UNIVERSITAT ROVIRA I VIRGILI
CHEMISTRY OF DAWSONITES AND APPLICATION IN CATALYSIS
Georgiana Stoica
ISBN:978-84-693-1533-0/DL:T-648-2010

UNIVERSITAT ROVIRA I VIRGILI
CHEMISTRY OF DAWSONITES AND APPLICATION IN CATALYSIS
Georgiana Stoica
ISBN:978-84-693-1533-0/DL:T-648-2010

UNIVERSITAT ROVIRA I VIRGILI
CHEMISTRY OF DAWSONITES AND APPLICATION IN CATALYSIS
Georgiana Stoica
ISBN:978-84-693-1533-0/DL:T-648-2010

Doctoral Thesis

CHEMISTRY OF DAWSONITES AND APPLICATION IN CATALYSIS

Georgiana Stoica

Supervised by Prof. Dr. Javier Pérez-Ramírez

ICIQ - URV

Tarragona

2010

UNIVERSITAT ROVIRA I VIRGILI
CHEMISTRY OF DAWSONITES AND APPLICATION IN CATALYSIS
Georgiana Stoica
ISBN:978-84-693-1533-0/DL:T-648-2010

UNIVERSITAT ROVIRA I VIRGILI
CHEMISTRY OF DAWSONITES AND APPLICATION IN CATALYSIS
Georgiana Stoica
ISBN:978-84-693-1533-0/DL:T-648-2010

Javier Pérez-Ramírez, Research Professor of the Catalan Institution for Research and Advanced Studies (ICREA) in Barcelona, and Group Leader of the Institute of Chemical Research of Catalonia (ICIQ) in Tarragona

CERTIFY:

That the present research study, entitled 'Chemistry of dawsonites and application in catalysis', presented by **Georgiana Stoica** for the award of the degree of Doctor, has been carried out under my supervision in ICIQ.

Tarragona, January 2010

Prof. Dr. Javier Pérez-Ramírez

Institut Català d'Investigació Química

Universitat Rovira i Virgili

UNIVERSITAT ROVIRA I VIRGILI
CHEMISTRY OF DAWSONITES AND APPLICATION IN CATALYSIS
Georgiana Stoica
ISBN:978-84-693-1533-0/DL:T-648-2010

UNIVERSITAT ROVIRA I VIRGILI
CHEMISTRY OF DAWSONITES AND APPLICATION IN CATALYSIS
Georgiana Stoica
ISBN:978-84-693-1533-0/DL:T-648-2010

Acknowledgments

First of all I would like to thank my supervisor, Dr. Javier Pérez-Ramírez, not only for his support, encouragement, and sometimes patience during this work, but also for trusting me when I joined his research group. These years have been very stimulating and instructive, with nice discussions and ideas. The pleasant research atmosphere was of course the product of all the other members of the group at different stages during this time. Of these I want to give special thanks to Marta, Sònia, and Yolanda. Thank you for your support, advices, joy, loyalty and friendship. That was of great fun.

I also want to take the opportunity to thank the research support units in ICIQ: Dr. Gisela Colet (Chemical Reaction Technologies), Eduardo Escudero (X-ray diffraction), Susana Delgado (Thermal Analysis), and Kerman Gomez (Nuclear Magnetic Resonance), for discussions and insights. Dr. Francesc Gispert and Mercè Moncusí from the Servei de Recursos Científics i Tècnics (Universitat Rovira i Virgili) are thanked for the *in situ* XRD and microscopy analyses, respectively.

Dr. Johan C. Groen (Delft Solids Solutions) and Dr. Miguel Antonio Gonzalez (ICIQ) are acknowledged for technical assistance and valuable discussions on the gas adsorption and density analyses. I am grateful to Dr. Paolo Pescarmona (K. U. Leuven) for the nice and fruitful collaboration on the alkenes epoxidation.

Last, but not least, I would also like to thank my personal friends from all over the world: thank you for all the good moments. To my friends who made life in Tarragona pleasant and friendly. I hesitate to include lists, as I will surely omit some who deserve mention. And everybody who positively influenced my life.

UNIVERSITAT ROVIRA I VIRGILI
CHEMISTRY OF DAWSONITES AND APPLICATION IN CATALYSIS
Georgiana Stoica
ISBN:978-84-693-1533-0/DL:T-648-2010

Finally, my greatest thanks to my parents and my brother, whose dedication, encouragement, and love was always of real importance. Thank you for the freedom to explore, discover, and pursue my dreams. You and your support, at home or from far away, inspired me to better myself and aim higher.

The Spanish MICINN (CTQ2006-01562/PPQ, AP2005-5147, and Consolider-Ingenio 2010, grant CSD2006-0003) and the ICIQ Foundation are acknowledged for the financial support of this research.

Georgiana Stoica

Tarragona, January 2010

UNIVERSITAT ROVIRA I VIRGILI
CHEMISTRY OF DAWSONITES AND APPLICATION IN CATALYSIS
Georgiana Stoica
ISBN:978-84-693-1533-0/DL:T-648-2010

UNIVERSITAT ROVIRA I VIRGILI
CHEMISTRY OF DAWSONITES AND APPLICATION IN CATALYSIS
Georgiana Stoica
ISBN:978-84-693-1533-0/DL:T-648-2010

UNIVERSITAT ROVIRA I VIRGILI
CHEMISTRY OF DAWSONITES AND APPLICATION IN CATALYSIS
Georgiana Stoica
ISBN:978-84-693-1533-0/DL:T-648-2010

Contents

UNIVERSITAT ROVIRA I VIRGILI
CHEMISTRY OF DAWSONITES AND APPLICATION IN CATALYSIS
Georgiana Stoica
ISBN:978-84-693-1533-0/DL:T-648-2010

UNIVERSITAT ROVIRA I VIRGILI
CHEMISTRY OF DAWSONITES AND APPLICATION IN CATALYSIS
Georgiana Stoica
ISBN:978-84-693-1533-0/DL:T-648-2010

Chapter 1

Introduction

A brief introduction on dawsonite-type materials is presented, stating the achievements of the state-of-the-art. However, their chemistry is not fully understood and examples of catalytic uses have been hardly published. In this purpose, the work herein focuses on the activation of the material by structure modification (Chapters 2-5) and the consequent application in selected catalytic reactions (Chapters 6 and 7). Finally, the main results and future work are highlighted in Chapter 8.

UNIVERSITAT ROVIRA I VIRGILI
CHEMISTRY OF DAWSONITES AND APPLICATION IN CATALYSIS
Georgiana Stoica
ISBN:978-84-693-1533-0/DL:T-648-2010

Dawsonite-type materials

Dawsonites are crystalline minerals generally present in nature as sodium aluminum carbonate hydroxide, $NaAlCO_3(OH)_2$. The mineral was discovered in 1862 during the construction of the Redpath Museum in a feldspathic dike on the campus of McGill University on the Island of Montreal, Quebec, Canada. It was first collected as 'probably new mineral specie' by John William Dawson, geologist and Principal of McGill University, and named in his honor by Harrington in 1874.[1] Up to date, dawsonite was found in many localities worldwide.

The crystal structure of the Montreal dawsonite was determined later by Frueh and Golightly,[2] and exhibits an orthorhombic-dipyramidal structure consisting of an assemblage of edge-sharing distorted $AlO_2(OH)_4$ and $NaO_4(OH)_2$ octahedra, and CO_3^{2-} groups (Figure 1.1). The structure of dawsonite is consistent with the space group *Imam*, displaying body-centered symmetry.[2] One oxygen of the carbonate is hydrogen-bonded to two hydroxyls groups, strengthening the three-dimensional framework.[3]

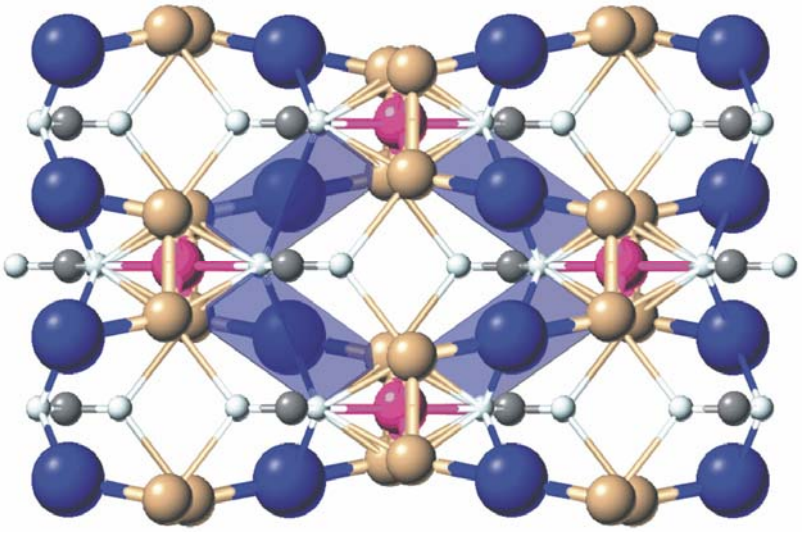

Figure 1.1. Structure of dawsonite, $NaAl(OH)_2CO_3$. Source: www.webmineral.com. Na: blue spheres, Al: purple sticks, C: grey sticks, and O: white sticks.

Besides $NaAlCO_3(OH)_2$, a variety of compositions with dawsonite-type structure have been synthesized by changing the nature of sodium or aluminum cations in the structure. These analogues of the mineral are generally denominated as double hydroxyl carbonates nominally described by the formula $XMCO_3(OH)_2$, where *X* is a monovalent cation and *M* is favorably a divalent or trivalent transition or nontransition metal.[4-6] Among them, the most studied

UNIVERSITAT ROVIRA I VIRGILI
CHEMISTRY OF DAWSONITES AND APPLICATION IN CATALYSIS
Georgiana Stoica
ISBN:978-84-693-1533-0/DL:T-648-2010

analogues of the mineral are ammonium and potassium dawsonites. The crystal structures of NH_4-dawsonite and K-dawsonite were found to be isostructural, and are composed of the same $AlO_2(OH)_4$ chains as the dawsonite mineral.[7] The space group of both $NH_4AlCO_3(OH)_2$ and $KAlCO_3(OH)_2$ has been determined as *Cmcm*, and such a structure is base-centered.

Most of the studies related to dawsonites touch upon their geological occurrence as well as their synthesis and characterization. However, the chemistry of synthetic dawsonites is not fully understood and, in particular, examples of catalytic uses have been hardly published. Dawsonite-type compounds can be used as-such or as precursors for derived materials. The as-synthesized samples have been applied as ingredient in antacids,[8] stabilizer in polymers,[9, 10] dry extinguisher in fuel leak fires,[11] and additive in synthetic fertilizers.[12] Recently, dawsonite has been reported as a possible mineral product resulting from the injection of CO_2 into many types of sandstone reservoirs.[13] This observation could represent an alternative to reduce the emission of this greenhouse gas by mineral trapping in the underground.

However, their application as precursors for other materials has attracted increasing attention lately considering that catalytic-grade alumina-based materials are very important from a practical perspective. NH_4-*M*-dawsonite composition is the appropriate precursor for pure *M*-oxides, whereas *X*-*M*-dawsonite systems are adequate precursors for alkalized and composite oxides. The annual world production of alumina was estimated in 2008 at 80 Mt, giving idea of the relevance of this compound in a number of industries (mining, ceramic, chemical). NH_4-dawsonite is a unique precursor for ultra-fine and highly-pure aluminas with enhanced properties compared to those derived from the conventional Bayer process (Figure 1.2).[5,14-16] The precursors were prepared by the in-line dispersion-precipitation (ILDP) method. The intrinsic features of this method, such as the continuous operation in a miniaturized precipitation chamber, the controlled residence time, and the excellent stirring, are partially responsible for the high surface area of the materials.[5,17,18] Based on this, several hydrotalcite-like compounds with different metal combination, and metal-substituted dawsonites were successfully synthesized as precursors for multimetallic oxide catalysts. This synthesis route was used extensively along the course of this thesis.

Previous studies reported that, due to the composition flexibility, calcination of dawsonite-type materials results in oxide compounds with outstanding component dispersion, porosity, thermal stability, and catalytic performance.[5,19] Yalfani *et al.*[6] investigated the thermal evolution in air of *M*-Al and La-*M*-Al dawsonite-type compounds (*M* = Mn, Fe, Co, Ni) using *in situ* methods. Depending on the combination of metals in the precipitate and temperature,

UNIVERSITAT ROVIRA I VIRGILI
CHEMISTRY OF DAWSONITES AND APPLICATION IN CATALYSIS
Georgiana Stoica
ISBN:978-84-693-1533-0/DL:T-648-2010

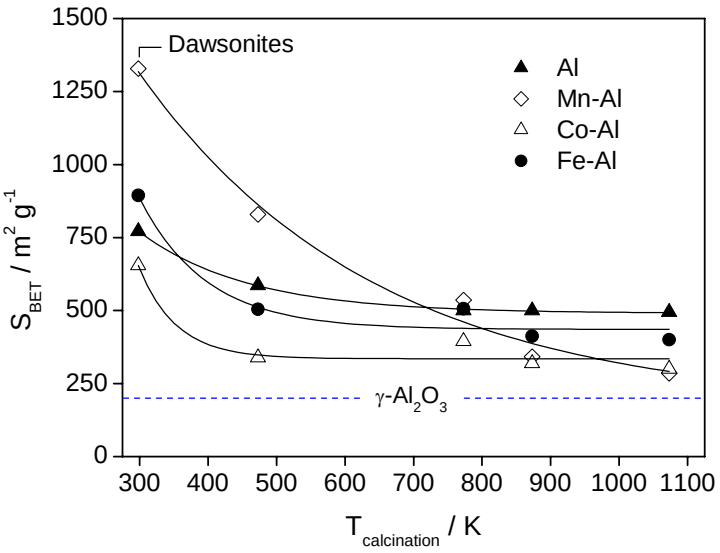

Figure 1.2. Total surface area (S_{BET}) of metal-substituted dawsonites, and the corresponding oxides at different calcination temperatures. The dashed line indicates typical S_{BET} of conventional γ-Al_2O_3 (catalyst support grade).[16]

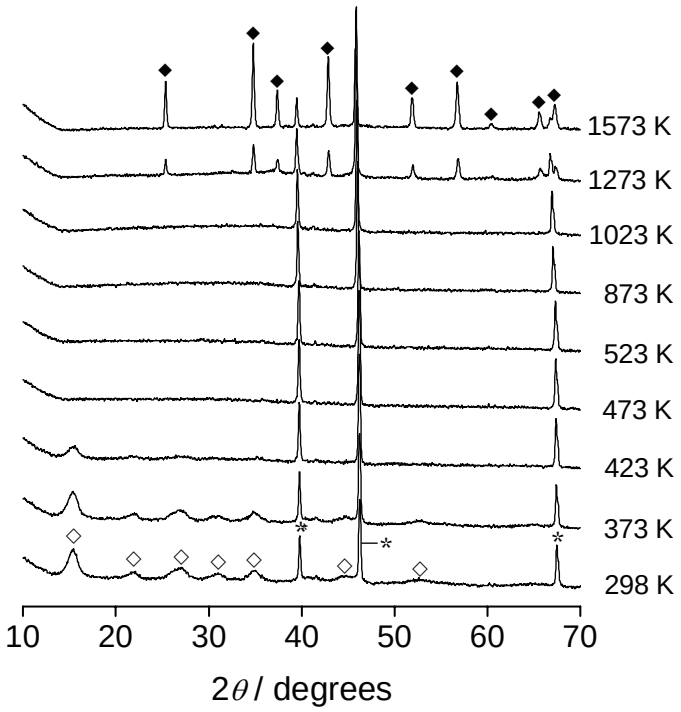

Figure 1.3. *In situ* X-ray diffraction patterns during decomposition in air of Fe-Al-dawsonite with Fe:Al = 1:11. Symbols: (◇) dawsonite, (◆) α-Al_2O_3, and (★) Pt-Rh alloy heater strip (JCPDS 4-802).

UNIVERSITAT ROVIRA I VIRGILI
CHEMISTRY OF DAWSONITES AND APPLICATION IN CATALYSIS
Georgiana Stoica
ISBN:978-84-693-1533-0/DL:T-648-2010

the products of metal-containing NH_4-dawsonite can be different forms of aluminas, single metal oxides, and mixed oxides with spinel, perovskite, and hexaaluminate structure. However, independent of the composition of the starting material, an amorphous alumina phase was formed after collapse of the dawsonite structure at 473 K, and temperatures above 1273 K were required in order to observe crystalline Al containing phases (α-Al_2O_3, $LaAlO_3$, $LaAl_{11}O_{18}$) by high temperature X-ray diffraction (Figure 1.3).[5] The transition temperature at which NH_4-dawsonite structure collapses (*ca.* 473 K) is independent of the metal composition of the samples.[5] The amorphous nature of the NH_4-dawsonite-derived alumina and its sintering stability, as described before, are very interesting and intriguing, and deserve further investigation. Finally, the acquired knowledge could be extrapolated to other dawsonite-type compounds.

Aim of the thesis

The work described in this thesis focuses on the chemistry of dawsonite-type compounds firstly understanding their stability in aqueous media, and secondly activating these materials *by structure modification* for consequent *application in several catalytic reactions* in order to demonstrate a more efficient utilization of dawsonites. Post-synthesis modifications of the dawsonites by thermal treatment, reconstruction, or as nanostructured composite materials represent a novel way to design materials with new properties and functionalities heretofore unavailable in the original material. The final goal is to benefit the acquired properties of the derived dawsonite-materials in selected catalytic reactions of practical relevance such as the production of dimethyl carbonate by transesterification of ethylene carbonate with methanol (base catalysis), or the alkene epoxidation of cyclooctene with hydrogen peroxide (redox catalysis). The above findings could have further practical implications as activated dawsonites open a new window of research with potential applications as catalysts, adsorbents, and additives.

Outline of the thesis

A short overview on dawsonite-type materials and current state-of–the-art, and the objectives and structure of this thesis are presented in ***Chapter 1***. ***Chapter 2*** discusses the stability of synthetic dawsonites in different aqueous media in the pH range 2-14. The influence of the carbonate solutions on dawsonite chemical structure will be presented in detail. The most interesting solid transformations were successively repeated in order to

UNIVERSITAT ROVIRA I VIRGILI
CHEMISTRY OF DAWSONITES AND APPLICATION IN CATALYSIS
Georgiana Stoica
ISBN:978-84-693-1533-0/DL:T-648-2010

investigate the stability of newly formed phases, and the reversibility of Na into NH_4-dawsonite and *vice versa* was demonstrated. Experiments at different periods of time provided insights on the mechanism of selected chemical transformations. The three dawsonite forms display relative different stability, *i.e.* the highly reactive Na and NH_4-dawsonite *versus* the stable K-dawsonite. Textural and morphological changes associated with the different phases and treatments will be highlighted.

Similarly to the dawsonites in the previous chapter, the reactivity of layered hydrotalcite-like compounds in aqueous ammonium carbonate solution was investigated in ***Chapter 3***. It is known that thermally decomposed or exfoliated hydrotalcites have the ability of recovering the original structure in very diverse media due to the memory property.[20] Rather than the typical restacking of the original phase, we endeavor the transformation of the hydrotalcites into other structured compounds by treatment in aqueous ammonium carbonate solution at ambient conditions. Remarkably, hydrotalcite transformed into nanostructured composite materials containing dawsonite, hydrotalcite and magnesium ammonium carbonate, under the conditions applied. In this purpose, two synthetic approaches were followed: (i) immersion of the solid hydrotalcites in $(NH_4)_2CO_3$ solution, and (ii) exfoliation of the layered hydrotalcites in formamide leading to positively charged nanosheets, and reactive stacking of the resulting colloid in aqueous $(NH_4)_2CO_3$. The influence of the treatment time on the phase composition of the resulting materials will be detailed. The mechanism of the exfoliation-restacking process will be discussed, highlighting the role of the Mg/Al ratio in the parent hydrotalcites.

Since post-synthesis modifications of dawsonites are one of the main objectives in this work, ***Chapter 4*** investigates the reactivity of aluminum oxides derived from thermal decomposition of dawsonite-type compounds in aqueous solutions. The influence of the thermal decomposition temperature on the starting material, aluminum metal-substituted dawsonites, and treatment media were studied. The importance of the ammonium carbonate aqueous solution is evidenced. Changes in crystallinity, porosity, and morphology of the reformed materials are highlighted. In connection to the previous chapter, ***Chapter 5*** studies the kinetics and mechanism of the reconstruction process in aqueous ammonium carbonate. The effect of dawsonite chemical composition and treatment conditions such as time, temperature, reactants molar ratio, and precipitating agent concentration, as well as the pH of the medium were investigated. The transition of alumina towards dawsonite follows a dissolution-precipitation mechanism accompanied by significant textural and morphological changes.

UNIVERSITAT ROVIRA I VIRGILI
CHEMISTRY OF DAWSONITES AND APPLICATION IN CATALYSIS
Georgiana Stoica
ISBN:978-84-693-1533-0/DL:T-648-2010

The second part of the thesis focuses on applications of the activated dawsonites as addressed in the previous chapters. ***Chapter 6*** presents the catalytic performance of thermally activated Na-dawsonite in the synthesis of dimethyl carbonate (DMC) via transesterification of ethylene carbonate with methanol. DMC is a versatile and eco-friendly building block compound, used as an alternative to the environmentally harmful phosgene, methyl halides, and dimethyl sulfate for producing a number of intermediates.[21] *In situ* X-ray diffraction studies have been complemented by other characterization techniques in order to derive structure-performance relationships. Additionally, the variation of the reaction parameters provided kinetic insights on the catalytic process. Stability of the catalysts in the title reaction was investigated in several consecutive runs. Scale-up studies were performed using two orders of magnitude higher reactors. Mechanistic information was obtained *via* on-line monitoring by ATR-FTIR spectroscopy, which couples the evolution of the liquid-phase reaction with vibrational spectroscopy. Basicity of activated dawsonites will be discussed.

Chapter 7 presents the epoxidation reaction of cyclooctene with hydrogen peroxide over catalysts derived from NH_4-Al and NH_4-Ga-dawsonites. The influence of the thermal activation temperature on the catalyst structure and the corresponding catalytic performance will be discussed, as well as stability aspects of the materials upon several consecutive recycling tests. NH_4-Ga-dawsonite derived materials are the most active transition metal-free catalysts developed so far for the epoxidation of cyclooctene.

Finally, the conclusions and outlook of the thesis are put in perspective in ***Chapter 8***.

References

[1] B. J. Harrington, *Can. Natural.* **1874**, 7, 305.
[2] A. J. Frueh, J. P. Golightly, *Can. Miner.* **1967**, 9, 51.
[3] E. Corazza, C. Sabelli, S. Vannucci, *Neues Jahrb. Mineral. Monatsh.* **1977**, 9, 381.
[4] A. A. Ali, M. A. Hasan, M. I. Zaki, *Chem. Mater.* **2005**, 17, 6797.
[5] M. Santiago, M. S. Yalfani, J. Pérez-Ramírez, *J. Mater. Chem.* **2006**, 16, 2886.
[6] M. S. Yalfani, M. Santiago, J. Pérez-Ramírez, *J. Mater. Chem.* **2007**, 17, 1222.
[7] T. Iga, S. Kato, *J. Ceram. Soc. Jpn.* **1978**, 86, 509.
[8] C. J. Serna, J. L. White, S. L. Hem, *J. Pharm. Sci.* **1978**, 67, 324.
[9] P. V. Bonsignore, *Plast. Eng.* **1976**, 32, 41.
[10] E. A. Woycheshin, R. J. Rigge, I. Sobolev, *U. S. Patent 3 878 166* **1975**.
[11] R. L. Altman, L. A. Mayer, A. C. Ling, *U. S. Patent 4 406 797* **1983**.
[12] G. Gillman, A.Noble, *Environ. Qual. Manage.* **2005**, 15, 59.

UNIVERSITAT ROVIRA I VIRGILI
CHEMISTRY OF DAWSONITES AND APPLICATION IN CATALYSIS
Georgiana Stoica
ISBN:978-84-693-1533-0/DL:T-648-2010

[13] W. D. Gunter, E. H. Perkins, T. J. McCann, *Energ. Convers. Manage.* **1993**, 34, 941.

[14] M. Giannos, M. Hoang, T. W. Turney, *Chem. Lett.* **1998**, 793.

[15] G. I. Horita, E. P. Goulart, O. Thomaz, A. Monteiro, D. G. de Souza, *Mater. Sci. Forum* **1999**, 299, 3.

[16] Handbook of Heterogeneous Catalysis, ed. F. Schütz, K. Unger, G. Ertl, H. Knözinger, J. Weitkamp, VCH, Weinheim, **1997**, vol. 2, pp. 72–86.

[17] S. Abelló, J. Pérez-Ramírez, *Adv. Mater.* **2006**, 18, 2436.

[18] J. Pérez-Ramírez , S. Abelló Cros, M. Santiago Redondo, *WO2007147881* **2007**.

[19] I. Pitsch, W. Gebner, A. Brückner, H. Mehner, S. Mohmel, D.-C. Uecker, M.-M. Pohl, *J. Mater. Chem.* **2001**, 11, 2498.

[20] J. Pérez-Ramírez, S. Abelló, N. M. van der Pers, *Chem. Eur. J.* **2007**, 13, 870.

[21] N. Keller, G. Rebmann, V. Keller, *J. Mol. Catal. A: Chemical* **2009**, doi:10.1016/j.molcata.2009.10.027.

UNIVERSITAT ROVIRA I VIRGILI
CHEMISTRY OF DAWSONITES AND APPLICATION IN CATALYSIS
Georgiana Stoica
ISBN:978-84-693-1533-0/DL:T-648-2010

UNIVERSITAT ROVIRA I VIRGILI
CHEMISTRY OF DAWSONITES AND APPLICATION IN CATALYSIS
Georgiana Stoica
ISBN:978-84-693-1533-0/DL:T-648-2010

UNIVERSITAT ROVIRA I VIRGILI
CHEMISTRY OF DAWSONITES AND APPLICATION IN CATALYSIS
Georgiana Stoica
ISBN:978-84-693-1533-0/DL:T-648-2010

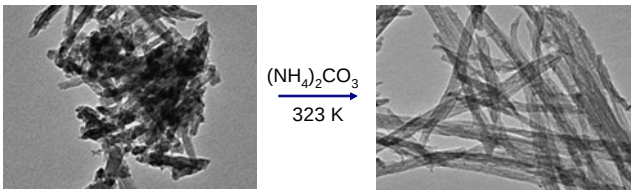

Na-dawsonite NH_4-dawsonite

Chapter 2

Stability and interconversion of synthetic dawsonites in aqueous media

The stability of synthetic dawsonites ($XAlCO_3(OH)_2$ with $X = NH_4$, Na, and K) in aqueous media was investigated at ambient pressure and 323 K. The three compositions dissolved under strong acid (pH 2) and basic (pH 14) conditions. In water (pH 7), dawsonites evolved into boehmite (NH_4 form) and bayerite (Na and K forms). The most interesting transformations occurred upon contacting the dawsonites with ammonium, potassium, and sodium carbonate solutions. NH_4-dawsonite was converted into Na-dawsonite and K-dawsonite in Na_2CO_3 and K_2CO_3 (pH 12), respectively. Na-dawsonite transformed into NH_4-dawsonite in $(NH_4)_2CO_3$ (pH 10). The NH_4-dawsonite and Na-dawsonite can be successively interconverted in the appropriate carbonate solution. The kinetics of these transformations was studied varying the treatment time from several minutes up to 24 h. In the pH range 10-12, K-dawsonite proved as the most stable among the three dawsonite compositions. Besides structural changes, the treatment of dawsonites in composite solutions also involved alterations of the morphology and porosity of the materials. Our results demonstrate the interconversion between various dawsonite compositions, and an improved understanding of the chemistry of these materials.

UNIVERSITAT ROVIRA I VIRGILI
CHEMISTRY OF DAWSONITES AND APPLICATION IN CATALYSIS
Georgiana Stoica
ISBN:978-84-693-1533-0/DL:T-648-2010

1. Introduction

Dawsonite is a mineral composed of sodium aluminum carbonate hydroxide with chemical formula $NaAlCO_3(OH)_2$. It exhibits various crystal habits including prisms, aciculae, fibers, spheres, rosettes, and random aggregates.[1] The crystal structure of Na-dawsonite is orthorhombic-dipyramidal (space group *Imam*), consisting of an assemblage of edge-sharing distorted $AlO_2(OH)_4$ and $NaO_4(OH)_2$ octahedra and CO_3^{2-} groups.[2,3] One oxygen of the carbonate is hydrogen-bonded to two hydroxyl groups, strengthening the three-dimensional framework. Besides $NaAlCO_3(OH)_2$, multiple compositions with dawsonite-type structure have been synthesized by changing the nature of sodium and/or aluminum cations.[4-6] Potassium and ammonium dawsonites are the most studied analogues, being composed of the same $AlO_2(OH)_4$ chains of octahedral as the mineral.[7] Dawsonite-type materials can also incorporate a variety of divalent and trivalent cations in Al^{3+} positions (*e.g.* Cr^{3+}, Fe^{3+}). Calcination of these materials results in oxidic compounds with outstanding properties and performance in catalytic applications.[5,8,9]

Various methods have been reported to synthesize dawsonites with high purity and crystallinity.[5] In contrast, little is known on the reactivity of dawsonite-type materials in aqueous media. This aspect is required for the preliminary assessment of the long-term stability of the material in the underground. Recently, Na-dawsonite has been reported as a possible mineral product resulting from the injection of CO_2 into Al-bearing silicates aquifers.[10] Dawsonite precipitation occurs at elevated partial pressures of CO_2 and alkaline environments, *i.e.* high Na^+ concentrations, assured by oligoclase dissolution according to the following reaction[11-16]:

$$KAlSi_3O_8 + Na^+ + CO_2(aq) + H_2O \rightarrow NaAlCO_3(OH)_2 + 3SiO_2 + K^+$$

This observation could be interesting for CO_2 mineralization.[17]

The thermodynamic stability of Na-dawsonite is a function of coexisting phases in the system, temperature, CO_2 pressure, and relative formation/dissolution kinetics of the phases. Hellevang *et al.*[11] investigated the stability of Na-dawsonite by means of dissolution experiments using the mineral itself. Results concluded that dawsonite dissolution rates are independent of pH in the range 3.5-8.6, and the limiting component for dawsonite precipitation is the concentration of aqueous aluminum. In addition, the lifetime of a dawsonite depends on a stable CO_2 source; once the CO_2 fugacity drops below the stability limits of Na-dawsonite, the material will persist only for a short period of time.[11,18] Bénézeth *et al.*[1] conducted solubility and stability experiments of synthetic Na-dawsonite in order to reevaluate thermodynamic parameters of dawsonite formation and dissolution in basic

UNIVERSITAT ROVIRA I VIRGILI
CHEMISTRY OF DAWSONITES AND APPLICATION IN CATALYSIS
Georgiana Stoica
ISBN:978-84-693-1533-0/DL:T-648-2010

aqueous media (NaOH, Na_2CO_3, $NaHCO_3$). These authors have shown that at temperatures below 423 K and moderate pH, dawsonite is in equilibrium with bayerite, while at higher temperatures, the equilibrium with boehmite dominates. Increased pH (> 11) will induce its complete dissolution and formation of the Al-(oxi)hydroxides.

No studies have yet been undertaken addressing the stability of synthetic NH_4 and K-dawsonite. Herein, the reactivity of synthetic NH_4-, Na-, and K-dawsonites with high purity was investigated at ambient pressure and 323 K in different aqueous media covering the pH range of 2-14 using solutions of NO_3^-, Cl^-, SO_4^{2-}, CO_3^{2-}, and OH^-. The three compositions dissolved under strong acid and basic conditions. The pH range of 10-12 comprises a window of interest to gather an improved understanding of the chemistry of dawsonite-type materials. In particular, interconversion of Na-dawsonite into NH_4-dawsonite, and *vice versa*, in the appropriate carbonate solution is reported for the first time. Insights into the kinetics and mechanism of the transformations were achieved studying the influence of time and temperature.

2. Experimental

2.1. Materials and treatments

Ammonium, sodium, and potassium dawsonites, with formulas $NH_4AlCO_3(OH)_2$, $NaAlCO_3(OH)_2$, and $KAlCO_3(OH)_2$, respectively, were prepared following the recipe of Fernández-Carrasco *et al.*[19] An appropriate amount of $Al(NO_3)_3{\cdot}9H_2O$ powder, corresponding to a concentration of 1 M, was added to aqueous solutions (2 M) of $(NH_4)_2CO_3$, Na_2CO_3, and K_2CO_3 at 353 K, yielding the corresponding dawsonites. The samples were synthesized in a round-bottom glass vessel at 353 K under reflux conditions and magnetic stirring (500 rpm). In the beginning of the synthesis, the pH dropped rapidly upon adding the aluminum source, *i.e.* from 11 to 8.3 for $NH_4AlCO_3(OH)_2$, and from 13 to 9.5 for $NaAlCO_3(OH)_2$ and $KAlCO_3(OH)_2$, respectively, and then remained constant. The resulting precipitate slurry was kept for 2 h at 353 K. The solids were filtered, washed with deionized water, and dried at 333 K for 12 h.

The as-synthesized dawsonites (0.1 g), referred to as NH_4-DW, Na-DW, and K-DW, were poured in 1 M aqueous solutions (50 cm^3) containing different anions, *i.e.* NO_3^-, Cl^-, SO_4^{2-}, CO_3^{2-}, OH^- in the pH range of 2-14 under magnetic stirring (500 rpm) at 323 K for 24 h. Treatment of the dawsonites in deionized water, was also performed using the same experimental conditions. The treatments summarized in Table 2.1 were carried out in a round-bottom glass vessel equipped with a reflux condenser. Selected experiments, *i.e.*

Na-dawsonite treated in $(NH_4)_2CO_3$, and NH_4-dawsonite treated in Na_2CO_3, were additionally done at 298 K and 24 h, respectively. All the resulting solids were filtered, washed, and dried at 333 K for 12 h.

2.2. Characterization

Powder X-ray diffraction (XRD) was measured in a Siemens D5000 diffractometer with Bragg-Brentano geometry and Ni-filtered CuKα radiation (λ = 0.1541 nm). Data were recorded in the range 10-70º 2θ with an angular step size of 0.0168º and a counting time of 4 s per step. Thermogravimetric analysis (TGA) was carried out in a Mettler Toledo TGA/SDTA851e microbalance. Analyses were performed in dry air flow of 50 cm^3 min^{-1} ramping the temperature from 298 to 1173 K at 5 K min^{-1}. Transmission electron microscopy (TEM) was carried out in a JEOL JEM-1011 microscope operated at 100 kV. A few droplets of the sample suspended in ethanol were placed on a carbon-coated copper grid followed by evaporation at ambient conditions. Nitrogen adsorption-desorption isotherms at 77 K were measured on a Quantachrome Quadrasorb-SI gas adsorption analyzer. Prior to analysis, the sample was degassed in vacuum at 373 K for 48 h. The BET method[20] was applied to calculate the total surface area, and the *t*-plot method[21] was used to discriminate between micro- and mesoporosity.

3. Results and discussion

3.1. As-synthesized dawsonites

Powder X-ray diffraction patterns of the as-synthesized samples (Figure 2.1) confirmed that dawsonite was the only crystalline phase in the precipitates: Na-dawsonite ($NaAlCO_3(OH)_2$, JCPDS 45-1359), K-dawsonite ($KAlCO_3(OH)_2$, JCPDS 21-979), and NH_4-dawsonite ($NH_4AlCO_3(OH)_2$, JCPDS 42-250). Thermogravimetric analyses in air (Figure 2.2) also demonstrated the high purity of the dawsonites. The total weight losses of the as-synthesized samples amounted to *ca.* 43% (Na-DW), 41% (K-DW), and 61% (NH_4-DW), *i.e.* very close to the theoretical values based on the dawsonite formulas (43% for Na-DW, 40% for K-DW, and 63% for NH_4-DW). Attending to the transition temperatures in Figure 2.2, the order of thermal stability was K-DW (580 K) > Na-DW (560 K) >> NH_4-DW (468 K). These results are in good correspondence with the literature.[22-24] The as-synthesized dawsonites featured different morphologies depending on the cation in the structure (Figure 2.3). TEM of Na-dawsonite showed the presence of

UNIVERSITAT ROVIRA I VIRGILI
CHEMISTRY OF DAWSONITES AND APPLICATION IN CATALYSIS
Georgiana Stoica
ISBN:978-84-693-1533-0/DL:T-648-2010

acicular particles, which is the most common appearance of the mineral.[25] K-dawsonite displayed spherical-like particles. This morphology is different from the fibrous K-dawsonite particles obtained by Hérnandez *et al.*[23] However, they carried out hydrothermal synthesis starting from a mixture of $AlCl_3$ and $KHCO_3$ at 403 K. NH_4-dawsonite exhibited the characteristic aggregated spherical-like particles.[24]

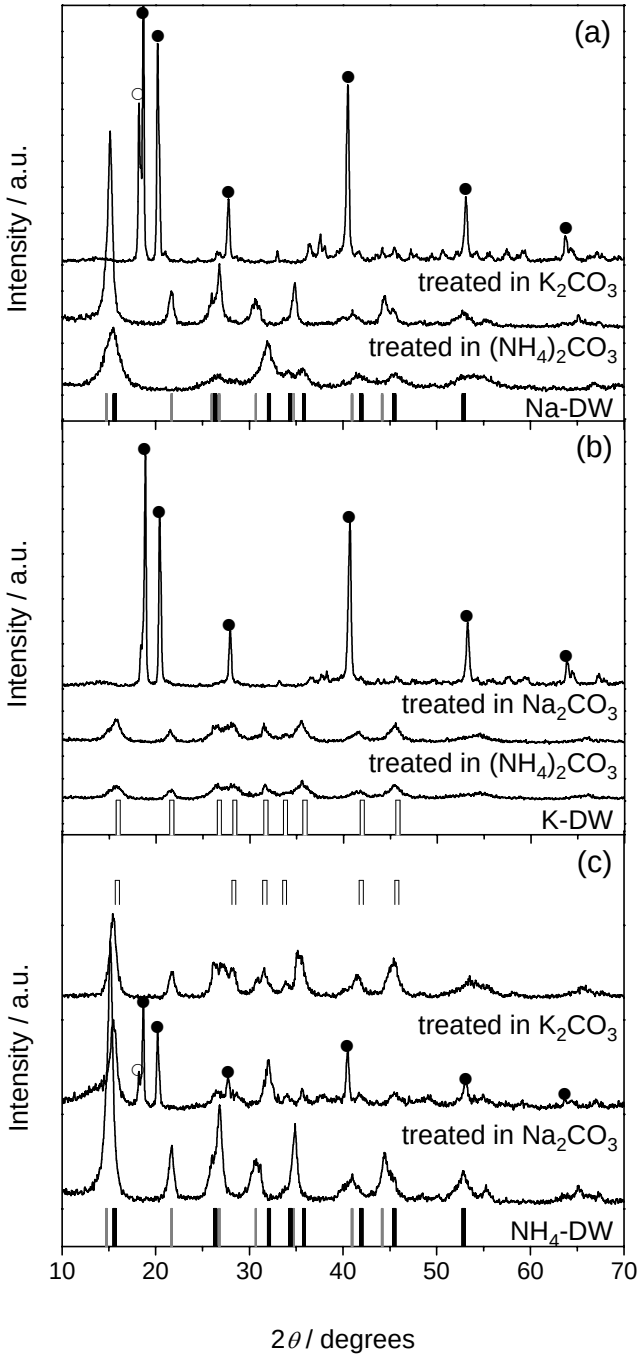

Figure 2.1. X-ray diffraction patterns of the solids resulting from treatment of the as-synthesized (a) Na-dawsonite, (b) K-dawsonite, and (c) NH_4-dawsonite in different media (1 M, 323 K, and 24 h). The reflections marked with (●) and (○) belong to bayerite and gibbsite, respectively. The lines are indicative for selected reflections of Na (black), K (white), and NH_4-dawsonite (gray), respectively, position-wise and not intensity (see text).

UNIVERSITAT ROVIRA I VIRGILI
CHEMISTRY OF DAWSONITES AND APPLICATION IN CATALYSIS
Georgiana Stoica
ISBN:978-84-693-1533-0/DL:T-648-2010

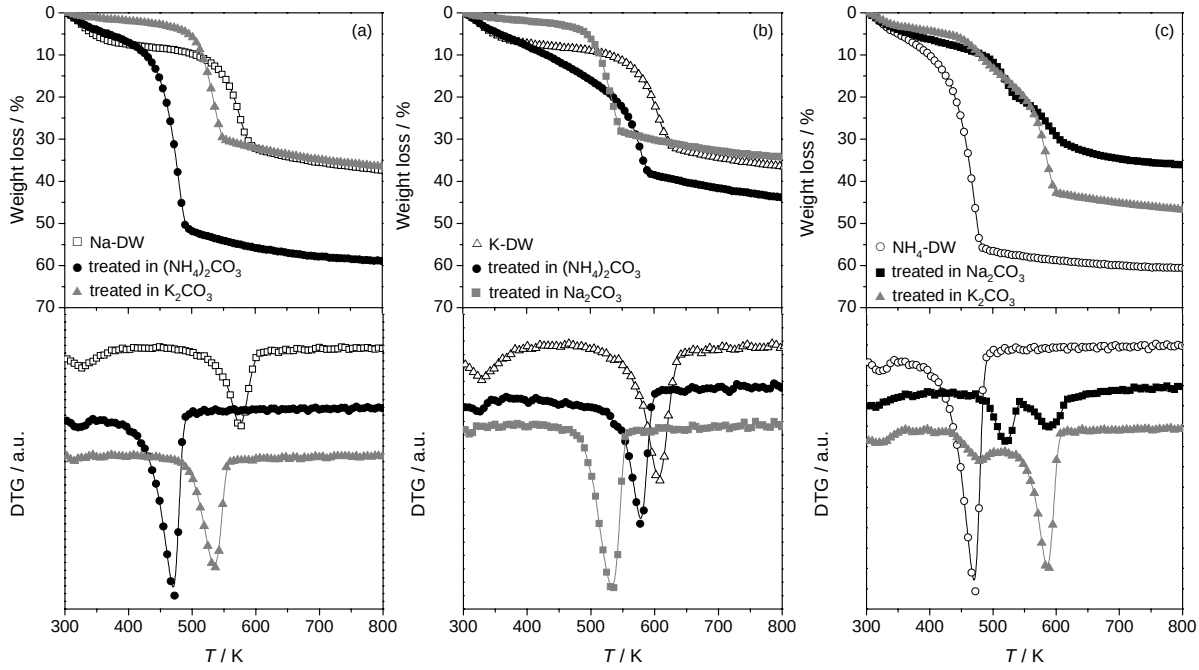

Figure 2.2. (Top) Thermogravimetric profiles and (bottom) derivative curves of the weight loss of as-synthesized (a) Na-dawsonite, (b) K-dawsonite, and (c) NH_4-dawsonite, and the solids resulting from their treatment in aqueous $(NH_4)_2CO_3$, K_2CO_3, and Na_2CO_3. Treatment conditions: 1 M, 323 K, and 24 h for 1 day.

3.2. Influence of the treatment media

The stability of the three dawsonites was investigated in a variety of aqueous solutions at a concentration of 1 M, a temperature of 353 K, and a period of time of 1 day (Table 2.1). As reported elsewhere, strong acids (HCl, H_2SO_4, and HNO_3, pH 2) and bases (NaOH and KOH, pH 14) caused complete dissolution of the solids under the experimental conditions applied.[19,26] Treatment in slightly acidic media (NH_4Cl, NaCl, and KCl, pH 6) transformed the dawsonite structures into boehmite (JCPDS 76-1871). None of the dawsonite was stable in deionized water: NH_4-dawsonite transformed into boehmite, while Na-dawsonite and K-dawsonite transformed into bayerite (JCPDS 8-96). At this pH, boehmite is expected to form, whilst bayerite precipitates at higher pH values in pure aluminum aqueous solutions.[27] Dissolution of Na- or K-dawsonites might increase the local alkalinity and favor the reprecipitation of aluminum in the form of aluminate at this pH, $Al(OH)_4^-$,[28] ultimately leading to Al-containing (oxi)hydroxides, *i.e.* boehmite and bayerite. The dawsonites were stable at moderate pH in aqueous solutions of $MgCO_3$ and $CaCO_3$ (pH 9), similar to previous results which showed a steady growth of dawsonite and other carbonates (calcite, magnesite, siderite, and ankerite) coupled to aluminosilicate dissolution.[29]

UNIVERSITAT ROVIRA I VIRGILI
CHEMISTRY OF DAWSONITES AND APPLICATION IN CATALYSIS
Georgiana Stoica
ISBN:978-84-693-1533-0/DL:T-648-2010

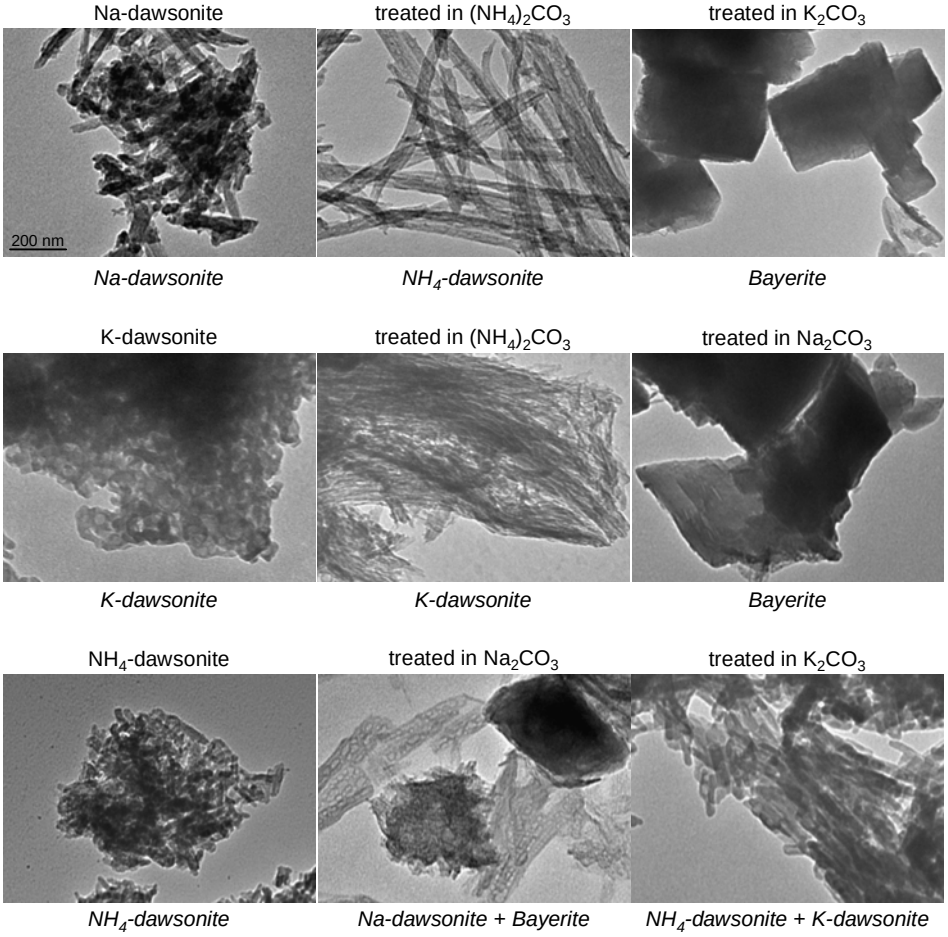

Figure 2.3. Transmission electron micrographs of the as-synthesized dawsonites and solids resulting from treatment in selected media (1 M, 323 K, and 24 h). Crystalline phases identified by XRD are stated in italics at the bottom of each illustration. The same scale bar applies to all micrographs.

Treatment at higher pH value (12), induced by aqueous NH_4OH 1 M, transformed the dawsonites in bayerite (Table 2.1). In the case of Na and K-dawsonite, additional gibbsite was determined in the XRD pattern due to local increased alkalinity induced by dissolution of Na and K, respectively. The dimorph bayerite-gibbsite is commonly reported at higher pH values and increasing temperature, *i.e.* pH ≥ 12 and 313-333 K, as an end result compound of $Al(OH)_3$ precipitation by the sequence aluminate → (pseudo)boehmite → bayerite → gibbsite.[30]

Remarkably, Na-dawsonite completely transformed into NH_4-dawsonite in aqueous $(NH_4)_2CO_3$ (pH 10). As shown by X-ray diffraction (Figure 2.1a), the (011) direction at 15.4º 2θ in Na-dawsonite shifted to 15.1º 2θ, which is characteristic of the (110) orientation in NH_4-dawsonite.[7] The diffraction pattern of Na-dawsonite vanished (black lines), and other reflections specific to $NH_4AlCO_3(OH)_2$ appeared (gray lines) as indicated

UNIVERSITAT ROVIRA I VIRGILI
CHEMISTRY OF DAWSONITES AND APPLICATION IN CATALYSIS
Georgiana Stoica
ISBN:978-84-693-1533-0/DL:T-648-2010

by the patterns of the reference materials in Figure 2.1a. Dissolution of Na-dawsonite in $(NH_4)_2CO_3$ is followed by precipitation of NH_4-dawsonite, which is thermodynamically favored over Na-dawsonite at this pH. The conversion of one dawsonite form into another has not been reported so far. Several studies reported that the optimal pH synthesis of NH_4-dawsonite is in the range 9.5-10.5, while synthesis of the sodium and potassium forms of dawsonite is favored at higher pH values, *i.e.* > 10.5.[31,32] In contrast to Na-dawsonite, K-dawsonite was stable in $(NH_4)_2CO_3$ (Figure 2.1b), as shown by the reflections specific to this compound (white lines).

Table 2.1. Summary of the influence of the treatment media on the XRD phase(s).

Treatment[a]	pH	NH4-dawsonite	Na-dawsonite	K-dawsonite
HNO_3	2	dissolution	dissolution	dissolution
HCl	2	dissolution	dissolution	dissolution
H_2SO_4	2	dissolution	dissolution	dissolution
NH_4Cl	6	NH_4-dawsonite	boehmite	boehmite
NaCl	6	NH_4-dawsonite	boehmite	boehmite
KCl	6	NH_4-dawsonite	boehmite	boehmite
H_2O	7	boehmite	bayerite	bayerite
$CaCO_3$	9	NH_4-dawsonite calcite	Na-dawsonite calcite	K-dawsonite calcite
$MgCO_3$	9	NH_4-dawsonite magnesite	Na-dawsonite magnesite	K-dawsonite magnesite
$(NH_4)_2CO_3$	10	-	NH_4-dawsonite	K-dawsonite
Na_2CO_3	12	Na-dawsonite bayerite gibbsite	-	bayerite
K_2CO_3	12	NH_4-dawsonite K-dawsonite	bayerite gibbsite	-
NH_4OH	12	bayerite	bayerite gibbsite	bayerite gibbsite
NaOH	14	dissolution	dissolution	dissolution
KOH	14	dissolution	dissolution	dissolution

[a] 1 M aqueous solutions, *T* 323 K, t 24 h.

UNIVERSITAT ROVIRA I VIRGILI
CHEMISTRY OF DAWSONITES AND APPLICATION IN CATALYSIS
Georgiana Stoica
ISBN:978-84-693-1533-0/DL:T-648-2010

Next, the as-synthesized dawsonites were treated in aqueous Na_2CO_3 and K_2CO_3 (pH 12). NH_4-dawsonite was converted into Na-dawsonite and K-dawsonite in Na_2CO_3 and K_2CO_3, respectively (Figure 2.1c). The (110) reflection at 2θ 15.1º in NH_4-dawsonite shifted to 15.4º, indicative of Na-dawsonite, and the reflections of $NH_4AlCO_3(OH)_2$ (gray lines) were completely replaced by those of Na-DW (black lines).[2] Besides, reflections of bayerite (JCPDS 8-96, solid circles in Figure 2.1b and c) and gibbsite (JCPDS 33-18, open circles in Figure 2.1c), respectively, were observed after treatment of K-dawsonite and NH_4-dawsonite in Na_2CO_3 as a consequence of the high pH. Treatment of NH_4-dawsonite in K_2CO_3 leads to a dimorph material (Figure 2.1c); the (110) reflection is displayed at 2θ 15.4º, *i.e.* intermediate between 15.1º in NH_4-dawsonite (gray line) and 15.6º in K-dawsonite (white line). Reflections characteristic to NH_4-dawsonie were visible at 27º and 33.8º, and new reflections belonging to $KAlCO_3(OH)_2$ appeared (white lines in Figure 2.1c). Due to the presence of the NH_4-dawsonite phase, the reflections of the K-form are shifted as compared to the pattern of the pure compound. This kind of mixed dawsonite was previously observed by Zhang *et al.*[33] Since there is only a small difference between the radius of K^+ (133 pm) and NH_4^+ (143 pm) ions, it is very possible that NH_4^+ would enter the lattice of $KAlCO_3(OH)_2$ when both cations co-exist in one reaction system leading to a dawsonite-type material with the formula $K_{1-x}(NH_4)_xAlCO_3(OH)_2$.[33] In support to this, the structures of NH_4-dawsonite and K-dawsonite are isomorphous.[31] Treatment of Na-dawsonite in aqueous K_2CO_3 (Figure 2.1a) and K-dawsonite in aqueous Na_2CO_3 (Figure 2.1b) led to bayerite. This can be expected based on thermodynamic studies by Bénézeth *et al.*[1] It was established that Na-dawsonite is not stable at pH > 11, leading to bayerite as the predominant phase. Additional gibbsite reflection at 2θ 18.3º is displayed in the diffractogram of Na-dawsonite sample treated in K_2CO_3. The symmetry of NH_4-dawsonite and K-dawsonite (base-centered) differs from that of Na-dawsonite (body-centered), although both structures are composed of the same $AlO_2(OH)_4$ chains of octahedra.[7]

Next sections will further elaborate on the different dawsonite forms phase transformation in carbonate media, and a general mechanism for the chemical transformation will be proposed.

3.3. Dawsonite transformation in carbonate solutions

The results obtained by X-ray diffraction in Figure 2.1 are substantiated by thermogravimetric analysis. Na-dawsonite treated in $(NH_4)_2CO_3$ displays a one-step weight loss profile amounting *ca.* 60% (Figure 2.2a**)**, with a transition temperature centered at 477 K specific to the NH_4-dawsonite phase (Figure 2.2a). This remark confirmed the transformation observed by X-ray diffraction analysis of the material. Based on the theoretical weight loss of NH_4-dawsonite, it was determined that 94% of the sample obtained after treatment in $(NH_4)_2CO_3$ consisted of $NH_4AlCO_3(OH)_2$. The solid obtained after treatment in aqueous K_2CO_3 presented a single step decomposition centered at 535 K, with a total weight loss of 35% (Figure 2.2a), in excellent agreement with the thermal decomposition of bayerite.[34] Additional evidences for dawsonite transformation were derived from morphological studies using transmission electron microscopy. As it can be seen in Figure 2.3, the acicular particles of Na-dawsonite transformed into very well defined nanoneedles by treatment in $(NH_4)_2CO_3$. Similar changes were observed by reconstruction of NH_4-dawsonite-derived alumina in ammonium carbonate, when the geometry evolved toward the most thermodynamically favored morphology specific to the dawsonite mineral.[25] Besides, comparing the morphology of as-synthesized NH_4-dawsonite and that obtained by treatment in Na_2CO_3, it can be deduced that the morphology of the same crystalline dawsonite is not influenced by the cation but is synthesis dependent. Treatment in potassium carbonate of Na-dawsonite led to big plate-like particles specific to bayerite, denominated as somatoid particles.[35]

The stability of K-dawsonite in $(NH_4)_2CO_3$ solution was confirmed by thermogravimetry. The weight loss profile in Figure 2.2b presented only one step centered at 577 K corresponding to $KAlCO_3(OH)_2$.[33] The transformation observed by electron microscopy, from spherical nanoparticles in the as-synthesized K-dawsonite to acicular crystals when treated with $(NH_4)_2CO_3$ (Figure 2.3), confirms the dissolution-precipitation step and is indicative of a structural and morphological transformation of the material towards the most stable geometry. Treatment of K-dawsonite in Na_2CO_3, generated a sample displaying the decomposition profile of bayerite (Figure 2.2b), in agreement with XRD results and similar to the transformation of Na-dawsonite in K_2CO_3 due to the high pH. The micrograph of this sample in Figure 2.3 showed particles characteristic of bayerite.

Thermogravimetric analysis of Na_2CO_3-treated NH_4-dawsonite (Figure 2.2c) displayed a two-step profile with transition temperatures at 520 and 588 K, respectively. Based on the weight loss of each step, corresponding to the phases existent in the material, it was concluded that NH_4-DW treated in Na_2CO_3 consisted of 47% Na-dawsonite and 53% bayerite,

respectively. These observations were nicely complemented by TEM of the sample in Figure 2.3 where morphologies specific to Na-dawsonite (aciculae) and bayerite (plate-like particles) can be identified. Treatment in K_2CO_3 led to a material displaying a two-step decomposition profile with transitions at 479 and 585 K, as shown in Figure 2.2c**.** From the total weight loss of 48%, a composition of 27% NH_4-dawsonite and 73% K-dawsonite was calculated. Nanoparticles in the as-synthesized NH_4-DW disposed in the form of aciculae (Figure 2.3), similar to the morphology of K-dawsonite treated in $(NH_4)_2CO_3$.

Since the most interesting solid changes occurred with NH_4-dawsonite and Na-dawsonite in the presence of Na_2CO_3 and $(NH_4)_2CO_3$, respectively, in the next paragraph the influence of treatment temperature and time on dawsonite transformation will be discussed. X-ray diffraction patterns of the samples upon treatment of Na-dawsonite in $(NH_4)_2CO_3$ and NH_4-dawsonite in Na_2CO_3, respectively, at 298 K and 24 h were silent. These observations indicate that the dawsonite structures were reactive, but under the conditions applied they will probably require longer time for crystalline structural changes. In line with this remark, Chesworth[36] reported that synthesis of dawsonite from an aluminum amalgam and 1 M Na_2CO_3 aqueous solution was possible at standard temperature and pressure conditions (298 K and 1 atm) only after 15 days. However, by increasing the treatment temperature to 323 K, major changes occurred as described before.

X-ray diffraction and transmission electron microscopy were used to monitor the structural and morphological transformations in time of Na-dawsonite upon treatment in aqueous $(NH_4)_2CO_3$ solution. In the first stages of the treatment in aqueous ammonium carbonate (5 min to 1 h), Na-dawsonite structure remained stable (Figure 2.4a), and the only morphologies observed were nanoparticles (Figure 2.5), similarly to the as-synthesized material. Between 1 h and 5 h, there is an important phase transformation, and characteristic reflections of NH_4-dawsonite become discernible. The (011) direction at 15.4º in Na-dawsonite, marked by the dashed line in the right top inset in Figure 2.4a, was shifted to 15.2º characteristic to NH_4-dawsonite (110), represented by the dot line in the bottom inset, and new reflections specific to $(NH_4)_2AlCO_3(OH)_2$ appeared. In addition, the morphology radically changes displaying acicular crystals (Figure 2.5) Longer treatment times led to dawsonite crystallization as the diffraction lines progressively get sharper and more intense.

The evolution of NH_4-dawsonite in sodium carbonate aqueous solution was investigated in a similar range of time and the results are shown in Figure 2.4b. The sample obtained after 1 h treatment displayed reflections characteristic to NH_4-dawsonite although the crystallinity decreased significantly due to the smaller particles as identified by electron microscopy.

UNIVERSITAT ROVIRA I VIRGILI
CHEMISTRY OF DAWSONITES AND APPLICATION IN CATALYSIS
Georgiana Stoica
ISBN:978-84-693-1533-0/DL:T-648-2010

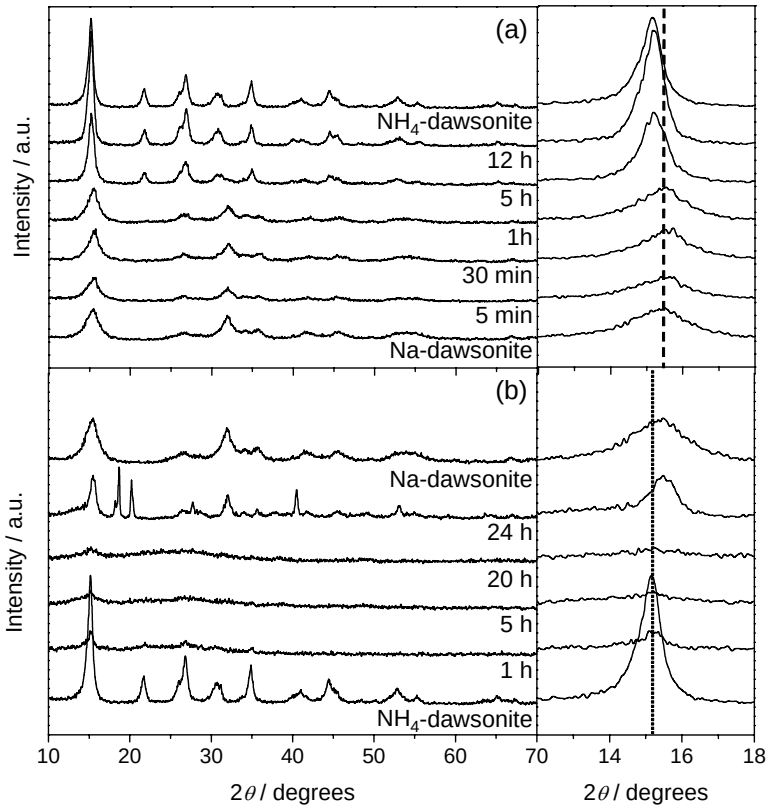

Figure 2.4. X-ray diffraction patterns of the solids resulting from treatment of (a) Na-dawsonite in 1 M $(NH_4)_2CO_3$ and (b) NH_4-dawsonite in 1 M Na_2CO_3 at 323 K and different times. Reference Na-dawsonite and NH_4-dawsonite are shown on top of each graph. Right inset: (011) direction in Na-dawsonite (top) marked by the dashed line, and (110) direction in NH_4-dawsonite (bottom) marked by the dot line.

Increasing the time up to 5 h, marked changes occurred, and the nanoparticles transformed into big plate-like crystals. Besides, the XRD pattern is almost silent. This structure was observed including at longer times, *i.e.* up to 20 h, both by XRD and electron microscopy analyses (Figure 2.5). After this time, the amorphous phase became unstable as the sample at 1 day consisted of bayerite and Na-dawsonite. We tentatively designate the amorphous compound as aluminum (oxi)hydroxide considering that various studies reported the use of Al-(oxi)hydroxides for the synthesis of dawsonite-type compounds,[31,37] and in addition, the transition amorphous Al-containing gels to bayerite was demonstrated by several authors during hydrolysis of aluminum metal. Bye *et al.*[38] determined that amorphous Al-containing gels crystallize by polymerization and condensation to a pseudo-boehmite phase, which further transformed into stable bayerite phase. The crystallographic changes after 24 h were confirmed by the morphologic observation of acicular crystals specific to Na-dawsonite, and bayerite somatoid particles, respectively (Figure 2.5).

UNIVERSITAT ROVIRA I VIRGILI
CHEMISTRY OF DAWSONITES AND APPLICATION IN CATALYSIS
Georgiana Stoica
ISBN:978-84-693-1533-0/DL:T-648-2010

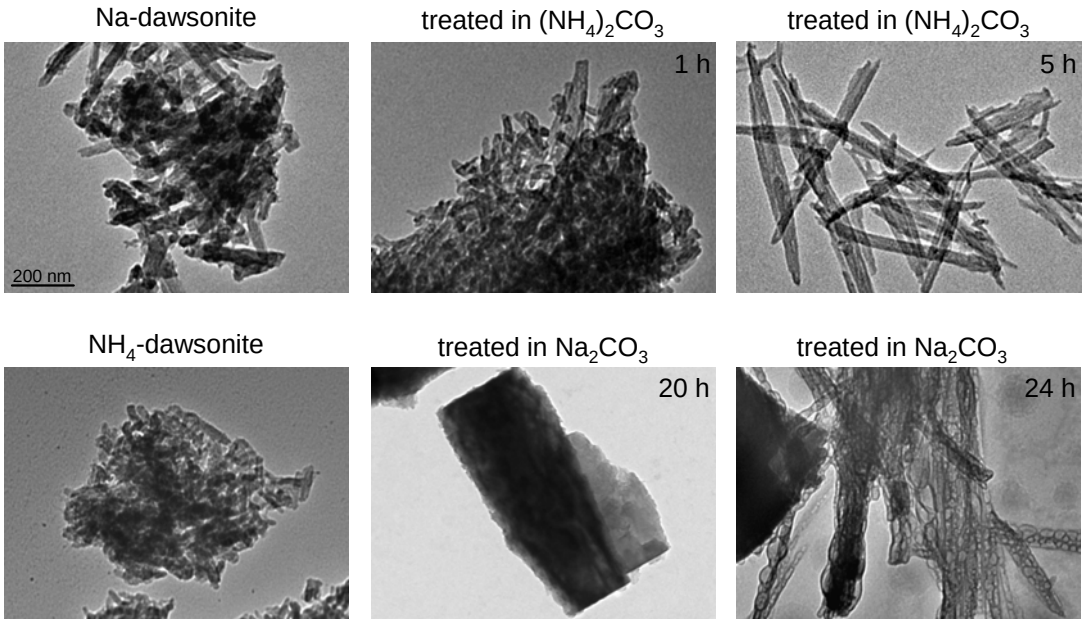

Figure 2.5. Transmission electron micrographs of selected samples at different times starting from Na-dawsonite treated in $(NH_4)_2CO_3$ (top), and NH_4-dawsonite treated in Na_2CO_3 (bottom). The same scale bar applies to all micrographs.

From the above results we preliminary concluded that NH_4-dawsonite and Na-dawsonite are interconvertible, while K-dawsonite seems to display a higher stability in aqueous carbonate media. In order to validate these observations, a second run of aqueous treatments in carbonate solutions was done. The solid NH_4-dawsonite treated in Na_2CO_3, consisting mostly of Na-dawsonite and bayerite, was immersed in $(NH_4)_2CO_3$ and the treatment led to a material displaying reflections of bayerite and NH_4-dawsonite (sample 3 in Figure 2.6a). The gibbsite phase is slightly present as indicated by the reflection present at 18.3º 2θ. Thermogravimetric analysis in Figure 2.6b confirmed there was a clear transformation of the $NaAlCO_3(OH)_2$ phase into the NH_4-counterpart since the thermal decomposition of Na-dawsonite at 586 K disappeared (sample 2) and a new transition at 467 K specific to NH_4-dawsonite is visible (sample 3). Bayerite decomposes at the same temperature as in the starting material, *i.e.* 520 K. The mass ratio dawsonite to bayerite changed from 47-53% before to 60-40% after the treatment (Figure 2.2a). These observations confirm the *reversible* transition of the two dawsonite phases one into the other, and the complete transformation of Na-dawsonite into NH_4-dawsonite, as in the case of the as-synthesized materials. Besides, as the amount of bayerite decreased, it might be possible that a small fraction of this structure transformed into NH_4-dawsonite.

UNIVERSITAT ROVIRA I VIRGILI
CHEMISTRY OF DAWSONITES AND APPLICATION IN CATALYSIS
Georgiana Stoica
ISBN:978-84-693-1533-0/DL:T-648-2010

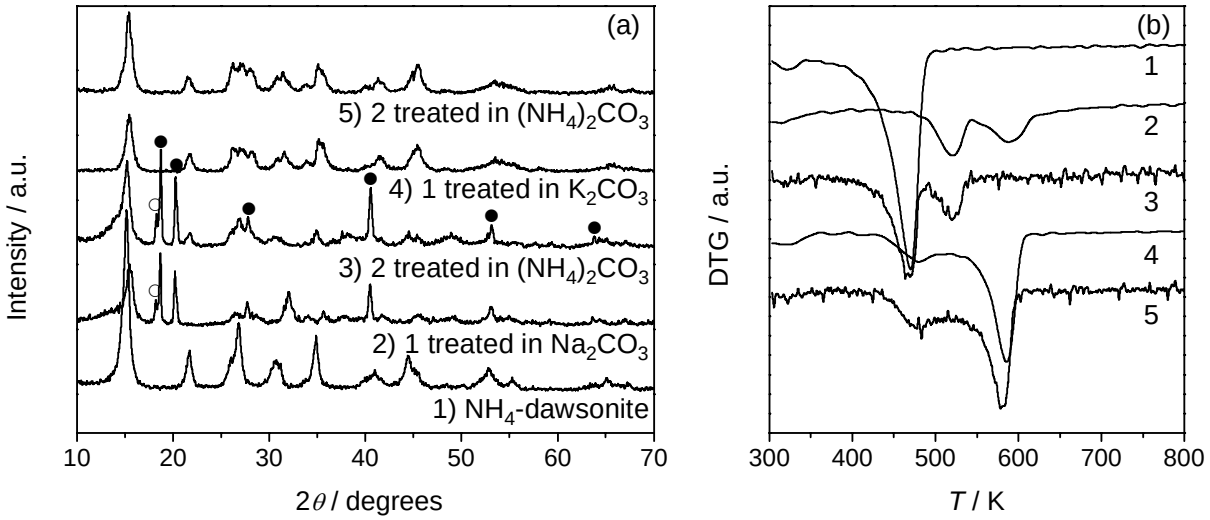

Figure 2.6. (a) X-ray diffraction patterns and (b) derivative curves of the weight loss profiles of the solids derived from treatment of the as-synthesized NH_4-dawsonite in Na_2CO_3 and K_2CO_3, respectively, and the resulting solids in $(NH_4)_2CO_3$, at 323 K for 1 day.

Treatment in aqueous $(NH_4)_2CO_3$ of NH_4-dawsonite previously immersed in K_2CO_3 (sample 4) had no influence on the material, and the same reflections characteristic to NH_4-dawsonite and K-dawsonite were visible in the sample 5 (Figure 2.6a). Thermal decomposition of this sample displayed a two-step profile with transition temperatures at 478 K and 580 K, respectively (Figure 2.6b), indicative of the presence of NH_4-dawsonite and K-dawsonite, respectively. The mass composition revealed a similar ratio between the two phases, *i.e.* 38% NH_4-dawsonite and 72% K-dawsonite, with an increase of the NH_4-dawsonite amount compared to the starting material, *i.e.* 27% NH_4-dawsonite (Figure 2.2b). This remark indicates there was a transformation of the $KAlCO_3(OH)_2$ phase but not sufficient to destabilize its structure and change it into compounds other than K-dawsonite. In other words, K-dawsonite is stable at this pH in the same way as determined with the as-synthesized material.

Additional information for the Na-dawsonite to NH_4-dawsonite phase transition was obtained from nitrogen adsorption (Figure 2.7). The N_2 uptake of Na-DW at intermediate and higher pressures is indicative of a mesoporous material. The total pore volume and specific surface area of Na-dawsonite are 0.21 $cm^3\ g^{-1}$ and 115 $m^2\ g^{-1}$, respectively. Treatment of Na-DW in ammonium carbonate aqueous solution induced radical morphological changes, and acicular crystals of NH_4-dawsonite are displayed (Figure 2.3). These transformations influenced significantly the textural properties of the resulting sample. The total uptake remarkably increased (Figure 2.7), indicating a higher surface area, *i.e.* 456 $m^2\ g^{-1}$. The

UNIVERSITAT ROVIRA I VIRGILI
CHEMISTRY OF DAWSONITES AND APPLICATION IN CATALYSIS
Georgiana Stoica
ISBN:978-84-693-1533-0/DL:T-648-2010

nitrogen uptake in various regions of relative pressure suggests the hierarchical nature of the material. Thus, the nitrogen uptake at lower relative pressures corresponds to small pores, which is in agreement with the newly generated microporosity, $V_{micro} = 0.08$ cm^3 g^{-1}, associated with the NH_4-dawsonite phase.[24] The total pore volume increased six times, up to 1.15 cm^3 g^{-1}.

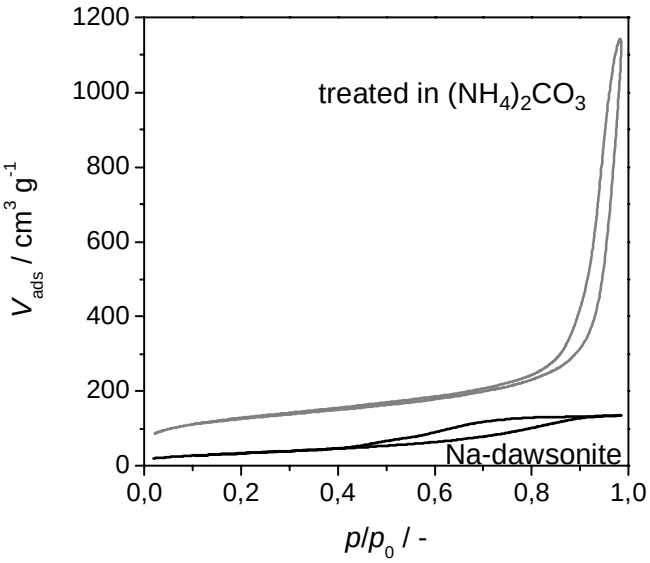

Figure 2.7. Nitrogen isotherms at 77 K of Na-dawsonite and the solid derived by treatment in 1 M $(NH_4)_2CO_3$ at 323 K for 24 h.

3.4. Mechanistic considerations

Taking into account the above observations, the following mechanism for dawsonite transformation is put forward. Dissolution of the original dawsonites leads in a first phase to precipitation of the aluminate $Al(OH)_4^-$ (eqs. 1 and 2), which further evolves into new structures depending on the treatment conditions.

$$NaAlCO_3(OH)_2 + 2H_2O = Na^+ + Al(OH)_4^- + HCO_3^- + H^+ \quad \text{(eq. 1)}$$

$$NH_4AlCO_3(OH)_2 + 2H_2O = NH_4^+ + Al(OH)_4^- + HCO_3^- + H^+ \quad \text{(eq. 2)}$$

No intermediate phase of crystalline nature was detected in the transition Na to NH_4-dawsonite. The moderate pH of the aqueous $(NH_4)_2CO_3$ solution and the excess of NH_4^+ compared to Na^+, favors the precipitation of the ionic species as NH_4-dawsonite after 5 h only (eq. 3).

$$Al(OH)_4^- + NH_4^+ + HCO_3^- + H^+ = NH_4AlCO_3(OH)_2 + 2H_2O \quad \text{(eq. 3)}$$

In contrast, an amorphous Al-(oxi)hydroxide was observed as intermediate compound in the conversion of NH_4-dawsonite to the Na-analogue and bayerite, α-$Al(OH)_3$ (eq. 4). However,

UNIVERSITAT ROVIRA I VIRGILI
CHEMISTRY OF DAWSONITES AND APPLICATION IN CATALYSIS
Georgiana Stoica
ISBN:978-84-693-1533-0/DL:T-648-2010

after 1 day of treatment, the Na-dawsonite was formed and coexists with the bayerite at this pH, in agreement with data in the literature.[1]

$2Al(OH)_4^- + Na^+ + HCO_3^- + 2H^+ = NaAlCO_3(OH)_2 + \alpha\text{-}Al(OH)_3 + 3H_2O$ (eq. 4)

In other words, the kinetics of NH_4-dawsonite formation is faster than Na-dawsonite. Several hypotheses are proposed for the transition NH_4-dawsonite to Na-dawsonite and bayerite. In a first step, the aluminate could transform concomitantly or sequentially into bayerite and Na-dawsonite, respectively (eq. 4). Secondly, the aluminate converts to boehmite (eq. 5) which becomes the precursor for bayerite and Na-dawsonite. Another possibility would be that boehmite will convert to bayerite (eq. 6) and a fraction of the latter will precipitate further as dawsonite (eq. 7).

$Al(OH)_4^- + OH^- + 2H^+ \rightarrow Al(OOH) + 3H_2O$ (eq. 5)

$Al(OOH) + 2OH^- + H^+ \rightarrow \alpha\text{-}Al(OH)_3 + H_2O$ (eq. 6)

$\alpha\text{-}Al(OH)_3 + Na^+ + HCO_3^- \rightarrow NaAlCO_3(OH)_2 + H_2O$ (eq. 7)

Additional experiments starting from pure boehmite, or bayerite and carbonate solution demonstrated that dawsonite was not formed, and the (oxi)hydroxides were stable. Only $NaAlO_2$ in $(NH_4)_2CO_3$ could crystallize as $NaAlCO_3(OH)_2$. These observations confirm the first hypothesis (eq. 4). Besides, the kinetics of Na-dawsonite and bayerite formation is similar in time. The aluminate will likely convert to bayerite since the precipitation of the latter is thermodynamically favored, *i.e.* $\Delta G = -918$ Kj mol^{-1} for boehmite *versus* $\Delta G = -1153$ Kj mol^{-1} for bayerite.[39] Crystallization from diluted aluminate solutions, at moderate pH (10-12) and temperature (313-333 K), occurs following the transformation amorphous aluminum hydroxide → pseudo-boehmite → bayerite.[40] van Straten *et al.*[30] observed the same precipitation sequence of $Al(OH)_3$ in the presence of Na^+ and K^+ at 298 K, due to super-saturation at high pH and Al concentration.

In summary, the composition of the final compounds obtained by the different dawsonites treatments is governed by the chemistry of aluminum. Dissolution of Al in the aqueous medium leads to the formation of distinctive Al-ionic species depending on the pH,[28] which further evolve into dawsonite and/or (oxi)hydroxides. This behavior was reported for dawsonite-derived aluminas which transformed into dawsonite uniquely in $(NH_4)_2CO_3$ solution, whereas other media originated various forms of aluminum hydroxides and (oxi)hydroxides.[24,32] However, the stability of dawsonites in carbonate solutions is higher when compared to the corresponding amorphous alumina due to the lower reactivity of the former materials induced by the presence of crystalline structures.

4. Conclusions

The stability of NH_4, Na, and K-dawsonites in different aqueous media with pH values in the range 2-14 was investigated. Strong acids (pH 2) or bases (pH 14) induced the complete dissolution of the materials. In water (pH 7), dawsonites evolved into boehmite (NH_4-form) and bayerite (Na and K-forms). The most interesting solid transformations occurred in the presence of ammonium, potassium, and sodium carbonates. NH_4-dawsonite was converted into Na-dawsonite and K-dawsonite in Na_2CO_3 and K_2CO_3 (pH 12), respectively. Na-dawsonite transformed into NH_4-dawsonite in $(NH_4)_2CO_3$ (pH 10), while treatment in K_2CO_3 led to bayerite. K-dawsonite was stable in $(NH_4)_2CO_3$, but changed to bayerite in Na_2CO_3 solution. The NH_4 and Na-dawsonite can be successively interconverted in the appropriate carbonate solution at mild temperature (323 K), and treatment at ambient conditions led to amorphous materials. The kinetics of Na-dawsonite is faster than the NH_4-analogue; that is, the transformation Na to NH_4-dawsonite takes place between 1-5 h, while NH_4-dawsonite needs between 20-24 h to convert into Na-dawsonite. Transformation of dawsonites into other dawsonite phase or (oxi)hydroxide composition follows a dissolution-precipitation mechanism. Dissolved aluminium precipitates as aluminate species, which further crystallizes as dawsonite isomorphs or Al-(oxi)hydroxides. The overall process is directed by the pH of the media. Besides the structural reorganization, a significant morphological refinement and hierarchical porosity were induced by the dissolution-precipitation process with formation of the characteristic acicular particles of the mineral dawsonite.

Acknowledgments

Francesc Guirado is thanked for technical assistance for the X-ray analyses.

References

[1] P. Bénézeth, D.A. Palmer, L.M. Anovitz, J. Horita, *Geochim. Cosmochim. Acta* **2007**, 71, 4438.

[2] A.J. Frueh, J.P. Golightly, *Can. Mineral.* **1967**, 9, 51.

[3] E. Corazza, C. Sabelli, S. Vannucci, *Neues Jahrb. Mineral. Monatsh.* **1977**, 9, 381.

[4] C.J. Serna, J.V. Garcia-Ramos, M.J. Peña, *Spectrochim. Acta* **1985**, 41A, 697.

[5] A.A. Ali, M.A. Hasan, M.I. Zaki, *Chem. Mater.* **2005**, 17, 6797.

[6] M.S. Yalfani, M. Santiago, J. Pérez-Ramírez, *J. Mater. Chem.* **2007**, 17, 1222.

[7] T. Iga, S. Kato, *J. Ceram. Soc. Jpn.* **1978**, 86, 509.

UNIVERSITAT ROVIRA I VIRGILI
CHEMISTRY OF DAWSONITES AND APPLICATION IN CATALYSIS
Georgiana Stoica
ISBN:978-84-693-1533-0/DL:T-648-2010

[8] I. Pitsch, W. Gessner, A. Brückner, H. Mehner, S. Moehmel, D.-C. Uecker, M.-M. Pohl, *J. Mater. Chem.* **2001**, 11, 2498.

[9] M. Santiago, M.S. Yalfani, J. Pérez-Ramírez, *J. Mater. Chem.* **2006**, 16, 2886.

[10] W.D. Gunter, E.H. Perkins, T.J. McCann, *Energy Conv. Manag.* **1993**, 34, 941.

[11] H. Hellevang, P. Aagaard, E.O. Oelkers, B. Kvamme, *Environ. Sci. Technol.* **2005**, 39, 8281.

[12] B. Zerai, B.Z. Saylor, G. Matisoff, *Appl. Geochem.* **2006**, 21, 223.

[13] B.N. Ryzhenko, *Geochem. Int.* **2004**, 44, 835.

[14] J.P. Kaszuba, D.R. Janecky, M.G. Snow, *Chem. Geol.* **2005**, 217, 277.

[15] S.J.T. Hangx, C.J. Spiers, *Chem. Geol.* **2009**, 265, 88.

[16] G.D. Saldi, G. Jordan, J. Schott, E.H. Oelkers, *Geochim. Cosmochim. Acta* **2009**, 73, 5646.

[17] L. Marini, *Developments in Geochemistry*, **2007**, Vol. 11, Elsevier, Amsterdam, p. 100.

[18] T. Xu, J.A. Apps, K. Pruess, *Appl. Geochem.* **2004**, 19, 917.

[19] L. Fernández-Carrasco, F. Puertas, M.T. Blanco-Varela, T. Vázquez, J. Rius, *Cem. Concr. Res.* **2005**, 35, 641.

[20] S. Brunauer, P.P. Emmett, E. Teller, *J. Am. Chem. Soc.* **1938**, 60, 309.

[21] B.C. Lippens, J.H. de Boer, *J. Catal.* **1965**, 4, 319.

[22] G. Stoica, S. Abelló, J. Pérez-Ramírez, *Appl. Catal. A-Gen.* **2009**, 365, 252.

[23] M.J. Hernandez, M.A. Ulibarri, J. Cornejo, M.J. Peña, C.J. Serna, *Thermochim. Acta* **1985**, 94, 257.

[24] G. Stoica, J. Pérez-Ramírez, *Chem. Mater.* **2007**, 19, 4785.

[25] J.W. Anthony, R.A. Bideaux, K.W. Bladh, M.C. Nichols, *Handbook of Mineralogy*, **2003**, Vol. V, Mineral Data Publishing: Tucson, AZ, p. 176.

[26] C. Palache, H. Berman, C. Frondel, *The System of Mineralogy of James Dwight Dana and Edward Salisbury Dana*, **1951**, 7th ed., Vol. II, John Wiley and Sons, Inc., New York, p. 276.

[27] P. Euzen, P. Raybaud, X. Krokidis, H. Toulhoat, J.-L. Le Loarer, J.-P. Jolivet, C. Froidefond, in *Handbook of Porous Solids*, **2002**, Eds. F. Schüth, K.S.W. Sing, J. Weitkamp, Part 4, Wiley-VCH Verlag, p. 1592.

[28] H. Tamura, J. Chiba, M. Ito, T. Takeda, S. Kikkawa, Y. Mawatari, M. Tabata, *J. Colloid Interface Sci.* **2006**, 300, 648.

[29] I. Gaus, M. Azarounal, I. Czernichowski-Lauriol, *Chem. Geol.* **2005**, 217, 319.

UNIVERSITAT ROVIRA I VIRGILI
CHEMISTRY OF DAWSONITES AND APPLICATION IN CATALYSIS
Georgiana Stoica
ISBN:978-84-693-1533-0/DL:T-648-2010

[30] H.A. van Straten, B.T.W. Holtkamp, P.L. de Bruyn, *J. Colloid Interface Sci.* **1984**, 98, 342.

[31] X. Zhang, Z. Wen, Z. Gu, X. Xu, Z. Lin, *J. Solid State Chem.* **2004**, 177, 849.

[32] G. Stoica, J.C. Groen, S. Abelló, R. Manchanda, J. Pérez-Ramírez, *Chem. Mater.* **2008**, 20, 3973.

[33] X. Zhang, Z. Wen, Z. Gu, X. Xu, Z. Li, *Thermochim. Acta* **2005**, 433, 116.

[34] J.T. Kloprogge, L.V. Duong, B.J. Wood, R.L. Frost, *J. Colloid Interface Sci.* **2006**, 296, 572.

[35] S. Music, D. Dragcevic, S. Popovic, N. Vdovic, *Mater. Chem. Phys.* **1999**, 59, 12.

[36] W. Chesworth, *Clay Clay Min.* **1971**, 19, 337.

[37] M. Giannos, M. Hoang, T.W. Turney, *Chem. Lett.* **1998**, 793.

[38] G.C. Bye, T.G. Robinson, *Colloid Polym. Sci.* **1964**, 198, 53.

[39] B.S. Hemingway, R.A. Robie, J.A. Kittrick, *Geochim. Cosmochim. Acta* **1978**, 42, 1533.

[40] H. Li, J. Addai-Mensah, J.C. Thomas, A.R. Gerson, *J. Cryst. Growth* **2005**, 279, 508.

UNIVERSITAT ROVIRA I VIRGILI
CHEMISTRY OF DAWSONITES AND APPLICATION IN CATALYSIS
Georgiana Stoica
ISBN:978-84-693-1533-0/DL:T-648-2010

UNIVERSITAT ROVIRA I VIRGILI
CHEMISTRY OF DAWSONITES AND APPLICATION IN CATALYSIS
Georgiana Stoica
ISBN:978-84-693-1533-0/DL:T-648-2010

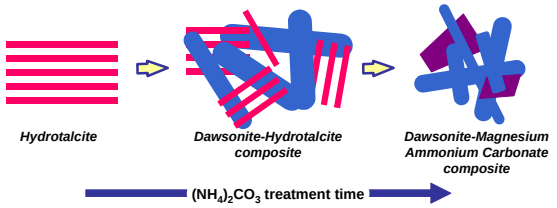

Chapter 3

Reactivity of Mg-Al hydrotalcites in solid and delaminated forms in ammonium carbonate solutions

Treatment of Mg-Al hydrotalcites (LDHs, layered double hydroxides) in aqueous $(NH_4)_2CO_3$ at 298 K leads to composites of dawsonite, hydrotalcite, and magnesium ammonium carbonate. The kinetics and mechanism of this transformation, ultimately determining the relative amounts of these components in the composite, depend on the treatment time (from 1 h to 9 days), the Mg/Al ratio in the hydrotalcite (2-4), and on the starting layered double hydroxide (solid or delaminated form). The progressive transformation of hydrotalcite towards crystalline dawsonite and magnesium ammonium carbonate phases occurs *via* a dissolution-precipitation mechanism. A gradual decrease of the Mg/Al ratio in the resulting solids was observed in time due to magnesium leaching in the reacting medium. Dawsonite-hydrotalcite composite formation is favored at high aluminum contents in the starting hydrotalcite, while the formation of magnesium ammonium carbonate is favored at high Mg/Al ratios. The synthetic strategy comprising hydrotalcite delamination in formamide prior to aqueous $(NH_4)_2CO_3$ treatment is more reactive towards composite formation than starting from the bulk solid hydrotalcite.

UNIVERSITAT ROVIRA I VIRGILI
CHEMISTRY OF DAWSONITES AND APPLICATION IN CATALYSIS
Georgiana Stoica
ISBN:978-84-693-1533-0/DL:T-648-2010

1. Introduction

Hydrotalcite-like compounds (HTlcs) or layered double hydroxides (LDHs) have a broad spectrum of applications, as catalyst precursor or support, in separation and membrane technologies, filtration, scavenging and controlled release of anions, *etc*. LDHs consist of layers of positively charged nanosheets with brucite-type structure neutralized by anions in the interlayer space, where water molecules are also present.[1]

In addition to the direct synthesis by coprecipitation from salt precursors, they have been subject of many post-synthesis transformations involving their well-known memory effect property and ion-exchange capacity.[2,3,4-7] That is, by recovering of the layered structure through calcination of the starting hydrotalcite and subsequent contact of the derived mixed oxide with solutions containing many different anions, or by direct exchange of the anions located in the interlayer space by others, an impressive variety of hydrotalcite-derived compounds have been synthesized.

Focusing on the layered nature of these compounds, LDHs act like the host structure for polymers, bio-active compounds, pillaring agents, *etc.*, leading to nanocomposite materials.[7,8] The use of intercalating agents by ion-exchange, like sodium dodecyl sulfate or alkyl carboxylates,[7] followed by exfoliation induces the separation of the layers into unilamellar positive nanosheets (colloids).[9-11] Polar[9,12-16] or nonpolar[17,18] solvents aided by heat,[18] ultrasounds,[18] or electric current[19] were also applied for delamination of HTlcs. Hibino and Jones[12] introduced the exfoliation of intercalated LDHs in formamide without the need of heat or reflux treatments, based on a two-stage mechanism: rapid swelling due to the very high ability of $HCONH_2$ for hydrogen bonding, followed by slow exfoliation.[20-22]

The subsequent restacking of the hydrotalcite nanosheets enables to fabricate nanostructured materials, offering an elegant alternative to the traditional intercalation of anionic species in their interlayer space by ion-exchange.[23] The restacking of colloidal LDHs, leading to the recovery of the native hydrotalcite structure, has been practiced by physical (solvent evaporation,[24,25] freeze-drying[8]) or chemical methods (treatment in aqueous solutions of Na_2CO_3[26] or NaCl,[8,10] and ethanol[26]). Grounded on the delamination-restacking concept, more sophisticated materials were recently reported. Venugopal *et al.*[25] prepared a randomly costacked Mg-Al/Co-Al LDH compound starting from colloidal dispersions of the individual hydrotalcites. Li *et al.*[27] applied a layer-by-layer assembly to obtain interstratified thin films of positively charged Mg-Al LDH nanosheets and negatively charged oxide nanosheets ($Ti_{0.91}O_2$ and $Ca_2Nb_3O_{10}$). In the cases reported so far, the fabrication of multicomponent composites requires starting from all individual components in delaminated form.

UNIVERSITAT ROVIRA I VIRGILI
CHEMISTRY OF DAWSONITES AND APPLICATION IN CATALYSIS
Georgiana Stoica
ISBN:978-84-693-1533-0/DL:T-648-2010

Rather than the typical delamination and restacking of the hydrotalcite phase, we endeavor the transformation of the LDH into other structured compounds, as well as by direct reaction of the starting LDH. Herein, the reactivity of Mg-Al hydrotalcites in solid or colloidal (delaminated) forms in aqueous ammonium carbonate at ambient conditions was investigated. Delamination was carried out by treatment of the as-synthesized hydrotalcites in formamide. Composite materials consisting of mixtures of hydrotalcite, dawsonite, and magnesium ammonium carbonate were obtained. Based on detailed characterization studies, it is concluded that the composition of the resulting composite is determined by the Mg/Al ratio of the starting hydrotalcite and the treatment time. The terms 'delamination' and 'exfoliation' are used indistinctly along the chapter.

2. Experimental

2.1. Materials and treatments

Synthesis of hydrotalcites. Mg-Al hydrotalcites (HT*x*) with molar Mg/Al ratios (*x*) of 2, 3, and 4 were synthesized by continuous coprecipitation using the ILDP method.[28,29] Briefly, aqueous solutions of $Mg(NO_3)_2 \cdot 6H_2O$ ($0.25 \cdot x$ M) and $Al(NO_3)_3 \cdot 9H_2O$ (0.25 M) and the precipitating agent ($NaOH+Na_2CO_3$, 1 M of each) were pumped into a 6 cm^3-reactor to a high-shear homogenizer rotating at 13,500 rpm. The pH of the slurry was measured and controlled by an in-line probe directly at the outlet of the precipitation chamber. The syntheses were carried out at pH 10 with an average residence time in the reactor of 18 s. The precipitate slurries were aged at 298 K for 12 h under mechanical stirring (500 rpm), followed by filtration, washing, and drying at 353 K for 12 h.

As detailed below, the synthetic strategy for the formation of composites followed two different experimental approaches, the first one by subjecting the hydrotalcite to delamination and subsequently treated in $(NH_4)_2CO_3$ solutions, and the second one, by treating directly the as-synthesized hydrotalcites with the same basic solution.

Delamination. A dispersion of the as-synthesized hydrotalcite in pure formamide (purity 99.5%) was prepared at a concentration of 5 g l^{-1}. In order to accelerate the exfoliation process, the suspension was ultrasonicated six times for a period of 30 min with an interval of 60 min between treatments. Then, the sample was left to stand for 12 h. The system remained turbid and was centrifuged at 4400 rpm for 30 min and two phases were observed: a colloidal suspension and the sediment. The supernatant colloidal dispersion, referred to as HTD*x* was collected and used for further treatment.

Treatment in $(NH_4)_2CO_3$. The colloidal suspension containing the delaminated

UNIVERSITAT ROVIRA I VIRGILI
CHEMISTRY OF DAWSONITES AND APPLICATION IN CATALYSIS
Georgiana Stoica
ISBN:978-84-693-1533-0/DL:T-648-2010

hydrotalcite was treated in aqueous 1 M $(NH_4)_2CO_3$ at room temperature in a 1:3 volume ratio. After stirring for 1 h, the mixture was left to rest at ambient conditions for periods of time raging from 1 hour to 9 days. The resulting solid was centrifuged at 4400 rpm for 30 min and redispersed in ethanol or water and centrifuged again at 4400 rpm for 30 min each. The washing procedure was repeated three times and the final solids were dried at 333 K for 12 h. The as-synthesized hydrotalcites in solid form were also treated in 1 M aqueous solution of $(NH_4)_2CO_3$ at room temperature using the same solid-to-liquid ratio as in the treatment of the colloid, stirred for 1 h, and let to stand for 1-3 days. The resulting solids were filtered, washed with deionized water, and dried at 333 K for 12 h.

Along the chapter, samples were designated by the codes HT*x*-*t* or R*x*-*t*, where HT refers to the protocol initiated from the solid hydrotalcite, R identifies the solids attained *via* the colloidal solutions, *x* is the Mg/Al ratio of the starting hydrotalcite, and *t* is the treatment time expressed in hours or days.

Reference samples. Reference dawsonite (DW) and magnesium ammonium carbonate (MAC) were synthesized in order to support assignments during transformation of delaminated hydrotalcites. DW ($NH_4AlCO_3(OH)_2$) was prepared at constant pH by precipitation of $Al(NO_3)_3{\cdot}9H_2O$ (1.1 M) and $(NH_4)_2CO_3$ (2 M) aqueous solutions using the ILDP method described above. The slurry was then filtered, washed with water, and dried at 333 K for 12 h. Calcination of the resulting solid at 723 K for 2 h, and further treatment in 1 M $(NH_4)_2CO_3$ were applied to obtain reformed dawsonite.[30] The precipitate was then filtered, washed with water, and dried at 333 K for 12 h. MAC ($(NH_4)_2Mg(CO_3)_2{\cdot}4H_2O$) was prepared by ILDP, adapting the recipe by Erdös *et al.*[31] An aqueous solution of $MgSO_4$ (0.5 M) was precipitated with an excess of 5 M $(NH_4)_2CO_3$ aqueous solution at pH 8.5. The precipitate was washed with methanol and dried at 333 K for 12 h.

2.2. Techniques

Magnesium and aluminum in the as-synthesized samples and some of the filtrates upon $(NH_4)_2CO_3$ treatment were determined by inductive coupled plasma-optical emission spectroscopy (ICP-OES) (Perkin-Elmer Optima 3200RL (radial)). Powder X-ray diffraction (XRD) patterns were measured in a Bruker AXS D8 Advance diffractometer equipped with a Cu tube, a Ge(111) incident beam monochromator, and a Vantec-1 PSD. Data were recorded in the range of 5-70º 2θ with an angular step size of 0.016º and a counting time of 6 s per step. Fourier transform infrared (FTIR) spectroscopy was carried out in a Bruker Optics Tensor 27 spectrometer equipped with a Golden Gate Diamond

UNIVERSITAT ROVIRA I VIRGILI
CHEMISTRY OF DAWSONITES AND APPLICATION IN CATALYSIS
Georgiana Stoica
ISBN:978-84-693-1533-0/DL:T-648-2010

ATR unit. Spectra were collected in the range 650-4000 cm^{-1} by co-addition of 32 scans at a nominal resolution of 4 cm^{-1}, taking the spectrum of the empty cell as the background. Thermogravimetric analysis (TGA) was carried out in a Mettler Toledo TGA/SDTA851e microbalance. Analyses were performed in dry air flow of 50 cm^3 min^{-1} from 298 to 1173 K using a heating rate of 5 K min^{-1}. Transmission electron microscopy (TEM) was carried out in a JEOL JEM-1011 microscope operated at 100 kV and equipped with a SIS Megaview III CCD camera. A few droplets of the sample suspended in ethanol were placed on a carbon-coated copper grid followed by evaporation at ambient conditions. Nitrogen isotherms at 77 K were measured on a Quantachrome Autosorb-1MP analyzer. Prior to analysis, the samples were degassed in vacuum at 373 K for 16 h. The BET method[32] was applied to calculate the total surface area, and the *t*-plot method[33] was used to discriminate between micro- and mesoporosity.

3. Results and discussion

3.1. Parent samples and exfoliation

The chemical composition of the as-synthesized hydrotalcites measured by ICP-OES indicated that the Mg/Al molar ratio in the solids were 1.8, 2.9, and 3.3, *i.e.* close to the nominal ratio in the solutions. X-ray diffraction confirmed that hydrotalcite (JCPDS 22-700) was the only crystalline phase in the precipitates. The pattern of one of the samples is illustrated in Figure 3.1. The materials featured the platelet-like morphology characteristic of these layered materials (Figure 3.2a). Thermogravimetric analysis of the as-synthesized hydrotalcites, represented by the open circles in Figure 3.3, shows the two-step weight loss profiles with respect to the Mg/Al ratio. The first transition, attributed to the loss of interlayer water, amounted *ca.* 17%, and is shifted to lower temperatures as the value of *x* decreases in the formula $[M^{2+}_{1-x}M^{3+}_{x}(OH)_2]^{x+}\ A^{n-}_{x/n})\cdot mH_2O$, *i.e.* at higher Mg/Al ratios.[2] The second transition, due to dehydroxylation of the brucite-like sheets and decarbonation, amounted 24-26%. The transition temperatures can be estimated from the derivative of the weight loss: 465 K and 665 K for HT2, 457 K and 668 K for HT3, and 403 K and 666 K for HT4, respectively (Figure 1 in Annex 1).

Exfoliation of the hydrotalcites in formamide at 298 K for 8 h led to translucent colloidal dispersions, which remain stable for more than 1 year. The amount of exfoliated hydrotalcite after delamination of 1 g of powder in 200 cm^3 of formamide represented a 54% of the initial amount of sample. The corresponding diffraction pattern, obtained by placing a drop of the colloidal suspension in the XRD holder, evidenced the disappearance

UNIVERSITAT ROVIRA I VIRGILI
CHEMISTRY OF DAWSONITES AND APPLICATION IN CATALYSIS
Georgiana Stoica
ISBN:978-84-693-1533-0/DL:T-648-2010

of the hydrotalcite reflections (pattern HTD in Figure 3.1), proving that the delamination of the LDH into positively charged brucite-like nanosheets was accomplished.[34] The broad reflection at 25º 2θ is due to formamide.[24]

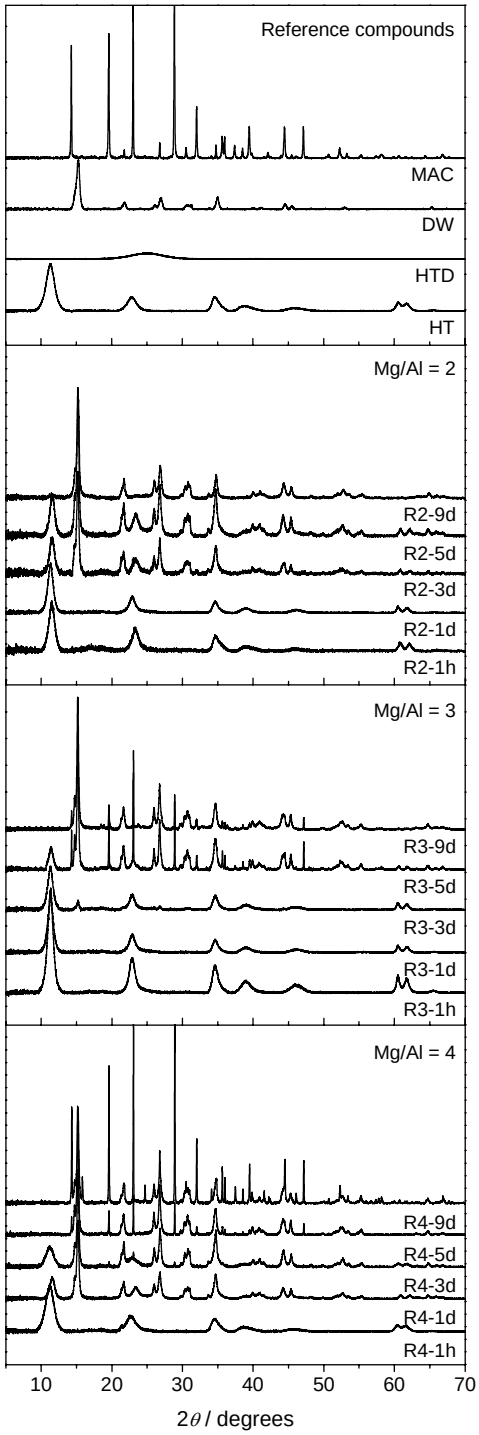

Figure 3.1. X-ray diffraction patterns of the solids resulting from treatment of delaminated Mg-Al hydrotalcites in 1 M $(NH_4)_2CO_3$ at 298 K and different times. The diffraction patterns of hydrotalcite (HT), delaminated hydrotalcite (HTD), dawsonite (DW), and magnesium ammonium carbonate (MAC) compounds are shown in the top graph (reference compounds).

UNIVERSITAT ROVIRA I VIRGILI
CHEMISTRY OF DAWSONITES AND APPLICATION IN CATALYSIS
Georgiana Stoica
ISBN:978-84-693-1533-0/DL:T-648-2010

3.2. Hydrotalcite transformation

Figure 3.1 shows the XRD patterns of the solids resulting from treatment of the colloidal hydrotalcite dispersions in 1 M $(NH_4)_2CO_3$ (pH 10) at 298 K and different times. Independently of the Mg/Al ratio, the hydrotalcite structure was recovered after 1 h due to restacking of the brucite-like layers (R*x*-1h). All specimens showed the same platelet morphology as the parent hydrotalcite. The XRD and TEM characterization techniques support the reported reversibility of the delamination-restacking process in hydrotalcites. The restacking of hydrotalcites is done typically in aqueous solutions of Na_2CO_3,[26] NaCl,[8,10] or ethanol[26] at ambient conditions for several days. In this chapter, we report for the first time the use of ammonium carbonate as restacking medium for hydrotalcites. The XRD patterns of the solids treated for 1 hour and 1 day were very similar for the samples derived from hydrotalcites with Mg/Al = 2 and 3, respectively. However, treatment of the colloid derived from the sample with Mg/Al = 4 in $(NH_4)_2CO_3$ for 1 day induced marked changes in the X-ray diffraction, unequivocally indicating the presence of a composite comprising both dawsonite (JCPDS 42-250) and hydrotalcite phases. Pure dawsonite (DW) was used as reference material. The morphology markedly differed from the starting materials, the micrograph displaying a high density of very well dispersed dawsonite acicular crystals[35] (Figure 3.2b), coexisting with the hydrotalcite whiskers in the composite. In contrast, physical mixtures of separately as-synthesized hydrotalcite and the reference dawsonite evidenced segregation of both phases (TEM in Annex 1, Figure 2).

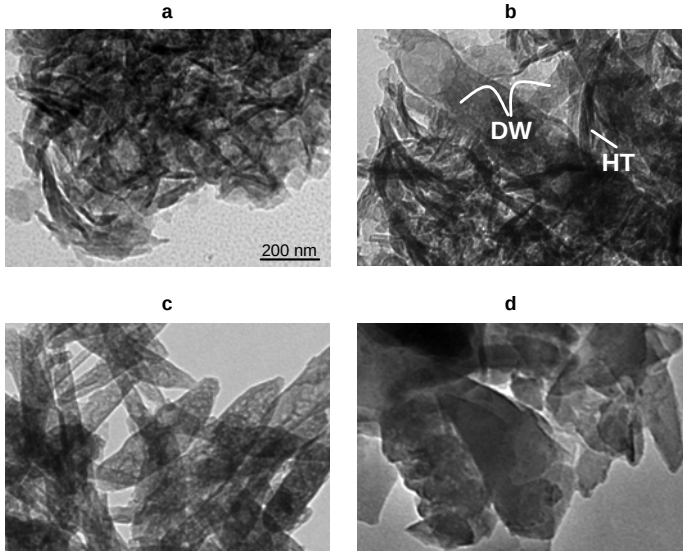

Figure 3.2. Transmission electron micrographs of (a) starting hydrotalcite (sample HT2), (b) dawsonite-hydrotalcite composite (sample R2-5d), (c) pure dawsonite (sample R2-9d), (d) dawsonite-magnesium ammonium carbonate composite (sample R3-9d). The same scale bar applies to all the micrographs.

UNIVERSITAT ROVIRA I VIRGILI
CHEMISTRY OF DAWSONITES AND APPLICATION IN CATALYSIS
Georgiana Stoica
ISBN:978-84-693-1533-0/DL:T-648-2010

In agreement with XRD, the thermogravimetric analysis of the samples derived from HT2 and HT3 after 1 day displayed the typical two-step behavior during hydrotalcite decomposition,[34] with transitions at 425-460 K and 650 K, and a total weight loss of *ca.* 45% (Figure 3.3). Distinctively, the total weight loss upon thermal decomposition of R4-1d increased to 54% as compared to 45% in R4-1h, due to the progressive crystallization of dawsonite. Sample R4-1d displayed a two-step weight loss profile with a significant decomposition temperature centered at *ca.* 450 K,[30,35] matching the decomposition temperature of NH_4-dawsonite (dashed line in Figure 1 in Annex 1). Concomitantly, the weight loss of the second transition (> 450 K), which is exclusively attributed to the HT phase, decreased due to the gradual conversion of hydrotalcite into dawsonite. We have quantified the relative amount of both phases from thermogravimetry (Figure 3.4) as detailed in Table 1 and Figure 3 in the Annex 1. Dawsonite was formed at the expense of hydrotalcite, and the former phase amounted 53% in the R4-1d sample.

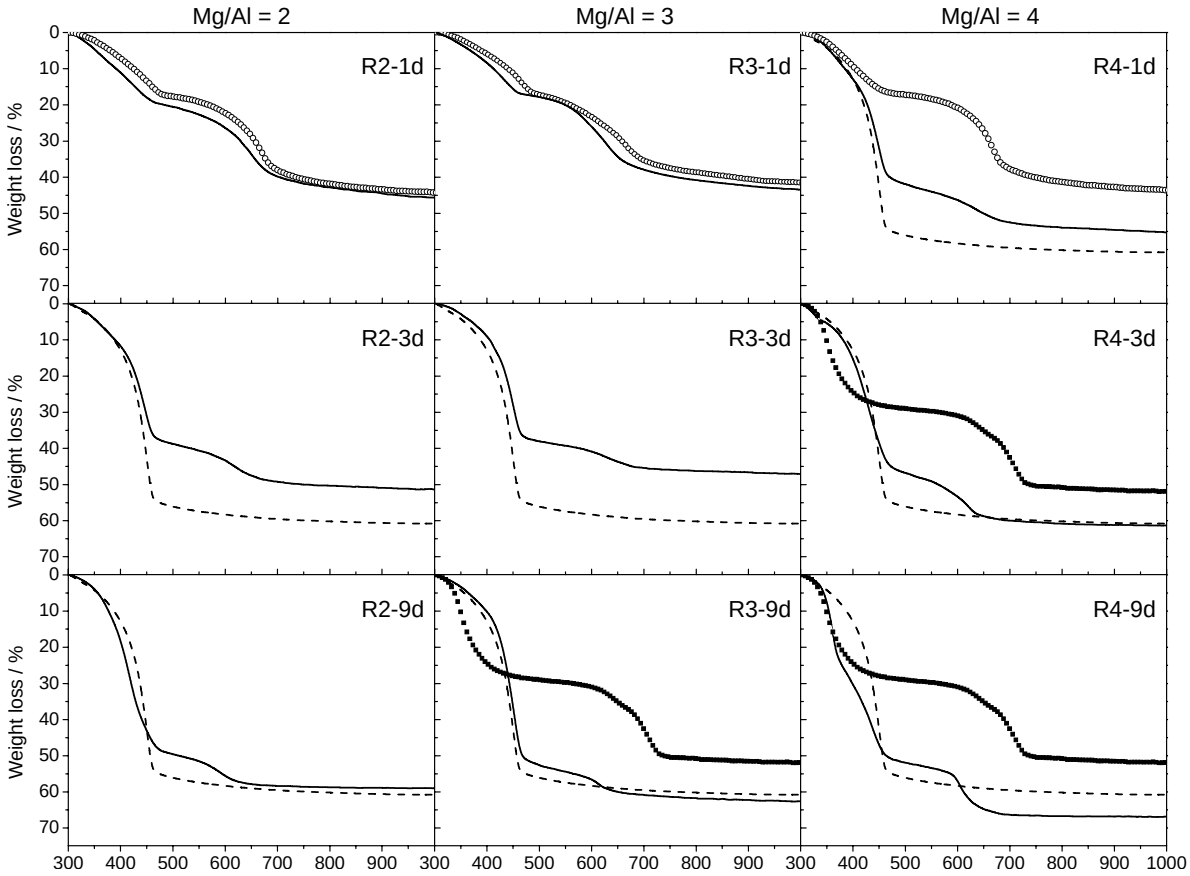

Figure 3.3. Thermogravimetric profiles of the solids resulting from treatment of delaminated hydrotalcites in 1 M $(NH_4)_2CO_3$ at 298 K and three representative times (1, 3, and 9 days). Pure compounds: (○) as-synthesized hydrotalcites, (**▪▪▪**) reference dawsonite, and (■) reference magnesium ammonium carbonate.

UNIVERSITAT ROVIRA I VIRGILI
CHEMISTRY OF DAWSONITES AND APPLICATION IN CATALYSIS
Georgiana Stoica
ISBN:978-84-693-1533-0/DL:T-648-2010

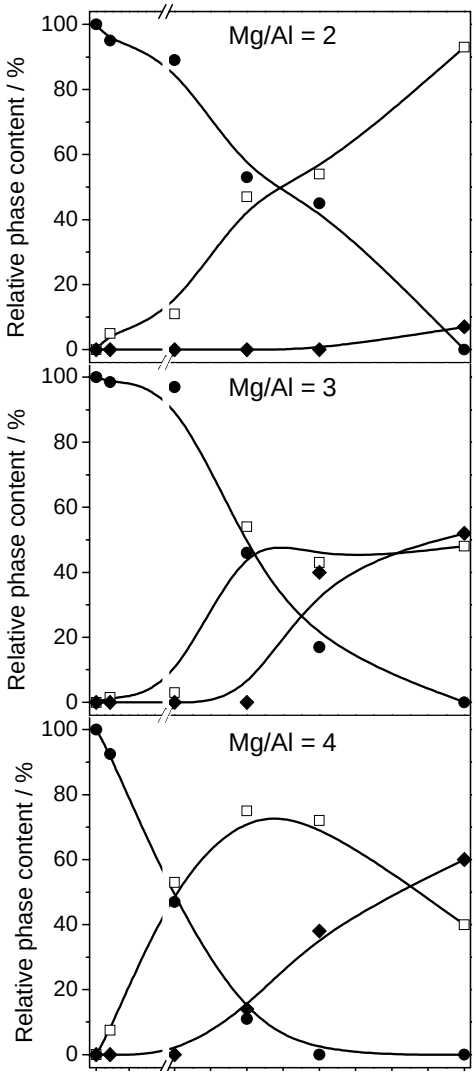

Figure 3.4. Evolution of the crystalline phases in the composites upon restacking of the delaminated hydrotalcites with different Mg/Al ratios: (●) hydrotalcite, (□) dawsonite, and (◆) magnesium ammonium carbonate. The relative amount of phases was determined by thermogravimetry as explained in the Annex 1.

Characterization by infrared spectroscopy (Figure 3.5) substantiated X-ray diffraction in the time scale at which phases appeared in the samples. For the sake of conciseness, we illustrate the spectra for the R2-*t* system as equivalent observations were obtained for the other two Mg/Al ratios. The infrared spectrum of R2-1h featured characteristic bands of hydrotalcite[34,36]: 3480 cm^{-1} (OH stretching), 3050 cm^{-1} (bridging mode of carbonate and water in the interlayer), 1370 cm^{-1} (ν_3 mode of the carbonate, antisymmetric stretching), 855 cm^{-1} (ν_2 mode of the carbonate, out-of-plane deformation), and 655 cm^{-1} (Mg-related OH translation modes). The vibration at 1640 cm^{-1} is due to the bending mode of water. The appearance of the ν_3 mode of the carbonate at 1370 cm^{-1} (being 1415 cm^{-1} in the

UNIVERSITAT ROVIRA I VIRGILI
CHEMISTRY OF DAWSONITES AND APPLICATION IN CATALYSIS
Georgiana Stoica
ISBN:978-84-693-1533-0/DL:T-648-2010

'free' carbonate anion) is related to its reorganization in the interlayer space due to electrostatic interaction with the nearby brucite-like layers.[37] Due to the loss of symmetry of the carbonate ion (from D_{3h} to C_{2v}), the ν_1 mode of the carbonate (symmetric stretching) became activated, thus leading to the shoulder at 1045 cm^{-1}.[37] This vibration mode is inactive when the carbonate ion retains its full symmetry.[38] The infrared spectrum of the sample after 1 day revealed new bands characteristic of NH_4-dawsonite, although the relatively small amount of this phase was not discernible by XRD. The most relevant ones are marked by solid dots in Figure 3.5 and belong to OH^- (δ_{OH} at 985 cm^{-1}), NH_4^+ (ν_{NH} at 3180 cm^{-1}), and CO_3^{2-} (ν_3 at 1560 and 1450 cm^{-1}, ν_2 at 855 cm^{-1}, and ν_1 at 1105 cm^{-1}).[30,39] For comparison, the spectrum of a pure dawsonite was also added, thus confirming the presence of dawsonite in the composite.

As expected, treatment in ammonium carbonate for longer times (3 days) led to the presence of the characteristic dawsonite reflections with different intensities in all the samples, clearly indicating the formation of the dawsonite-hydrotalcite composite (Figure 3.1). Besides, sample R4-3d contained low-intensity reflections assigned to magnesium ammonium carbonate hydrated (MAC, $(NH_4)_2Mg(CO_3)_2{\cdot}4H_2O$, JCPDS 33-66), as it can be seen by comparison with the reference material in Figure 3.1.

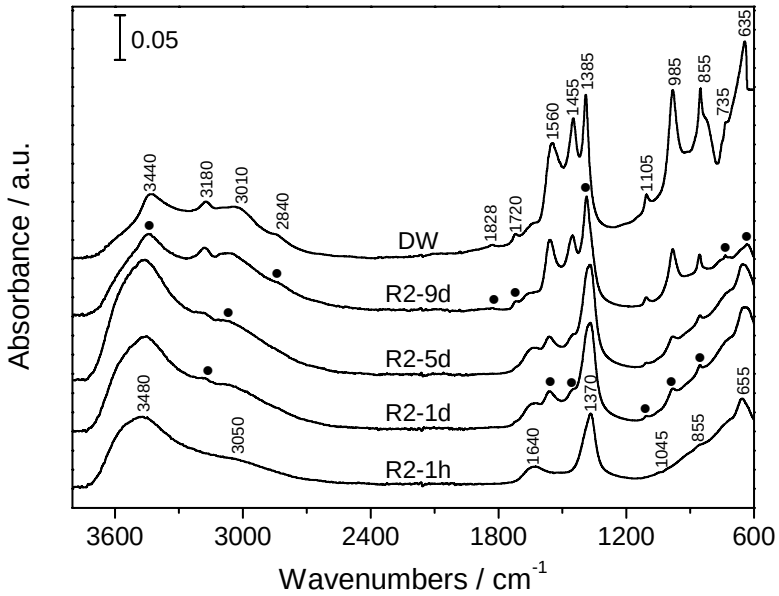

Figure 3.5. Infrared spectra of solids resulting from treatment of delaminated hydrotalcite (Mg/Al = 2) in 1 M $(NH_4)_2CO_3$ at 298 K. Solid dots indicate characteristic absorptions of dawsonite appearing in the hydrotalcite-dawsonite composite at different times (assignments detailed in text). The spectrum of the reference dawsonite sample is also shown.

Extension of the treatment for 5 days led to the progressive hydrotalcite disappearance in R2-5d and R3-5d, respectively, which was complete in R4-5d. The higher the Mg/Al ratio in the parent material, the higher the amount of MAC formed. The reflections of both dawsonite and magnesium ammonium carbonate hydrate phases became more intense in R*x*-9d as a consequence of the enhanced crystallization at longer treatment times. These changes were also observed by transmission electron microscopy. After 9 days, typical dawsonite particles were predominant in R2-9d (Figure 3.2c), while samples R3-9d and R4-9d still displayed a mixed morphology of the porous dawsonite particles and MAC (Figure 3.2d).

In agreement with X-ray diffraction, the infrared analysis revealed new bands in R2-5d characteristic to dawsonite (solid dots in Figure 3.5) at 3070 cm^{-1} (ν_{NH}). R2-9d displayed more developed and additional characteristic dawsonite bands at 2836 cm^{-1} (ν_{NH}) and 1830 and 1720 cm^{-1} (δ_{NH}), 735 cm^{-1} (ν_4 mode of carbonate), and 635 cm^{-1} (Al-O stretching vibration). The spectra also showed that the ν_{OH} and the $\nu_3(CO_3^{2-})$ modes in Mg-Al hydrotalcite (3480 and 1370 cm^{-1}, respectively) shifted to typical values of NH_4-dawsonite as the time of the treatment was increased (3445 and 1385 cm^{-1}, respectively, in R2-9d).

The changes displayed by the XRD patterns at longer times were further confirmed by thermogravimetry. The total weight loss upon thermal decomposition increased to 57% (R2-3d) and 67% (R2-9d), respectively, as compared to 42% in HT2 (Figure 3.3), and the weight loss in the first transition (centered at *ca.* 420 K in Figure 1 in Annex 1) gradually increased from R2-3d to R2-9d as the amount of dawsonite increased. No crystalline hydrotalcite was visible anymore by XRD after 9 days. Additional decompositions at 350 and 615 K, observed in R2-9d, were attributed to an amorphous phase. The percentage of dawsonite in the composite was 47% (R2-3d), 54% (R2-5d), and 93% (R2-9d), respectively (Figure 3.4).

The total weight loss upon thermal decomposition of R3-3d (51%) and R3-9d (62%) increased significantly as compared to 44% in HT3 as a consequence of the progressive crystallization of dawsonite and magnesium ammonium carbonate (dashed line and solid squares, respectively, in Figure 3.3) in line with XRD. A discrete shoulder centered at *ca.* 360 K (Figure 1 in Annex 1) can be seen in R3-9d, and was attributed to the decomposition of magnesium ammonium carbonate.[40] While the transition temperature in the range 590-700 K belongs to the hydrotalcite fraction in R3-3d, in R3-9d the same

UNIVERSITAT ROVIRA I VIRGILI
CHEMISTRY OF DAWSONITES AND APPLICATION IN CATALYSIS
Georgiana Stoica
ISBN:978-84-693-1533-0/DL:T-648-2010

transition belongs to magnesium ammonium carbonate (Figure 1 in Annex 1). According to Figure 3.4, the percentage of dawsonite in the composite materials was 54% for R3-3d, 43% for R3-5d, and 48% for R3-9d, respectively.

Considering the similarities between the transition temperatures of R2-9d and MAC in Figure 1 in Annex 1, the amorphous phase in R2-9d could be identified as MAC. Due to the low Mg/Al ratio 2 in the starting hydrotalcite, crystallization of MAC would require longer times, or a higher carbonate concentration in the solution. However, distinctive absorption bands of MAC were not visible by infrared spectroscopy.

Thermogravimetric results of the HT4-derived samples indicated that the total weight loss increased from 44% in HT4 to 60% (R4-3d), and 68% (R4-9d), respectively, due to the newly formed dawsonite and magnesium ammonium carbonate. The transition at 420-440 K in samples R4-3d, R4-5d, and R4-9d (Figure 1 in Annex 1) was attributed to NH_4-dawsonite, whose relative amount was estimated at 75%, 72%, and 40%, respectively (Figure 3.4). Magnesium ammonium carbonate displayed two transition temperatures at 350 K and > 600 K, respectively, and induced the shift of dawsonite decomposition to lower temperatures. The relative amount of MAC increased (Figure 3.4) due to the higher Mg concentration in the starting hydrotalcite sample. The relative amount of dawsonite decreased in R4-9d with respect to R4-5d (Figure 3.4) due to the extensive formation of MAC. These results show that dawsonite crystallized in detriment of hydrotalcite, and the fraction of the different phases in the composite material strongly depends on the treatment time.

Additional characterization by nitrogen adsorption further accounts for the formation of composites. As exemplified for the R2 series in Figure 4 (Annex 1) and Table 3.1, adsorption at 77 K revealed substantial porosity changes with respect to the starting hydrotalcite, with a significant increase of the total surface area (from 58 $m^2\ g^{-1}$ in HT2 to 243 $m^2\ g^{-1}$ in R2-5d) and pore volume due to newly generated microporosity when dawsonite was formed (0.13 $cm^3\ g^{-1}$ in R2-9d).[30]

The behavior of the starting hydrotalcites (Mg/Al = 2-4) in the layered form in ammonium carbonate aqueous solution was investigated as well. The hydrotalcite powders were directly treated in 1 M $(NH_4)_2CO_3$ aqueous solution at ambient conditions for 1 day, and no changes in the XRD pattern were observed. Apparently, the hydrotalcite phase was stable even when additional ultrasonication was applied for the same time. Longer treatment times, *i.e.* 3 days, of the as-synthesized hydrotalcites in the ammonium carbonate solution led to the discrete appearance of dawsonite bands in the XRD pattern

UNIVERSITAT ROVIRA I VIRGILI
CHEMISTRY OF DAWSONITES AND APPLICATION IN CATALYSIS
Georgiana Stoica
ISBN:978-84-693-1533-0/DL:T-648-2010

of samples HT3-3d and HT4-3d, respectively, indicating the formation of a hydrotalcite-dawsonite composite. However, sample HT2-3d did not display any dawsonite reflections. These observations were logical since the recovered hydrotalcite by delamination/restacking after 1 h is able to transform at longer times into new phases when treated with ammonium carbonate. Following the solid route, the formation of the dawsonite-hydrotalcite composites was slower than the treatment *via* delamination-restacking. Accordingly, although exfoliation is not certainly a prerequisite for the transformation, we want to highlight that the higher reactivity of the LDH nanosheets with respect to the powder hydrotalcite is likely responsible for the above mentioned features.

3.3. Mechanism of the hydrotalcite-dawsonite transformation

ICP-OES analyses of selected solids (obtained *via* delamination in formamide and treatment in ammonium carbonate) and the corresponding filtrates were in agreement with the results presented so far. The Mg/Al ratio in the solids decreased from 1.8 in HT2 to 0.23 in HT2-9d, *i.e.* one order of magnitude lower as compared to the starting hydrotalcite (Figure 3.6). The sample obtained after 9 days contains only 13% of the initial Mg^{2+} concentration in the parent hydrotalcite. Similar trends were observed for the R3-*t* and R4-*t* systems, which contained 15% and 40% of the starting Mg^{2+} concentration, respectively. This result can be expected considering that the final composites mainly consisted of Al-containing phases.

Table 3.1. Characterization data of selected samples.

Sample	Phases[a]	V_{pore} ($cm^3\ g^{-1}$)	V_{micro}[b] ($cm^3\ g^{-1}$)	S_{meso}[b] ($m^2\ g^{-1}$)	S_{BET}[c] ($m^2\ g^{-1}$)
HT2	HT	0.26	0	58	58
R2-1h	HT	0.34	0.00	91	116
R2-5d	HT + DW	0.13	0.06	124	243
R2-9d	DW	0.25	0.13	181	457
DW	DW	0.94	0.12	198	462

[a] Determined by X-ray diffraction. HT and DW stand for hydrotalcite and dawsonite, respectively. [b] *t*-plot method. [c] BET method.

UNIVERSITAT ROVIRA I VIRGILI
CHEMISTRY OF DAWSONITES AND APPLICATION IN CATALYSIS
Georgiana Stoica
ISBN:978-84-693-1533-0/DL:T-648-2010

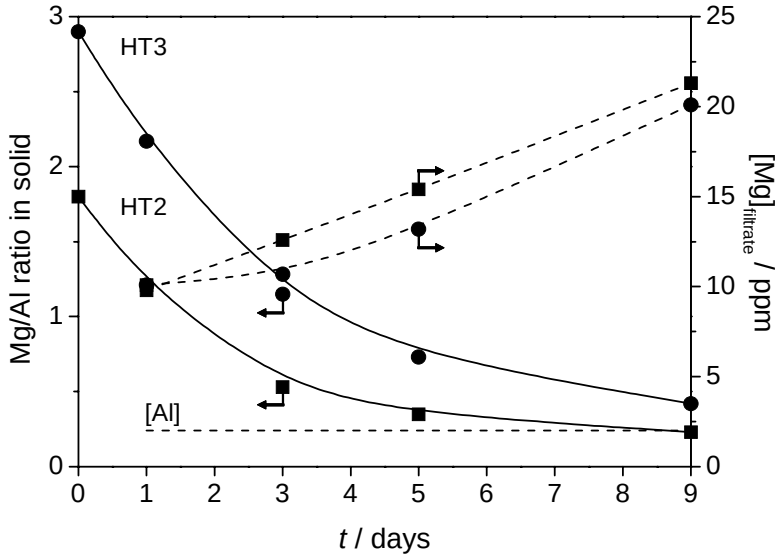

Figure 3.6. Variation of the Mg/Al ratios in the solids (solid line), and variation of the Mg concentration in the filtrates (dashed line) as a function of treatment time. The Mg/Al ratio decreases due to dissolution of Mg, followed by precipitation of Al as dawsonite when hydrotalcite is not stable anymore. Consequently, Mg crystallizes as magnesium ammonium carbonate at longer restacking times. Concentration of Al was determined below 2 ppm in the filtrates, indicating its precipitation into dawsonite.

Besides, the Al^{3+} content in the filtrates was found in a very low amount, *i.e.* < 2 ppm, thus suggesting that the decrease in Mg/Al ratio was provoked by the gradual dissolution of magnesium (as observed by the increase in Mg^{2+} concentration in the filtrate, Figure 3.6). Therefore, the amount of MAC in the final solids increased upon increasing the starting Mg/Al ratio of the LDH.

Taking into account the above observations, the following mechanism for the formation of the composite materials can be put forward (Figure 3.7). As previously explained, hydrotalcite became exfoliated upon contacting the coprecipitated solid in formamide under ultrasounds, giving rise to colloidal suspensions with pH 9.5. After addition of ammonium carbonate, the pH of the final solution was 9.2, and the restacking of the hydrotalcite structure rapidly occurred, as observed by their corresponding reflections in the XRD patterns in Figure 3.1. The solubility of the pre-formed hydrotalcite was likely affected by the pH of the solution, which slightly declined during the course of the treatment from 9.2 to 9. This induced the presence of magnesium (Mg^{2+}) and aluminum ions in solution, the latter being in the form of $Al(OH)_4^-$.[41] As observed by ICP-OES analysis, the amount of Mg in the filtrates increased, thus implying a removal of this metal from the hydrotalcite, and therefore, its progressive dissolution. A similar dissolution behavior likely occurred when the original as-prepared hydrotalcite was directly treated with $NH_4(CO_3)_2$, as schematically shown in

UNIVERSITAT ROVIRA I VIRGILI
CHEMISTRY OF DAWSONITES AND APPLICATION IN CATALYSIS
Georgiana Stoica
ISBN:978-84-693-1533-0/DL:T-648-2010

Figure 3.7. This is supported by the higher lability and solubility of Mg^{2+} with respect to Al^{3+}: $Mg(OH)_2$, ΔG_{diss} = -96.1 kJ mol^{-1}, $Al(OH)_3$, ΔG_{diss} = -46.7 kJ mol^{-1},[41,42] that is, the larger the negative value of the free energy of dissolution, the more soluble the metal. As concluded from XRD and TGA, the amount of hydrotalcite decreased as the treatment time increased. At the same time, new reflections associated with dawsonite appeared, following the equation below for the dawsonite[43] (thermodynamic data calculated from Wagman *et al.*[44]):

$$Al(OH)_4^- + NH_4^+ + CO_3^{2-} + 2H^+ = NH_4AlCO_3(OH)_2 + 2H_2O \qquad \Delta G = -1483 \text{ kJ mol}^{-1}$$

$Al(OH)_4^-$ ions present at the pH of the solution started to precipitate in the form of dawsonite, leading in a first stage to a dawsonite-hydrotalcite composite. This was expected, as alumina precursors crystallize into ammonium dawsonite when precipitated with ammonium carbonate.[30] The relative amount of dawsonite and hydrotalcite can be controlled (as shown before by thermogravimetric analysis in Figure 3.4), as the latter is the precursor of the former phase *via* a dissolution-precipitation mechanism. Based on the obtained results complemented by thermodynamic data, it was suggested that the magnesium dissolution represents the rate-controlling process. From a thermodynamic point of view, the standard Gibbs energy of precipitation of dawsonite (ΔG = -1483 kJ mol^{-1})[44] is higher than that of hydrotalcite (ΔG = -843.8 kJ mol^{-1} for Mg/Al = 3 LDH, as calculated from Allada *et al.*[5]), clearly indicating the higher tendency of dawsonite to precipitate. As a consequence, all ingredients present in solution favored the formation of dawsonite rather than the permanence of hydrotalcite. Besides, the standard Gibbs free energies of dissolution of dawsonite and hydrotalcite in basic media are 102.1 kJ mol^{-1},[1,43] and -107.4 kJ mol^{-1},[1,3], respectively, indicating the higher tendency of hydrotalcite to dissolve than dawsonite.

The starting Mg/Al ratio played an important role on the evolution of the dawsonite-hydrotalcite composite. When the composition of the hydrotalcite was brought to the limit (higher Mg/Al ratios), the restacking procedure ultimately resulted into the depletion of the hydrotalcite phase, *i.e.* giving rise to the formation of crystalline dawsonite and ammonium magnesium carbonate hydrate phases (Figures 3.1 and 3.7). Despite the relative high Mg/Al ratio, no brucite was discernable, and MAC precipitated due to the presence of ammonium and carbonate ions in the aqueous medium.[31]

The same mechanism holds for the as-synthesized hydrotalcites when poured directly in the $(NH_4)_2CO_3$ aqueous solution. However, the transformation of the solid took longer due to the higher stability of the original lamellar hydrotalcites than the metastable hydrotalcites formed

UNIVERSITAT ROVIRA I VIRGILI
CHEMISTRY OF DAWSONITES AND APPLICATION IN CATALYSIS
Georgiana Stoica
ISBN:978-84-693-1533-0/DL:T-648-2010

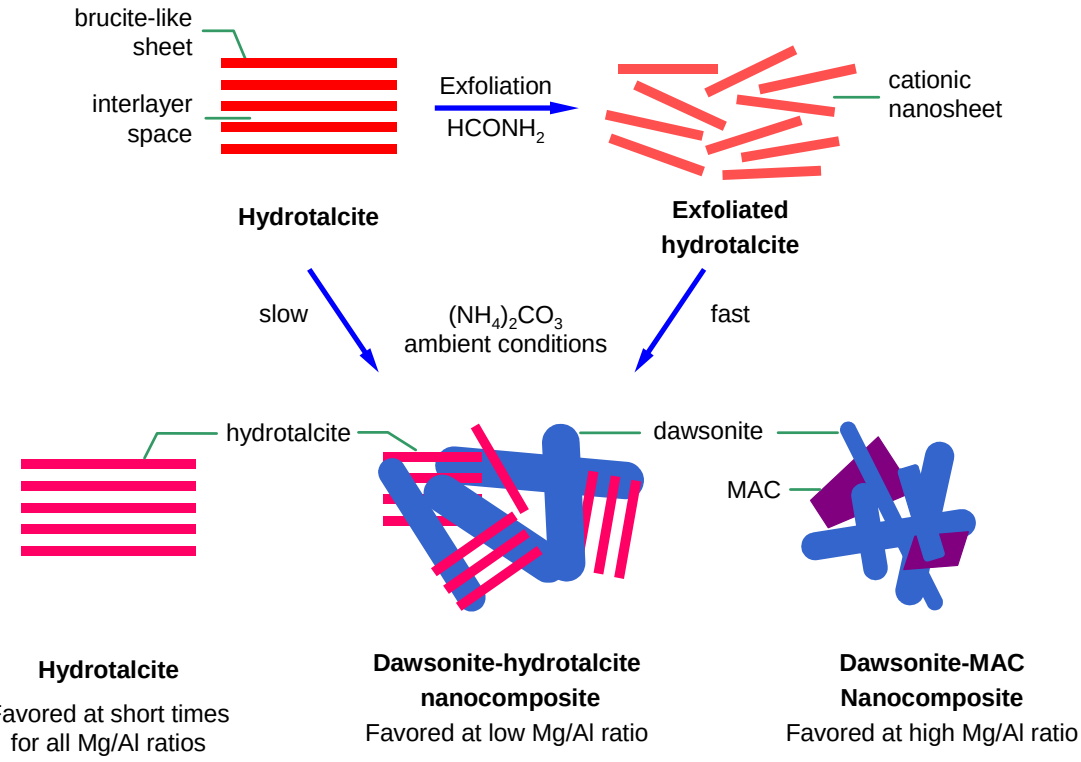

Figure 3.7. Pictorial scheme of the synthetic approach used in this work. Short treatment times of solid or delaminated Mg-Al hydrotalcites recover the pure hydrotalcite phase, while longer exposure transformed the layered material into composites containing dawsonite and/or magnesium ammonium carbonate.

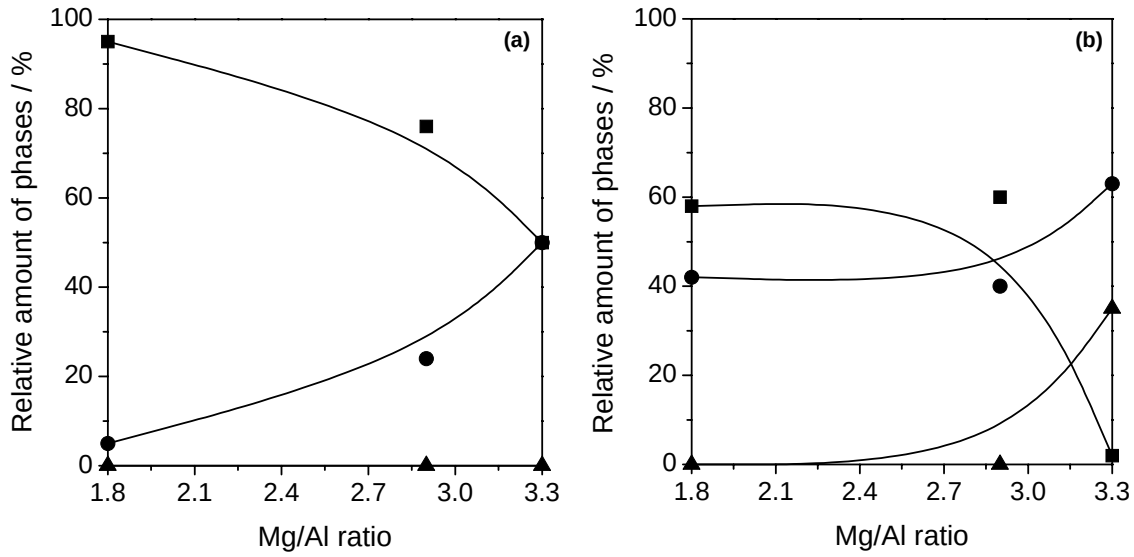

Figure 3.8. Relative amount of hydrotalcite (■), dawsonite (●), and magnesium ammonium carbonate (▲) at 3 days by (a) direct reaction of the solid hydrotalcite with aqueous $(NH_4)_2CO_3$ solution, and (b) delamination-restacking approach. Formation of the composite is faster by delamination-restacking due to the increased reactivity of the hydrotalcite nanosheets induced by prior exfoliation. The relative amount of phases was determined by thermogravimetry as explained in the Annex 1.

UNIVERSITAT ROVIRA I VIRGILI
CHEMISTRY OF DAWSONITES AND APPLICATION IN CATALYSIS
Georgiana Stoica
ISBN:978-84-693-1533-0/DL:T-648-2010

by restacking of the colloidal solutions. Comparative thermogravimetric calculations of the relative amount of phases, after 3 days by the two synthetic approaches, are presented in Figure 3.8 and confirmed not only the faster formation of composites following the delamination route, but also the higher reactivity of the hydrotalcites in the order HT4 > HT3 > HT2. Using the model proposed by Allada *et al.*,[5] we computed the standard Gibbs free energies of formation of the hydrotalcites with different Mg/Al ratios as -848.3 kJ mol^{-1} (HT2), -843.8 kJ mol^{-1} (HT3), and -842.7 kJ mol^{-1} (HT4), indicating that in aqueous media HT4 will be the first to suffer chemical transformations. This order of reactivity is in agreement with previous thermodynamic studies in LDHs,[5] and supported the XRD *vs.* time results presented earlier in the chapter.

4. Conclusions

Composite materials consisting of mixtures of dawsonite, hydrotalcite, and magnesium ammonium carbonate have been synthesized starting from a single component, *i.e.* hydrotalcites with Mg/Al = 2-4. This synthesis route comprises the treatment of the original or exfoliated hydrotalcite in ammonium carbonate aqueous solution at ambient conditions. At short treatment times (1 h to 1 day) the reformed samples displayed the original layered structure, which further transformed into dawsonite-hydrotalcite composite materials. However, longer treatment times and high Mg content in the starting material were unfavorable for the stability of the composite due to excessive hydrotalcite dissolution. Hydrotalcites with lower Mg/Al ratio displayed a similar behavior at early stages of the treatment, while hydrotalcites with higher Mg/Al ratio were similar at longer treatment times due to the increased Mg content in the starting material. The hydrotalcite in delaminated (colloidal) form, attained by treatment in formamide, was significantly more reactive in $(NH_4)_2CO_3$ than the parent hydrotalcites in solid form. As supported by previously published thermodynamic data, the progressive transformation of hydrotalcite towards crystalline dawsonite and magnesium ammonium carbonate phases occurred *via* a dissolution-precipitation mechanism.

Acknowledgments

Sònia Abelló and Marta Santiago are gratefully acknowledged for their valuable contribution to this chapter.

UNIVERSITAT ROVIRA I VIRGILI
CHEMISTRY OF DAWSONITES AND APPLICATION IN CATALYSIS
Georgiana Stoica
ISBN:978-84-693-1533-0/DL:T-648-2010

References

[1] P.S. Braterman, Z.P. Xu, F. Yarberry, Layered Double Hydroxides (LDHs). In *Handbook of Layered Materials*, S.M. Auerbach, K.A. Carrado, P.K. Dutta (Eds.), Taylor & Francis: New York, 2004; p. 313.

[2] F. Cavani, F. Trifiro, A. Vaccari, *Catal. Today* **1991**, 11, 173.

[3] J.J. Bravo-Suárez, E.A. Páez-Mozo, S.T. Oyama, *Quim. Nova* **2004**, 27, 601.

[4] S. Miyata, *Clays Clay Miner.* **1983**, 4, 305.

[5] R.K. Allada, A. Navrotsky, H.T. Berbeco, W.H. Casey, *Science* **2002**, 296, 721.

[6] R.K. Allada, J.D. Pless, T.M. Nenoff, A. Navrotsky, *Chem. Mater.* **2005**, 17, 2455.

[7] V. Rives, M.A. Ulibarri, *Coord. Chem. Rev.* **1999**, 181, 61.

[8] F. Leroux, M. Adachi-Pagano, M. Intissar, S. Chauvière, C. Forano, J.-P. Besse, *J. Mater. Chem.* **2001**, 11, 105.

[9] N. Iyi, Y. Ebina, T. Sasaki, *Langmuir* **2008**, 24, 5591.

[10] M. Adachi-Pagano, C. Forano, J.-P. Besse, *Chem. Commun.* **2000**, 91.

[11] M.S. San Román, M.J. Holgado, C. Jaubertie, V. Rives, *Solid State Sci.* **2008**, 10, 1333.

[12] T. Hibino, W. Jones, *J. Mater. Chem.* **2001**, 11, 1321.

[13] S. O'Leary, D. O'Hare, G. Seeley, *Chem. Commun.* **2002**, 1506.

[14] T. Hibino, M. Kobayashi, *J. Mater. Chem.* **2005**, 15, 653.

[15] J.T. Rakamathi, A. Arulraj, N. Ravishankar, J. Arulraj, M. Rajamathi, *Langmuir* **2008**, 24, 11164.

[16] C. Jaubertie, M.J. Holgado, M.S. San Román, V. Rives, *Chem. Mater.* **2006**, 18, 3114.

[17] M. Jobbagy, A.E. Regazzoni, *J. Colloid Interface Sci.* **2004**, 275, 345.

[18] B.R. Venugopal, C. Shivakumara, M. Rajamathi, *J. Colloid Interface Sci.* **2006**, 294, 234.

[19] W. Hou, L. Kang, R. Sun, Z.-H. Liu, *Colloids Surf., A* **2008**, 312, 92.

[20] Z. Liu, R. Ma, M. Osada, N. Iyi, Y. Ebina, K. Takada, T. Sasaki, *J. Am. Chem. Soc.* **2006**, 128, 4872.

[21] T. Hibino, *Chem. Mater.* **2004**, 16, 5482.

[22] Z. Liu, R. Ma, Y. Ebina, N. Iyi, K. Takada, T. Sasaki, *Langmuir* **2007**, 23, 861.

[23] M. Alexandre, P. Dubois, *Mater. Sci. Eng.* **2000**, R28, 1.

[24] C.R. Gordijo, V.R. Leopoldo Constantino, D. de Oliveira Silva, *J. Solid State Chem.* **2007**, 180, 1967.

[25] B.R. Venugopal, C. Shivakumara, M. Rajamathi, *Solid State Sci.* **2007**, 9, 287.

UNIVERSITAT ROVIRA I VIRGILI
CHEMISTRY OF DAWSONITES AND APPLICATION IN CATALYSIS
Georgiana Stoica
ISBN:978-84-693-1533-0/DL:T-648-2010

[26] Q. Wu, A. Olafsen, Ø.B. Vistad, J. Roots, P. Norby, *J. Mater. Chem.* **2005**, 15, 4695.

[27] L. Li, R. Ma, Y. Ebina, K. Fukuda, K. Takada, T. Sasaki, *J. Am. Chem. Soc.* **2007**, 129, 8000.

[28] S. Abelló, J. Pérez-Ramírez, *Adv. Mater.* **2006**, 18, 2436.

[29] M. Santiago, M.S. Yalfani, J. Pérez-Ramírez, *J. Mater. Chem.* **2006**, 16, 2886.

[30] G. Stoica, J. Pérez-Ramírez, *Chem. Mater.* **2007**, 19, 4783.

[31] E. Erdös, H. Altorfer, J. Witt, *J. Appl. Cryst.* **1979**, 12, 611.

[32] S. Brunauer, P.H. Emmett, E. Teller, *J. Am. Chem. Soc.* **1938**, 60, 309.

[33] B.C. Lippens, J.H. de Boer, *J. Catal.* **1965**, 4, 319.

[34] J.T. Kloprogge, R.L. Frost, *J. Solid State Chem.* **1999**, 146, 506.

[35] G. Stoica, J.C. Groen, S. Abelló, R. Manchanda, J. Pérez-Ramírez, *Chem. Mater.* **2008**, 20, 3973.

[36] J. Pérez-Ramírez, G. Mul, F. Kapteijn, J.A. Moulijn, *J. Mater. Chem.* **2001**, 11, 821.

[37] V. Rives, *Mater. Chem. Phys.* **2002**, 75, 19.

[38] J.I. Di Cosimo, V.K. Diez, M. Xu, E. Iglesia, C.R. Apesteguia, *J. Catal.* **1998**, 178, 499.

[39] C.J. Serna, J.V. Garcia-Ramos, M.J. Peña, *Spectrochim. Acta* **1985**, 41A, 697.

[40] R.M. Dell, S.W. Weller, *Trans. Faraday Soc.* **1959**, 55, 2203.

[41] H. Tamura, J. Chiba, M. Ito, T. Takeda, S. Kikkawa, Y. Mawatari, M. Tabata, *J. Colloid Interface Sci.* **2006**, 300, 648.

[42] U. Costantino, F. Marmottini, M. Nocchetti, R. Vivani, *Eur. J. Inorg. Chem.* **1998**, 10, 1439.

[43] P. Bénézeth, D.A. Palmer, L.M. Anovitz, J. Horita, *Geoch. Cosmoch. Acta* **2007**, 71, 4438.

[44] D.D. Wagman, W.H. Evans, V.B. Parker, R.H. Schumm, I. Halow, S.M. Bailey, K.L. Churney, R.L. Nuttal, *J. Phys. Chem. Ref. Data* **1982**, 11, 1.

UNIVERSITAT ROVIRA I VIRGILI
CHEMISTRY OF DAWSONITES AND APPLICATION IN CATALYSIS
Georgiana Stoica
ISBN:978-84-693-1533-0/DL:T-648-2010

Annex 1

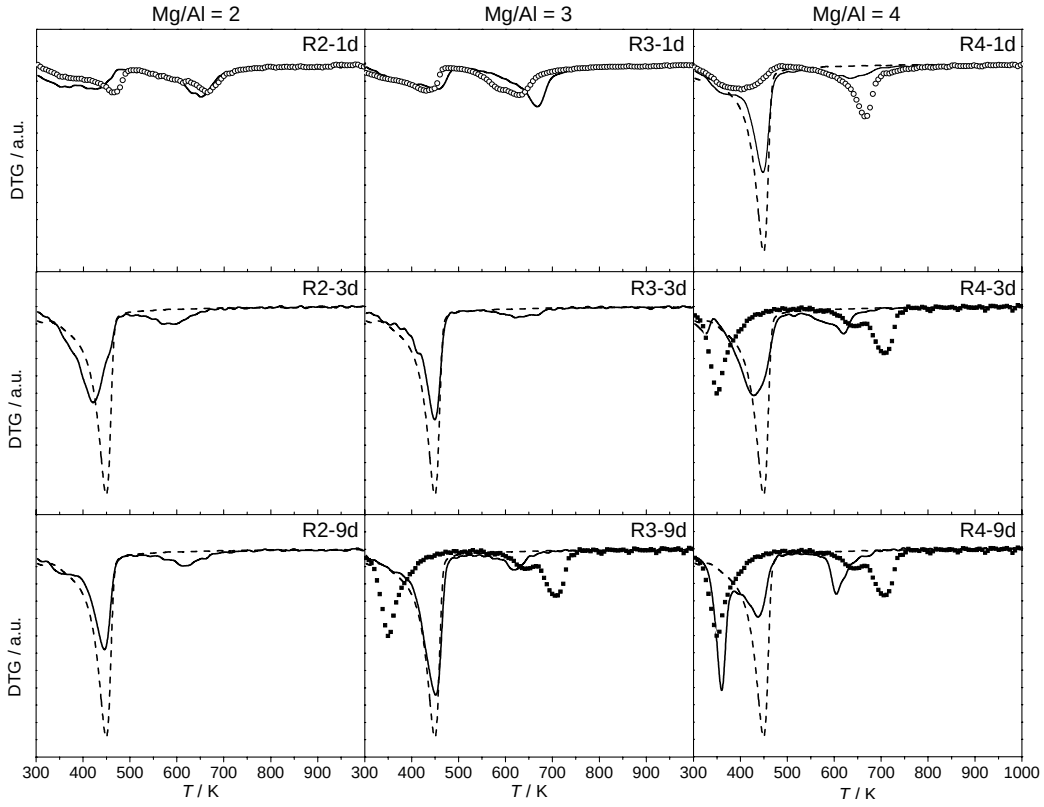

Figure 1. Derivatives of the weight loss profiles shown in Figure 3.3. Pure compounds: (○) parent hydrotalcites, (**---**) reference dawsonite, and (■) reference magnesium ammonium carbonate.

UNIVERSITAT ROVIRA I VIRGILI
CHEMISTRY OF DAWSONITES AND APPLICATION IN CATALYSIS
Georgiana Stoica
ISBN:978-84-693-1533-0/DL:T-648-2010

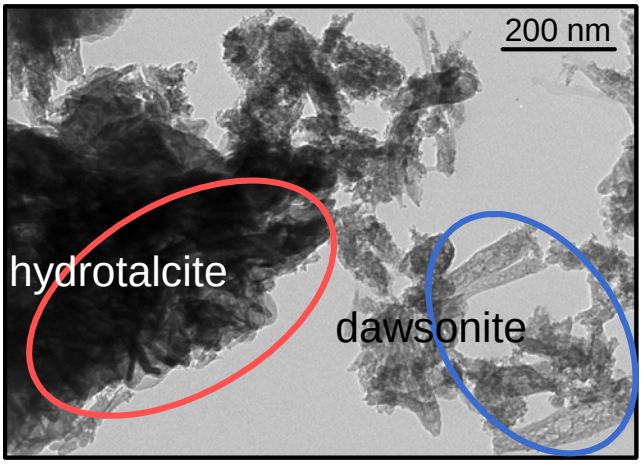

Figure 2. TEM image of a physical mixture of as-synthesized hydrotalcite and reconstructed dawsonite (by ball milling), evidencing the segregation of both phases, in contrast to the well intermixed dawsonite-hydrotalcite composite.

UNIVERSITAT ROVIRA I VIRGILI
CHEMISTRY OF DAWSONITES AND APPLICATION IN CATALYSIS
Georgiana Stoica
ISBN:978-84-693-1533-0/DL:T-648-2010

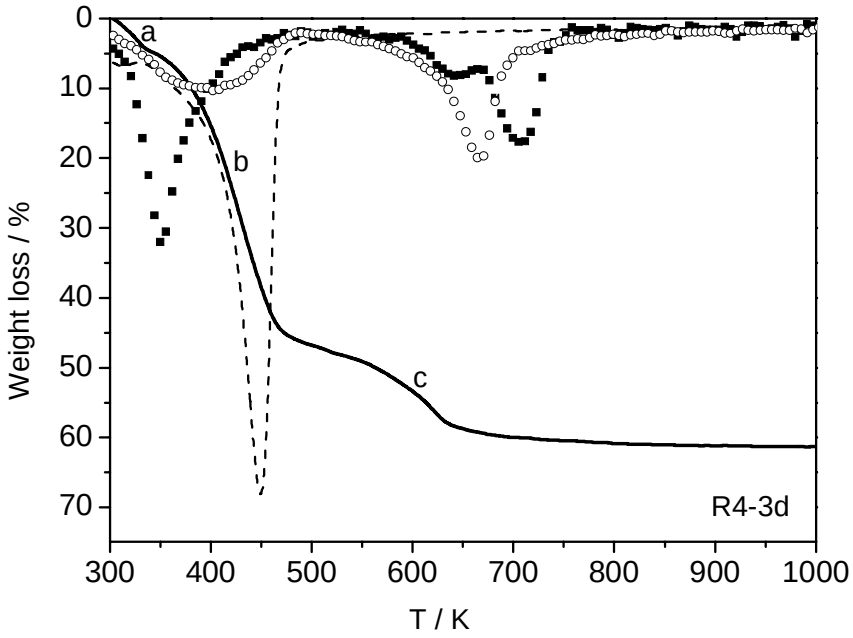

Figure 3. For a better understanding of the quantification process using TGA, we exemplify the case of sample R4-3d consisting of hydrotalcite, dawsonite, and MAC. Thermogravimetric analysis profile displays a three-step profile marked by a, b, and c, respectively. The first weight loss (a) at 350 K is attributed to MAC decomposition (indicate by squares), with transitions at 350 K (28% due to water and ammonia removal) and > 600 K (21% due to decomposition of carbonates). The second weight-loss step, marked by b, corresponds to both dawsonite (dashed line; one-step weight loss centered at *ca.* 450 K) and hydrotalcite (open circles; interlayer water removal at 423-473 K, 16% theoretical). The weight loss at higher temperatures (> 600 K, c), due to dehydroxylation of the brucite-like sheets and decomposition of interlayer carbonates in hydrotalcite (28% from the theoretical formula of HT), overlaps with the second weight loss of MAC. Knowing the *a* value, the second weight loss of MAC contributing to *c* can be calculated from the theoretical formula. The difference from *c* corresponds to the second weight loss of hydrotalcite, $WL2_{HT}$. Further, based on the theoretical formula of HT, we calculate $WL1_{HT}$. The difference *b*-$WL1_{HT}$ represents the weight loss of dawsonite, WL_{DW}.

When the final material consists only of dawsonite and hydrotalcite, the *a* value is 0, and *c* corresponds to $WL2_{HT}$. From the theoretical formula of HT, we calculate $WL1_{HT}$ in *b*. The difference *b*-$WL1_{HT}$ represents the weight loss of dawsonite, WL_{DW}. If the sample consists of

UNIVERSITAT ROVIRA I VIRGILI
CHEMISTRY OF DAWSONITES AND APPLICATION IN CATALYSIS
Georgiana Stoica
ISBN:978-84-693-1533-0/DL:T-648-2010

dawsonite and MAC, *a* and *c* correspond to the first and second weight loss, respectively, of MAC. And *b* is attributed only to dawsonite decomposition.

UNIVERSITAT ROVIRA I VIRGILI
CHEMISTRY OF DAWSONITES AND APPLICATION IN CATALYSIS
Georgiana Stoica
ISBN:978-84-693-1533-0/DL:T-648-2010

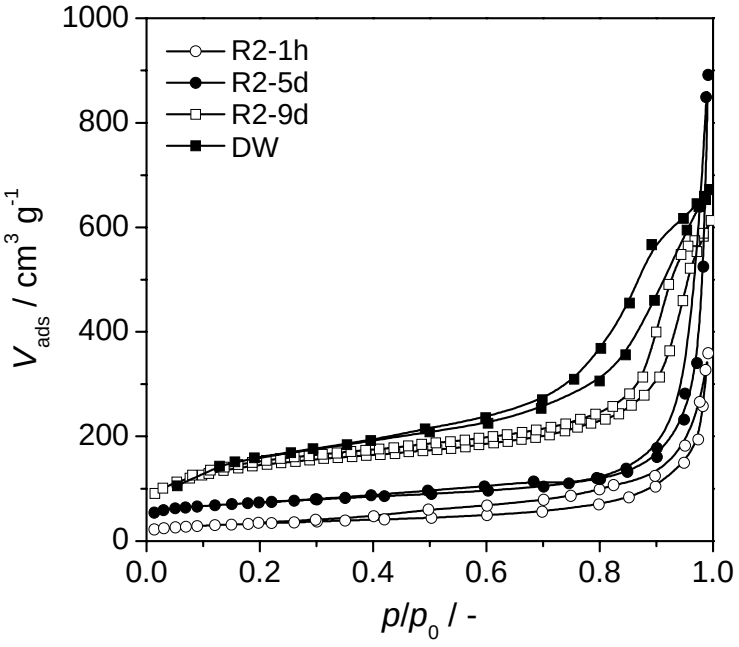

Figure 4. Nitrogen adsorption-desorption isotherms at 77 K of selected solids resulting from treatment of delaminated hydrotalcite with Mg/Al = 2 in 1 M $(NH_4)_2CO_3$. The isotherm of R2-1h is characteristic of the hydrotalcite clay compounds with a significant increase of the total surface area, *i.e.* 116 m^2 g^{-1}. This is due to the interparticle mesoporosity generated by the exfoliation-restacking treatment. Longer restacking times induced substantial porosity changes in the composite with respect to the starting hydrotalcite. The nitrogen uptake is remarkably higher, especially at high relative pressure. There is also a low-pressure contribution due to the presence of microporosity in the composite, associated with the presence of dawsonite (Stoica *et al.*, Chem. Mater. 20 (2008) 3973). The micropore volume, determined by the *t*-plot method, increased from 0 in HT2 to 0.06 cm^3 g^{-1} in R2-5d. Due to the newly generated microporosity, the total surface area experienced a significant increase, from 58 m^2 g^{-1} in HT2 to 243 m^2 g^{-1} in R2-5d. The total pore volume and surface area of R2-9d increased significantly, although the N_2 uptake at higher pressures decreased. However, the uptake at lower pressures remarkably increased due to the presence of micropores, amounting to 0.13 cm^3 g^{-1}. Sample R2-9d exhibits similar textural and porous properties as those in the reconstructed dawsonite used as reference.

UNIVERSITAT ROVIRA I VIRGILI
CHEMISTRY OF DAWSONITES AND APPLICATION IN CATALYSIS
Georgiana Stoica
ISBN:978-84-693-1533-0/DL:T-648-2010

Table 1. Determination of the relative amount of hydrotalcite (HT), dawsonite (DW) and magnesium ammonium carbonate (MAC) from thermogravimetric analysis.

Sample	$WL_{total}MAC$[a] / %	$WL1_{total}$[b] / %	$WL2_{HT}$[c] / %	$WL1_{HT}$[d] / %	WL_{DW}[e] / %	HT[f] / %	DW[g] / %	MAC[h] / %
HT2	0	17.2	24.4	17.2	0	100	0	0
R2-1h	0	18.4	26.6	16.2	2.2	95	5	0
R2-1d	0	22	24	16.6	5.4	89	11	0
R2-3d	0	39	18	12.2	26.8	53	47	0
R2-5d	0	46.4	21	11.2	35.2	45	54	0
R2-9d	0	55	6.2	4.1	51	7	93	0
HT3	0	17.7	26.5	17.7	0	100	0	0
R3-1h	0	16.6	27.8	16	0.65	98.5	1.5	0
R3-1d	0	17	27	15.8	1.2	97	3	0
R3-3d	0	35	16.7	11.4	23.6	46	54	0
R3-5d	19.4	24.5	5	3.3	21.2	17	43	40
R3-9d	31.7	29.7	0	0	29.7	0	48	52
HT4	0	17.2	26.4	17.2	0	100	0	0

UNIVERSITAT ROVIRA I VIRGILI
CHEMISTRY OF DAWSONITES AND APPLICATION IN CATALYSIS
Georgiana Stoica
ISBN:978-84-693-1533-0/DL:T-648-2010

R4-1h	0	19.8	25.7	16.4	3.4	92.5	7.5	0
R4-1d	0	44	19.5	10.2	33.8	47	53	0
R4-3d	8	46	4	2.6	43.4	11	75	14
R4-5d	16.9	43.6	0	0	43.6	0	72	38
R4-9d	39.6	26	0	0	26	0	40	60

[a] Weight loss of MAC in the composite material, calculated as $WL_{350\ K} + WL_{600\ K}$.

[b] Weight loss at 450 K; includes removal of interlayer water in hydrotalcite and dawsonite decomposition.

[c] Weight loss at 450-700 K; includes dehydroxylation and decarbonation of hydrotalcite.

[d] Contribution of hydrotalcite to $WL1_{total}$, calculated from the general hydrotalcite formula.

[e] Contribution of dawsonite to $WL1_{total}$, calculated as $WL1_{total}$-$WL1_{HT}$.

[f] Weight percent of hydrotalcite in the composite material, calculated as $\%HT = 100\times(WL1_{HT} + WL2_{HT})/(WL_{total}MAC + WL1_{total}+WL2_{HT})$

[g] Weight percent of dawsonite in the composite material, calculated as $\%DW = 100\times WL_{DW}/(WL_{total}MAC + WL1_{total}+WL2_{HT})$.

[h] Weight percent of MAC in the composite material, calculated as $\%MAC = 100\times WL_{total}MAC/(WL_{total}MAC + WL1_{total}+WL2_{HT})$.

UNIVERSITAT ROVIRA I VIRGILI
CHEMISTRY OF DAWSONITES AND APPLICATION IN CATALYSIS
Georgiana Stoica
ISBN:978-84-693-1533-0/DL:T-648-2010

Chapter 3

UNIVERSITAT ROVIRA I VIRGILI
CHEMISTRY OF DAWSONITES AND APPLICATION IN CATALYSIS
Georgiana Stoica
ISBN:978-84-693-1533-0/DL:T-648-2010

UNIVERSITAT ROVIRA I VIRGILI
CHEMISTRY OF DAWSONITES AND APPLICATION IN CATALYSIS
Georgiana Stoica
ISBN:978-84-693-1533-0/DL:T-648-2010

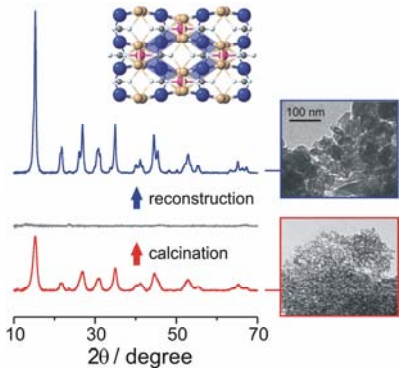

Chapter 4

Reforming Dawsonite by Memory Effect of AACH-Derived Aluminas

Ammonium aluminum carbonate hydroxide (AACH), a material isostructural with the mineral dawsonite ($NaAl(OH)_2CO_3$), leads to finely dispersed and high-surface area Al_2O_3 upon thermal decomposition. This family of compounds exhibits memory effect, *i.e.* the dawsonite structure can be recovered upon treatment of the derived aluminas in $(NH_4)_2CO_3$ solutions at 323 K. Treatment of the oxides in water or NH_4OH, NH_4Cl, and Na_2CO_3 solutions led to aluminum (oxi)hydroxides. The memory effect holds in aluminas doped with transition metals such as chromium or iron. The reconstruction of dawsonite in ammonium carbonate was complete for the solids calcined at 523 and 723 K, consisting of a highly amorphous and low-skeleton density alumina phase with well-developed porosity. The recrystallization was incomplete upon formation of larger γ-Al_2O_3 crystals by calcination at 1073 K, and no reconstruction occurred when α-Al_2O_3 was obtained by calcination at 1473 K. Characterization of the reconstructed samples indicates the attainment of NH_4-dawsonite with higher purity than in the parent material. This is due to the presence of amorphous Al-containing phase(s) in the as-synthesized sample coexisting with AACH. All the phases were selectively converted into dawsonite by thermal decomposition and $(NH_4)_2CO_3$ treatment. The *reformed* samples consist of relatively large crystals with developed microporosity as compared to the parent material. These results extend the unique memory property of oxides derived from particular layered materials such as hydrotalcites to other families of mineral-like compounds.

This chapter is based on the following publication:
G. Stoica, J. Pérez-Ramírez, *Chem. Mater.* **2007**, 19, 4783.

UNIVERSITAT ROVIRA I VIRGILI
CHEMISTRY OF DAWSONITES AND APPLICATION IN CATALYSIS
Georgiana Stoica
ISBN:978-84-693-1533-0/DL:T-648-2010

1. Introduction

The annual world production of alumina (Al_2O_3) is estimated at 80 Mtonnes, giving idea of the relevance of this compound in a number of industries (mining, ceramic, chemical). Ammonium aluminum carbonate hydroxide (AACH, with formula $NH_4Al(OH)_2CO_3$) is a unique precursor for aluminas with enhanced properties compared to those derived from the conventional Bayer process. Several works have reported on the preparation of submicrometer high-purity α-Al_2O_3 powders for fine-grained ceramics or composites by thermal decomposition of AACH above 1173 K.[1,2] Besides, the porous Al_2O_3 resulting from thermal decomposition of AACH at lower temperatures (< 873 K) exhibits surface areas around 500 $m^2\ g^{-1}$,[3,4] superior to the typical 200-300 $m^2\ g^{-1}$ in commercial γ-alumina used as adsorbent, desiccant, catalyst, and catalyst support.

AACH is the NH_4-analogue of the mineral dawsonite ($NaAl(OH)_2CO_3$). The structure of dawsonite is orthorhombic-dipyramidal (space group *Imam*), consisting of an assemblage of edge-sharing distorted $AlO_2(OH)_4$ and $NaO_4(OH)_2$ octahedra and CO_3^{2-} groups.[5,6] One oxygen of the carbonate is hydrogen-bonded to two hydroxyl groups, strengthening the three-dimensional framework.[6] The symmetry of NH_4-dawsonite (base-centered) differs from that of Na-dawsonite (body-centered), although both structures are composed of the same $AlO_2(OH)_4$ chains of octahedra.[7] Consequently, a larger *c* dimension is observed in the ammonium analogue of the mineral.[7,8]

Various methods have been used to synthesize dawsonite, which can be classified attending to the phase composition of the reactants (gas-liquid, gas-solid, solid-solid, and liquid-liquid).[9] Preparation of AACH is typically practiced by precipitation of aqueous solutions of aluminum salts ($NH_4Al(SO_4)_2$, $AlCl_3$, or $Al(NO_3)_3$) or $Al(OH)_3$ suspensions with aqueous solutions of ammonium (bi)carbonate.[1,3,4,10,11] Dawsonite compounds have been applied as an ingredient in antiacids,[12] a stabilizer in polymers,[13,14] a dry extinguisher in fuel leak fires,[15] and an additive in synthetic fertilizers.[16] However, the above-mentioned use as precursor for ceramic and catalytic-grade alumina-based materials is the most relevant from a practical perspective. Dawsonite-type materials are compositionally flexible, *i.e.* the structure can accommodate a variety of divalent and trivalent cations in Al^{3+} positions and calcination results in oxide compounds with outstanding component dispersion, porosity, thermal stability, and catalytic performance.[3,4]

We have recently investigated the thermal evolution in air of *M*-Al and La-*M*-Al dawsonite-type compounds (*M* = Mn, Fe, Co, Ni) using *in situ* methods.[17] Depending on the combination

UNIVERSITAT ROVIRA I VIRGILI
CHEMISTRY OF DAWSONITES AND APPLICATION IN CATALYSIS
Georgiana Stoica
ISBN:978-84-693-1533-0/DL:T-648-2010

of metals in the precipitate and temperature, the products of metal-containing AACH can be different forms of aluminas, single metal oxides, and mixed oxides with spinel, perovskite, and hexaaluminate structure. However, independent of the composition of the starting material, an amorphous alumina phase was formed after collapse of the dawsonite structure at 473 K, and temperatures above 1273 K were required in order to observe crystalline Al-containing phases (α-Al_2O_3, $LaAlO_3$, $LaAl_{11}O_{19}$) by high-temperature X-ray diffraction.[17]

The amorphous nature of the AACH-derived alumina and its sintering stability was very interesting and intriguing, leading us to investigate the chemical transformations of this oxidic phase upon contact with aqueous solutions containing different ions. It can be envisaged that at a certain condition the original dawsonite structure can recrystallize, equivalently to the unique memory effect displayed by Mg-Al mixed oxides derived from hydrotalcite-like compounds (layered double hydroxides).[18] Related to this hypothesis, the patent literature claims procedures to obtain MAl$(OH)_2CO_3$ (referred to as alkalized alumina) by treatment of hydrated aluminas (gibbsite, bayerite, and boehmite) in aqueous solutions of bicarbonate salts (MHCO$_3$, M = Li, K, Na, NH_4) above 373 K,[19] or by heating a solid mixture of the bicarbonate salt and aluminum hydroxide under CO_2 pressure.[20]

This study demonstrates for the first time that aluminum oxides resulting from thermal decomposition of AACH up to 1073 K, or Al-substituted AACH, have the ability to recover the dawsonite structure by treatment in $(NH_4)_2CO_3$ solutions under mild conditions. Treatment in other solutions (NH_4OH, NH_4Cl, Na_2CO_3) led to aluminum (oxi)hydroxide phases. The physico-chemical properties of the as-synthesized, calcined, and reconstructed samples have been assessed and comparatively discussed on the basis of chemical composition analyses, X-ray diffraction, infrared and Raman spectroscopies, transmission electron microscopy, density measurements, gas adsorption, and thermal analyses.

2. Experimental

2.1. Materials and treatments

Ammonium aluminum carbonate hydroxide (AACH) was synthesized by co-precipitation at constant pH using the ILDP (in-line dispersion precipitation) method.[4,21] Peristaltic pumps were used to continuously feed an aqueous solution of $Al(NO_3)_3 \cdot 9H_2O$ (1.1 M) and an aqueous solution of $(NH_4)_2CO_3$ (2 M) at 333 K to the precipitation chamber (volume of *ca.* 6 cm^3), which was stirred at 13,500 rpm. The synthesis was carried out at pH 8, with an average residence time of 18 s. Metal-substituted aluminum dawsonites with a molar Fe:Al or Cr:Al ratio of 1:11 were prepared in the same way by incorporating $Cr(NO_3)_3 \cdot 9H_2O$ and

UNIVERSITAT ROVIRA I VIRGILI
CHEMISTRY OF DAWSONITES AND APPLICATION IN CATALYSIS
Georgiana Stoica
ISBN:978-84-693-1533-0/DL:T-648-2010

$Fe(NO_3)_3 \cdot 9H_2O$ (0.1 M) in the 1.1 M Al^{3+} solution. In all cases, the resulting slurry was aged at 333 K for 3 h, followed by filtration, washing, and drying at 333 K for 12 h. The as-synthesized Al-samples were treated in static air at temperatures of 523, 723, 1073, and 1473 K during 2 h using a ramp of 5 K min^{-1}. The resulting oxide samples (0.2 g) were dispersed in 50 ml of water or 1 M aqueous solutions of $(NH_4)_2CO_3$, NH_4OH, NH_4Cl, and Na_2CO_3 at 323 K using reflux conditions and mechanical stirring (300 rpm), and treated during periods ranging from 5 min to 24 h. The samples were then filtered, thoroughly washed with deionized water until the pH of the filtrate was 7, and dried at 333 K for 12 h. All chemicals used were purchased from Panreac and Sigma-Aldrich and had purities > 98%. Along the manuscript, the as-synthesized, calcined, and reconstructed samples are identified by the codes AS, C, and R, respectively. The number in the sample code refers to the calcination temperature of the as-synthesized material, *i.e.* C1 at 523 K, C2 at 723 K, C3 at 1073 K, and C4 at 1473 K. Samples R1, R2, R3, and R4 resulted from treatment of C1, C2, C3, and C4, respectively, in a 1 M ammonium carbonate solution at 323 K for 24 h. Treatments in different media or for a different period of time are explicitly indicated.

2.2. Characterization methods

The aluminum content in the samples was determined by inductive coupled plasma-optical emission spectroscopy (ICP-OES) (Perkin-Elmer Optima 3200RL (radial)). Before analysis, the solids were treated by an alkaline fusion method with NaOH and Na_2O_2, followed by dilution with HCl. Elemental analysis (C, H, and N) was measured in a Carlo Erba EA1108 instrument. Powder X-ray diffraction (XRD) patterns were acquired in transmission using a Bruker AXS D8 Advance diffractometer equipped with a Cu tube, a Ge(111) incident beam monochromator (λ = 0.1541 nm), and a Vantec-1 PSD. Data were recorded in the 2θ range of 5 to 70º with an angular step size of 0.016º and a counting time of 6 s per step. The cell parameters were determined by the Bragg equation,[22] taking into account the orthorhombic dipyramidal crystal structure of the dawsonite mineral. The average crystallite size was determined using the Scherrer formula[23] in selected reflections, taking into account the instrumental broadening. The skeleton density of selected solids was measured by helium pycnometry at 295 K in a Quantachrome Pentapycnometer. Previous to the measurement, the sample was dried at 393 K for 12 h. Fourier transform infrared (FTIR) spectroscopy was carried out in a Bruker Optics Tensor 27 spectrometer equipped with a Golden Gate Diamond ATR unit. Spectra were collected at 298 K in the range 650-4000 cm^{-1} by co-addition of 32 scans at a nominal resolution of 4 cm^{-1}, taking the spectrum of the empty cell at ambient

UNIVERSITAT ROVIRA I VIRGILI
CHEMISTRY OF DAWSONITES AND APPLICATION IN CATALYSIS
Georgiana Stoica
ISBN:978-84-693-1533-0/DL:T-648-2010

conditions as the background. Raman spectroscopy was carried out in a NXR Raman module connected to a Thermo Nicolet 5700 spectrometer equipped with a thermoelectrically-cooled InGaAs detector. Raman scattering was excited by a Nd:YVO_4 laser operating at 1064 nm. The power of the laser at the surface of the sample was *ca.* 1 W. Spectra were collected at 298 K in the range 100-1200 cm^{-1} by co-addition of 100 scans at a nominal resolution of 4 cm^{-1}, taking the spectrum of the empty capillary at ambient conditions as the background. Transmission electron microscopy (TEM) was carried out in a JEOL JEM-1011 microscope operated at 80 kV and equipped with a SIS Megaview III CCD camera. A few droplets of the sample suspended in ethanol were placed on a carbon-coated copper grid followed by evaporation at ambient conditions. N_2 adsorption-desorption isotherms at 77 K were measured on a Quantachrome Autosorb 1-MP analyzer. Before analysis, the samples were degassed in vacuum at 393 K for 16 h. The BET method[24] was applied to calculate the total surface area, and, the *t*-plot method[25] was used to discriminate between micro- and mesoporosity. The BJH model[26] applied to the desorption branch of the isotherm provided information on the mesopore size distribution. High-resolution Ar adsorption at 87 K was measured in a Micromeritics ASAP 2010 apparatus. The pore size distribution was calculated using a DFT model that assumes cylindrical pore geometry.[27] Thermogravimetric analysis (TGA) was carried out in a Mettler Toledo TGA/SDTA851e microbalance. Analyses were performed in dry air flow of 50 cm^3 STP min^{-1}, ramping the temperature from 298 to 1173 K with a heating rate of 5 K min^{-1}. Differential scanning calorimetry (DSC) was carried out in a Mettler Toledo DSC822e calorimeter following the same procedure as in thermogravimetry.

3. Results and discussion

3.1. As-synthesized material

As shown in Table 4.1, the empirical formula of the as-synthesized (AS) sample was $C_{0.25}H_{3.0}N_{0.2}O_{3.1}Al_{1.0}$, differing from the ammonium-form of dawsonite ($C_{1.0}H_{6.0}N_{1.0}O_{5.0}Al_{1.0}$ or $NH_4AlCO_3(OH)_2$). The ratios C/Al, H/Al, and N/Al were significantly lower in AS, suggesting the presence of additional aluminum-containing phases besides AACH. The formula of AS resembles that of ammonium aluminum carbonate hydroxide reported by Vogel *et al.*[28] ($C_{0.5}H_{3.65}N_{0.3}O_{3.8}Al_{1.0}$ or $(NH_4)_2Al_6(CO_3)_3(OH)_{14}$). These authors prepared AACH by precipitation of aluminum nitrate with ammonium hydroxide and ammonium bicarbonate at pH = 8. Groppi *et al.*[29,30] assumed the same chemical formula for samples prepared using ammonium carbonate at pH = 7.5-8.0, *i.e.* the same route applied in this work. Scholtz *et al.*[31] investigated the influence of pH on the composition of the solid resulting from

precipitation of Al^{3+} ions using Na_2CO_3. In the pH range 6-7, amorphous carbonate-containing aluminum hydroxide was the only component in the precipitate, determined by infrared spectroscopy. However, this amorphous phase coexisted with Na-dawsonite at higher pH. For example, the dawsonite content was 42% when the precipitation was carried out at pH = 8.5.[31]

The conclusions derived by these authors, the similar pH used in the present study, and our composition analyses made it possible to conclude the coexistence of AACH with Al-containing phase(s) in AS. However, as shown in Figure 4.1, the X-ray diffraction pattern of the as-synthesized sample only presented characteristic reflections of ammonium aluminum carbonate hydroxide ($NH_4AlCO_3(OH)_2$, JCPDS 42-250). The material collected in this card was prepared by aging boehmite in a solution of NH_4HCO_3 at 333 K and was claimed to be isostructural with the mineral dawsonite, *i.e.* $NaAlCO_3(OH)_2$.[7] The cell parameters of AS (Table 4.1) are in close correspondence with those reported in JCPDS 42-250). Additionally, the diffraction pattern of AS was indistinguishable to those measured by Vogel *et al.*[28] and Groppi *et al.*[29] for $(NH_4)_2Al_6(CO_3)_3(OH)_{14}$. Consequently, in line with early findings by Scholtz *et al.*,[31] Al-containing phases other than AACH in the precipitate are amorphous. Despite this, the skeleton density of the AS sample measured by helium pycnometry was 2.2 g cm^{-3} (Table 4.1), resembling the reported value for the naturally occurring Na-dawsonite mineral (2.4 g cm^{-3}).[5]

Table 4.1. Characterization data of the samples.

Code	Empirical formula[a]	Cell parameters			ρ_{He}[b]	V_{pore}	V_{micro}[c]	S_{BET}[d]
		a (nm)	*b* (nm)	*c* (nm)	(g cm^{-3})	(cm^3 g^{-1})	(cm^3 g^{-1})	(m^2 g^{-1})
AS	$C_{0.25}H_{3.0}N_{0.2}O_{3.1}Al_{1.0}$	0.661	1.163	0.575	2.18	1.6	0.10	773
C1	-	-	-	-	-	1.7	0	586
C2	-	-	-	-	2.74	1.5	0	500
C3	-	-	-	-	-	0.8	0	210
R1	$C_{1.0}H_{7.2}N_{0.9}O_{5.8}Al_{1.0}$	0.662	1.163	0.579	-	1.2	0.33	1046
R2	$C_{0.7}H_{5.8}N_{0.8}O_{5.6}Al_{1.0}$	0.662	1.163	0.579	2.15	0.7	0.25	782
R3	$C_{0.3}H_{2.4}N_{0.3}O_{3.5}Al_{1.0}$	0.662	1.164	0.578	-	0.7	0	300

[a] Determined from chemical composition analyses. Oxygen was calculated by difference. [b] Skeletal density determined by He pycnometry. [c] *t*-plot method. [d] BET method.

UNIVERSITAT ROVIRA I VIRGILI
CHEMISTRY OF DAWSONITES AND APPLICATION IN CATALYSIS
Georgiana Stoica
ISBN:978-84-693-1533-0/DL:T-648-2010

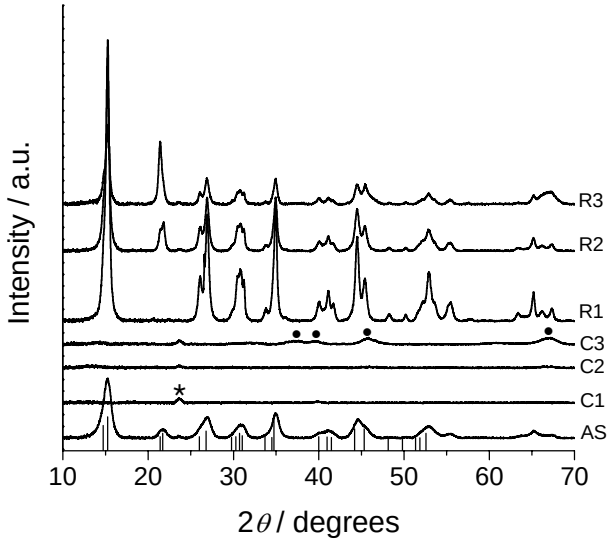

Figure 4.1. XRD patterns of the samples. Vertical lines represent the pattern of $NH_4AlCO_3(OH)_2$ (JCPDS 42-250). The reflections marked by dots in C3 belong to γ-Al_2O_3 (JCPDS 29-63) and the reflection at the position of the asterisk is due to the sample holder.

The Fourier transform infrared spectrum of the as-synthesized sample at room temperature (Figure 4.2) was consistent with X-ray diffraction and only exhibited characteristic absorptions of the hydroxyl, ammonium, and carbonate groups in dawsonite[8]: OH^- (ν_{OH} at 3435 cm^{-1}; δ_{OH} at 985 cm^{-1}), NH_4^+ (ν_{NH} at 3170, 3005, and 2840 cm^{-1}; δ_{NH} at 1830 and 1720 cm^{-1}), and CO_3^{2-} (ν_3 at 1545, 1445, and 1387 cm^{-1}, ν_1 at 1105 cm^{-1}, ν_2 at 852 cm^{-1}, and ν_4 at 755 and 735 cm^{-1}). The weak shoulder at 820 cm^{-1} has been identified in earlier studies but no assignment was made.[32] We tentatively attribute this feature to the deformation of structural OH groups in the dawsonite framework, in analogy with infrared investigations over Al-containing silicate minerals.[33,34] The characteristic Al-O stretching vibration, which typically appears at 740 cm^{-1},[5,9] cannot be clearly distinguished in the spectrum because of strong overlapping with the in-plane bending mode of the carbonate. The Raman spectrum of the AS sample, shown in Figure 4.3, corresponds well to those published over the reference Na-dawsonite mineral.[8,35] Raman shifts related to the carbonate group were identified at 725 and 762 cm^{-1} (ν_4) and 1101 cm^{-1} (ν_1), whereas the bands at 200, 289, and 560 cm^{-1} have been assigned to lattice vibrations.

Transmission electron microscopy evidenced the presence of the ultra-fine particles (< 10 nm) with remarkable size uniformity in AS (Figure 4.4). In line with this observation, the average crystallite size was estimated at *ca.* 6 nm from the XRD pattern of this sample in Figure 4.1, applying the Scherrer equation in the (110) reflection at 15º 2θ. The occurrence of

UNIVERSITAT ROVIRA I VIRGILI
CHEMISTRY OF DAWSONITES AND APPLICATION IN CATALYSIS
Georgiana Stoica
ISBN:978-84-693-1533-0/DL:T-648-2010

very small crystallites has been attributed to the intrinsic characteristics of the AACH precursor as well as to the features of the in-line dispersion-precipitation method.[4]

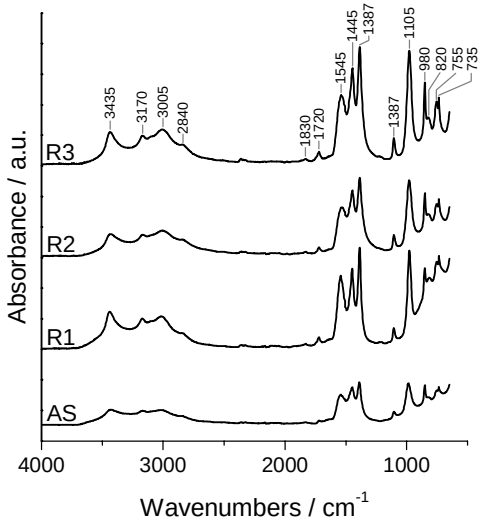

Figure 4.2. FTIR spectra of the as-synthesized and reconstructed samples.

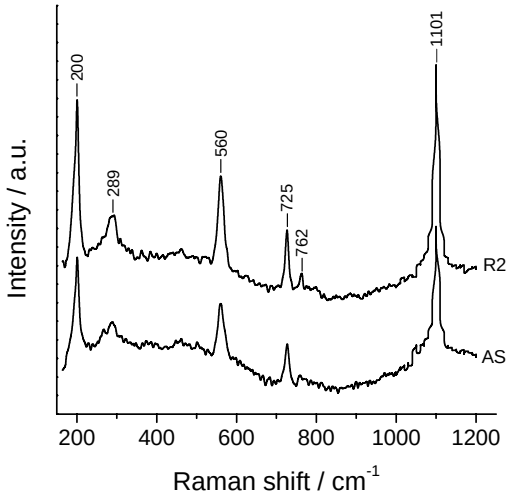

Figure 4.3. Raman spectra of the as-synthesized and reconstructed samples.

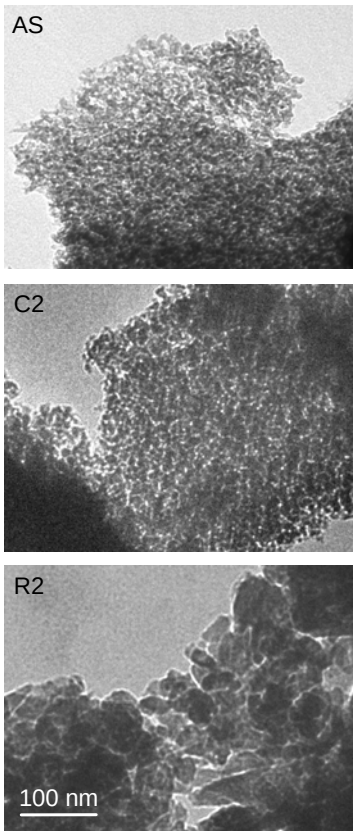

Figure 4.4. TEM micrographs of AS, C2, and R2. The scale bar in the bottom micrograph applies to all the samples.

UNIVERSITAT ROVIRA I VIRGILI
CHEMISTRY OF DAWSONITES AND APPLICATION IN CATALYSIS
Georgiana Stoica
ISBN:978-84-693-1533-0/DL:T-648-2010

The small particle and crystallite sizes determined by TEM and XRD, respectively, made it possible to anticipate a high degree of interparticle porosity in the as-synthesized sample. The textural properties of the solid were determined by adsorption of nitrogen at 77 K (Figure 4.5). Following IUPAC recommendations,[36] the N_2 isotherm of AS can be classified as type IV with H1 hysteresis. These fingerprints are characteristic of a purely mesoporous material with uniform pore size. The latter statement was substantiated by the narrow pore size distribution in the sample, which is centered around 10 nm (inset of Figure 4.5). The total pore volume and specific surface area of AS were 1.6 $cm^3\ g^{-1}$ and 773 $m^2\ g^{-1}$, respectively (Table 4.1). The absence of microporosity was confirmed by application of the *t*-plot method.

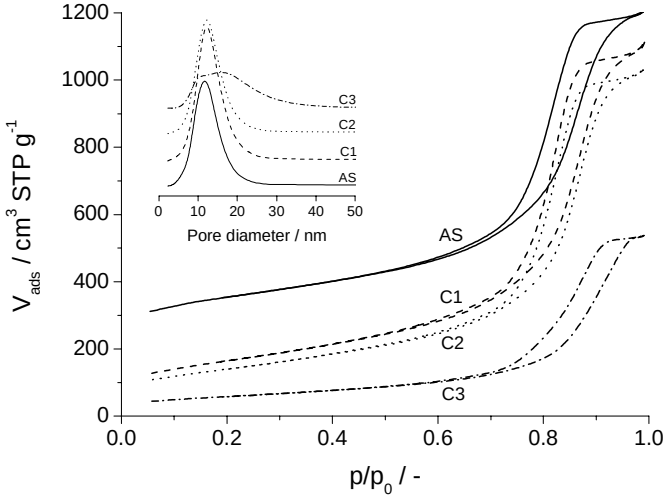

Figure 4.5. N_2 isotherms at 77 K of the as-synthesized and calcined samples. Inset: BJH pore size distributions.

3.2. Thermal decomposition

The thermogravimetric profile of AS in Figure 4.6 showed the one-step weight loss at 420-480 K, assigned to the decomposition of AACH to alumina.[4,17] The transition temperature was estimated at 450 K from the derivative of the weight loss (see inset of Figure 4.6). In good correspondence, the DSC profile of the as-synthesized sample presented a single endothermic transition centered at 470 K (Figure 4.7). The total weight loss of the as-synthesized sample amounted *ca.* 50%, lower than the theoretical weight loss of pure ammonium dawsonite, *i.e.* $NH_4AlCO_3(OH)_2$ (63%). This difference is expected since AS contains some amorphous aluminum hydroxycarbonates in addition to dawsonite.

The XRD patterns of the calcined samples at different temperatures are shown in Figure 4.1. The patterns of C1 (calcined at 523 K) and C2 (calcined at 723 K) were silent, indicating the amorphous nature of the resulting aluminas. The XRD pattern of C3 (calcined

UNIVERSITAT ROVIRA I VIRGILI
CHEMISTRY OF DAWSONITES AND APPLICATION IN CATALYSIS
Georgiana Stoica
ISBN:978-84-693-1533-0/DL:T-648-2010

at 1073 K) exhibited broad reflections associated with γ-Al_2O_3. From these, an average crystallite size of *ca.* 5 nm was estimated by application of the Scherrer equation. As shown elsewhere,[17] the pattern of C4 (calcined at 1473 K) showed a well-crystallized α-Al_2O_3 phase.

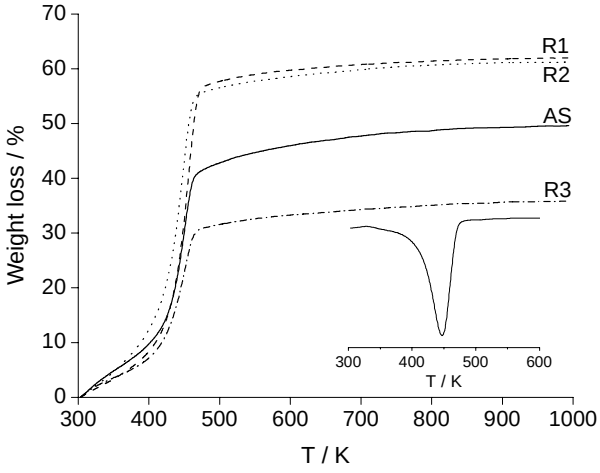

Figure 4.6. TGA profiles of the as-synthesized and reconstructed samples upon thermal treatment in air at 5 K min^{-1}. Inset: derivative of the weight loss for R2.

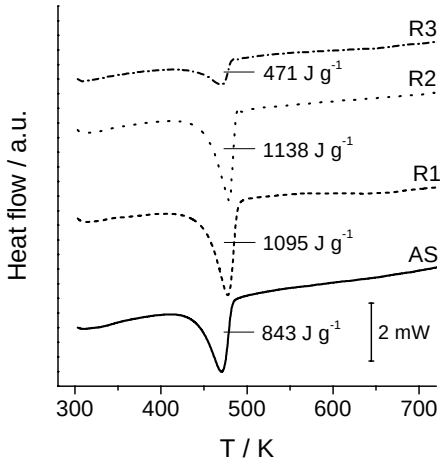

Figure 4.7. DSC profiles of the as-synthesized and reconstructed samples upon thermal treatment in air at 5 K min^{-1}.

The remarkable resistance of the AACH-derived oxides to sinter into large gamma-alumina crystals upon thermal treatment in the broad temperature range of 523-1073 K was additionally demonstrated by TEM and N_2 adsorption. As illustrated in Figure 4.4, the particles in C2 were somewhat larger (10-20 nm) than in AS (< 10 nm) because of a certain degree of sintering, although their remarkable uniform size was maintained. In excellent agreement with microscopy, the N_2 uptake in the calcined samples was lower than in the as-synthesized sample, but the shape of the isotherms in AS, C1, and C2 was identical (type IV with H1 hysteresis) as well as the BJH-pore size distributions (centered at 10 nm) (Figure 4.5). As shown in Table 4.1, the BET surface area decreased by 25% in C1 and C2 samples with respect to AS, due to the disappearance of the original microporosity in AS upon calcination. However, the total pore volume was practically unchanged. In summary, the particle morphology and type of mesoporosity in the as-synthesized material were kept upon calcination at 523 and 723 K. The isotherm of C3 in Figure 4.5 was also characteristic of a mesoporous material, although both S_{BET} and V_{pore} experienced a substantial decrease with respect to C1 and C2 (Table 4.1). The sample calcined at 1073 K experienced a marked degree of sintering, leading to the progressive collapse of the mesoporous network due to the

formation of larger γ-Al_2O_3 crystallites. Consequently, the size of the pores in this sample is less uniform, as revealed by the broadening of the BJH pore size distribution (inset in Figure 4.5). The porous properties of C4 were determined elsewhere.[37] As expected, α-Al_2O_3 exhibited a type II nitrogen isotherm, characteristic of a macroporous material,[36] and a very low surface area (S_{BET} = 4 m^2 g^{-1}).

The skeleton density of C2 was measured by He pycnometry in order to get further insights into the nature of the alumina phase in this particular sample (Table 4.1). The resulting value (2.74 g cm^{-3}) was higher than that determined in AS (2.2 g cm^{-3}). However, it was significantly lower than typical values reported for γ-Al_2O_3 prepared by conventional methods (3.6 g cm^{-3}) or transition aluminas with AlOOH formula like boehmite (3.04 g cm^{-3}) or diaspore (3.38 g cm^{-3}). Accordingly, the unique features of the alumina phase resulting from thermal activation of the as-synthesized material can be further highlighted, exhibiting a highly amorphous character, a low skeleton density, and a well-developed porosity.

3.3. Reconstruction

The oxides obtained by calcination of the as-synthesized material were treated in a 1 M aqueous solution of $(NH_4)_2CO_3$ at 323 K for 24 h. After this treatment, the materials calcined at 523 K, 723 K, and 1073 K recovered the original AACH structure, as corroborated by X-ray diffraction (Figure 4.1). The cell parameters of the orthorhombic crystal structure in the as-synthesized and reconstructed dawsonite-type samples matched (Table 4.1). The infrared and Raman spectra of the R1, R2, and R3 samples also substantiated the reconstruction of the dawsonite structure (Figures 4.2 and 4.3). Treatment of C4 in the ammonium carbonate solution did not lead to any phase change, which can be understood attending to the high stability of the α-alumina phase in this sample. Consequently, this specimen was not used for further investigations.

Figure 4.8 illustrates the XRD patterns of the sample calcined at 723 K after treatment in 1 M aqueous solutions of $(NH_4)_2CO_3$ (pH = 10), Na_2CO_3 (pH = 12), NH_4OH (pH = 12), and NH_4Cl (pH = 6). All treatments led to chemical transformation of C2, indicating the highly reactive nature of this alumina phase. However, the transition from alumina to dawsonite was only induced in $(NH_4)_2CO_3$, whereas other media originated various forms of aluminum hydroxides and (oxi)hydroxides. Treatment in basic solutions of sodium carbonate and ammonia led to bayerite (JCPDS 8-0096) and gibbsite (JCPDS 33-0018), respectively. Treatment in ammonium chloride originated diaspore (JCPDS 1-1284) and treatment in

UNIVERSITAT ROVIRA I VIRGILI
CHEMISTRY OF DAWSONITES AND APPLICATION IN CATALYSIS
Georgiana Stoica
ISBN:978-84-693-1533-0/DL:T-648-2010

distilled water led to boehmite (JCPDS 01-076-1871). These results indicate that both pH and nature of the ions in the solution determined the structural evolution of the AACH-derived alumina. The specificity of ammonium and carbonate ions in the recovery of dawsonite was surprising, taking into account that sodium carbonate can be also used as a precipitating agent of Al^{3+} ions to synthesize Na-dawsonite.[11] In the next chapter, the unique capability of ammonium carbonate as reconstructing agent will be investigated.

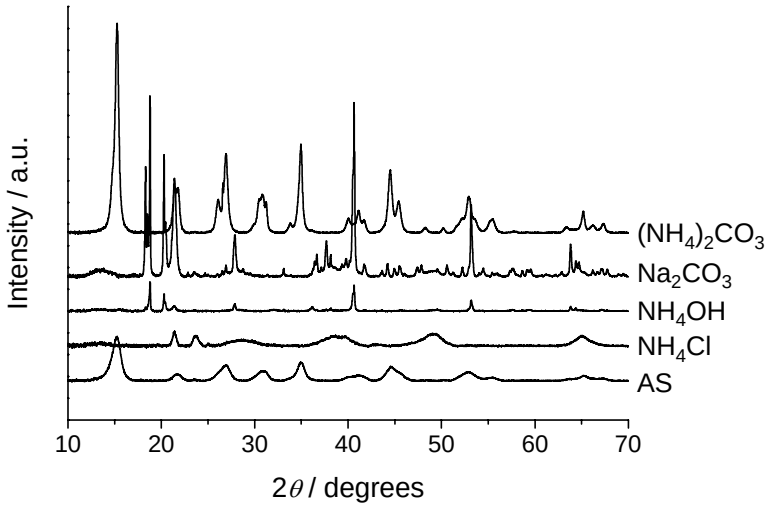

Figure 4.8. XRD patterns of the solids resulting from treatment of C2 in different aqueous media at 323 K for 24 h. The pattern of the AS sample is included for comparative purposes.

The reflections of the dawsonite phase in the reconstructed samples were more intense and sharper than in the parent material (Figure 4.1). Similarly, the definition of the FTIR and Raman spectra in Figures 4.2 and 4.3, respectively, was significantly improved in the reconstructed samples. The average crystallite size, determined by the Scherrer formula in the (110) reflection at 15º 2θ, was 2-3 times higher in the reconstructed samples. In excellent agreement, the TEM image of R2 in Figure 4.4 revealed a substantial increase in particle dimensions. The particle size distribution in R2 is in the broad range of 15-50 nm in contrast with < 10 nm in AS. The above observations indicated that the treatment in $(NH_4)_2CO_3$ brought not only the recovery of the AACH phase, but also an improved crystallization with respect to the original solid. The skeleton density of the as-prepared and reconstructed samples was practically identical (Table 4.1).

We have also investigated whether dawsonite can be recovered if transition metals are structurally incorporated during the synthesis. It is known that this type of materials can accommodate different cations in Al^{3+} positions.[9] Single-phased iron and chromium-

UNIVERSITAT ROVIRA I VIRGILI
CHEMISTRY OF DAWSONITES AND APPLICATION IN CATALYSIS
Georgiana Stoica
ISBN:978-84-693-1533-0/DL:T-648-2010

substituted NH_4-dawsonites, denoted as $Fe_{0.1}$-$Al_{1.1}$ and $Cr_{0.1}$-$Al_{1.1}$, were successfully synthesized (Figure 4.9). As expected, calcination of the precipitates at 723 K for 2 h led to an amorphous oxidic phase, *i.e.* no reflections specific of crystalline Fe_2O_3, Cr_2O_3, or Al_2O_3 were identified. Treatment of the oxide in 1 M $(NH_4)_2CO_3$ aqueous solution at 323 K for 24 h induced the recovery of the dawsonite phase, largely resembling the transformation experienced by the sample without transition metals.

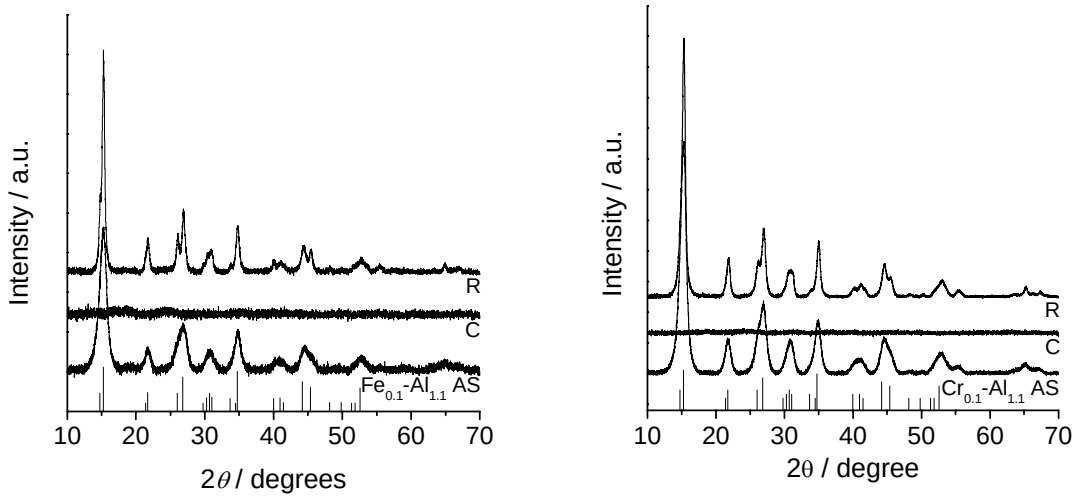

Figure 4.9. XRD patterns of the chromium and iron-substituted dawsonites and the products of calcination and reconstruction in 1 M $(NH_4)_2CO_3$ aqueous solution at 323 K for 30 min. Vertical lines belong to $NH_4AlCO_3(OH)_2$ (JCPDS 42-250).

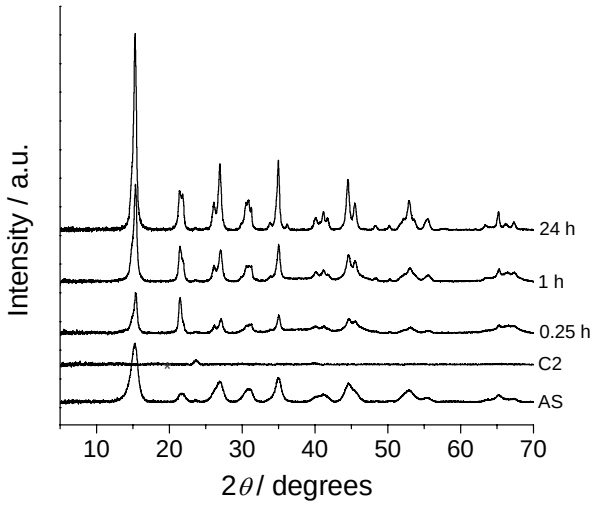

Figure 4.10. XRD patterns during reconstruction of C2 in 1 M $(NH_4)_2CO_3$ aqueous solution at 323 K and different times. The reflection at the position of the asterisk is due to the sample holder.

UNIVERSITAT ROVIRA I VIRGILI
CHEMISTRY OF DAWSONITES AND APPLICATION IN CATALYSIS
Georgiana Stoica
ISBN:978-84-693-1533-0/DL:T-648-2010

The memory effect of AACH-derived Al_2O_3 can be explained on the basis of a dissolution-precipitation mechanism by which the amorphous, highly porous, and low-framework density alumina dissolved to form hydroxyaluminum complexes reacting with ammonium and carbonate anions to precipitate as dawsonite $NH_4AlCO_3(OH)_2$. The reconstruction process was very fast, as revealed by the X-ray diffraction patterns of the solids treated in 1 M $(NH_4)_2CO_3$ solution at 323 K and different times (Figure 4.10). *Ca.* 15 min were sufficient to fully recover the AACH phase. Longer reconstruction times led to further crystallization, as concluded from the development of sharper and more intense diffraction lines. The crystal growth when comparing the as-synthesized and reconstructed materials is likely due to the presence of aluminum in the parent sample as XRD-invisible AACH crystallites or in other amorphous phases.

The molar ratio between $(NH_4)_2CO_3$ and Al_2O_3 in the reconstruction treatment was *ca.* 25, *i.e.* ammonium and carbonate ions are in great excess with respect to aluminum in the solid if considering the reconstruction reaction:

$$Al_2O_3 + 2\,NH_4^+ + 2\,HCO_3^- + H_2O \rightarrow 2\,NH_4AlCO_3(OH)_2$$

Following this line of reasoning, the reconstruction of AS should in principle originate a dawsonite with higher purity. This was unequivocally confirmed by chemical composition analyses of the reconstructed samples. As shown in Table 4.1, the empirical formulas of R1 and R2 differed considerably from that of AS, practically matching the nominal formula of ammonium-dawsonite, *i.e.* $NH_4AlCO_3(OH)_2$. However, the empirical formula of R3 was very similar to AS, indicating only partial reconstruction. Similar conclusions were derived from thermal analysis. The thermogravimetric profiles of R1, R2, and R3 showed the one-step decomposition pattern described for AS. The transition temperature for all samples determined from the derivative of the weight loss was remarkably similar (*ca.* 450 K, see inset of Figure 4.6). The total weight loss of R1 and R2 (*ca.* 65%) was significantly higher than that of AS (*ca.* 50%). The 65% value is very close to the theoretical weight loss in $NH_4AlCO_3(OH)_2$ (*ca.* 63%). Differently, the total weight loss of R3 (*ca.* 35%) was even lower than that of AS (*ca.* 50%). Results from differential scanning calorimetry were in line with thermogravimetry. The position of the endothermic transition due to the decomposition process was very similar (*ca.* 470 K) in the as-synthesized and reconstructed materials. However, the enthalpy associated with the transition in R1 and R2 (*ca.* 1100 J g^{-1}) was higher than in AS (843 J g^{-1}), and a significantly lower value was obtained in R3 (471 J g^{-1}).

UNIVERSITAT ROVIRA I VIRGILI
CHEMISTRY OF DAWSONITES AND APPLICATION IN CATALYSIS
Georgiana Stoica
ISBN:978-84-693-1533-0/DL:T-648-2010

These results proved that reconstruction of AACH-derived aluminas calcined in the range of 523-723 K leads to a *reformed* dawsonite, compositionally corresponding to the nominal formula of the mineral. The sample calcined at 1073 K experienced certain recrystallization attending to the XRD patterns in Figure 4.1. However, the reconstruction process was incomplete. The γ-Al_2O_3 phase visualized in C3 is held responsible for the partial reconstruction of this sample. The memory effect of AACH-derived oxides vanished upon sintering of γ-Al_2O_3 crystals due to relatively high calcination temperatures. The crystallization of gamma-alumina inhibited the dissolution-precipitation mechanism governing the reconstruction process. Therefore, the amorphous, low-skeleton density, and high-surface area properties of the alumina phase in the C1 and C2 samples seem to be essential for the materials to exhibit memory effect.

A certain parallelism can be drawn with the memory effect displayed by Mg-Al oxide obtained by thermal decomposition of hydrotalcite ($Mg_6Al_2(OH)_{16}CO_3{\cdot}4H_2O$).[18] For the latter family of compounds, a dissolution-precipitation mechanism has been proposed to explain the memory effect[38,39] and is thought to be promoted by the poor crystallinity and high-surface area of the resulting $Mg(Al)O_x$ oxide (with periclase structure).[40] Calcined Mg-Al hydrotalcite displays memory effect in very diverse media (vapor-containing gas streams, water, or aqueous solutions of NH_4OH or Na_2CO_3). Differently, the conditions under which AACH-derived aluminas reconstruct are more restricted (limited to $(NH_4)_2CO_3$ solution).

The reconstructed dawsonites exhibited different structural, morphological, and compositional features *vis à vis* the parent material. The former changes should also impact on the porous properties of the reformed materials, as quantitatively assessed by gas adsorption analysis. Figure 4.11 compares the N_2 adsorption-desorption isotherms at 77 K of the as-synthesized and reconstructed samples. The nitrogen uptake decreased in the order AS > R1 > R2 > R3, causing a progressive drop of the total pore volume (V_{pore}, Table 4.1). This is attributed to the occurrence of larger crystals in the reconstructed samples, inducing a diminished interparticle volume. In relation to the as-synthesized sample, larger crystals were induced by sintering due to calcination of AACH as well as the crystallization during reconstruction. In addition to the lower N_2 uptake, indicative of decreased porosity, the hysteresis loops in the isotherms of R1 and R2 were expanded in the p/p_0 range with respect to that of AS, indicating a broader distribution of mesopores. In accordance, TEM investigations showed larger particles and a broader particle size distribution in R2 (Figure 4.4). Consequently, the isotherms of the R1 and R2 samples are indicative of a less

UNIVERSITAT ROVIRA I VIRGILI
CHEMISTRY OF DAWSONITES AND APPLICATION IN CATALYSIS
Georgiana Stoica
ISBN:978-84-693-1533-0/DL:T-648-2010

regular porous network compared to that of AS, and a classification to a particular type in the former samples cannot be rigorously made.

Despite the lower pore volume and larger average mesopore size of R1 compared to AS, the BET surface area of R1 (1046 $m^2\ g^{-1}$) was considerably higher than AS (773 $m^2\ g^{-1}$). This is due to the newly generated micropores in the reconstructed material. Application of the *t*-plot method resulted in an estimated V_{micro} = 0.3 $cm^3\ g^{-1}$ in R1, *i.e.* more than three times higher than in the starting AS material. Consequently, the surface area due to the microporosity in R1 largely exceeds the reduced N_2 uptake due to the calcination and reconstruction steps. Micropore generation in R2 was also confirmed (V_{micro} = 0.25 $cm^3\ g^{-1}$), although in this case the BET surface area was very similar to the parent material (*ca.* 780 $m^2\ g^{-1}$). The N_2 adsorption of R3 deviated from the trend in R1 and R2, showing a complex step-wise hysteresis loop (Figure 4.11). In addition, this sample contained no microporosity (Table 4.1).

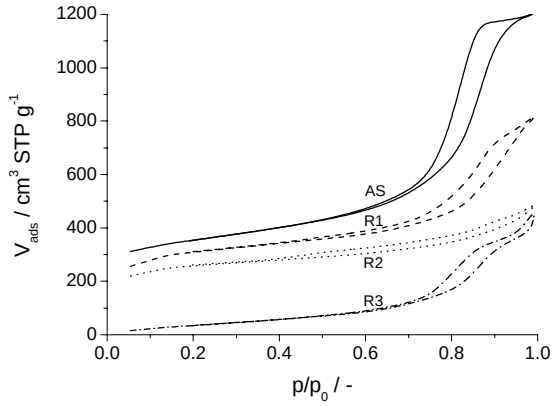

Figure 4.11. N_2 adsorption-desorption isotherms at 77 K of AS and reconstructed samples.

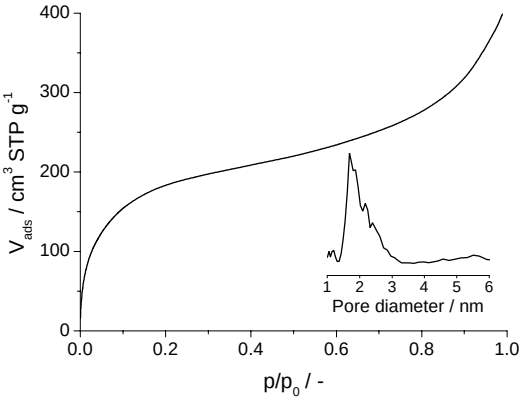

Figure 4.12. Ar adsorption isotherms at 87 K of R2. Inset: DFT pore size distribution.

More detailed assessment of the micropore region in the samples was tackled by high-resolution Ar adsorption at 87 K. Figure 4.12 illustrates the adsorption isotherm of argon over R2. The micropores in the sample are responsible of the Ar uptake at low relative pressures ($p/p_0 < 0.2$), whereas the filling of the mesopores occurred mainly at $p/p_0 > 0.6$. As expected from proper gas adsorption measurements, the total uptake of R2 in the N_2 and Ar measurements coincided (400 cm^3 STP g^{-1}). As shown in the inset of Figure 4.12, the micropore size distribution was relatively narrow, being centered at 2 nm. However, the absence of a well-defined plateau between the low (< 0.2) and high (> 0.6) relative pressure indicated that the micropores in the range of 1.5-4 nm overlapped the lower segment of mesopores.

Our discovery made it possible to extend the unique memory property of oxides derived from particular layered materials such as hydrotalcites to other families of minerals. The structural, compositional, and porous changes induced by the reconstruction treatment open exciting possibilities to alter the properties of dawsonite-type compounds in their various applications (catalyst, ingredient in antiacids, polymer-stabilizer, fire retardant). A more quantitative description of the mechanism and kinetics of the reconstruction process will be presented in the next chapter.

4. Conclusions

Aluminas resulting from thermal decomposition of NH_4-(B_x-Al_{1+x}), where B = Fe or Cr, and x = 0 or 0.1, have the ability to recover the dawsonite structure by treatment in ammonium carbonate solutions at 323 K. The memory effect of dawsonite took place uniquely with $(NH_4)_2CO_3$; treatment in solutions of NH_4OH, NH_4Cl, and Na_2CO_3 led to aluminum (oxi)hydroxides. The reconstruction was complete for the solids calcined at 523 and 723 K. The latter materials were characterized by a highly amorphous and low-density alumina phase, with a well-developed and uniform mesoporosity. Formation of larger γ-Al_2O_3 crystals by calcination at 1073 K and ultimately α-Al_2O_3 by calcination at 1473 K led to partial or no recovery, respectively. The reconstruction can be explained on the basis of a dissolution-precipitation mechanism by which the amorphous alumina dissolved to form hydroxyaluminum complexes reacting with ammonium and carbonate anions to precipitate as $NH_4AlCO_3(OH)_2$. The reconstructed samples displayed higher purity than the parent material. This is due to the presence of amorphous Al-containing phase(s) in the as-synthesized sample coexisting with AACH. All the phases were selectively converted into dawsonite by thermal decomposition and $(NH_4)_2CO_3$ treatment. The *reformed* samples consisted of relatively large crystals with developed microporosity, in contrast to the smaller crystals in the purely mesoporous as-synthesized solid. Our results extend the unique memory property of layered materials such as hydrotalcites to other families of mineral-like compounds.

Acknowledgments

Johan C. Groen is thanked for the technical assistance and valuable related discussions on the gas adsorption and density analyses.

References

[1] M. Giannos, M. Hoang, T. W. Turney, *Chem. Lett.* **1998**, 793.

[2] G. I. Horita, E. P. Goulart, O. Thomaz, A. Monteiro, D. G. de Souza, *Mater. Sci. Forum* **1999**, 299-300, 3.

[3] I. Pitsch, W. Gebner, A. Brückner, H. Mehner, S. Mohmel, D.-C. Uecker, M.-M. Pohl, *J. Mater. Chem.* **2001**, 11, 2498.

[4] M. Santiago, M.S. Yalfani, J. Pérez-Ramírez, *J. Mater. Chem.* **2006**, 16, 2886.

[5] A. J. Frueh, J. P. Golightly, *Can. Mineral.* **1967**, 9, 51.

[6] E. Corazza, C. Sabelli, S. Vannucci, *Neues Jahrb. Mineral. Monatsh.* **1977**, *9*, 381.

[7] T. Iga, S. Kato, *J. Ceram. Soc. Jpn.* **1978**, 86, 509.

[8] C. J. Serna, J. V. Garcia-Ramos, M. J. Peña, *Spectrochim. Acta* **1985**, 41A, 697.

[9] A. A. Ali, M. A. Hasan, M. I. Zaki, *Chem. Mater.* **2005**, 17, 6797.

[10] C. Ma, X. Zhou, T. Zhu, *Mater. Chem. Phys.* **2001**, 72, 374.

[11] X. Zhang, Z. Wen, Z. Gu, X. Xu, Z. Lin, *J. Solid State Chem.* **2004**, 177, 849.

[12] C. J. Serna, J. L. White, S. L. Hem, *J. Pharm. Sci.* **1978**, 67, 324.

[13] P. V. Bonsignore, *Plast. Eng.* **1976**, 32, 41.

[14] E. A. Woycheshin, R. J. Rigge, I. Sobolev, *US Patent 3,878,166*, **1975**.

[15] R. L. Altman, L. A. Mayer, A.C. Ling, *US Patent 4,406,797*, **1983**.

[16] G. Gillman, A. Noble, *Environmental Quality Management* **2005**, 15, 59.

[17] M. S. Yalfani, M. Santiago, J. Pérez-Ramírez, *J. Mater. Chem.* **2007**, 17, 1222.

[18] F. Cavani, F. Trifiro, A. Vaccari, *Catal. Today* **1991**, 11, 173.

[19] R. B. Emerson, W. A. Brian, *US Patent 3,557,025*, **1971**.

[20] R. L. Altman, *US Patent 4,356,157*, **1982**.

[21] S. Abelló, J. Pérez-Ramírez, *Adv. Mater.* **2006**, 18, 2436.

[22] B. D. Cullity, S. R. Stock; In *Elements of X-Ray Diffraction*; Prentice-Hall: New Jersey, 2001, p. 93.

[23] P. Scherrer, *Gottingen Nachr.* **1918**, 2, 98.

[24] S. Brunauer, P. H. Emmett, E. Teller, *J. Am. Chem. Soc.* **1938**, 60, 309.

[25] B. C. Lippens, J. H. de Boer, *J. Catal.* **1965**, 4, 319.

[26] E. P. Barret, L. G. Joyner, P. P. Hallenda, *J. Am. Chem. Soc.* **1951**, 73, 373.

[27] M. Thommes; In *Nanoporous Materials: Science and Engineering*; G. Q. Lu, X. S. Zhao, Eds.; Imperial College Press: London, 2004; pp. 317-364.

[28] R. F. Vogel, G. Marcelin, W. L. Kehl, *Appl. Catal.* **1984**, *12*, 234.

UNIVERSITAT ROVIRA I VIRGILI
CHEMISTRY OF DAWSONITES AND APPLICATION IN CATALYSIS
Georgiana Stoica
ISBN:978-84-693-1533-0/DL:T-648-2010

[29] G. Groppi, M. Belloto, C. Cristiani, P. Forzatti, P. L. Villa, *Appl. Catal. A* **1993**, 104, 101.

[30] G. Groppi, C. Cristiani, P. Forzatti, M. Belloto, *J. Mater. Sci.* **1994**, 29, 3441.

[31] E. C. Scholtz, J. R. Feldkamp, J. L. White, S. L. Hem, *J. Pharm. Sci.* **1984**, 73, 967.

[32] C. J. Serna, J. L. White, L. S. Hem, *Clays Clay Miner.* **1977**, 25, 384.

[33] T. Delineau, T. Allard, J.-P. Muller, O. Barres, J. Yvon, J.-M. Cases, *Clays Clay Miner.* **1994**, 42, 308.

[34] J. T. Kloprogge, S. Komarneni, K. Yanagisawa, R. Fry, R. L. Frost, *J. Colloid Interface Sci.* **1999**, 212, 562.

[35] M.-L. C. Sirbescu, P. I. Nabelek, *Am. Mineral.* **2003**, 88, 1055.

[36] K. S. W. Sing, D. H. Everett, R. A. W. Haul, L. Moscou, R. A. Pierotti, J. Rouquerol, T. Siemieniewska, *Pure Appl. Chem.* **1985**, 57, 603.

[37] M. Santiago, J. Pérez-Ramírez, *Environ. Sci. Technol.* **2007**, 41, 1704.

[38] M. Rajamathi, G. D. Nataraja, S. Ananthamurthy, P. V. Kamath, *J. Mater. Chem.* **2000**, 10, 2754.

[39] F. Millange, R. I. Walton, D. O'Hare, *J. Mater. Chem.* **2000**, 10, 1713.

[40] J. Pérez-Ramírez, S. Abelló, N. M. van der Pers, *Chem. Eur. J.* **2007**, 13, 870.

UNIVERSITAT ROVIRA I VIRGILI
CHEMISTRY OF DAWSONITES AND APPLICATION IN CATALYSIS
Georgiana Stoica
ISBN:978-84-693-1533-0/DL:T-648-2010

UNIVERSITAT ROVIRA I VIRGILI
CHEMISTRY OF DAWSONITES AND APPLICATION IN CATALYSIS
Georgiana Stoica
ISBN:978-84-693-1533-0/DL:T-648-2010

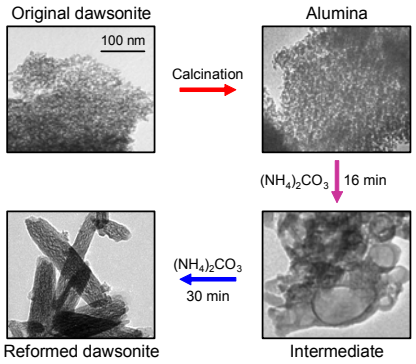

Chapter 5

Reconstruction of Dawsonite by Alumina Carbonation in $(NH_4)_2CO_3$: Requisites and Mechanism

The products derived from thermal decomposition of NH_4, K, and Na-dawsonites have structural memory, *i.e.* the original mineral structure in ammonium form ($NH_4AlCO_3(OH)_2$) was recovered upon treatment of the oxide in aqueous $(NH_4)_2CO_3$ solution under mild conditions at pH ~ 10. In contrast, treatment of calcined dawsonites in K_2CO_3 and Na_2CO_3 solutions led to bayerite. The mechanism and kinetics of the reconstruction process were investigated by experiments in a parallel-reactor system varying treatment, time, temperature, molar $(NH_4)_2CO_3/Al_2O_3$ ratio, $(NH_4)_2CO_3$ concentration, solvent, and dawsonite composition. The reconstruction of the dawsonite structure from alumina followed a dissolution-precipitation mechanism and was accomplished in 10-30 minutes depending on the temperature. The transformation went through an intermediate carbonate-containing aluminum hydroxide compound of amorphous nature followed by progressive dawsonite crystallization upon ammonium incorporation. In contrast with other families of materials having structural memory such as hydrotalcites, the original and reconstructed dawsonites presented marked morphological and porosity differences. Upon reconstruction, nanoparticles in the as-made and calcined materials gradually transformed by way of complex intermediate morphologies into acicular nano-needles with newly developed microporosity.

This chapter is based on the following publication:
G. Stoica, J. C. Groen, S. Abelló, R. Manchanda, J. Pérez-Ramírez, *Chem. Mater.* **2008**, 20, 3973.

UNIVERSITAT ROVIRA I VIRGILI
CHEMISTRY OF DAWSONITES AND APPLICATION IN CATALYSIS
Georgiana Stoica
ISBN:978-84-693-1533-0/DL:T-648-2010

1. Introduction

Considerable effort is being deployed to develop smart materials and structures for creating hitherto novel products and for performance enhancement of existing products in a broad range of applications. Smart materials have the ability to respond in a controlled manner to external stimuli, such as mechanical deformation, stress, pressure, temperature, chemicals, incident radiation, electric and magnetic fields, electric charges, *etc*.[1] Materials responses to these types of stimuli include the rearrangement of atomic and molecular structures, the creation and motion of crystallographic defects, chemical reactions, absorption and emission of photons, generation of charge and voltage, and other effects. Well-known examples of smart materials are piezoelectric sensors,[2] shape-memory metal alloys,[3] shape-memory polymers,[4] magnetic-memory metal alloys,[5] halochromic and chromogenic systems,[6] and compounds with structural memory.[7,8]

In the context of the latter category, hydrotalcite-like compounds can be considered as prototypic materials. This family of anionic clays consists of brucite-like layers that transform into high-surface area well-dispersed mixed oxides on calcination.[9,10] The oxide is able to recover the original layered structure in contact with humid gas, water, and aqueous salt solutions.[7,9,11-17] The memory property of hydrotalcites has multiple applications: removal of anions in contaminated water,[18,19] development of drug delivery systems,[20,21] and insertion of new functionalities and active catalytic sites.[22,23] The retrotopotactic transformation in hydrotalcites is accepted to occur via a dissolution-precipitation mechanism,[24,25] by which the regeneration takes place through crystallization from solution. The poorly crystalline nature of the mixed oxide derived by calcination of hydrotalcites is thought to be key in the attainment of the memory effect.[17] As anticipated for a reversible transformation, the platelet-like morphology and type of mesoporosity in the original and reconstructed hydrotalcites are essentially maintained.[16,26]

As concluded in the previous chapter, we have extended the unique structural memory property of oxides derived from hydrotalcites to dawsonite-type compounds.[8] Natural dawsonite is a mineral with formula $NaAlCO_3(OH)_2$ exhibiting various crystal habits including prisms, aciculae, fibers, spheres, rosettes, and random aggregates.[27] It exhibits an orthorhombic-dipyramidal structure, consisting of an assemblage of edge-sharing distorted $AlO_2(OH)_4$ and $NaO_4(OH)_2$ octahedra and CO_3^{2-} groups.[28,29] One oxygen of the carbonate is hydrogen-bonded to two hydroxyl groups, strengthening the three-dimensional framework.[28]

UNIVERSITAT ROVIRA I VIRGILI
CHEMISTRY OF DAWSONITES AND APPLICATION IN CATALYSIS
Georgiana Stoica
ISBN:978-84-693-1533-0/DL:T-648-2010

Besides $NaAlCO_3(OH)_2$, a variety of compositions with dawsonite-type structure have been synthesized by changing the nature of sodium or aluminum cations in the structure.[30-32] Potassium and ammonium dawsonites are the most studied analogues of the mineral and are composed of the same $AlO_2(OH)_4$ chains of octahedra as the dawsonite mineral. The structure of K-dawsonite is visualized in Figure 5.1. The NH_4-analogue, *i.e.* $NH_4AlCO_3(OH)_2$, is often denoted as ammonium aluminum carbonate hydroxide or by the acronym AACH.

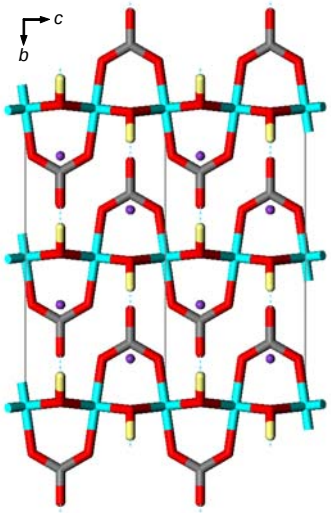

Figure 5.1. Structure of potassium dawsonite ($KAlCO_3(OH_2)$) in the (100) direction. Cell parameters and atomic coordinates taken from Fernández-Carrasco *et al.*[47] K: purple spheres, Al: blue sticks, C: grey sticks, O: red sticks, and H: yellow sticks. Dashed lines represent hydrogen bonds.

As presented in ***Chapter 4***, amorphous and low-skeleton density aluminas obtained by decomposition of AACH at 523 and 773 K reformed the original dawsonite structure upon treatment in 1 M $(NH_4)_2CO_3$ solution at 323 K and ambient pressure for 24 h according to:

$$Al_2O_3 + 2\,NH_4^+ + 2\,HCO_3^- + H_2O \rightarrow 2\,NH_4AlCO_3(OH)_2 \qquad (1)$$

The retrotopotactic transformation of dawsonite did not solely imply the recovery of the original structure but also originated changes in composition, morphology, and porosity with respect to the parent material.[8] However, dawsonite reconstruction from AACH-derived Al_2O_3 by $(NH_4)_2CO_3$ treatment was attained in a single set of conditions with respect to temperature, time, and composition of the starting dawsonite. Consequently, a detailed mechanistic and kinetic picture of the reconstruction process was not provided. This understanding is needed to exploit the memory property of this family of materials. For example, the ability of tailoring the physico-chemical characteristics (shape, size, porosity) by reconstruction may impact on the properties of dawsonite in reported applications as antiacid,

polymer stabilizer, fertilizer additive, flame retardant, adsorbent for industrial flue gases, and catalyst precursor.[33-38] Besides, the carbonation of alumina leading to dawsonite (eq. 1) is linked to CO_2 mineralization, a topic of great environmental relevance for alleviating global warming. Several authors reported that dawsonite is a product of CO_2 trapping by aluminosilicate minerals, such as feldspars, at high pressure.[27,39] Accordingly, investigating the interaction of alumina with carbonate-containing solutions is interesting to preliminary assess the potential of Al-containing compounds in sequestration of carbon dioxide.

This chapter reports the mechanism and kinetics of dawsonite recrystallization from amorphous alumina by carbonation in aqueous $(NH_4)_2CO_3$ solution. Reconstruction was specific to ammonium carbonate, since treatment in other carbonate salts such as K_2CO_3 and Na_2CO_3 led to bayerite. The influence of time, temperature, reconstruction media (salt and solvent), molar $(NH_4)_2CO_3/Al_2O_3$ ratio, $(NH_4)_2CO_3$ concentration, and chemical composition and precipitation conditions of the original dawsonite on the reconstruction process have been investigated using a parallel reactor system. Structural, morphological, and porosity changes along the course of the treatments have been systematically studied by a number of characterization techniques and key factors conferring the unique memory feature to this family of materials are discussed.

2. Experimental

2.1. Materials and treatments

NH_4-Al, K-Al, and Na-Al dawsonites were synthesized by co-precipitation at constant pH using the in-line dispersion-precipitation (ILDP) method.[40] Briefly, aqueous solutions of $Al(NO_3)_3 \cdot 9H_2O$ (1.1 M) and the precipitating agent ($(NH_4)_2CO_3$, K_2CO_3 or Na_2CO_3, 2 M) were continuously fed to the miniaturized precipitation chamber (volume of *ca.* 6 cm^3), which was stirred at 13 500 rpm. The synthesis was carried out at pH 8 or 10 (by adjusting the flow of the basic solution) with an average residence time of 18 s. The resulting slurry was aged at 333 K for 3 h, followed by filtration, washing, and drying at 333 K for 12 h. The as-synthesized samples were calcined in static air at 723 K during 2 h using a heating rate of 5 K min^{-1}.

Reconstruction experiments were conducted in a fully automated Multimax liquid-phase parallel chemical synthesizer from Mettler Toledo, consisting of 16 parallel-batch glass reactors (17 mm i.d., total volume 50 cm^3) in four independent blocks and enabling high-throughput experimentation.[41,42] The treatment consisted in dispersing the oxide powder in a solution under magnetic stirring (350 rpm). The influence of various parameters such as time

(0-30 min), temperature (298-343 K), media ($(NH_4)_2CO_3$, K_2CO_3, Na_2CO_3), concentration of the carbonate salt (0.01-2 M), molar $(NH_4)_2CO_3/Al_2O_3$ ratio (2-25), solvent (water, methanol), and dawsonite composition (*X*-Al where *X* = NH_4, K, Na) on the reconstruction process was investigated. The treated samples were filtered, thoroughly washed with deionized water until neutral pH, and dried at 333 K for 12 h. All chemicals used were purchased from Panreac and Sigma-Aldrich and had purities > 98%. Along the chapter, the as-synthesized, calcined, and reconstructed samples are generally identified by the codes AS, C, and R, respectively. The number in the code of the reconstructed samples refers to the treatment time in minutes. If not explicitly mentioned, the AS sample refers to NH_4-Al dawsonite.

2.2. Techniques

Powder X-ray diffraction patterns were acquired in transmission using a Bruker AXS D8 Advance diffractometer equipped with a Cu tube, a Ge(111) incident beam monochromator (λ = 0.1541 nm), and a Vantec-1 PSD. Data were recorded in the 2θ range of 5-70º with an angular step size of 0.016º and a counting time of 6 s per step. Fourier transform infrared spectroscopy was carried out in a Bruker Optics Tensor 27 spectrometer equipped with a Golden Gate Diamond ATR unit. Spectra were collected at room temperature in the range 650-4000 cm^{-1} by co-addition of 32 scans at a nominal resolution of 4 cm^{-1}, taking the spectrum of the empty cell at ambient conditions as the background. Transmission electron microscopy (TEM) was carried out in a JEOL JEM-1011 microscope operated at 80 kV and equipped with a SIS Megaview III CCD camera. A few droplets of the sample suspended in ethanol were placed on a carbon-coated copper grid followed by evaporation at ambient conditions. Environmental scanning electron microscopy (ESEM) was carried out in a FEI Quanta 600 FEG microscope operated at 30 kV. Nitrogen adsorption-desorption isotherms at 77 K were measured on a Quantachrome Autosorb-6B analyzer. Before analysis, the samples were degassed in vacuum at 393 K for 16 h. The BET method[43] was applied to calculate the total surface area, and the *t*-plot method[44] was used to discriminate between micro- and mesoporosity. The BJH model[45] applied to the adsorption branch of the isotherm provided information on the mesopore size distribution. Mercury porosimetry was measured on Pascal 140 and 440 porosimeters (Thermo Electron), which operate in the pressure range of 0.001-400 MPa. Prior to the intrusion-extrusion experiment, the sample was degassed (10^{-1} Pa) at 373 K for 16 h. Thermogravimetric analysis (TGA) was carried out in a Mettler Toledo TGA/SDTA851e microbalance. Analyses were performed in dry air flow of 50 cm^3 STP min^{-1}, ramping the temperature from 298 to 1173 K at 5 K min^{-1}.

UNIVERSITAT ROVIRA I VIRGILI
CHEMISTRY OF DAWSONITES AND APPLICATION IN CATALYSIS
Georgiana Stoica
ISBN:978-84-693-1533-0/DL:T-648-2010

3. Results and discussion

3.1. Reconstruction kinetics

Chapter 4 reported the reconstruction of the dawsonite structure from amorphous alumina derived from calcination of AACH (ammonium aluminum carbonate hydroxide) by treatment under the following conditions: 1 M $(NH_4)_2CO_3$ aqueous solution, $(NH_4)_2CO_3/Al_2O_3$ ratio of 25, 323 K, and 24 h. As stressed in the *Introduction*, a wider examination of conditions is needed in order to gain in-depth mechanistic and kinetic understanding of the reconstruction process. This includes temperature, time, and concentration, molar ratio of reactants, reconstruction media, and chemical composition of the starting dawsonite.

X-ray diffraction made it possible to follow the evolution in time of amorphous alumina to crystalline dawsonite upon treatment at the above conditions (Figure 5.2). The solid remained amorphous in the first stages of the treatment and the characteristic (110) reflection of the dawsonite phase at $2\theta = 15^o$ became discernible after 8 min in the ammonium carbonate aqueous solution at 323 K. No intermediate phase of crystalline nature was detected in this transition. The X-ray diffraction pattern of ammonium dawsonite ($NH_4AlCO_3(OH)_2$, JCPDS 42-250) was fully developed after *ca.* 15 min. Longer treatment times led to dawsonite crystallization as the diffraction lines progressively get sharper and more intense. The experiment illustrated in Figure 5.2 was conducted at different temperatures in the range of 298-343 K maintaining other conditions expressed above.

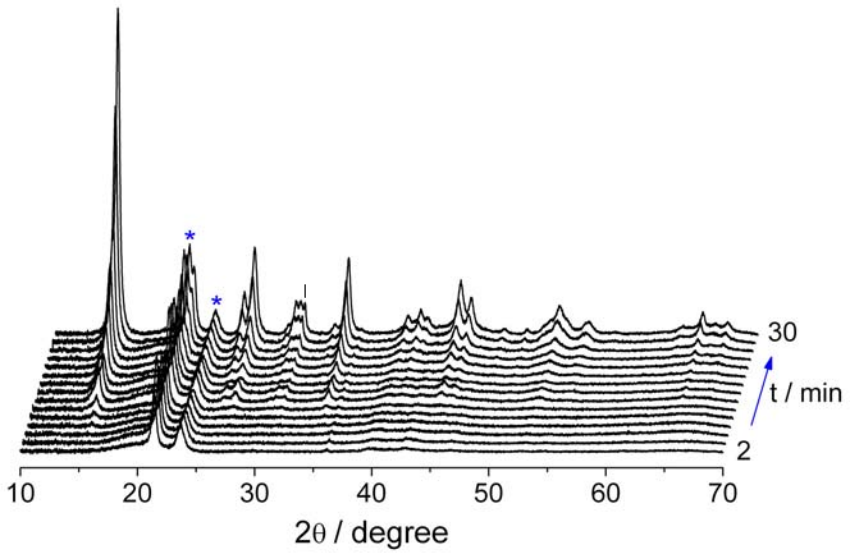

Figure 5.2. XRD patterns during treatment of AACH-derived alumina in 1 M $(NH_4)_2CO_3$ aqueous solution at 323 K. The reflections marked with asterisk are due to the sample holder.

UNIVERSITAT ROVIRA I VIRGILI
CHEMISTRY OF DAWSONITES AND APPLICATION IN CATALYSIS
Georgiana Stoica
ISBN:978-84-693-1533-0/DL:T-648-2010

For the sake of conciseness, Figure 5.3 shows the XRD patterns of the solids after treatment at different temperatures for 30 min. The diffractograms of the as-synthesized dawsonite (AS) and calcined product at 723 K (C) are also shown for comparison. Sample C exhibited very broad reflections at 2θ = 45º and 67º, indicating the presence of tiny crystallites of γ-Al_2O_3 (JCPDS 29-63) in the sub-nanometer range. The pattern of the sample upon 30 min treatment at 298 K in 1 M $(NH_4)_2CO_3$ did not show any sign of reconstruction.

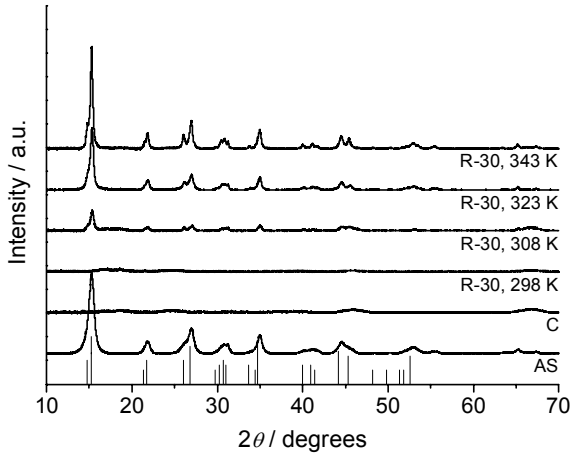

Figure 5.3. XRD patterns of the as-synthesized, calcined, and reconstructed samples at different temperatures for 30 min. The starting dawsonite was in the ammonium form and the reconstruction of the oxide was conducted in 1 M $(NH_4)_2CO_3$ aqueous solution. Vertical lines belong to $NH_4AlCO_3(OH)_2$ (JCPDS 42-250).

Dawsonite reconstruction was accelerated upon increasing temperature from 308 K to 343 K, since the diffraction lines of the mineral-like phase become sharper and more intense at the same treatment time. Consequently, the time at which the first reflection of dawsonite appeared in a similar experiment to that shown in Figure 5.2 was shorter on increasing the treatment temperature: 20 min at 308 K, 8 min at 323 K, and only 4 min at 343 K. In other words, the carbonation of alumina to dawsonite in $(NH_4)_2CO_3$ at 343 K was 2 and 5 times faster than at 323 K and 308 K, respectively. Besides, comparison of R-30 treated at 323 and 343 K with AS in Figure 5.3 indicated sharper reflections in the reconstructed samples, indicative of the occurrence of larger crystals than in the as-synthesized dawsonite. The average crystallite size, estimated by the Scherrer formula in the (110) reflection, was *ca.* 4-6 times larger in the R-30 samples (25 nm at 323 K and 35 nm at 343 K) than in the AS sample (6 nm). This further confirmed that the structural retrotransformation of AACH-derived alumina to dawsonite is accompanied by a marked crystal growth, which we have referred to as dawsonite *reforming* in the previous chapter.

UNIVERSITAT ROVIRA I VIRGILI
CHEMISTRY OF DAWSONITES AND APPLICATION IN CATALYSIS
Georgiana Stoica
ISBN:978-84-693-1533-0/DL:T-648-2010

The influence of the concentration of the ammonium carbonate solution and the molar ratio ammonium carbonate-to-alumina were also investigated. The experiments reported in Figures 5.2 and 5.3 applied 1 M $(NH_4)_2CO_3$ aqueous solution (pH 10) and excess of ammonium carbonate ($(NH_4)_2CO_3/Al_2O_3$ = 25) compared to the stoichiometric ratio of 2 according to eq. 1. As anticipated, the structural memory of dawsonite was also manifested when the ammonium carbonate to alumina ratio was 10 and 2. The reconstruction proceeded in a similar time scale for all ratios at 323 K with respect to the appearance of the first dawsonite reflection and the crystallite sizes after 30 min treatment did not vary significantly. The pH of the ammonium carbonate solution plays an important role on the reconstruction process. No sign of dawsonite formation or any other transformation was observed after 30 min at 323 K when the $(NH_4)_2CO_3$ concentration was 0.2 M (pH 8.8). It can be inferred that the pH of this solution did not ensure the minimum concentration of ions required to convert alumina into dawsonite. Increasing the concentration to 0.5 M and up to 2 M led to pH in the relatively narrow range of 9.5-10.5, where dawsonite formation within the practiced treatment time of 30 min occurred. Next section further elaborates on the influence of pH on the product of alumina treatment in solutions of different carbonate salts and concentrations.

3.2. Influence of dawsonite composition and treatment media

Reconstruction treatments have so far been conducted over NH_4-Al dawsonite. In order to determine how general the memory property is, the dependence of the process on the chemical composition of the starting material has been studied. The main results of the treatments are summarized in Table 5.1.

Similarly to NH_4-Al dawsonite, Na-Al and K-Al dawsonites were synthesized by precipitation at pH 8, using Na_2CO_3 and K_2CO_3 as precipitating agents, respectively. These samples are labeled as Na-Al and K-Al. The X-ray diffraction patterns of the as-synthesized materials (Figure 5.4) showed dawsonite as the only crystalline phase, *i.e.* $NaAlCO_3(OH)_2$ (JCPDS 45-1359) and $KAlCO_3(OH)_2$ (JCPDS 21-979). The calculated cell parameters for the sodium, ammonium, and potassium dawsonites corresponded well with crystallographic data in the literature.[28,46,47] As visualized in Figure 5.1, the three forms of dawsonite have an orthorhombic lattice and are composed of the same $AlO_2(OH)_4$ chains of octahedra.[46] The different symmetry of NH_4 and K-dawsonites (base-centered, space group *Cmcm*) and Na-dawsonite (body-centered, space group *Imma*) renders a larger *c* dimension in the former two materials.[30,46,47]

UNIVERSITAT ROVIRA I VIRGILI
CHEMISTRY OF DAWSONITES AND APPLICATION IN CATALYSIS
Georgiana Stoica
ISBN:978-84-693-1533-0/DL:T-648-2010

Thermal treatment of Na-AS and K-AS at 723 K led to sodium aluminum oxide ($NaAlO_2$, JCPDS 2-985) and potassium aluminum oxide ($K_6Al_2O_6$, JCPDS 1-82-916), respectively. Crystalline aluminates in Na and K-dawsonites calcined above 900 K were previously reported.[48] In our case, the intensity of the $NaAlO_2$ reflections was considerably higher than that of the $K_6Al_2O_6$, suggesting a larger amount of the former crystalline phase. Therefore, the presence of amorphous alumina in the K-dawsonite calcined at 723 K can be also expected.

Table 5.1. Summary of results upon reconstruction of calcined dawsonites in different media[a]

	Synthesis	Reconstruction			Product[d]
Precursor	pH[b]	Medium	Concentration (M)	pH[c]	
NH_4-dawsonite	8	$(NH_4)_2CO_3$	2	10.5	Dawsonite
	8	$(NH_4)_2CO_3$	1	10	Dawsonite
	8	$(NH_4)_2CO_3$	0.5	9.5	Dawsonite
	8	$(NH_4)_2CO_3$	0.2	8.8	Amorphous
	8	Na_2CO_3	1	12	Bayerite
	8	Na_2CO_3	0.1	10.9	Bayerite
	8	Na_2CO_3	0.01	10.6	Bayerite
	8	K_2CO_3	1	12	Bayerite
	8	K_2CO_3	0.1	11.2	Bayerite
	8	K_2CO_3	0.01	10.6	Bayerite
	8	NH_4Cl	1	6	Diaspore
	8	water	-	7	Boehmite
	8	NH_4OH	1	12	Gibbsite
Na-dawsonite	8	$(NH_4)_2CO_3$	1	10	Dawsonite+Bayerite
	8	Na_2CO_3	1	12	Bayerite
	8	K_2CO_3	1	12	Bayerite
	11	$(NH_4)_2CO_3$	1	10	Dawsonite+Bayerite
K-dawsonite	8	$(NH_4)_2CO_3$	1	10	Dawsonite
	8	Na_2CO_3	1	12	Bayerite
	8	K_2CO_3	1	12	Bayerite

[a] The precursors were calcined at 723 K for 2 h. Other construction conditions: 323 K, 30 min, 350 rpm. [b] Constant pH during precipitation by the ILDP method. [c] Initial pH of the carbonate solution. [d] Phases detected by XRD.

UNIVERSITAT ROVIRA I VIRGILI
CHEMISTRY OF DAWSONITES AND APPLICATION IN CATALYSIS
Georgiana Stoica
ISBN:978-84-693-1533-0/DL:T-648-2010

Additionally, the calcined Na-AS sample displayed distinctive reflections of sodium orthonitrate (Na_3NO_4, JCPDS 44-1051). Na_3NO_4 is likely derived from the reaction of residual $NaNO_3$ and Na_2O formed upon thermal decomposition of Na-dawsonite but no reflection of $NaNO_3$ was observed in the pattern of Na-AS.

Treatment of the calcined materials in 1 M $(NH_4)_2CO_3$ aqueous solution (pH 10) at 323 K for 30 min originated the transformation into dawsonite by a dissolution-precipitation mechanism. Exceptionally, bayerite (α-$Al(OH)_3$, JPCPS 8-96) was observed as a secondary phase in the reconstructed sample derived from calcined Na-dawsonite (see Figure 5.4). In great contrast, equivalent treatment of the calcined materials in sodium or potassium

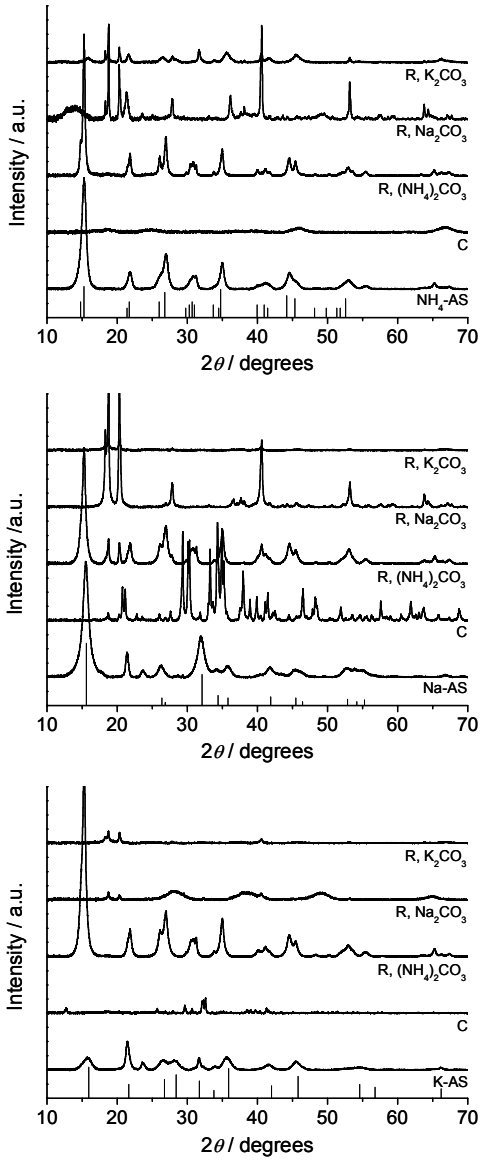

Figure 5.4. XRD patterns of NH_4, K, and Na-AS, the oxides resulting from calcination (C), and the products of treatment in 1 M $(NH_4)_2CO_3$, K_2CO_3 or Na_2CO_3 aqueous solutions at 323 K for 30 min (R).

UNIVERSITAT ROVIRA I VIRGILI
CHEMISTRY OF DAWSONITES AND APPLICATION IN CATALYSIS
Georgiana Stoica
ISBN:978-84-693-1533-0/DL:T-648-2010

carbonate solutions induced no sign of dawsonite recovery. Instead, any of the calcined dawsonites fully transformed into bayerite (α-$Al(OH)_3$, JCPDS 8-96) on treatment in 1 M Na_2CO_3 (pH 12) or K_2CO_3 (pH 12) aqueous solutions for 30 min (Figure 5.4 and Table 5.1). *A priori*, bayerite crystallization can be associated with the excessively high pH of the 1 M sodium and potassium carbonate solutions. In good correspondence, thermodynamic studies by Bénézeth *et al.*[27] established that Na-dawsonite is not stable at pH > 11.5, leading to bayerite as the predominant phase. In all our reconstruction treatments using 1 M $(NH_4)_2CO_3$ (pH 10), the pH of the solution was monitored with time. As expected, pH dropped from 10 to *ca.* 9.5 immediately after pouring the calcined samples in the carbonate solution followed by a slow decrease in the course of the treatment until values around 9.25-9.4 after 30 min (Annex 2).

The pH 10 of the 1 M ammonium carbonate solution was essential to convert the calcined samples into dawsonite, while pH ≥ 12 led to bayerite (Table 5.1). As shown here and in the previous chapter,[8] pH ≥ 12 induced crystallization of aluminum hydroxides (bayerite and gibbsite), while pH = 6-7 (ammonium chloride and distilled water) led to boehmite and diaspore (Table 5.1). The relatively narrow pH window where the reconstruction occurs represents a limiting factor for potential application of Al-containing compounds in CO_2 mineralization. This is particularly relevant in case of large pH fluctuations leading to dawsonite destabilization. Besides pH, the use of water as solvent is required. Treatment of alumina in 1 M $(NH_4)_2CO_3$ methanolic solution resulted in no transformation, although the attained value of pH was 9.6. Alumina in aqueous solutions at pH > 6 first hydrates and then forms aluminate anions, $Al(OH)_4^-$. This did not occur with other protic solvents such as methanol. Subsequently, in analogy with Bénézeth *et al.*[27] for $NaAlCO_3(OH)_2$ synthesis, NH_4-dawsonite can precipitate according to the global reaction in eq. 1. Tightly related to this, Zhang *et al.*[49] determined that the optimal conditions to synthesize dawsonite require moderately basic solutions (optimum at pH 10.3).

Originally, for systematic reasons, it was decided to compare samples derived from parent dawsonites synthesized by ILDP at the same pH (8), calcined at the same conditions (723 K for 2 h), and treated in solutions of carbonate salts with the same concentration (1 M) and conditions (temperature, time). As mentioned in the previous paragraph, fixing the concentration of the carbonate solution led to treatments in the pH range of 10.5-12. Further insights into pH effects were obtained by varying the pH of the synthesis or comparing samples treated in different carbonate salts at the same initial pH. First of all, dawsonite recovery occurred independent of the synthesis pH of the parent NH_4, K, and Na-dawsonites

UNIVERSITAT ROVIRA I VIRGILI
CHEMISTRY OF DAWSONITES AND APPLICATION IN CATALYSIS
Georgiana Stoica
ISBN:978-84-693-1533-0/DL:T-648-2010

by precipitation (pH 8 and 11 were used), as long as 1 M $(NH_4)_2CO_3$ was used for reconstruction. Secondly, the concentration of the sodium and potassium carbonate solutions was lowered in order to approach the optimal value of 10 in 1 M $(NH_4)_2CO_3$. This was not strictly possible; the pH did not decrease below 10.6 (even if using very diluted solutions, 0.01 M) and bayerite was the only crystalline phase obtained (Table 5.1). The nearly identical pH between a 2 M $(NH_4)_2CO_3$ solution (10.5, where reconstruction occurred) and a 0.01 M Na_2CO_3 solution (10.6, where bayerite is obtained) suggests the specificity of the ammonium cation in inducing reconstruction. However, it should be mentioned that the concentration of carbonate ions (required to transform Al_2O_3 into $NH_4AlCO_3(OH)_2$) was much higher in 2 M $(NH_4)_2CO_3$ than in a 0.01 M Na_2CO_3.

The formation of bayerite as a residual phase on treatment of calcined Na-dawsonites in $(NH_4)_2CO_3$ can be tentatively related to the local increase in alkalinity by dissolution of sodium orthonitrate, favoring aluminum reprecipitation as crystalline $Al(OH)_3$. The latter is supported by the absence of both Na_3NO_4 and $NaAlO_2$ in the pattern of the reconstructed sample. In fact, the pH *versus* time in the solution of calcined Na-dawsonite decreased slower than those of calcined NH_4-dawsonite and K-dawsonite (Annex 2). As a result, despite the significant changes in the first 5 min, the final pH of NH_4 and K coincided while that of Na was higher. Surprisingly, the unique ability of $(NH_4)_2CO_3$ to reconstruct dawsonite is not exclusively applicable to amorphous alumina (derived from NH_4-dawsonite) but additionally to alkaline aluminas or aluminates (derived from Na and K-dawsonites at 723 K). Broadening the range of Al-containing compounds able to form dawsonite requires further investigation.

3.3. Mechanism of alumina carbonation

The evolution of alumina to dawsonite was followed by thermogravimetric analysis and infrared spectroscopy in order to gain additional mechanistic insights into the reconstruction process. Herein, we elaborate on the treatment of the calcined NH_4-dawsonite under standard conditions (1 M $(NH_4)_2CO_3$ aqueous solution, $(NH_4)_2CO_3/Al_2O_3 = 25$, and 323 K). The investigation concentrated on the first 30 min, *i.e.* the period where most significant changes in X-ray diffraction occurred (see Figure 5.2).

Thermogravimetric analyses of the solid samples treated at different times (after filtration and drying) made it possible to monitor the reconstruction process and to estimate the degree of dawsonite recovery with time. As shown in Figure 5.5 (left), the as-synthesized sample (AS) presented a characteristic one-step weight loss of *ca.* 50% centered at 450 K, which has been assigned to the decomposition of ammonium aluminum carbonate hydroxide.[8,32] The

UNIVERSITAT ROVIRA I VIRGILI
CHEMISTRY OF DAWSONITES AND APPLICATION IN CATALYSIS
Georgiana Stoica
ISBN:978-84-693-1533-0/DL:T-648-2010

total weight loss of the treated samples increased upon increasing the duration of the treatment (*e.g.* 26% in R-4, 35% in R16, and 47% in R-30). This information is more complete in Figure 5.5 (right), where the total weight loss of the treated solids every two minutes in the period 0-30 min is plotted. The weight loss in the first 10 min of the treatment was practically constant (*ca.* 26%) and steeply increased on longer treatments, reaching 47% after 30 min. The weight loss of the samples at t < 10 min was assigned to the decomposition of an intermediate phase in the transition from Al_2O_3 and $NH_4AlCO_3(OH)_2$, which is amorphous attending to X-ray diffraction results. This compound was identified and characterized by FTIR.

Figure 5.6 shows the infrared spectra of the AS and C samples, and the solids at selected reconstruction times. The AS sample showed characteristic bands of the hydroxyl, ammonium, and carbonate groups in dawsonite,[8,30] which practically disappear in the calcined sample. In the first stages of the treatment in $(NH_4)_2CO_3$ (t < 10 min), the material progressively developed bands in the hydroxyl and carbonate regions. As illustrated more specifically in Figure 5.6, the sample R-6 (0% reconstruction) showed a broad adsorption band at 3420 cm^{-1} attributed to OH stretching in $Al(OH)_3$, a band at 1640 cm^{-1} corresponding to OH bending, and bands corresponding to carbonate groups (ν_3 at 1514 cm^{-1} and 1408 cm^{-1} and ν_2 at 835 cm^{-1}). These fingerprints are unequivocal evidence of the presence of carbonate-containing aluminum hydroxide as intermediate phase in early stages of the reconstruction process corresponding to the amorphous phase anticipated by X-ray diffraction and thermogravimetry. Our assignment was based on infrared characterization reported by several authors,[33,50] who explicitly reported the amorphous nature of this compound.

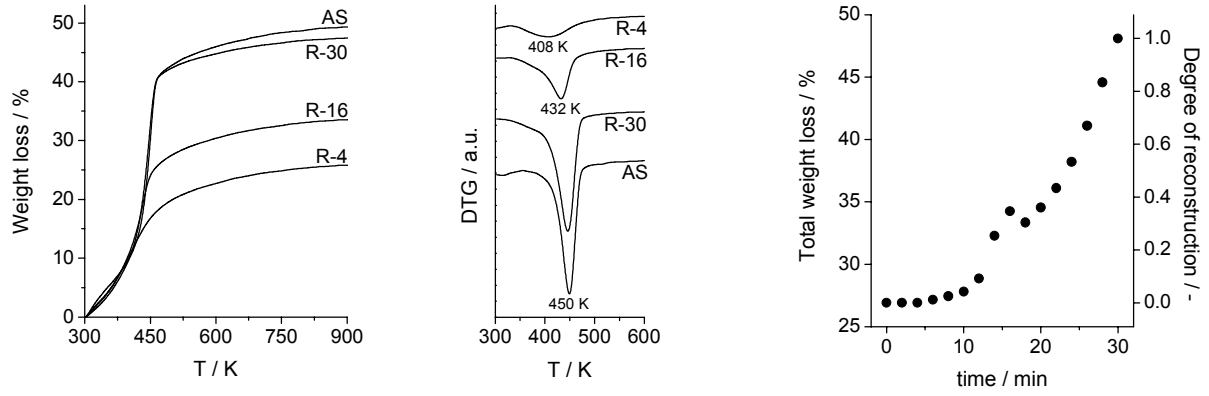

Figure 5.5. Thermogravimetric profiles (left) and derivative of the weight loss (center) of selected samples upon decomposition in air at 5 K min^{-1}. The right figure plots the total weight loss of the samples and calculated degree of reconstruction *versus* the reconstruction time.

UNIVERSITAT ROVIRA I VIRGILI
CHEMISTRY OF DAWSONITES AND APPLICATION IN CATALYSIS
Georgiana Stoica
ISBN:978-84-693-1533-0/DL:T-648-2010

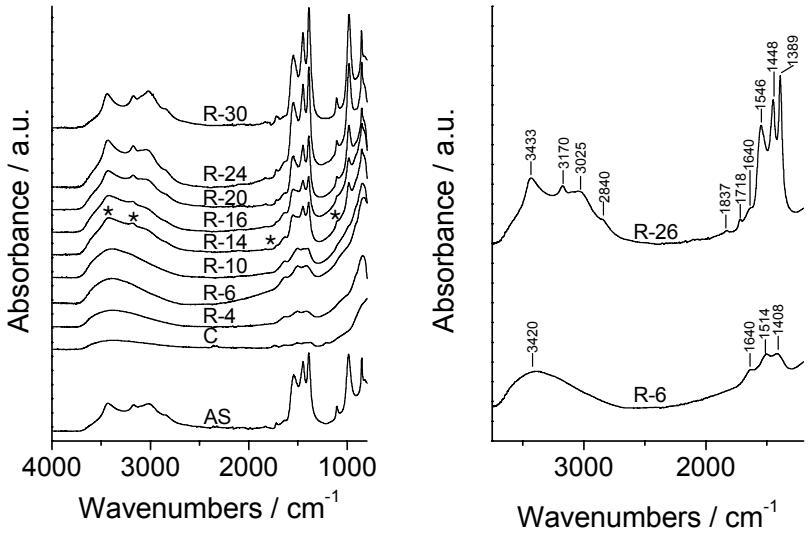

Figure 5.6. FTIR spectra during reconstruction of AACH-derived alumina in 1 M $(NH_4)_2CO_3$ at 323 K and different times. The spectra of the as-synthesized sample and calcined samples are shown for reference.

The steep weight loss increase experienced by the samples at t > 10 min was attributed to the progressive formation of dawsonite. The time scale agreed very well with the appearance of the dawsonite phase in XRD analyses (Figure 5.2). The thermogravimetric profile and total weight loss of R-30 practically matched that of AS, indicating that the dawsonite reconstruction was completed after 30 min. Considering the weight loss of the R-2 and R-30 samples as 0% and 100% reconstruction, the degree of dawsonite recovery *versus* the treatment time can be determined. This quantification is illustrated in Figure 5.5, right. The derivative of the weight loss (Figure 5.5, center) provided additional information on the evolution of the phases in the solids along the treatment. As expected, the fully reconstructed R-30 and the as-synthesized samples showed the same transition temperature, *i.e.* 450 K. The transition temperature was shifted to lower temperature at shorter times. For example, R-4 (0% reconstruction) displayed a transition temperature of 408 K, indicating the lower stability of the intermediate amorphous phase compared to dawsonite. As expected, the transition temperature of R-16 (35% reconstruction, 432 K) was intermediate between of R-4 and R-30.

The time at which dawsonite was first identified in the infrared spectra (Figure 5.6) was in excellent agreement with XRD and TGA. Based on assignments made elsewhere,[8,28] the marked changes in the spectrum of R-14 (see asterisks) were consequence of the incipient crystallization of dawsonite:

- Characteristic NH_4^+ vibrations, which were absent in the intermediate phase, appeared at 3170, 3005, and 2840 cm^{-1} (ν_{NH}) and 1830 and 1720 cm^{-1} (δ_{NH}).

- The broad OH stretching vibration at 3420 cm^{-1} in $Al(OH)_3$ shifted to the characteristic absorption at 3435 cm^{-1} in $NH_4AlCO_3(OH)_2$.
- Characteristic vibrations of CO_3^{2-} groups in $NH_4AlCO_3(OH)_2$ were distinguished, *i.e.* ν_3 at 1545, 1445, and 1387 cm^{-1}, ν_1 at 1105 cm^{-1}, ν_2 at 852 cm^{-1}). This implies a drastic reorganization of the carbonates upon crystallization of the dawsonite phase. The vibration at 1514 cm^{-1} in R-6 shifted to 1545 cm^{-1} in R-24 and the vibration at 1408 cm^{-1} split into two carbonate bands at 1445 cm^{-1} and 1390 cm^{-1} as a consequence of a decreased carbonate symmetry, leading to the appearance of the 1105 cm^{-1} band in the reconstructed sample.
- A sharp vibration band at 985 cm^{-1}, assigned to Al-OH deformation in dawsonite, was evidenced.

As expected, the above assigned vibrations sharpened as the reconstruction of dawsonite proceeds.

3.4. Morphology and textural changes during reconstruction

Transmission electron microscopy and N_2 adsorption measurements were used to monitor the morphological and textural transformations of the as-synthesized material upon calcination and subsequent reconstruction. The TEM micrograph of the AS sample showed the presence of aggregated relatively uniform spherical-like aggregates (< 10 nm), which were mostly preserved after calcination at 723 K (Figure 5.7). It can be anticipated that clusters of small particles will induce a high degree of interparticle porosity in both samples. This was indeed confirmed by N_2 porosity showing a combined type I and IV isotherm, following IUPAC guidelines (Figure 5.8).[51] The presence of mesopores is responsible for the type IV behavior while the enhanced uptake at lower relative pressures (corresponding to type I) denoted the presence of micropores. Application of the *t*-plot confirmed the combined micro- and mesoporous character; a substantial micropore volume of 0.10 $cm^3\,g^{-1}$ (Table 5.2) and a contribution of mesoporosity amounting to 555 $m^2\,g^{-1}$. The isotherm of the calcined alumina sample reflected similar porous characteristics in the mesopore regime as the AS sample, though lacking the distinct uptake at low relative pressure. The latter observation strongly suggested the absence of microporosity in the calcined sample, which was supported by the *t*-plot results in Table 5.1 evidencing a purely mesoporous material. These changes in porosity induced a decrease in BET surface area from 773 $m^2\,g^{-1}$ in AS to 500 $m^2\,g^{-1}$ in C. The BJH pore size distributions concluded a similar narrow distribution of mesopores centered at 10 nm (Figure 5.9).

UNIVERSITAT ROVIRA I VIRGILI
CHEMISTRY OF DAWSONITES AND APPLICATION IN CATALYSIS
Georgiana Stoica
ISBN:978-84-693-1533-0/DL:T-648-2010

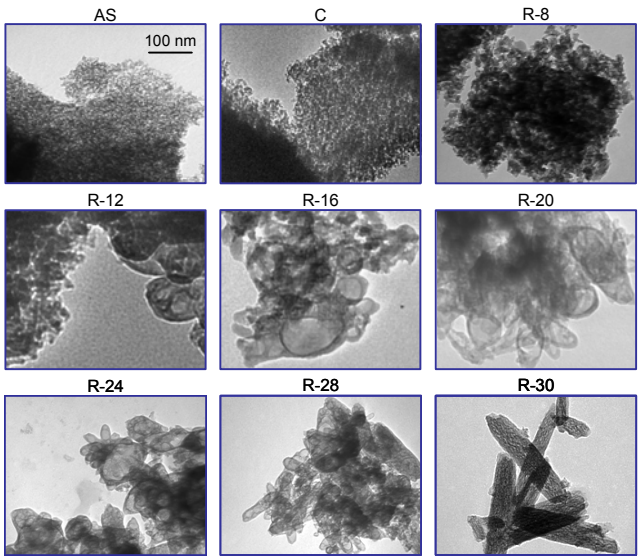

Figure 5.7. TEM micrographs of the as-synthesized, calcined, and treated samples at different times. The scale bar applies to all the samples. The starting dawsonite was in the ammonium form and the oxide reconstruction was conducted 1 M $(NH_4)_2CO_3$ aqueous solution at 323 K.

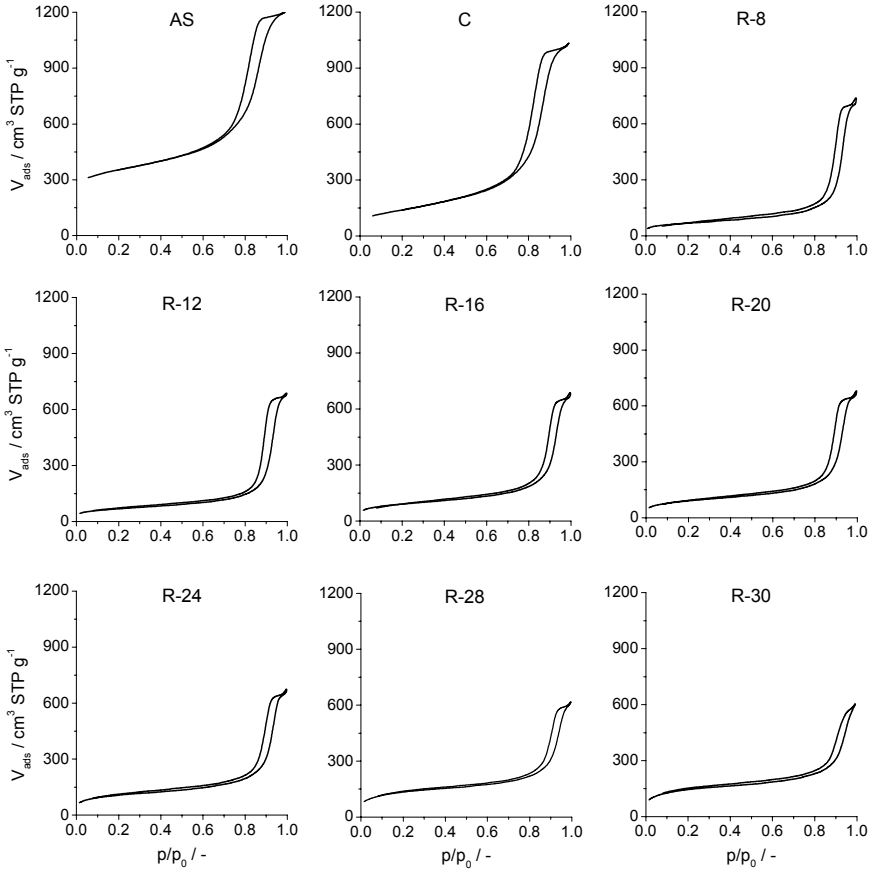

Figure 5.8. Nitrogen isotherms at 77 K of the as-synthesized, calcined, and reconstructed samples.

UNIVERSITAT ROVIRA I VIRGILI
CHEMISTRY OF DAWSONITES AND APPLICATION IN CATALYSIS
Georgiana Stoica
ISBN:978-84-693-1533-0/DL:T-648-2010

Treatment of alumina in $(NH_4)_2CO_3$ solution for 8 min led to moderate morphological changes as depicted in the TEM micrographs and rendered a material with larger, irregular, and agglomerated particles. As a consequence, the adsorption isotherm displayed a hysteresis loop at higher relative pressures with a lower N_2 uptake, pointing to the presence of larger mesopores. The latter was clearly substantiated by the shift in the maximum of the pore size distribution from 10 nm to 30 nm. Only after longer treatment times, marked changes in the morphology occurred (see R-12). New architectures of bigger spherical-like particles with a darker outer rim and a lighter layer core appeared. The latter observation suggested the presence of a denser phase in the edges likely corresponding to the dawsonite phase that started to develop. With increasing reconstruction time, also the micropore volume progressively increased. This can tentatively be attributed to the formation of the dawsonite phase that typically is microporous.[8] This in turn provoked an enhanced total BET surface area, as the mesoporosity was kept fairly constant.

At longer reconstruction times, the outer rim became thicker, enabling to hypothesize that NH_4^+ and CO_3^{2-} species gradually diffused from the outside to the centre of the particle, driving the progressive precipitation of dawsonite and a further increase in microporosity.

Table 5.2. Textural characterization of selected samples

Sample code[a]	V_{pore} ($cm^3\ g^{-1}$)	V_{micro}[b] ($cm^3\ g^{-1}$)	S_{meso}[b] ($m^2\ g^{-1}$)	S_{BET}[c] ($m^2\ g^{-1}$)
AS	1.60	0.10	555	773
C	1.40	0.00	500	500
R-8	1.10	0.02	189	236
R-12	1.05	0.03	176	240
R-16	1.03	0.05	218	316
R-20	1.02	0.05	210	319
R-24	1.02	0.07	210	371
R-28	0.94	0.12	198	462
R-30	0.90	0.14	197	497

[a] AS: as-synthesized NH4-dawsonite sample. C: calcined sample. R-*x*: reconstructed samples. The number *x* indicates the reconstruction time in minutes at 323 K. [b] *t*-plot method. [c] BET method.

UNIVERSITAT ROVIRA I VIRGILI
CHEMISTRY OF DAWSONITES AND APPLICATION IN CATALYSIS
Georgiana Stoica
ISBN:978-84-693-1533-0/DL:T-648-2010

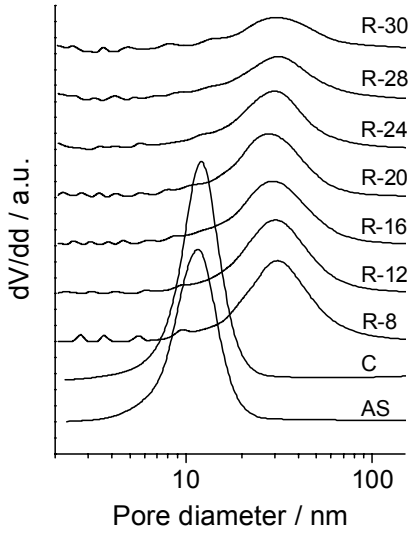

Figure 5.9. BJH desorption pore size distribution of the samples derived from the N_2 isotherms.

In excellent agreement, XRD reflections and IR absorption bands of the ongoing dawsonite formation appeared in the same time range correlating with the changes in morphology. The latter observations suggested a phase transition from the amorphous carbonate-containing aluminum hydroxide phase to dawsonite. As the reconstruction process proceeded (R-20 to R-24), the contrast in the zoned particles became more uniform suggesting an increase of the material density as dawsonite recrystallized.

As the TEM micrographs tentatively suggested the presence of hollow porous particles, mercury intrusion porosimetry was applied to assess the accessibility of the porosity as determined by N_2 adsorption. The intrusion and extrusion curves acquired over sample R-20 showed a two-step behavior (Figure 5.10). The step at low pressure was attributed to the voids

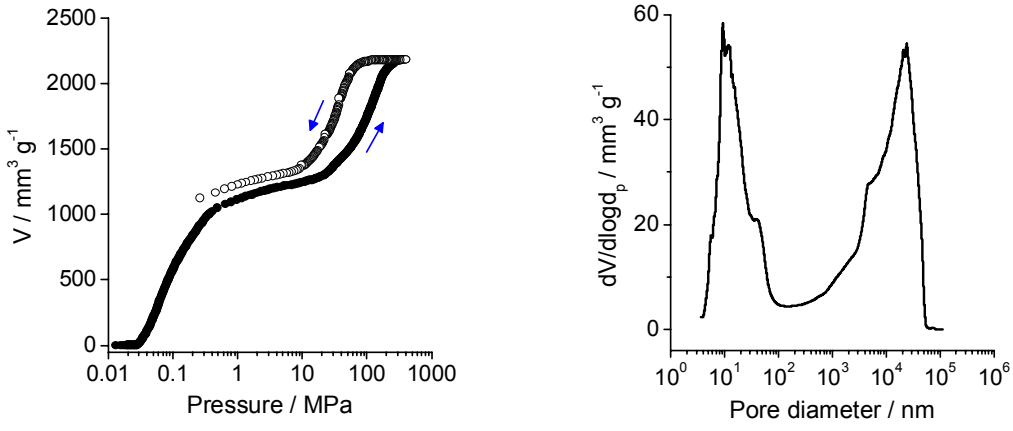

Figure 5.10. Hg intrusion (solid symbols) and extrusion (open symbols) curves of R-20 (left) and derived pore size distribution using the Washburn equation (right).

UNIVERSITAT ROVIRA I VIRGILI
CHEMISTRY OF DAWSONITES AND APPLICATION IN CATALYSIS
Georgiana Stoica
ISBN:978-84-693-1533-0/DL:T-648-2010

between the aggregates whereas the second transition at higher pressure was the result of interparticle porosity. The interparticle volume of *ca.* 0.95 $cm^3 g^{-1}$ associated with the latter step was in excellent agreement with the porous properties derived from N_2 adsorption. The full reversibility of the intrusion and extrusion curve coupled to the good correlation between both two pore size distributions further evidenced that the porosity was readily accessible and not encapsulated within the apparent partially hollow particles.

From R-24 to R-30, the morphology evolved towards the more thermodynamically favored acicular crystals specific to the dawsonite mineral.[52] Related to this, Ma *et al.*[53] observed that pH > 8 induced formation of acicular to stick fibers rather than the disordered hairy particles obtained at pH < 7. Scanning electron microscopy also evidenced the acicular geometry of the reformed dawsonite crystals (Figure 5.11). Similar morphological and textural transformations leading to acicular configurations were also observed at other reconstruction conditions.

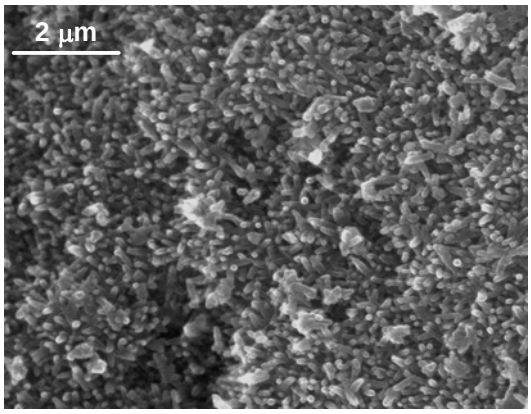

Figure 5.11. Scanning transmission micrograph of R-30.

4. Conclusions

Aluminas derived from thermal decomposition of dawsonite-type compounds exhibited structural memory, *i.e.* the original mineral structure in ammonium form ($NH_4AlCO_3(OH)_2$) was recovered by treatment in aqueous solutions of ammonium carbonate under mild conditions at pH ~ 10. Alumina carbonation to dawsonite was specific to $(NH_4)_2CO_3$, and the memory property applied to dawsonite compounds with different compensating cations (NH_4^+, K^+, Na^+). In great contrast, treatment of calcined dawsonites in other carbonate salts such as K_2CO_3 and Na_2CO_3 solutions led to bayerite. Similarly to layered-double hydroxides with hydrotalcite structure, the term memory was used since we start from the dawsonite structure, decompose it by thermal treatment, and recover it upon specific treatment and

conditions. Accordingly, calcined dawsonite 'remembers' the way back to dawsonite and this transformation is thermodynamic and kinetically favored. The kinetics and mechanism of the reconstruction process have been successfully studied. The alumina-to-dawsonite transition was relatively fast (10-30 min depending on the temperature) and followed a dissolution-precipitation mechanism. By this, alumina formed an amorphous carbonate-containing aluminum hydroxide phase followed by dawsonite recrystallization. The original and reconstructed dawsonites presented striking morphological and porosity differences. Nanoparticles in the as-made and calcined materials transformed through complex intermediate morphologies into well-crystallized acicular nanoneedles with newly developed microporosity in the reconstructed material. Our results can be of significance to improve current applications of dawsonites associated to the modified properties induced by the memory effect. Besides, this work opens a route for CO_2 mineralization using Al-containing compounds through dawsonite formation.

Acknowledgments

The author thanks to Sònia Abelló for contribution to this chapter. Gisela Colet is acknowledged for the technical assistance with the automated liquid-phase parallel chemical synthesizer. Johan C. Groen is thanked for the technical assistance and valuable related discussions on the porosimetry analyses.

References

[1] A. R. Wilson; In *Kirk-Othmer Encyclopedia of Chemical Technology*; A. Seidel, Ed.; John Wiley & Sons, Inc., New York, 2006, vol. 22, pp. 705-722.

[2] S. B. Lang, S. Muensit, *Appl. Phys. A: Mater. Sci. Process.* **2006**, 85, 125.

[3] E. Hornbogen, *Adv. Eng. Mater.* **2006**, 8, 101.

[4] D. Ratna, J. Karger-Kocsis, *J. Mater. Sci.* **2008**, 43, 254.

[5] R. Kainuma, Y. Imano, W. Ito, Y. Sutou, H. Morito, S. Okamoto, O. Kitakami, K. Oikawa, A. Fujita, T. Kanomata, K. Ishida, *Nature* **2006**, 439, 957.

[6] C. M. Lampert, *Mater. Today* **2004**, 7, 28.

[7] P. S. Braterman, Z. P. Xu, F. Yarberry; In *Handbook of Layered Materials*; S. M. Auerbach, K. A. Carrado, P. K. Dutta, Eds.; Taylor & Francis, New York, 2004, pp. 313-372.

[8] G. Stoica, J. Pérez-Ramírez, *Chem. Mater.* **2007**, 19, 4783.

UNIVERSITAT ROVIRA I VIRGILI
CHEMISTRY OF DAWSONITES AND APPLICATION IN CATALYSIS
Georgiana Stoica
ISBN:978-84-693-1533-0/DL:T-648-2010

[9] F. Cavani, F. Trifiro, A. Vaccari, *Catal. Today* **1991**, 11, 173.

[10] W. T. Reichle, *J. Catal.* **1985**, 94, 547.

[11] F. Kooli, C. Depège, A. Ennaqadi, A. D. Roy, J. P. Besse, *Clays Clay Miner.* **1997**, 45, 92.

[12] A. J. Marchi, C. R. Apesteguía, *Appl. Clay Sci.* **1998**, 13, 35.

[13] F. Millange, R. I. Walton, D. O'Hare, *J. Mater. Chem.* **2000**, 10, 1713.

[14] J. A. van Bokhoven, J. C. A. A.; Roelofs, K. P. de Jong, D. C. Koningsberger, *Chem. Eur. J.* **2001**, 7, 1258.

[15] S. Abelló, F. Medina, D. Tichit, J. Pérez-Ramírez, J. C. Groen, J. E. Sueiras, P. Salagre, Y. Cesteros, *Chem. Eur. J.* **2005**, 11, 728.

[16] J. Pérez-Ramírez, S. Abelló, N. M. van der Pers, *Chem. Eur. J.* **2007**, 13, 870.

[17] J. Pérez-Ramírez, S. Abelló, N. M. van der Pers, *J. Phys. Chem. C* **2007**, 111, 3642.

[18] A. E. Palomares, J. G. Prato, F. Rey, A. Corma, *J. Catal.* **2004**, 221, 62.

[19] M. Shiraga, T. Kawabata, D. Li, T. Shishido, K. Komaguchi, T. Sano, K. Takehira, *Appl. Clay Sci.* **2006**, 33, 247.

[20] H. Nakayama, N. Wada, M. Tsuhako, *Int. J. Pharm.* **2004**, 269, 469.

[21] G. R. Williams, D. O'Hare, *J. Mater. Chem.* **2006**, 16, 3065.

[22] V. Rives, M. A. Ulibarri, *Coord. Chem. Rev.* **1999**, 181, 61.

[23] D. Tichit, B. Coq, *CATTECH* **2003**, 7, 206.

[24] M. Rajamathi, G. D. Nataraja, S. Ananthamurthy, P. V. Kamath, *J. Mater. Chem.* **2000**, 10, 2754.

[25] T. S. Stanimirova, G. Kirov, E. Dinolova, *J. Mater. Sci. Lett.* **2001**, 20, 453.

[26] F. Prinetto, G. Ghiotti, P. Graffin, D. Tichit, *Microporous Mesoporous Mater.* **2000**, 39, 229.

[27] P. Bénézeth, D. A. Palmer, L. M. Anovitz, J. Horita, *Geochim. Cosmochim. Acta* **2007**, 71, 4438.

[28] A. J. Frueh, J. P. Golightly, *Can. Mineral.* **1967**, 9, 51.

[29] E. Corazza, C. Sabelli, S. Vannucci, *Neues Jahrb. Mineral. Monatsh.* **1977**, 9, 381.

[30] C. J. Serna, J. V. Garcia-Ramos, M. J. Peña, *Spectrochim. Acta* **1985**, 41A, 697.

[31] A. A. Ali, M. A. Hasan, M. I. Zaki, *Chem. Mater.* **2005**, 17, 6797.

[32] M. S. Yalfani, M. Santiago, J. Pérez-Ramírez, *J. Mater. Chem.* **2007**, 17, 1222.

[33] C. J. Serna, J. L. White, S. L. Hem, *J. Pharm. Sci.* **1978**, 67, 324.

[34] P. V. Bonsignore, *Plast. Eng.* **1976**, 32, 41.

[35] G. Gillman, A. Noble, *Environmental Quality Management* **2005**, 15, 59.

[36] R. L. Altman, L. A. Mayer, A. C. Ling, *US Patent 4,406,797*, **1983**.

[37] J. B. Doyle, ED. A. Pirsh, W. Downs, *EP0268353*, **1988**.

[38] M. Santiago, M. S. Yalfani, J. Pérez-Ramírez, *J. Mater. Chem.* **2006**, 16, 2886.

[39] H. Hellevang, P. Aagaard, E. O. Oelkers, B. Kvamme, *Environ. Sci. Technol.* **2005**, 39, 8281.

[40] S. Abelló, J. Pérez-Ramírez, *Adv. Mater.* **2006**, 18, 2436.

[41] S. Abelló, S. Dhir, G. Colet, J. Pérez-Ramírez, *Appl. Catal. A* **2007**, 325, 121.

[42] J. C. Groen, J. A. Moulijn, J. Pérez-Ramírez, *Ind. Eng. Chem. Res.* **2007**, 46, 4193.

[43] S. Brunauer, P. H. Emmett, E. Teller, *J. Am. Chem. Soc.* **1938**, 60, 309.

[44] B. C. Lippens, J. H. de Boer, *J. Catal.* **1965**, 4, 319.

[45] E. P. Barret, L. G. Joyner, P. P. Hallenda, *J. Am. Chem. Soc.* **1951**, 73, 373.

[46] T. Iga, S. Kato, *J. Ceram. Soc. Jpn.* **1978**, 86, 509.

[47] L. Fernandez-Carrasco, F. Puertas, M. T. Blanco-Varela, T. Vázquez, J. Rius, *Cem. Concr. Res.* **2005**, 35, 641.

[48] M. J. Hernandez, M. A. Ulibarri, J. Cornejo, M. J. Peña, C. J. Serna, *Thermochim. Acta* **1985**, 94, 257.

[49] X. Zhang, Z. Wen, Z. Gu, X. Xu, Z. Lin, *J. Solid State Chem.* **2004**, 177, 849.

[50] E. C. Scholtz, J. R. Fedlkamp, J. L. White, S. L. Hem, *J. Pharm. Sci.* **1984**, 73, 967.

[51] K. S. W. Sing, D. H. Everett, R. A. W. Haul, L. Moscou, R. A. Pierotti, J. Rouquerol, T. Siemieniewska, *Pure Appl. Chem.* **1985**, 57, 603.

[52] J. W. Anthony, R. A. Bideaux, K. W. Bladh, M. C. Nichols; In *Handbook of Mineralogy*, vol. V; Mineral Data Publishing, Ed.; Tucson, Arizona, 2007, pp. 176.

[53] C.-C. Ma, X.-X. Zhou, X. Xu, T. Zhu, *Mater. Chem. Phys.* **2001**, 72, 374.

UNIVERSITAT ROVIRA I VIRGILI
CHEMISTRY OF DAWSONITES AND APPLICATION IN CATALYSIS
Georgiana Stoica
ISBN:978-84-693-1533-0/DL:T-648-2010

Annex 2

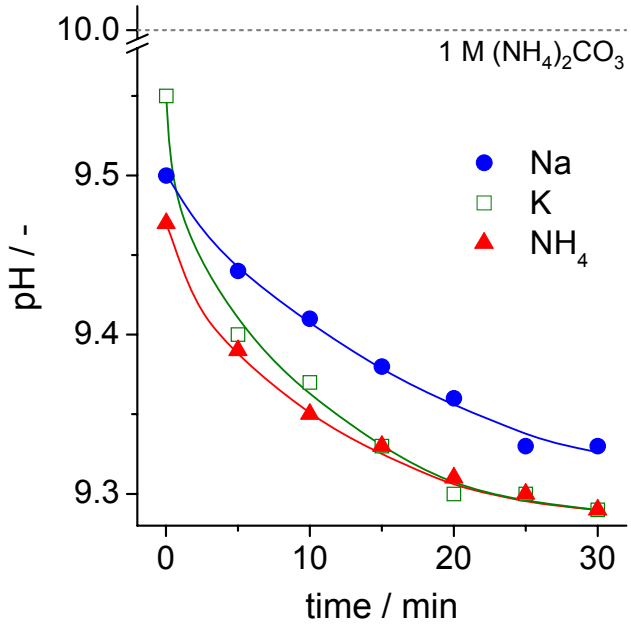

Evolution of pH with time during reconstruction of calcined NH_4, Na, and K-dawsonites at 723 K in 1 M $(NH_4)_2CO_3$ aqueous solution at 323 K. The pH of the original solution (10) dropped immediately after pouring the solids (first value at $t \rightarrow 0$) and progressively decreased along the treatment.

UNIVERSITAT ROVIRA I VIRGILI
CHEMISTRY OF DAWSONITES AND APPLICATION IN CATALYSIS
Georgiana Stoica
ISBN:978-84-693-1533-0/DL:T-648-2010

UNIVERSITAT ROVIRA I VIRGILI
CHEMISTRY OF DAWSONITES AND APPLICATION IN CATALYSIS
Georgiana Stoica
ISBN:978-84-693-1533-0/DL:T-648-2010

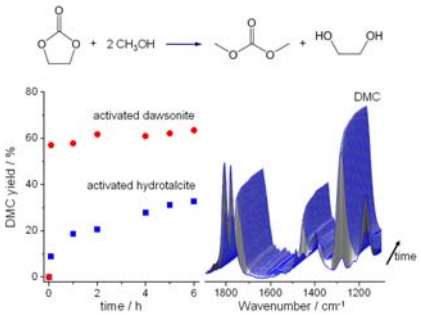

Chapter 6

Synthesis of Dimethyl Carbonate (DMC) by Transesterification of Ethylene Carbonate over Activated Dawsonites

The transesterification of ethylene carbonate with methanol to dimethyl carbonate, an alternative phosgene-free route to DMC, was investigated over aluminas derived from calcination at different temperatures of Na and NH_4-dawsonites. The influence of the monovalent cation (NH_4^+, Na^+) on the thermal decomposition of the starting dawsonites and derived crystallinity, morphology, and porosity of the resulting aluminates was studied. Phase transitions during thermal decomposition are dependent on the monovalent cation in the original dawsonite, *i.e.* the NH_4-counterpart is transformed into finely dispersed and highly amorphous aluminas with well-developed porosity in the range 473-1073 K, while Na-dawsonite exhibits an intermediate amorphous sodium-containing alumina phase at 523-773 K, which crystallizes into sodium aluminate at 773-1073 K. Tests were carried out in a parallel reactor system at 298-343 K, methanol-to-ethylene carbonate ratios of 2-12, and 0.1-10 wt.% catalyst amount. Tailoring the catalyst activation conditions is essential to optimize the transesterification performance, and consequently the production of DMC, a valuable environment-friendly chemical for many potential applications. Any of the oxides derived from NH_4-dawsonite were inactive in the reaction. The basicity of the Na-containing oxides, attained by calcination of Na-dawsonite at 973 K, is required to obtain an active catalyst, which rendered a maximum DMC yield up to *ca.* 65%. Recycling experiments demonstrated that activated dawsonites can be effectively reused. Additionally, the title reaction was successfully scaled up.

This chapter is based on the following publications:
G. Stoica, S. Abelló, J. Pérez-Ramírez, *ChemSusChem.* **2009**, 2, 301.
G. Stoica, S. Abelló, J. Pérez-Ramírez, *Appl. Catal. A* **2009**, 365, 252.

UNIVERSITAT ROVIRA I VIRGILI
CHEMISTRY OF DAWSONITES AND APPLICATION IN CATALYSIS
Georgiana Stoica
ISBN:978-84-693-1533-0/DL:T-648-2010

1. Introduction

Solid bases have been investigated for more than 45 years but they have been protagonists of an increased research over the past decade, especially on the synthesis of fine chemicals. In fact, they offer an environmentally benign and economical pathway in well-recognized reactions such as isomerizations, C-C bond formation, transesterification, additions, or oxidations.[1,2] However, solid-base catalysts are not used so extensively in industry as compared to solid acid catalysts. In 2001, only 10 solid bases were applied in industrial processes compared to the 103 acids.[3] Although these figures have certainly increased, the replacement of homogeneous catalysts by heterogeneous catalysts is still a challenge to be overcome. This motivated us to find new fundamental directions to develop solid bases, which may fulfill the desirable activity, selectivity, and reusability requirements. In this trajectory, dawsonites, *i.e.* $NaAlCO_3(OH)_2$, could be potential candidates in base-catalyzed reactions, attending to the formation of well-dispersed oxides obtained by thermal decomposition, the possibility to incorporate other metals instead of the sodium or aluminum cations in the structure, and their easy (re)activation procedure.[4]

In this chapter we investigated a novel family of heterogeneous catalysts for the synthesis of dimethyl carbonate (DMC) by transesterification of ethylene carbonate (EC) with methanol (Scheme 6.1).[5] This relatively unexplored reaction is proclaimed as an environmentally-friendly alternative for the replacement of harmful and undesirable compounds like phosgene or dimethyl sulphate, and is an interesting path for the production of a great number of chemical intermediates.[6,7] The industrial routes to produce DMC, namely, phosphogenation and oxidative carbonylation of methanol, involve high-risk and expensive compounds such as $COCl_2$ and CO. At present, greener methods such as 1) the direct reaction of methanol with CO_2, 2) the methanolysis of urea, and 3) the transesterification of cyclic carbonates with methanol are being investigated.[6-8] Homogeneous alkali metals and heterogeneous catalysts such as zeolites,[9] basic metal oxides,[10] smectites,[11] hydrotalcites,[12] basic salts (Na_3PO_4 and Na_2CO_3),[13] quaternary ammonium salts,[14] composites,[15] and ionic liquids[16] have been used in the transesterification of ethylene carbonate with methanol under mild conditions, leading to DMC and ethylene glycol (Scheme 6.1). Ethylene carbonate is an attractive feedstock, enabling phosgene-free operation and the utilization of carbon dioxide as a chemical (cyclic carbonates are produced by insertion of CO_2 into the corresponding epoxide[17]). DMC can also be produced by a one-pot process starting directly from ethylene epoxide, but the corresponding yields are relatively low owing to the undesired alcoholysis of the epoxide.[9]

UNIVERSITAT ROVIRA I VIRGILI
CHEMISTRY OF DAWSONITES AND APPLICATION IN CATALYSIS
Georgiana Stoica
ISBN:978-84-693-1533-0/DL:T-648-2010

Besides providing kinetic data to reach the thermodynamic DMC yield, comprehensive relationships between the different bases, their basicity, and their resulting transesterification performance have not been established. A common aspect in these works is that the catalytic efficiency of these systems increases with the degree of basicity, but prospects in reusability and scalability were not derived.

Herein, we have systematically investigated the activation of NH_4 and Na-dawsonites into their oxides for subsequent use in the transesterification of ethylene carbonate and methanol to dimethyl carbonate. Well-known solid bases such as activated hydrotalcites and magnesium oxide were used as reference materials for the title reaction. *In situ* XRD studies have been complemented by other characterization techniques (TGA-MS, TEM, N_2 adsorption, FTIR, and NMR) to derive structure-performance relationships associated with the activation of the dawsonite precursor. Influence of the synthesis method, optimal catalyst activation, and the study of the effect of reaction variables (methanol-to-EC ratio, catalyst amount) were attained in a 16 parallel-batch reactor system. The best catalyst was used for reusability and scalability tests. Additionally, the evolution of the reaction was monitored by means of real-time infrared spectroscopy under *operando* conditions.

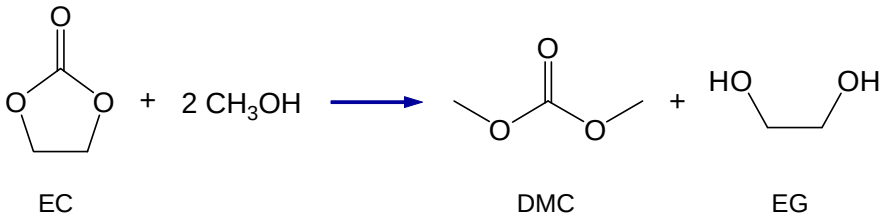

Scheme 6.1. Transesterification of ethylene carbonate with methanol.

2. Experimental

2.1. Materials and treatments

NH_4 and Na-dawsonites and Mg-Al hydrotalcite (Mg/Al = 3) were prepared by co-precipitation at constant pH using the in-line dispersion-precipitation (ILDP) method.[18] For dawsonite synthesis, aqueous solutions of $Al(NO_3)_3 \cdot 9H_2O$ (1.1 M) and the precipitating agent ($(NH_4)_2CO_3$ or Na_2CO_3 2 M) were continuously fed to the miniaturized precipitation chamber (volume of *ca.* 6 cm^3), which was stirred at 13 500 rpm. Syntheses were carried out at pH ranging from 6 to 11 with an average residence time of 18 s. The resulting slurry was aged at 333 K for 3 h, followed by filtration, washing, and drying at 333 K for 12 h. The dawsonite samples were calcined by thermal treatment in static air at 473 or 973 K for 2 h using a

heating rate of 5 K min^{-1}. Along the chapter, the as-synthesized and calcined dawsonites are generally identified by the codes *X*-DW-as and *X*-DW-*y*, respectively, where *X* corresponds to NH_4, or Na, and *y* represents the calcination temperature in K. For the synthesis of hydrotalcite, aqueous solutions of $Mg(NO_3)_2 \cdot 6H_2O$ (0.75 M) and $Al(NO_3)_3 \cdot 9H_2O$ (0.25 M) were precipitated with a mixture of $NaOH+Na_2CO_3$ (1 M of each) at pH 10. The resulting slurry was aged at 298 K for 12 h under mechanical stirring (500 rpm), followed by filtration, washing, and drying at 353 K for 12 h. The as-synthesized hydrotalcite (HT-as) was decomposed in static air at 723 K for 15 h to obtain the corresponding Mg-Al mixed oxide (HT-c). The rehydrated hydrotalcite (HT-rh) was obtained by immersing the calcined material in decarbonated water for 1 h at room temperature. MgO was prepared by calcination of $Mg(OH)_2$ at 723 K for 15 h.

2.2. Characterization methods

The chemical composition of the as-synthesized dawsonites was determined by inductive coupled plasma-optical emission spectroscopy (ICP-OES) (Perkin-Elmer Optima 3200RL (radial)). Elemental analysis (C, H, and N) was measured in a Carlo Erba EA1108 instrument. *In situ* X-ray diffraction patterns during calcination of NH_4-DW-as and Na-DW-as were recorded in a Siemens D5000 diffractometer with Bragg-Brentano geometry and Ni-filtered Cu Kα radiation (λ = 0.1541 nm). Diffraction patterns were measured at intervals of 50 K in the temperature range 303-973 K after 5 min of equilibration at each temperature. The heating rate used was 10 K min^{-1}. Data were recorded in the range 10-70º 2θ with an angular step size of 0.016º and a counting time of 4 s per step. Fourier transform infrared spectroscopy was carried out in a Bruker Optics Tensor 27 spectrometer equipped with a Golden Gate Diamond ATR unit. Spectra were collected at room temperature in the range 650-4000 cm^{-1} by co-addition of 32 scans at a nominal resolution of 4 cm^{-1}, taking the spectrum of the empty cell at ambient conditions as the background. Solid-state magic-angle spinning nuclear magnetic resonance (MAS-NMR) spectra were recorded on a Bruker AV 400MHz Wide Bore spectrometer equipped with a 4 mm BB/1H probe. The samples were spun in 4 mm zirconia rotors with a spinning frequency of 12 kHz. ^{27}Al spectra were recorded using 1160 accumulations at 4 ms pulses, an angle of 90º, and a relaxing time of 10 s. A total of 4000 scans were collected with a sweep width of 100 kHz and an acquisition time of 0.2 s. An acquisition delay of 5 s between successive accumulations was selected to avoid saturation effects. The ^{27}Al chemical shifts were referenced to $NH_4SO_4Al \cdot 12H_2O$. Thermogravimetric analysis (TGA) was carried out in a Mettler Toledo TGA/SDTA851e microbalance. Analyses

UNIVERSITAT ROVIRA I VIRGILI
CHEMISTRY OF DAWSONITES AND APPLICATION IN CATALYSIS
Georgiana Stoica
ISBN:978-84-693-1533-0/DL:T-648-2010

were performed in air (50 cm^3 STP min^{-1}), ramping the temperature from 298 to 1173 K at 5 K min^{-1}. The evolution of the gases during calcination of the dawsonites was studied by temperature programmed desorption mass spectrometry (TPD-MS). The as-synthesized material (50 mg) was decomposed in dry air (50 cm^3 STP min^{-1}) in a quartz fixed-bed reactor (10 mm i.d.) and the temperature was raised from room temperature to 973 K at 5 K min^{-1}. Masses *m/z* 17 (NH_3), *m/z* 18 (H_2O) and *m/z* 44 (CO_2) were continuously monitored with a quadrupole mass spectrometer (Pfeiffer OmniStar GSD 301O). Transmission electron microscopy was carried out in a JEOL JEM-1011 microscope operated at 80 kV. A few droplets of the sample suspended in ethanol were placed on a carbon-coated copper grid followed by evaporation at ambient conditions. Nitrogen isotherms at 77 K were measured on a Quantachrome Autosorb-1MP analyzer. Prior to analysis, the samples were degassed in vacuum at 393 K for 16 h. The BET method[19] was applied to calculate the total surface area and, the *t*-plot method[20] was used to discriminate between micro- and mesoporosity. The Hammett indicator was used to determine the basic strength of sodium aluminate sample ($H\_$).[21] About 200 mg of sample were well mixed with 10 ml methanol solution of the Hammett indicator and left for 1 hour to achieve equilibration. The concentrations of 0.02 mol/l phenolphthalein ($H\_ = 9.8$), 2,4-dinitroaniline ($H\_ = 15.0$), and 4-nitroaniline ($H\_ = 18.4$) were used for Hammett indicators. When a change in color of the indicator was observed, the $H\_$ value of the basic sites was taken to be higher than the pK_a value of the indicator.

2.3. Catalytic tests

The parallel screening and scale-up of the transesterification reaction were performed in a fully automated MultiMax™ liquid-phase parallel chemical synthesizer and LabMax setup, from Mettler Toledo, respectively. Briefly, 16-glass vessels (17 mm i.d. and total volume 50 ml) were filled with catalyst, carefully sealed, and placed in the reactor block. The reaction mixture was dosed to the reactors and samples were collected at six different times in the period of 6 h, with a sampling volume of 150 μl. Tests were carried out at ambient pressure using the following conditions: methanol-to-ethylene carbonate ratio = 2-12, temperature = 298-343 K, amount of catalyst with respect to ethylene carbonate = 0.1-10%, and stirring speed = 350 rpm. Fresh, reused, and regenerated catalysts were evaluated. Reusability tests were conducted over a used catalyst from a typical experiment after cooling down the reactor to room temperature, recovery of the solid by filtration, and drying. The regenerated samples were obtained by calcination of a used catalyst (same treatment as for the

UNIVERSITAT ROVIRA I VIRGILI
CHEMISTRY OF DAWSONITES AND APPLICATION IN CATALYSIS
Georgiana Stoica
ISBN:978-84-693-1533-0/DL:T-648-2010

activation). The most promising catalyst was further evaluated in a 2 L batch reactor. The liquid samples were analyzed off-line by a gas chromatograph (Agilent 6890N/G1530N) equipped with a flame ionization detector and HP-5 capillary column. Biphenyl was used as internal standard in a concentration of 5% with respect to ethylene carbonate. The yield of DMC was calculated as moles of DMC formed divided by initial moles of EC. Additionally, the products were monitored by ATR-IR by means of a React-IR^{TM} 4000 spectrometer equipped with an ASI Applied Systems 16 mm-probe with a diamond crystal as the sensing element. Spectra were collected in the range 650-4000 cm^{-1}, by co-addition of 32 scans at a nominal resolution of 4 cm^{-1}.

3. Results and discussion

3.1. Materials

As-synthesized samples

The as-synthesized NH_4-dawsonite consists of an assemblage of edge-sharing distorted $AlO_2(OH)_4$ and $NH_4O_4(OH)_2$ octahedras.[22] The X-ray diffraction pattern of this sample in Figure 6.1 only displayed characteristic reflections of ammonium aluminum carbonate hydroxide ($NH_4AlCO_3(OH)_2$, JCPDS 42-250) indicating that the synthesis step was carried out effectively.

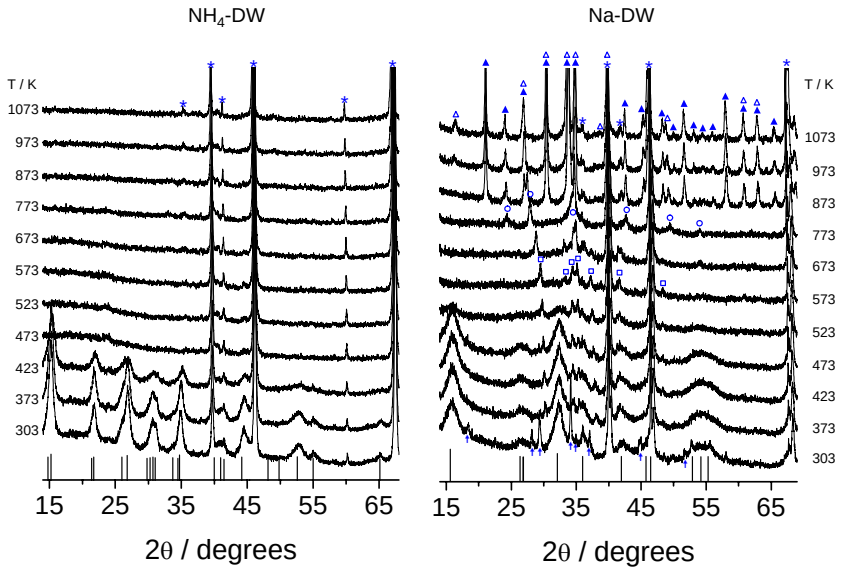

Figure 6.1. *In situ* XRD patterns during thermal decomposition of dawsonites in static air. Crystalline phases: (↟) $Na_3H(CO_3)_2{\cdot}2H_2O$, (□) Na_2CO_3 (JCPDS 1-77-2082), (○) Na_2CO_3 (JCPDS 1-84-176), (▲) $NaAlO_2$ (JCPDS 19-1179), and (△) $NaAlO_2$ (JCPDS 1-79-1475). Vertical lines represent the pattern of dawsonite in the corresponding NH_4 (JCPDS 42-250) or Na form (JCPDS 45-1359). The reflections with asterisk (★) belong to the Pt_{95}-Rh_5 strip where the samples were mounted.

UNIVERSITAT ROVIRA I VIRGILI
CHEMISTRY OF DAWSONITES AND APPLICATION IN CATALYSIS
Georgiana Stoica
ISBN:978-84-693-1533-0/DL:T-648-2010

The formula of Na-DW-as was $C_{0.92}H_{5.69}O_{4.94}Na_{0.90}Al$. The ratios C/Al and Na/Al were lower than 1, suggesting the presence of additional aluminum-containing phases besides dawsonite. Comparing these values to a pure sodium dawsonite, $NaAlCO_3(OH)_2$, it can be inferred that this sample consists of 90% Na-dawsonite. The corresponding XRD pattern at 303 K exhibited the characteristic reflections of $NaAlCO_3(OH)_2$ (JCPDS 45-1359) accompanied by an additional phase, $Na_3H(CO_3)_2{\cdot}2H_2O$ (trona, JCPDS 29-1447) (Figure 6.1). This phase is a hydrate double salt of sodium carbonate and bicarbonate, also known as sodium sesquicarbonate, $Na_2CO_3{\cdot}NaHCO_3{\cdot}2H_2O$.[23] As this additional phase contains the same elements than the starting dawsonite, the remaining 10% could well corresponding to extra Al-containing amorphous phases in the precipitate. In this sample, the intensity of the dawsonite reflections was considerably lower than that of the NH_4 counterpart, suggesting the lower crystallinity of the former. Besides, a marked broadening of the dawsonite reflections was observed in the diffractogram of the Na sample as compared to the NH_4 sample. In fact, the average crystallite size of Na-DW-as, as estimated by the Scherrer equation applied to the (110) reflection at 15º 2θ, resulted in *ca.* 3 nm, respectively, which was considerably smaller than the crystallite size of 8 nm for the NH_4 sample.

The Fourier transform infrared spectra of the as-synthesized samples (Figure 6.2) were consistent with XRD, and exhibited characteristic absorptions bands of the hydroxyl and carbonate groups in dawsonites, and additional ammonium bands specifics of the NH_4 counterpart.[22] For NH_4-DW-as, the following bands were identified: OH^- (ν_{OH} at 3435 cm^{-1}; δ_{OH} at 982 cm^{-1}), NH_4^+ (ν_{NH} at 3170, 3020, and 2840 cm^{-1}; δ_{NH} at 1830 and 1720 cm^{-1}), and CO_3^{2-} (ν_3 at 1545, 1445, and 1385 cm^{-1}, ν_1 at 1105 cm^{-1}, ν_2 at 850 and 827 cm^{-1}, and ν_4 at 758 and 735 cm^{-1}). In the case of Na-DW-as, the bands appeared at: OH^- (ν_{OH} at 3435 and 3270 cm^{-1}; δ_{OH} at 954 and 928 cm^{-1}), and CO_3^{2-} (ν_3 at 1547 and 1388 cm^{-1}, ν_1 at 1094 cm^{-1}, ν_2 at 844 cm^{-1}, and ν_4 at 730 cm^{-1}). The band at 671 cm^{-1} corresponds to the lattice vibration.

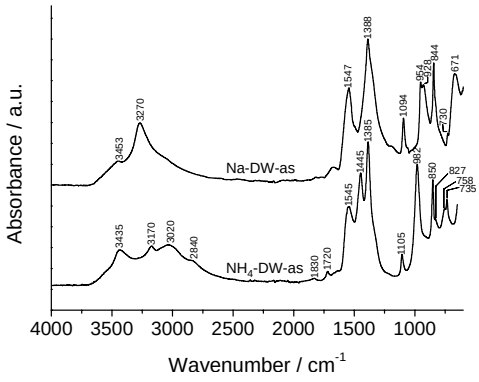

Figure 6.2. FTIR spectra of the as-synthesized NH_4 and Na-dawsonites.

UNIVERSITAT ROVIRA I VIRGILI
CHEMISTRY OF DAWSONITES AND APPLICATION IN CATALYSIS
Georgiana Stoica
ISBN:978-84-693-1533-0/DL:T-648-2010

Thermal decomposition

A previous study has investigated the *in situ* thermal decomposition of metal-substituted dawsonite-type materials, including Fe, La or Mn.[24] This approach enables an accurate monitoring of the decomposition process and provides valuable information on the nature and stability of the resulting oxide phases. However, no studies have evaluated the decomposition process of Na-derived dawsonites *in situ* and compared it with the NH_4-counterpart. This can be complemented with spectroscopic techniques to gain insights into changes of metal coordination upon heating (for example, XAFS, ^{27}Al MAS-NMR) and the evolution of chemical species such as hydroxyls and carbonate groups (for example, FT-IR, Raman, TGA-MS). The information is essential to optimize the activation treatment for subsequent catalytic applications.

Thermal decomposition of the dawsonite-type compounds in the temperature range 303-1073 K led to different oxide phases as a function of the metal combination in the original material (Figure 6.1). Up to 423 K, the NH_4-sample experienced a progressive decrease in intensity of the dawsonite reflections, and at 473 K, all reflections have vanished. This corresponds to the reported evolution of the crystalline dawsonite to an alumina phase,[4] which displayed a highly amorphous character, a low skeleton density and a well-developed porosity (*vide infra*). Above this temperature, only the amorphous alumina phase was present and no other crystalline Al-containing phases were discernible up to 873 K. *Ex situ* diffraction studies of the NH_4-dawsonite reported that AlOOH was the most stable phase above 473 K,[25] and transformed into γ-Al_2O_3 at *ca.* 773 K.[26]

The stability of the Na sample in the low-temperature range was higher, as the most intense dawsonite reflections were visible up to 473 K. At 373 K, the reflections attributed to $Na_3H(CO_3)_2{\cdot}2H_2O$ (diffraction lines at *ca.* 18º, 28º, 29º, and 34º 2θ) completely vanished, and new reflections in the 2θ range 28-45º emerged, attributed to sodium carbonate (JCPDS 1-77-2082). The diffractograms at 423 and 473 K were very similar, although partial dehydration of the dawsonite precursors is expected in this range, attending to their corresponding thermogravimetric decomposition profile (*vide infra*). As determined by dividing the total integral area of the most intense reflection at 2θ 16º by that of the starting dawsonite, the amount of dawsonite has decreased more than 76% at 523 K. The absence of dawsonite reflections was evident at 573 K, at which temperature only Na_2CO_3 was present. Thermal treatment of Na-DW-as between 573 and 773 K revealed the progressive crystallization of Na_2CO_3. Up to 773 K, the reflection at 30º 2θ experienced a progressive

shift to lower angles, and the reflection at 35º begun to sharpen. This observation is related to the polymorphism associated with sodium carbonate,[27] with the corresponding increase in the size of the cell parameters *c* and *a* of the monoclinic (γ phase) to the orthorhombic structure (α phase, JCPDS 01-084-0176). Infrared spectroscopic studies demonstrated that the nature of these carbonates is very different from the starting dawsonite and is associated with the disappearance of the original dawsonite and the formation of intermediate less crystalline metastable phases.[28] Further increase of the temperature led to a significant change of the XRD pattern. Above 873 K, sodium aluminum oxide ($NaAlO_2$, JCPDS 19-1179) occurred as a highly crystalline phase. However, carbonates were still present in a less extent but shifted, and appeared together with the aluminate phase as a double reflection at 27.45º 2θ. At 973 K, sodium carbonate was completely decomposed, and another $NaAlO_2$ phase (JCPDS 1-79-1475) was slightly visible beside the one formed previously. Higher temperatures, *i.e.* 1073 K, led to coexistence and crystallization of the aluminate phases. The occurrence of crystalline aluminate in Na-dawsonite calcined above 900 K was previously reported.[28]

These results were substantiated by thermogravimetric analysis and TPD-MS (Figure 6.3), which mainly presented a one-step weight loss in the temperature range 300-650 K for NH_4-DW-as sample. This was attributed to the decomposition of the dawsonite phase into the corresponding alumina in the alkaline precursor. The transition temperature can be estimated from the derivative of weight loss at 441 K for NH_4. These results are supported by XRD observations in Figure 6.1. Thermogravimetric analysis of Na-DW-as displayed a three-step weight-loss profile. Several transition temperatures can be observed at 356, 514, 580, and 930 K, respectively, and were assigned to the decomposition of hydroxyls and carbonates in the structure. The total weight losses of the as-synthesized samples towards alumina or alkaline aluminate amounted to *ca.* 60%, and 42%, respectively. These values are similar to the theoretical weight losses of the pure dawsonites (63% and 43%). The weight loss of NH_4-DW-as is practically matching the theoretical weight loss of the mineral dawsonite (63%) and it can be estimated that 95% of the sample consisted of ammonium dawsonite and only an insignificant part is amorphous. In a similar way, Na-DW-as consisted of 97% Na-dawsonite, in good agreement with the elemental analysis.

Additional evidences for the decomposition process of the dawsonite-type compounds in air were also derived from TPD-MS (Figure 6.3). In the case of NH_4-DW-as, the masses associated with water and carbon dioxide simultaneously evolved from the sample, showing a maximum at the same temperature than that observed by thermogravimetry.

UNIVERSITAT ROVIRA I VIRGILI
CHEMISTRY OF DAWSONITES AND APPLICATION IN CATALYSIS
Georgiana Stoica
ISBN:978-84-693-1533-0/DL:T-648-2010

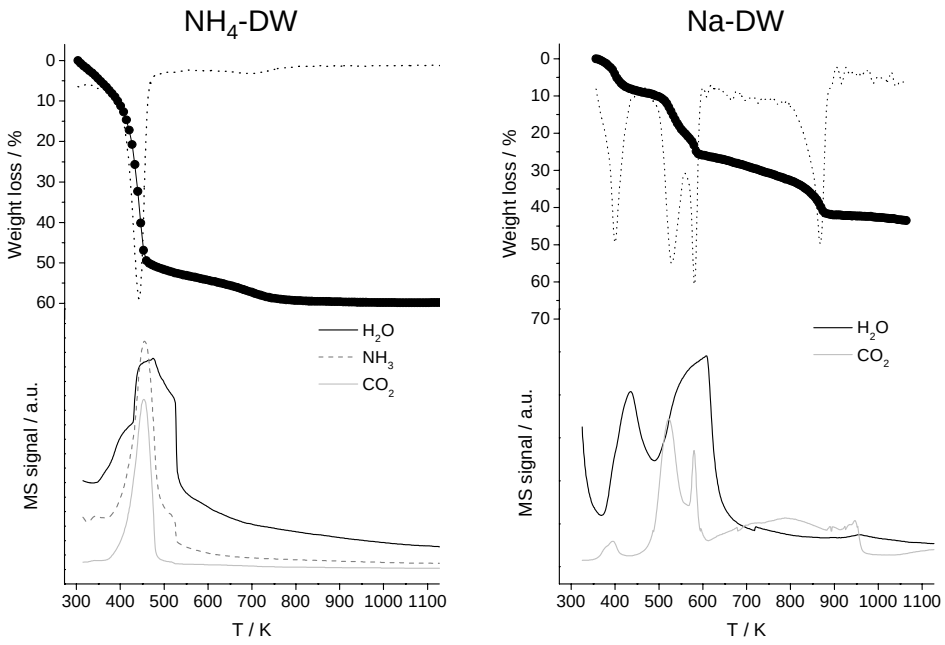

Figure 6.3. TGA-DTG and MS profiles during thermal decomposition of the as-synthesized dawsonites in air at 5 K min^{-1}.

As expected, the presence of ammonia at the reactor outlet upon decomposition of the NH_4-dawsonite was confirmed. Na-dawsonite showed a first endothermic effect up to 500 K, attributed to the decomposition of dawsonite and trona releasing water and CO_2, as well as surface effects, such as contamination from the atmosphere. The second endothermic peak in the range 500-700 K is consistent with the loss of all the hydroxyls and most of the carbonates. At higher temperatures, the rest of the remaining carbonate groups was progressively lost by decomposition of sodium carbonate polymorphs visualized by XRD (Figure 6.1), giving rise to the formation of sodium aluminate.

The textural properties of the materials were determined by adsorption of nitrogen at 77 K (Table 6.1 and Figure 6.4). The N_2 isotherms of the calcined NH_4-DW-as (Figure 6.4) were similar to the as-synthesized material (data not shown). NH_4-DW-473 displayed N_2 uptake in various regions of relative pressure suggesting the hierarchical nature of the material. The N_2 adsorption at lower pressures corresponds to small pores, which is in agreement with the extensive microporosity (V_{micro} = 0.22 $cm^3\,g^{-1}$) attained by application of the *t*-plot method. The presence of small crystals led to the enhanced uptake at higher relative pressures (hysteresis loop type H1). The total pore volume and specific surface area of this sample were 0.38 $cm^3\,g^{-1}$ and 752 $m^2\,g^{-1}$, respectively (Table 6.1). The high total surface area is a consequence of the high external surface area (271 $m^2\,g^{-1}$) due to the newly generated

UNIVERSITAT ROVIRA I VIRGILI
CHEMISTRY OF DAWSONITES AND APPLICATION IN CATALYSIS
Georgiana Stoica
ISBN:978-84-693-1533-0/DL:T-648-2010

microporosity. The micropores were formed by the partial decomposition of the material at this particular temperature as shown before by other techniques (*i.e. in situ* XRD, TG, and TPD-MS). In contrast, the surface area and the total pore volume substantially decreased upon calcination at 973 K, *i.e.* $S_{BET} = 385\ m^2\ g^{-1}$, and $V_{pore} = 0.21\ cm^3\ g^{-1}$ (Table 6.1). This is likely due to the progressive collapse of the mesoporous network upon formation of the larger alumina crystallites, leading to a marked degree of sintering.

The textural and porous properties of Na-dawsonite were also investigated. The total uptake of Na-DW-473 was much lower that in the NH_4-analogue indicating a lower BET surface area of $630\ m^2\ g^{-1}$. However, the total pore volume was similar to NH_4-DW-473, *i.e.* $V_{pore} = 0.35\ cm^3\ g^{-1}$. The N_2 uptake at lower pressures is in agreement with the microporosity displayed by this sample ($V_{micro} = 0.13\ cm^3\ g^{-1}$ in Table 6.1). In addition to the decreased porosity, this sample reflected distinct porous characteristics in the mesopore regime (hysteresis loop type H3), as the isotherm is expanded to the lower p/p_0 range. Thermal decomposition at 973 K induced a marked decrease of the surface area and total pore volume, $S_{BET} = 295\ m^2\ g^{-1}$ and $V_{pore} = 0.18\ cm^3\ g^{-1}$, respectively. Besides, the lack of distinct uptake at low relative pressure evidenced the absence of microporosity. This observation is due to the sintering of the network upon formation of the aluminate crystallites at temperatures above 900 K.

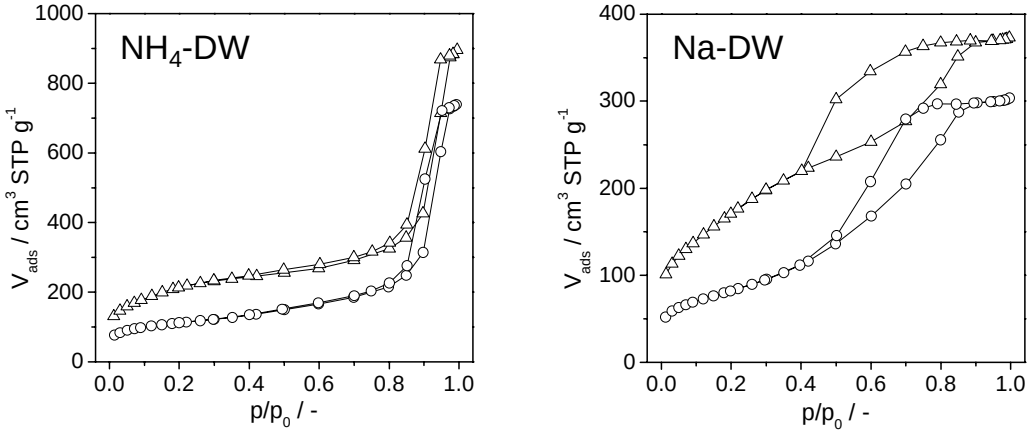

Figure 6.4. N_2 adsorption-desorption isotherms at 77 K of thermal treated dawsonites at 473 (□) or 973 K (○).

UNIVERSITAT ROVIRA I VIRGILI
CHEMISTRY OF DAWSONITES AND APPLICATION IN CATALYSIS
Georgiana Stoica
ISBN:978-84-693-1533-0/DL:T-648-2010

Table 6.1. Characterization data of dawsonites and derived products.

Sample	Phases[a]	V_{pore} ($cm^3\ g^{-1}$)	V_{micro}[b] ($cm^3\ g^{-1}$)	S_{meso} ($m^2\ g^{-1}$)	S_{BET}[c] ($m^2\ g^{-1}$)
NH_4-DW-473	amorphous alumina	0.38	0.22	271	752
NH_4-DW-973	amorphous alumina	0.21	0.05	270	385
Na-DW-473	$NaAlCO_3(OH)_2$ Na_2CO_3	0.35	0.13	350	630
Na-DW-973	$NaAlO_2$	0.18	0	295	295

[a] Determined by powder X-ray diffraction. [b] *t*-plot method. [c] BET method.

The structure of sodium aluminate ($NaAlO_2$) consists of a three dimensional framework of corner linked AlO_4 tetrahedra.[29] The hydrated form has layers of AlO_4 tetrahedra joined into rings and the layers are held together by sodium ions and water molecules that are hydrogen bonded to oxygen atoms in the AlO_4 tetrahedra. As depicted in the ^{27}Al MAS-NMR spectra in Figure 6.5, the structure of the as-synthesized dawsonites contains only octahedrally coordinated aluminum, set to a chemical shit of *ca.* 2 ppm. Calcination at 473 K did not alter the aluminum coordination (not shown). However, the relative amounts of the three different aluminum coordinations (Al^{IV}, Al^{V} and Al^{VI}) upon calcination at 973 K were visible at approximately 70, 35 and 10 ppm, respectively. Specifically for the NH_4-dawsonite, the solid obtained at the highest calcination temperature consisted of alumina phase with significant inherent disorder, as indicated by the presence of five-coordinated aluminum in the sample. In agreement with *in situ* XRD results, this suggests that after calcination at 973 K, the sample still displayed some aluminum-containing amorphous phases with octahedral coordination, coexisting with the corresponding aluminates with tetrahedral coordination. Thermal treatment of Na-dawsonite at 973 K induced a total transformation of the octahedrally coordinated aluminum in Na-DW-as into the tetrahedrally coordinated metal in $NaAlO_2$ (visible at 78 ppm). This observation is in excellent agreement with the *in situ* XRD showing that at 973 K $NaAlO_2$ was already formed, and exhibited well defined crystalline reflections.

Transmission electron microscopy in Figure 6.6 evidenced the presence of fine particles with remarkable size and uniformity in both NH_4 and Na-dawsonites.

UNIVERSITAT ROVIRA I VIRGILI
CHEMISTRY OF DAWSONITES AND APPLICATION IN CATALYSIS
Georgiana Stoica
ISBN:978-84-693-1533-0/DL:T-648-2010

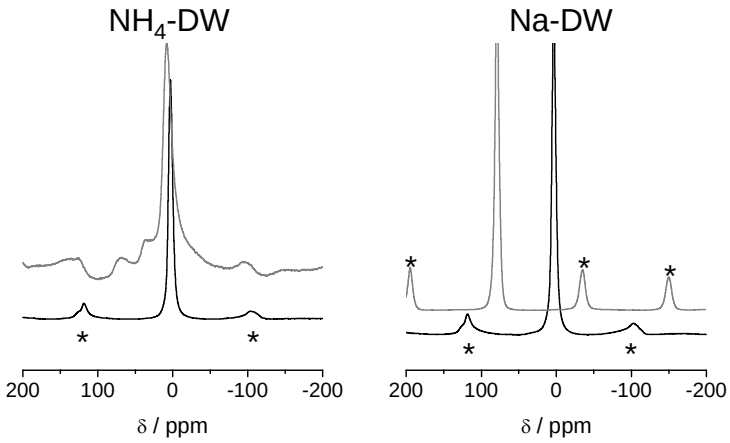

Figure 6.5. ^{27}Al MAS-NMR spectra of the as-synthesized dawsonites (black line) and thermal treated products at 973 K (grey line). Spinning sidebands are denoted with asterisks.

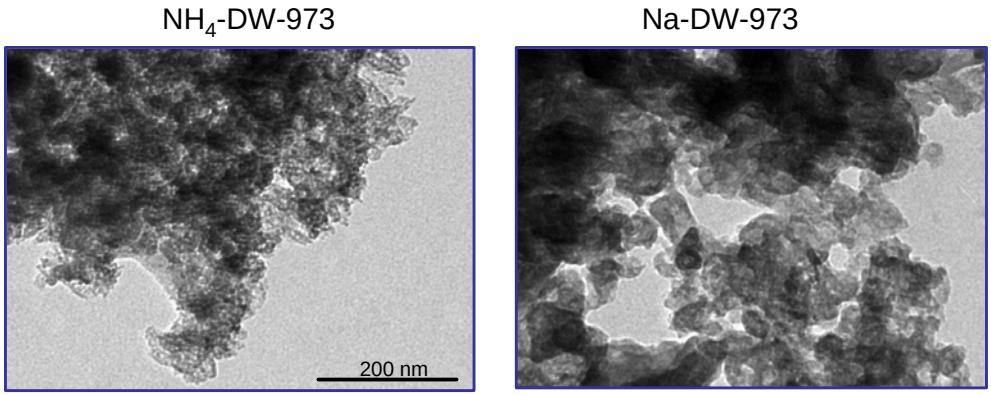

Figure 6.6. TEM of the products derived by thermal treatment of dawsonite at 973 K. The scale bar applies to both micrographs.

3.2. Catalyst screening

The samples were tested in the transesterification of ethylene carbonate with methanol in a fully automated parallel batch reactor,[30] which enables fast catalyst screening. The reaction was conducted at 343 K for 6 h, using a methanol-to-EC ratio of 4 and a W_{cat}/W_{EC} = 10%. Reactants and products were analyzed by off-line gas chromatography. The as-synthesized dawsonites were virtually inactive, leading to DMC yields of about 5% after 6 h (Figure 6.7). A blank experiment without catalyst was performed under the same conditions and led to the formation of DMC in 3% yield. The thermally activated dawsonites were tested in the reaction under the same conditions. The alumina derived from calcination of the NH_4 precursor was inactive.

UNIVERSITAT ROVIRA I VIRGILI
CHEMISTRY OF DAWSONITES AND APPLICATION IN CATALYSIS
Georgiana Stoica
ISBN:978-84-693-1533-0/DL:T-648-2010

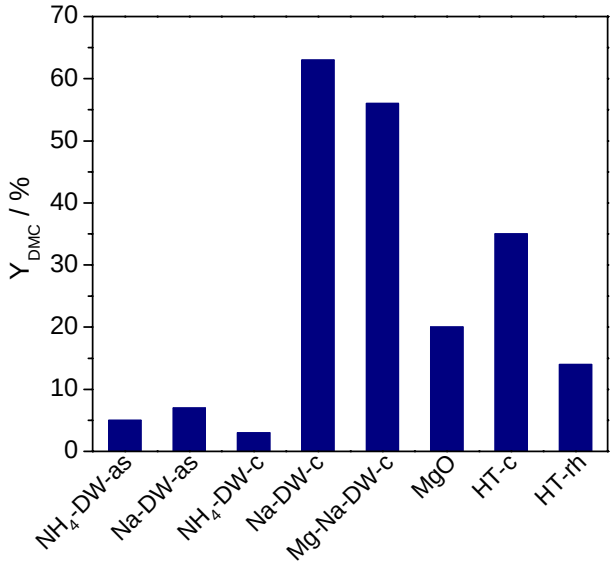

Figure 6.7. Variation in the DMC yield in the transesterification of ethylene carbonate with methanol over selected materials (*T* = 343 K, methanol/EC = 4, 10 wt.% catalyst, t = 6 h).

In contrast, basic aluminates containing Na in the structure reached a maximum yield of DMC of 62%, considering the fact that the conversion is limited to equilibrium. The reaction was extremely fast over these materials, giving a DMC yield of 50% in 5 min. Ethylene glycol was the only by-product identified in the reaction.

In addition to dawsonite-derived materials, hydrotalcite-derived materials and MgO were tested as reference catalysts. Hydrotalcite is a good model system as its basic sites can be tuned by means of the activation method. Thus, Lewis basic sites (O^{2-}) in calcined hydrotalcite (HT-c) are generated by thermal activation of the as-synthesized sample, while Brønsted basic sites (OH^-) can be obtained by rehydration leading to meixnerite (HT-rh).[31] $Mg(Al)O_x$ resulting from calcination of the Mg-Al hydrotalcite (Mg/Al = 3) at 723 K led to a DMC yield of 35% after 6 h (Figure 6.7). The rehydrated hydrotalcite is less active than its calcined counterpart, strongly suggesting that Lewis basic O^{2-} sites are more efficient in the reaction than Brønsted OH^- sites. Our results do not substantiate the work by Watanabe and Tatsumi,[32] who reported that as-synthesized hydrotalcite was the most active catalyst for this reaction. MgO provided lower yields than calcined hydrotalcite (Figure 6.7).

Considering that the mixed oxide obtained by calcination of Mg-Al displays activity, we evaluated whether the introduction of Mg in the structure of dawsonite would further improve its catalytic performance. The oxides obtained by calcination of the Mg-containing Na-dawsonite (Mg/Al = 1:11) did not lead to any improvement in activity (Figure 6.7). Taking into account that the alumina derived from the ammonium precursor was not active and that

UNIVERSITAT ROVIRA I VIRGILI
CHEMISTRY OF DAWSONITES AND APPLICATION IN CATALYSIS
Georgiana Stoica
ISBN:978-84-693-1533-0/DL:T-648-2010

the presence of Mg in the calcined dawsonites did not affect the catalytic performance, the catalytic activity in the calcined dawsonites is assigned to the particular formation of Na aluminate phases.

Since the reaction investigated is a well-known base-catalyzed system, the Hammett indicator was used to determine the basic strength ($H\_$) of the solid derived by thermal activation of Na-dawsonite, according to literature protocols.[21] So far, the basicity of these systems has not been investigated. The sodium aluminate fresh sample transformed the colorless phenolphthalein solution ($H\_ = 9.3$) into pink, but it could not change the color of 2,4-dinitroaniline ($H\_ = 15$) from yellow to purple, but only to orange (Figure 6.8). The material had no influence on the 4-dinitroaniline ($H\_ = 18$). Accordingly, these samples ($10 < H\_ < 15$) could be regarded as moderate bases, following the definition of acids and bases by Tanabe.[33] Our results were different from those of Wan *et al.*[34] who claimed that the commercial $NaAlO_2$ with no treatment is a strong base. Besides, this sample showed the highest activity in the transesterification of soybean oil, and they attributed the high performance to its strong basicity character. However, it has to be reminded that the non-treated Na-aluminate used in that work consisted of three phases, *i.e.* dawsonite, $NaAlO_2{\cdot}xH_2O$, and $NaAlO_2$ which could influence the overall basicity of the catalyst.[34]

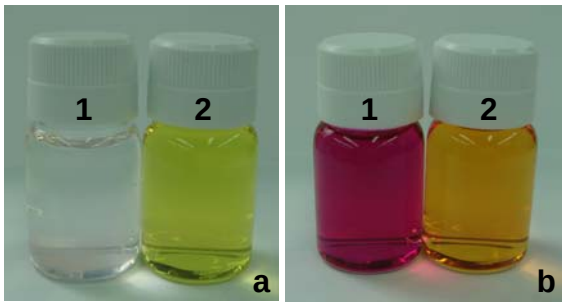

Figure 6.8. Basic strength test of Na-dawsonite derived $NaAlO_2$ using Hammett indicators (1: phenolphtalein, 2: 2,4-dinitroaniline): (a) methanolic solution of the indicators, and (b) methanolic solutions of the indicators and catalyst.

3.3. Transesterification performance

We demonstrated above that the as-synthesized dawsonites were inactive in the reaction, and the NH_4-counterpart displayed no activity independently of the calcination treatment. In contrast, $NaAlO_2$ obtained by thermal decomposition of Na-dawsonite was active for the transesterification of ethylene carbonate with methanol. However, these results attained the DMC thermodynamic equilibrium in a single set of conditions with respect to temperature

UNIVERSITAT ROVIRA I VIRGILI
CHEMISTRY OF DAWSONITES AND APPLICATION IN CATALYSIS
Georgiana Stoica
ISBN:978-84-693-1533-0/DL:T-648-2010

(343 K), molar ratio (methanol-to-EC = 4), and catalyst amount (10% with respect to EC). Consequently, a detailed kinetic picture of the transesterification reaction and an appropriate activation of the starting dawsonite, including deeper studies on the synthesis method were not provided. In line with this, Wan *et al.*[34] reported the commercial sodium aluminate as an active catalyst for the transesterification of soybean oil to biodiesel. Catalytic tests were carried out over a non-treated Na-aluminate, consisting of a mixture of three phases, *i.e.* dawsonite, $NaAlO_2{\cdot}xH_2O$ and $NaAlO_2$. The high performance is attributed to its strong basicity character. Although the authors provided a detailed characterization of this material calcined at different temperatures, the influence thereof on transesterification was not examined. This understanding is needed to exploit the use of dawsonite-derived aluminates in base catalysis.

Accordingly, catalytic tests for the transesterification of ethylene carbonate with methanol at varying conditions will be presented over the Na-dawsonite sample. Figure 6.9 summarizes the DMC yields attained under different experimental conditions. If not mentioned otherwise, each subfigure includes the catalytic data performed under the specified conditions, with the exception of the variable under study.

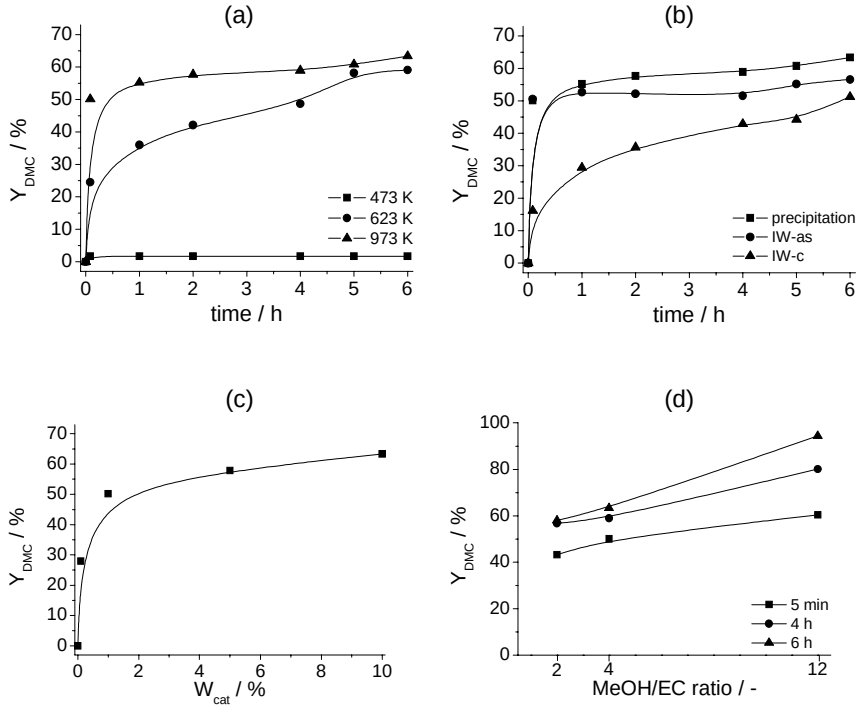

Figure 6.9. DMC yield *vs.* time over calcined Na-DW catalysts. Influence of (a) the calcination temperature, (b) the synthesis method of the dawsonite precursor, (c) the catalyst amount (t = 6 h), and (d) the methanol-to-EC ratio. Standard conditions: T = 343 K, methanol/EC = 4, 10 wt.% catalyst.

UNIVERSITAT ROVIRA I VIRGILI
CHEMISTRY OF DAWSONITES AND APPLICATION IN CATALYSIS
Georgiana Stoica
ISBN:978-84-693-1533-0/DL:T-648-2010

Calcination temperature

The influence of the thermal decomposition temperature of the Na-dawsonite on the yield of DMC is shown in Figure 6.9a, at 343 K, using a molar methanol-EC ratio of 4 and 10% of catalyst with respect to EC. Based on the thermogravimetric decomposition profile (Figure 6.4), three calcination temperatures were chosen for the catalytic activity, *i.e.* 473 K, 623 K, and 973 K, according to the existence of dehydrated dawsonite, partially decomposed dawsonite, and sodium aluminate, respectively. The sample calcined at 473 K was inactive, comparable to the as-synthesized material. The catalyst obtained by calcination at 623 K displayed an increased activity leading to a DMC yield up to 58%. As determined by the *in situ* XRD, the sample at this temperature consisted of sodium carbonate. Commercial Na_2CO_3 was also reported by De Filippis *et al.*[13] to be active in this reaction. When dawsonite was calcined at 973 K, a DMC yield of 62% was obtained. The responsible active phase is $NaAlO_2$ obtained by complete decomposition of Na-DW-as at 973 K as displayed from the XRD and TGA analyses. The transesterification of ethylene carbonate with methanol proceeded very fast, reaching a DMC yield of *ca.* 50% within 5 min. Longer reaction times had a positive effect on the conversion of ethylene carbonate reaching the equilibrium yield after 4 h of reaction.

Synthesis pH and method

Originally, for systematic reasons, the catalytic tests were performed by using samples derived from starting dawsonites synthesized by the ILDP method at pH 8 and calcined at the same conditions. However, other tests varying the synthesis pH of the dawsonite or the synthesis method were conducted in order to assess the occurrence of additional aspects related to the final active phase.

Firstly, the synthesis of the Na-dawsonite was successfully achieved independently of the pH synthesis, which included the range 6-11. Additional reflections of NH_4-dawsonite were only observed in the XRD pattern of the sample precipitated at pH 11. This is due to the fact that NH_4OH was used as precipitating agent besides Na_2CO_3 in order to increase the pH. Thermal decomposition at 973 K of the as-synthesized materials at different pHs led to $NaAlO_2$ in all the cases. The influence of the pH synthesis on the DMC yield showed a very fast reaction in all cases, and the DMC yields were in a narrow range indicating that the process is material-dependent as long as the active phase is $NaAlO_2$. Besides, DMC yields seemed to be slightly higher when the dawsonite precursor is precipitated at pH 8.

UNIVERSITAT ROVIRA I VIRGILI
CHEMISTRY OF DAWSONITES AND APPLICATION IN CATALYSIS
Georgiana Stoica
ISBN:978-84-693-1533-0/DL:T-648-2010

Another important aspect to investigate was the influence of $NaAlO_2$ synthesis method. Besides co-precipitation by the ILDP method, Na-aluminate was also prepared by incipient wetness impregnation. First of all, the as-synthesized NH_4-dawsonite was impregnated with NaOH 10 wt.%, dried at 373 K, and calcined at 673 K for 12 h . The resulting compound (IW-as) exhibited reflections specific to $NaAlO_2$. Additionally, this sample displayed distinctive reflections of sodium nitrite ($Na_2N_2O_2$, JCPDS 50-1853), which is likely derived from the reaction of thermal decomposition products of NH_4-DW-as and NaOH. $NaAlO_2$ was also prepared by calcination of NH_4-DW-as at 723 K, which leads to amorphous γ-Al_2O_3 (JCPDS 26-93), followed by impregnation with NaOH 10 wt.%, and final calcination at 673 K for 12 h. The thermally decomposed sample, *i.e.* IW-c consists of pure $NaAlO_2$. Figure 6.9b shows the catalytic activity over $NaAlO_2$ prepared by the three different methods. The reaction was very fast when using the ILDP method or IW-as, and the DMC yields experienced a major increase in the first 5 min, independently of the method used for the preparation of $NaAlO_2$. However, sodium aluminate prepared from impregnation of the amorphous alumina led to somewhat lower DMC yields. This observation enabled us to conclude that the dawsonite precursor influenced the structure and, consequently, the catalytic performance of the final material.

Subsequent experiments were carried out with $NaAlO_2$ derived from precipitation by the ILDP method at pH 8 and calcination at 973 K.

Temperature and catalyst amount

As expected, there was a progressive increase of the DMC yield with increasing the temperature. After 1 h of reaction, 47, 53, and 55% of DMC was attained at 298, 313 and 343 K, respectively. The DMC equilibrium yield of 62% was completely achieved after 4 h at the highest temperature.

The influence of the catalyst loading was studied in the range 0.1-10 wt.% with respect to ethylene carbonate and the results obtained are shown in Figure 6.9c. A decrease in catalyst weight caused a significant decrease of DMC formation. This dependency indicated that the overall process is controlled by the chemical reaction.

Methanol-to-ethylene carbonate ratio

It is well known that the transesterification of ethylene carbonate with methanol is an equilibrium reaction. Accordingly, a molar ratio higher than the stoichiometric ratio of methanol and EC is required to shift the equilibrium of the reaction towards DMC production.

The DMC yield at different molar methanol-to-EC ratios is shown in Figure 6.9d. The reaction was carried out at the stoichiometric ratio of 2 according to the Scheme 6.1, and besides, excess conditions such as 4 and 12 were applied as well. As it can be anticipated, the reaction also proceeded when the molar ratio between reactants was 2. Moreover, the process occurred in a similar time scale for the ratios 2 and 4 with respect to the formation of DMC. A significant increase in DMC yield up to 90% was observed when methanol was used in large excess (MeOH/EC = 12). Ethylene glycol was the only by-product identified in the reaction, irrespective of the methanol-to-EC ratio. Consequently, the enhancement of the molar ratio was beneficial for this reaction, although the selectivity of DMC and EG did not change. Similar results were obtained by Bhanage *et al.*[11] and Cao *et al.*[35], respectively. Methanol-to-EC ratios in the range 4-16 led to DMC yields up to 90% over Mg-containing smectites or anion exchange resins, respectively, in the one-pot synthesis of DMC.

3.4. Recycling studies

The above results show that calcined Na-dawsonite is highly active catalyst for the transesterification of ethylene carbonate with methanol in comparison with well-established solid bases. Another important characteristic for their performance is the stability. For comparative purposes, we approached this aspect over the most active material, Na-DW-as thermally treated at 973 K, and the reference catalyst, calcined hydrotalcite. Recycling tests were approached by two different strategies: reusability and regenerability, respectively, and are shown in the next paragraph.

Reusability tests were conducted over a used catalyst from a typical experiment after cooling down the reactor to room temperature, recovering the solid by filtration, and drying it. The DMC yield decreased from 35% with the freshly calcined hydrotalcite to 20% in the reused counterpart (Figure 6.10). The DMC yield over calcined Na-dawsonite (Na-DW-ru) decreased by 8% after the first run only, but the activity remained constant in consecutive runs. Apparently, the slight activity lose of these samples is likely due to adsorption of reaction products along the process and/or products derived from cooling down the reactor at the end of the catalytic run. These deposits likely modify the nature of the active centers and/or its accessibility by reactants in subsequent reactions due to steric hindrance, leading to lower DMC selectivity. In order to investigate the presence of adsorbed deposits, XRD and thermogravimetric analyses were conducted over the catalyst used in the first catalytic run, after filtering the reaction mixture and drying the solid in air (data not shown). The XRD pattern of Na-DW-ru showed only very crystalline reflections of sodium aluminate. This

UNIVERSITAT ROVIRA I VIRGILI
CHEMISTRY OF DAWSONITES AND APPLICATION IN CATALYSIS
Georgiana Stoica
ISBN:978-84-693-1533-0/DL:T-648-2010

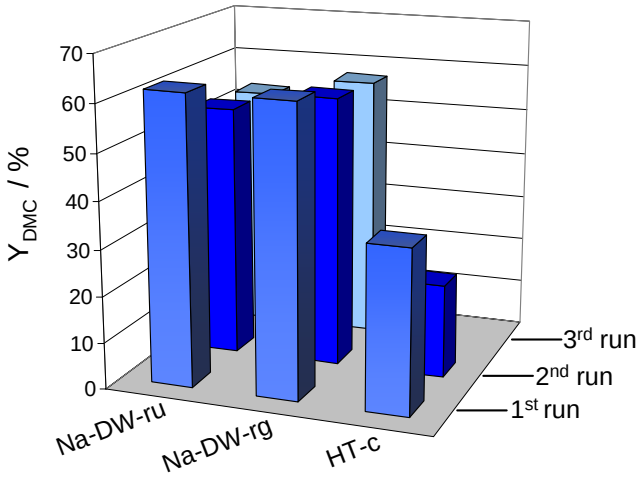

Figure 6.10. DMC yield over Na-DW-c calcined at 973 K upon consecutive runs. Conditions: T = 343 K, methanol/EC = 4, w_{cat}/w_{EC} = 10%, t = 6 h.

observation explains the high catalytic activity observed in the following runs and confirmed that the title reaction is promoted in the presence of $NaAlO_2$. However, the presence of adsorbed species was quantified by thermal analysis and the total weight loss of Na-DW-ru was 7%.

Although only a minor drop of the catalytic activity was observed over Na-DW-ru, the regeneration of the catalyst by calcination after each run was also considered. As shown in Figure 6.10, the DMC activity was slightly recovered over Na-DW-rg, but it was somewhat lower compared to the fresh sample (58% *vs.* 62% at t = 4 h). The yield of DMC remained constant when Na-DW-rg was used for consecutive catalytic runs. These results were consistent with a previous study using commercial sodium aluminate calcined at 873 K in the transesterification of soybean oil with methanol.[16] The variation in the percentage yield for DMC was relatively small, up to 10%, by both approaches. Moreover, the selectivities for DMC and ethylene glycol were unchanged after three consecutive runs and no additional by-products were formed, indicating the high activity of these novel heterogeneous catalysts.

3.5. Scale-up of the transesterification of ethylene carbonate with methanol

Finally, we briefly assessed the scalability of the transesterification reaction over calcined Na-dawsonite. The reaction conditions for Na-DW-c on the gram scale were applied to a 2 L reactor (*i.e.* two orders of magnitude higher than the reactor volume in lab-scale experiments, Figure 6.11). The results over the bench-scale reactor demonstrated the agreement with those obtained in the lab-scale reactor, with a DMC yield of 55% observed after 6 h and a very similar profile for DMC production.

UNIVERSITAT ROVIRA I VIRGILI
CHEMISTRY OF DAWSONITES AND APPLICATION IN CATALYSIS
Georgiana Stoica
ISBN:978-84-693-1533-0/DL:T-648-2010

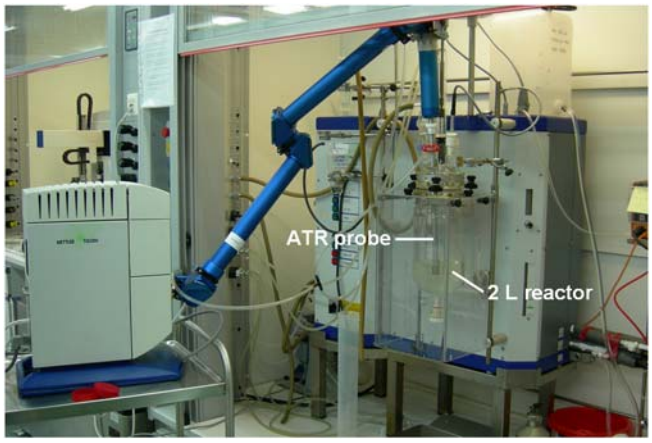

Figure 6.11. The platform used for scale-up studies (T = 343 K, methanol/EC = 4, 10 wt.% (10g) catalyst).

The transesterification reaction over calcined Na-dawsonite at 973 K was also monitored by on-line ATR-FTIR spectroscopy. Attenuated total reflection (ATR) enables kinetic and mechanistic studies by coupling the evolution of liquid-phase reactions with vibrational spectroscopy.[36] Figure 6.12 shows typical infrared spectra for the reaction mixture in the 1100-1800 cm^{-1} region, in which the most important vibrations undergo changes with time. Bands corresponding to ethylene carbonate and DMC were assigned with reference to the spectra of the pure single compounds.

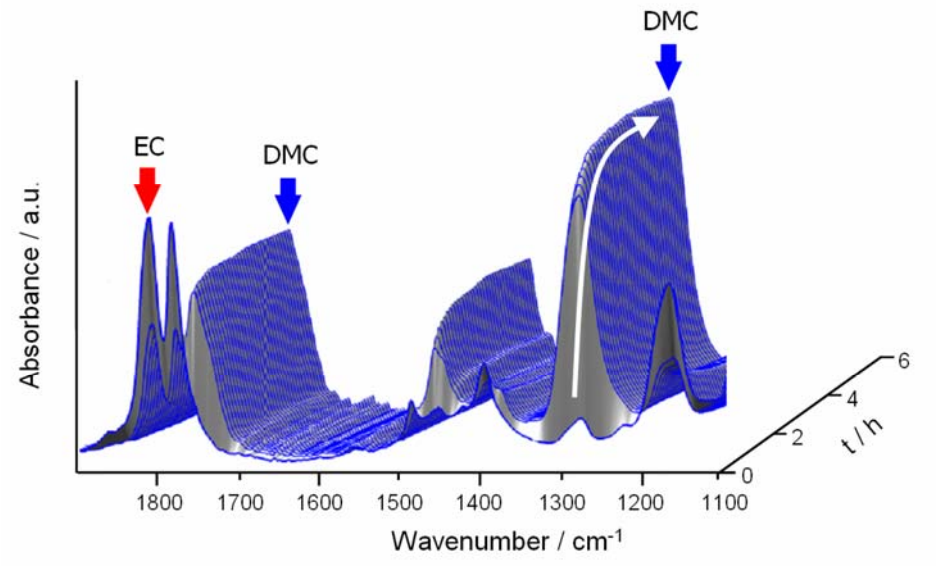

Figure 6.12. Waterfall ATR-IR plot for the transesterification reaction vs. time over Na-DW-973 (T = 343 K, methanol/EC = 4, 10 wt.% catalyst). The band marked with the white arrow was used to quantify the DMC yield.

UNIVERSITAT ROVIRA I VIRGILI
CHEMISTRY OF DAWSONITES AND APPLICATION IN CATALYSIS
Georgiana Stoica
ISBN:978-84-693-1533-0/DL:T-648-2010

At the onset of the reaction, several intense bands in the region 1750-1860 cm^{-1} are related to the asymmetric C=O stretching frequency of ethylene carbonate. As a result of the presence of two ester groups located close together in the molecule, a doublet in the latter zone is observed with maxima at 1772 and 1804 cm^{-1}. Other bands corresponding to ethylene carbonate are attributed to symmetric and asymmetric C-O stretching vibrations at 1185-1275 cm^{-1} and 1050-1160 cm^{-1} (not shown in the plot), respectively. The fast decrease of the bands assigned to ethylene carbonate was accompanied by an increase in absorbance of the DMC bands at 1751 and 1270 cm^{-1}. The latter bands are related to the C=O stretching of an alkyl carbonate (-O-CO-O-) and the C-O-C asymmetric stretching for aliphatic esters, respectively.[37] The disappearance of the bands related to ethylene carbonate at 1770 and 1800 cm^{-1} and the appearance of the band at 1270 cm^{-1} were nicely complemented by off-line GC analysis of the reaction mixture with time, displaying yields of DMC of around 60% after 6 h.

4. Conclusions

Basic alumina derived by thermal activation of Na-dawsonite is efficient, selective, and stable basic catalyst for the green synthesis of DMC by transesterification of ethylene carbonate with methanol. The aluminates are more active than calcined hydrotalcite and magnesium oxide, and, more importantly, they can be successfully recycled. The adequate selection of the activation conditions of the dawsonite precursor, namely the calcination temperature, is decisive to maximize the transesterification activity. Thermal decomposition of the Na-dawsonite precursor at 973 K renders a basic aluminate containing sodium in the structure, which is an active catalyst for the title reaction. The reaction proceeds very fast (in 5 min the yield of DMC reaches 50%) and the process is material-dependent as long as the active phase is the aluminate / basic alumina, finally leading to a maximum DMC yield of *ca.* 65%. The kinetics of the transesterification reaction has been approached by variation of different experimental parameters. The conciliation of the catalytic data on the lab and bench scales is remarkable, which indicates that the reaction can be scaled up. The ATR-IR technique provided real-time infrared spectra under *operando* conditions, avoiding laborious batch-wise sampling of the reaction. The inherent characteristics of these basic catalysts open attractive routes for the use of activated dawsonites in base catalysis.

Acknowledgments

Sònia Abelló is gratefully thanked for valuable contribution to this chapter. Gisela Colet is acknowledged for technical assistance in the scale up tests.

References

[1] Y. Ono, *J. Catal.* **2003**, 216, 406.

[2] H. Hattori, *Appl. Catal. A* **2001**, 222, 247.

[3] K. Tanabe, W. F. Hölderich, *Appl. Catal. A* **1999**, 181, 399.

[4] G. Stoica, J. C. Groen, S. Abelló, R. Manchanda, J. Pérez-Ramírez, *Chem. Mater.* **2008**, 20, 3973.

[5] H. J. Buysch, H. Krimm, H. Rudolph, *US Patent 4181676* **1980**.

[6] D. Delledonne, F. Rivetti, U. Romano, *Appl. Catal. A* **2001**, 221, 241.

[7] P. Tundo, M. Selva, *Acc. Chem. Res.* **2002**, 35, 706.

[8] N. Keller, G. Rebmann, V. Keller, *J. Mol. Catal. A: Chemical* **2009**, doi:10.1016/j.molcata.2009.10.027.

[9] B. M. Bhanage, S. Fujita, Y. Ikushima, M. Arai, *Appl. Catal. A* **2001**, 219, 259.

[10] N. Sheppard, J. W. Ward, *J. Catal.* **1969**, 15, 50.

[11] B. M. Bhanage, S. Fujita, Y. Ikushima, K. Torii, M. Arai, *Green Chem.* **2003**, 5, 71.

[12] Y. Watanabe, T. Tatsumi, *Micropor. Mesopor. Mater.* **1998**, 22, 399.

[13] P. de Fillipis, M. Scarsella, C. Borgianni, F. Pochetti, *Energ. Fuel.* **2006**, 20, 17.

[14] E. S. Jeong, K. H. Kim, D. W. Park, S. W. Park, J. W. Lee, *React. Kinet. Catal. Lett.* **2005**, 86, 241.

[15] T. Wei, M. Wang, W. Wei, Y. Sun, B. Zhong, *Green Chem.* **2003**, 5, 343.

[16] H.-Y. Ju, M. D. Manju, D. W. Park, Y. Choe, S. W. Park, *React. Kinet. Catal. Lett.* **2007**, 90, 3.

[17] P. de Filippis, M. Scarsella, C. Borgianni, F. Pochetti, *Energy Fuels* **2006**, 20, 17.

[18] S. Abelló, J. Pérez-Ramírez, *Adv. Mater.* **2006**, 18, 2436.

[19] S. Brunauer, P. H. Emmet, E. Teller, *J. Am. Chem. Soc.* **1938**, 60, 309.

[20] B. C. Lippens, J. H. de Boer, *J. Catal.* **1965**, 4, 319.

[21] W. Xie, H. Li, *J. Mol. Catal A: Chemical* **2006**, 255, 1.

[22] C. J. Serna, J. V. García-Ramos, M. J. Peña, *Spectrochim. Acta* **1985**, 41A, 697.

[23] R. S. Gärtner, G.-J. Witkamp, *Hydrometallurgy* **2007**, 88, 75.

[24] M. S. Yalfani, M. Santiago, J. Pérez-Ramírez, *J. Mater. Chem.* **2007**, 17, 1222.

UNIVERSITAT ROVIRA I VIRGILI
CHEMISTRY OF DAWSONITES AND APPLICATION IN CATALYSIS
Georgiana Stoica
ISBN:978-84-693-1533-0/DL:T-648-2010

[25] L. A. O'Deall, S. L. P. Savin, A. V. Chadwick, M. E. Smith, *Solid State Nucl. Magn. Reson.* **2007**, 31, 169.

[26] G. Groppi, C. Cristiani, P. Forzatti and M. Belloto, *J. Mater. Sci.* **1994**, 29, 3441.

[27] M. Dusek, G. Chapuis, M. Meyer, V. Petricek, *Acta Crystallogr., Sect. B : Struct. Sci.* **2003**, B59, 337.

[28] M. J. Hernández, M. A. Ulibarri, J. Cornejo, M. J. Peña, C. J. Serna, *Thermochim. Acta* **1985**, 94, 257.

[29] J. A. Kaduk, S. Y. Pei, *J. Solid State Chem.* **1995**, 115, 126.

[30] S. Abelló, S. Dhir, G. Colet, J. Pérez-Ramírez, *Appl. Catal. A* **2007**, 325, 121.

[31] S. Abelló, F. Medina, D. Tichit, J. Pérez-Ramírez, J. C. Groen, J. E. Sueiras, P. Salagre, Y. Cesteros, *Chem. Eur. J* **2005**, 11, 728.

[32] Y. Watanabe, T. Tatsumi, *Microporous Mesoporous Mater.* **1998**, 22, 399.

[33] K. Tanabe, B. Imelik, in *Catalysis by Acids and Bases*; B. Imelik, C. Nacceche, G. Condurier, Y. B. Taarti, J. C. Vedrine, Eds.; Elsevier, Amsterdam, **1985**, p. 1.

[34] T. Wan, P. Yu, S. Wang, Y. Luo, *Energ. Fuel.* **2009**, 23, 1089.

[35] M. Cao, Y. Meng, Y. Lu, *React. Kinet. Catal. Lett.* **2006**, 88, 251.

[36] J. C. Groen, G. M. Hamminga, J. A. Moulijn, J. Pérez-Ramírez, *Phys. Chem. Chem. Phys.* **2007**, 9, 4822.

[37] G. Socrates, *Infrared Characteristic Group Frequencies*, John Wiley & Sons, New York, **1980**, p. 71.

UNIVERSITAT ROVIRA I VIRGILI
CHEMISTRY OF DAWSONITES AND APPLICATION IN CATALYSIS
Georgiana Stoica
ISBN:978-84-693-1533-0/DL:T-648-2010

UNIVERSITAT ROVIRA I VIRGILI
CHEMISTRY OF DAWSONITES AND APPLICATION IN CATALYSIS
Georgiana Stoica
ISBN:978-84-693-1533-0/DL:T-648-2010

UNIVERSITAT ROVIRA I VIRGILI
CHEMISTRY OF DAWSONITES AND APPLICATION IN CATALYSIS
Georgiana Stoica
ISBN:978-84-693-1533-0/DL:T-648-2010

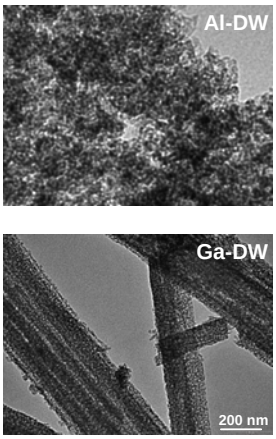

Chapter 7

Epoxidation Catalysts Derived from Aluminum and Gallium Dawsonites

As-synthesized and reconstructed NH_4-Al-dawsonite and NH_4-Ga-dawsonite, and the materials obtained by thermal treatment in the range 373-873 K, were studied as heterogeneous catalysts for the epoxidation of cyclooctene with hydrogen peroxide at 353 K and ambient pressure by means of High-Throughput Experimentation. The temperature at which the dawsonite precursors were treated proved to be crucial in determining the activity of the catalysts. The best catalyst identified in this work was obtained by calcination at 573 K of reconstructed Ga-dawsonite. This material provided an epoxide yield of 51% and 99% selectivity after 4 h at 353 K. Remarkably, many of the catalysts derived from Al-dawsonite displayed an enhanced epoxidation activity upon recycling, reaching up to 30% epoxide yield with 98% selectivity over Al-dawsonite treated at 473 K.

This chapter is based on the following publication:
G. Stoica, M. Santiago, P. A. Jacobs, J. Pérez-Ramírez, P. P. Pescarmona, *Appl. Catal. A* **2009**, 371, 43.

UNIVERSITAT ROVIRA I VIRGILI
CHEMISTRY OF DAWSONITES AND APPLICATION IN CATALYSIS
Georgiana Stoica
ISBN:978-84-693-1533-0/DL:T-648-2010

1. Introduction

The efficient and sustainable production of fine chemicals requires the use of suitable catalytic processes to convert the selected substrates into the desired products with high atom efficiency, thus generating a minimal amount of waste, and using environmentally friendly reagents and solvents. Epoxides are versatile compounds with many applications in the fine chemical industry.[1] Therefore, the development of active and selective catalysts for the sustainable synthesis of this family of compounds is an attractive and relevant research target. Epoxides are generally produced by oxidation of alkenes. Aiming at an environmentally friendly process, aqueous hydrogen peroxide is the oxidant of choice since it is readily available, relatively cheap, safe, and produces water as by-product of the epoxidation.[2]

A promising class of heterogeneous catalysts for the epoxidation of alkenes with H_2O_2 is represented by partially hydroxylated aluminum and gallium oxides.[3-6] These transition-metal-free materials are active in the epoxidation of a wide range of alkenes in environmentally acceptable solvents and generally display high epoxide selectivities.[7] It has been proposed that the catalytically active sites are provided by mildly acidic surface Al-OH or Ga-OH groups that react with H_2O_2 to form surface hydroperoxide species, which in turn are able to transfer an oxygen atom to the alkene with formation of the epoxide.[8] The method used to prepare the oxides has a strong influence on their catalytic behavior. The synthesis protocol for both types of oxides was optimized by means of High-Throughput Experimentation (HTE) and a gallium oxide prepared by the hydrolysis of $GaCl_3$ proved to be the most active among a large set of aluminum and gallium oxides.[3] Although this class of catalysts presents many of the ideal features for a sustainable epoxidation process, a major drawback is that both the aluminum and gallium oxides undergo deactivation upon few successive catalytic runs.[3,9,10] Besides, the turnover (moles of product per gram of catalyst) of these materials could be improved by enlarging their specific surface area, thus increasing the fraction of aluminum or gallium species located in accessible sites for the catalytic reaction. In this context, a promising method for preparing aluminum and gallium oxides with improved catalytic performance comprises the thermal decomposition of ammonium aluminum carbonate hydroxide ($NH_4AlCO_3(OH)_2$) and of its gallium analogue ($NH_4GaCO_3(OH)_2$). $NH_4AlCO_3(OH)_2$ is isostructural with the mineral dawsonite, $NaAlCO_3(OH)_2$.[11] Dawsonite-type compounds are excellent precursors for catalytic materials with high specific surface area, uniform particle size, well-defined porosity, and resistance to thermal sintering.[12-16] However, no study has reported the synthesis of Ga-dawsonite and its thermal evolution to the corresponding oxide.

UNIVERSITAT ROVIRA I VIRGILI
CHEMISTRY OF DAWSONITES AND APPLICATION IN CATALYSIS
Georgiana Stoica
ISBN:978-84-693-1533-0/DL:T-648-2010

Herein, we report a study of aluminum and gallium compounds prepared from the respective NH_4-Al and NH_4-Ga dawsonite precursors using thermal treatment at different temperatures, with the purpose of generating high-surface area materials with improved catalytic performance in alkene epoxidation with aqueous hydrogen peroxide. Cyclooctene was chosen as substrate to provide an easy comparison with previously reported aluminum and gallium oxide catalysts (Scheme 7.1). The thermal treatment conditions influence the formation of certain crystalline and amorphous phases, the specific surface area, the number and type of surface hydroxyls of the oxides and, consequently, their catalytic behavior.

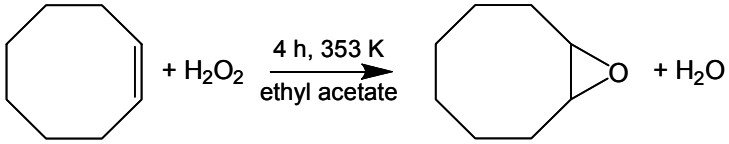

Scheme 7.1. Epoxidation of cyclooctene with hydrogen peroxide.

2. Experimental

2.1. Materials and treatments

NH_4-Al and NH_4-Ga dawsonites were synthesized by continuous precipitation at constant pH using the in-line dispersion-precipitation (ILDP) method.[14,17] Briefly, aqueous solutions of $Al(NO_3)_3 \cdot 9H_2O$ (0.48 M) (Scharlau, purity 98%) or $Ga(NO_3)_3 \cdot 9H_2O$ (0.48 M) (Alfa Aesar, purity 99.9%) and the precipitating agent ($(NH_4)_2CO_3$, 1 M) (Scharlau, purity 99%) were pumped into a 6 cm^3 microreactor attached to a high-shear homogenizer rotating at 13 500 rpm. The pH of the slurry was measured and controlled by an in-line probe directly at the outlet of the precipitation chamber. The synthesis was carried out at pH 8 with an average residence time of 18 s. The resulting slurry was aged at 333 K for 3 h, followed by filtration, washing, and drying at 333 K for 12 h. GaO(OH) was prepared by precipitation of an aqueous solution of $Ga(NO_3)_3$ (0.48 M) with K_2CO_3 (1 M) at pH 8 using the ILDP method described above.

The as-synthesized samples were subjected to thermal treatments at different temperatures. In a typical treatment, the solid sample was weighed in a porcelain crucible, placed in a calcination oven, and heated to the desired temperature in the range 373-873 K in static air during 2 h. The heating rate was 5 K min^{-1}.

Reconstruction experiments were conducted in a round bottom flask under reflux conditions at 323 K. The treatment consisted in dispersing the oxide powder, obtained by calcination of

UNIVERSITAT ROVIRA I VIRGILI
CHEMISTRY OF DAWSONITES AND APPLICATION IN CATALYSIS
Georgiana Stoica
ISBN:978-84-693-1533-0/DL:T-648-2010

the as-synthesized dawsonites at 723 K, in 1 M $(NH_4)_2CO_3$ aqueous solution under magnetic stirring (350 rpm) at 323 K for 24 h.[15] The treated samples were filtered, washed with deionized water until neutral pH, dried at 333 K for 12 h, and finally thermally treated as described above.

In this manuscript, the as-synthesized, reconstructed, and thermally treated samples are identified by the codes *X*-AS, *X*-R, and *X*-*y* and *X*-R-*y*, respectively, where *X* is Al or Ga, and *y* is the calcination temperature in Kelvin. Samples reused in consecutive catalytic tests are labelled as follows: *X*-*y*-rec#, where # is the number of recycling runs. Table 7.1 lists the catalysts studied in this work.

2.2. Characterization

The aluminum and gallium content in the as-synthesized samples was determined by inductive coupled plasma-optical emission spectroscopy (ICP-OES) (Perkin-Elmer Optima 3200RL (radial)). Elemental analysis (C, H, and N) was performed on a Carlo Erba EA1108 instrument. Powder X-ray diffraction (XRD) patterns were measured on a Bruker AXS D8 Advance diffractometer equipped with a Cu tube, a Ge(111) incident beam monochromator (λ = 0.1541 nm), and a Vantec-1 PSD. Data were recorded in the range of 10-70º 2θ with an angular step size of 0.016º and a counting time of 6 s per step. Fourier transform infrared spectroscopy (FTIR) measurements were carried out on a Bruker Optics Tensor 27 spectrometer equipped with a Golden Gate Diamond ATR unit. Spectra were collected at room temperature in the range 650-4000 cm^{-1} by co-addition of 32 scans at a nominal resolution of 4 cm^{-1}. The spectrum of the empty cell at ambient conditions was taken as the background. Transmission electron microscopy (TEM) analysis was carried out in a JEOL JEM-1011 microscope operated at 80 kV. A few droplets of the sample suspended in ethanol were placed on a carbon-coated copper grid followed by evaporation at ambient conditions. Nitrogen isotherms at 77 K were measured in a Quantachrome Autosorb-1MP analyzer. Prior to analysis, the samples were degassed in vacuum at 373 K for 16 h. The BET method[18] was applied to calculate the total surface area, and the *t*-plot method[19] was used to discriminate between micro- and mesoporosity. Thermogravimetric analysis (TGA) was carried out in a Mettler Toledo TGA/SDTA851e microbalance. Analyses were performed in dry air flow of 50 cm^3 STP min^{-1}, ramping the temperature from 298 to 1173 K at 5 K min^{-1}.

2.3. Catalytic tests

The catalysts were tested in the epoxidation of cis-cyclooctene with a 50 wt.% aqueous

UNIVERSITAT ROVIRA I VIRGILI
CHEMISTRY OF DAWSONITES AND APPLICATION IN CATALYSIS
Georgiana Stoica
ISBN:978-84-693-1533-0/DL:T-648-2010

solution of hydrogen peroxide (Scheme 7.1) using similar conditions to those reported previously for testing aluminum and gallium oxides.[3,7] An amount of solid catalysts containing 0.50 mmol of either Al or Ga was used in each test. The amount of catalyst (in grams) was calculated under the assumption that the as-synthesized or reconstructed material had the formula $NH_4AlCO_3(OH)_2$ or $NH_4GaCO_3(OH)_2$, and taking into account the weight loss after the thermal treatment. First, a solution of cyclooctene (2.50 mmol) and di-*n*-butyl ether (1.25 mmol) in ethyl acetate (2.50 g) was added to each solid catalyst while stirring, followed by addition of the aqueous solution of hydrogen peroxide (5.00 mmol). Both solutions were dispensed using an automated High-Throughput Experimentation (HTE) workstation.[1] The samples were stirred for 4 h at 500 rpm and 353 K in capped vials placed in a 60-well parallel reaction block. When the temperature in the vials reached 353 K, the rubber septa of the caps were pierced with a sharp needle to prevent development of overpressure inside the reactors.

Cyclooctene conversion (*X*, %), epoxycyclooctane and by-products yield (*Y*, %), and selectivity (*S*, %) were determined by gas chromatography (GC) analysis using an Interscience Finnigan Trace GC Ultra equipped with a RTX-5 fused silica column (5 m, 0.1 mm). The analysis time for each sample was 2.25 min. Before GC analysis, the samples were centrifuged for 5 min at 3000 rpm. An aliquot of the reaction mixture (*ca.* 0.3 ml) was added to an equal volume of decane to induce phase separation of any H_2O that might have been present in the sample, thus preventing its injection into the chromatograph. The conversions and yields were calculated by normalizing the areas of the GC peaks by means of the area of the internal standard peak (di-*n*-butyl ether). A number of catalytic tests were conducted in duplicate: in such case, the average of the obtained conversions and yields is reported. Gas chromatography-mass spectrometry analysis (GC-MS) on an Agilent 6890N gas chromatograph coupled to an Agilent 5973 MSD mass spectrometer was used to identify reaction by-products. The GC was equipped with a WCOT fused silica column (30 m, 0.25 mm) coated with a 0.25-μm-thick HP-5 MS film.

For the recycling of the catalysts, first the reaction solution was removed from each sample, then 7 ml of ethanol was added to each vial and the samples were stirred for 5 min. Next, the samples were centrifuged for 7 min at 3500 rpm to settle the solid catalyst, after which the supernatant ethanol solution was removed. The washing procedure was repeated 3 times. Finally, the samples were dried at 363 K for 16 h and used for further catalytic runs.

The amount of H_2O_2 decomposed into H_2O and O_2 during the catalytic test was determined by titration with a 0.1 M solution of $Ce(SO_4)_2$.[20]

UNIVERSITAT ROVIRA I VIRGILI
CHEMISTRY OF DAWSONITES AND APPLICATION IN CATALYSIS
Georgiana Stoica
ISBN:978-84-693-1533-0/DL:T-648-2010

3. Results and discussion

3.1. Characterization

As-synthesized samples

The empirical formula of the as-synthesized NH_4-Al-dawsonite (Al-AS), as determined by elemental analysis and ICP-OES, was $C_{0.78}H_{6.20}N_{0.68}O_{5.40}Al$. As reported previously, this composition differs from the theoretical formula of a pure ammonium-form of dawsonite ($C_1H_6N_1O_5Al_1$ or $NH_4AlCO_3(OH)_2$) indicating that besides the predominant dawsonite phase (estimated at 70-80% from the empirical formula) the sample contained additional aluminum-containing phase(s). However, the X-ray diffraction pattern of Al-AS in Figure 7.1a only showed the characteristic reflections of ammonium aluminum carbonate hydroxide ($NH_4AlCO_3(OH)_2$, JCPDS 42-250). Consequently, the extra Al-containing phases in the precipitate were ascribed to amorphous species. The empirical formula of the as-synthesized NH_4-Ga-dawsonite (Ga-AS) was $C_{0.22}H_{2.70}N_{0.22}O_{3.26}Ga$. The ratios C/Ga, H/Ga, and N/Ga were significantly lower in Ga-AS than in the theoretical formula of a pure gallium dawsonite, $NH_4GaCO_3(OH)_2$. This indicated the presence of extra gallium-containing phases besides Ga-dawsonite. Based on the empirical and theoretical formulas, it can be inferred that only 22% of Ga-AS consisted of dawsonite. Indeed, the XRD pattern of Ga-AS in Figure 7.1b exhibited reflections characteristic to ammonium gallium carbonate hydroxide ($NH_4GaCO_3(OH)_2$, (JCPDS 33-60) as well as of gallium (oxi)hydroxide (GaO(OH), JCPDS 6-180). This is the first time Ga-dawsonite has been reported, although the applied synthesis route did not render it as pure. For the sake of conciseness and when no specific disambiguation is needed, the Ga-AS sample is referred to as Ga-dawsonite along the chapter.

The Fourier transform infrared spectra of the as-synthesized samples at room temperature (Figure 7.2) exhibited characteristic absorptions of the hydroxyl, ammonium, and carbonate groups in dawsonite.[21] For Al-AS, the following bands were identified: OH^- (ν_{OH} at 3435 cm^{-1}; δ_{OH} at 985 cm^{-1}), NH_4^+ (ν_{NH} at 3170, 3005, and 2840 cm^{-1}; δ_{NH} at 1830 and 1720 cm^{-1}), and CO_3^{2-} (ν_3 at 1545, 1445, and 1387 cm^{-1}, ν_1 at 1105 cm^{-1}, ν_2 at 852 cm^{-1}, and ν_4 at 755 and 735 cm^{-1}). In the case of Ga-AS, the same bands found in Al-AS were identified. However, the ν_3 mode of the carbonates at 1387 cm^{-1} in Al-AS is shifted to lower wavenumbers in Ga-AS (1362 cm^{-1}). The vibrational modes corresponding to the OH groups appeared at lower wavenumbers, *i.e.* ν_{OH} at 3360 cm^{-1} and δ_{OH} at 977 cm^{-1}, respectively. Several hypotheses are proposed for the observed OH groups shift: it could be due to the different structure of Ga-AS

UNIVERSITAT ROVIRA I VIRGILI
CHEMISTRY OF DAWSONITES AND APPLICATION IN CATALYSIS
Georgiana Stoica
ISBN:978-84-693-1533-0/DL:T-648-2010

compared to Al-AS or it could be related to the presence of the hydroxyls from the GaO(OH) phase, which is the main component of the gallium as-synthesized material.

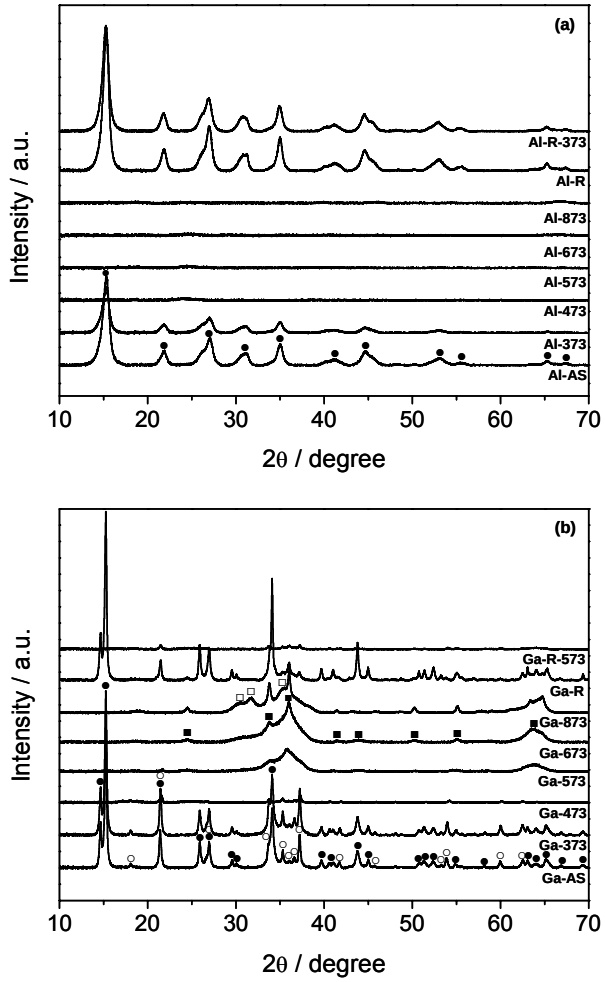

Figure 7.1. X-ray diffraction patterns of (a) Al-AS and (b) Ga-AS and derived materials. Crystalline phases: (●) dawsonite, (○) GaO(OH), (■) α-Ga_2O_3, and (□) β-Ga_2O_3.

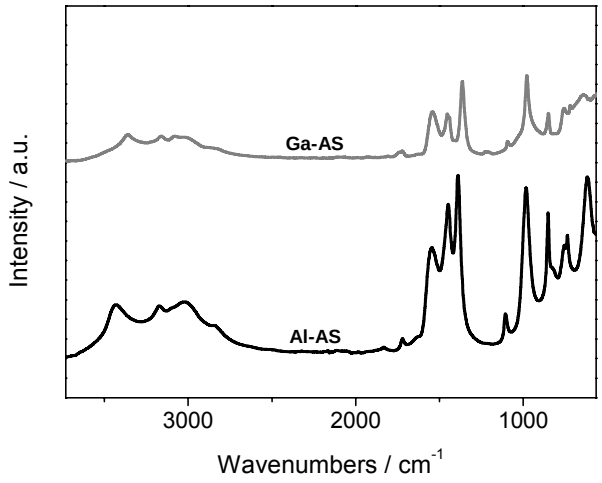

Figure 7.2. Infrared spectra of Al-AS (black) and Ga-AS (grey).

UNIVERSITAT ROVIRA I VIRGILI
CHEMISTRY OF DAWSONITES AND APPLICATION IN CATALYSIS
Georgiana Stoica
ISBN:978-84-693-1533-0/DL:T-648-2010

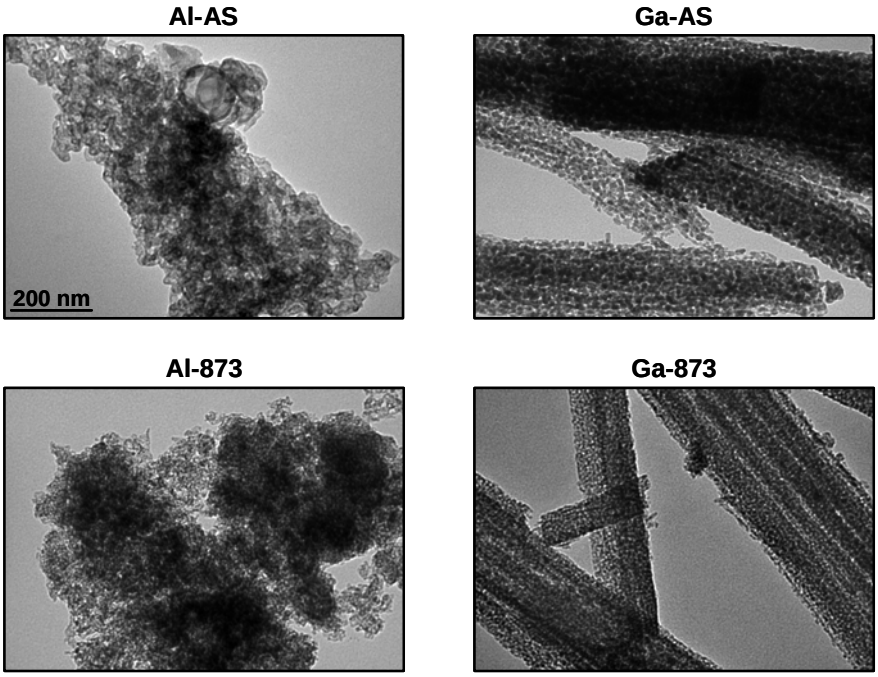

Figure 7.3. Transmission electron micrograph of Al-AS and Ga-AS and thermally derived products (at 873 K). The scale bar applies to all micrographs.

The morphology of both as-synthesized samples determined by TEM is shown in Figure 7.3. Al-AS was composed of agglomerates of nanoparticles, while the particles in Ga-AS were assembled in very long and uniform aciculae. The acicular morphology of Ga-AS resembles more the mineral dawsonite,[22] than the typically reported zeppelin-like, spindle-like, or rod-like morphologies of the additional GaO(OH) phase.[23] The textural properties of the materials were determined by nitrogen adsorption at 77 K (Figure 7.4). The N_2 uptake at lower pressures corresponded to small pores, while intermediate and higher uptakes were indicative of mesopores. The total pore volume and specific surface area of Al-AS were 1.27 $cm^3\ g^{-1}$ and 832 $m^2\ g^{-1}$, respectively (Table 7.1). The sample contained extensive microporosity, *i.e.* 0.14 $cm^3\ g^{-1}$, as determined by application of the *t*-plot method. The external surface area is high (500 $m^2\ g^{-1}$) due to the presence of small particles. Since the particles are uniform in size, the pore size distribution, determined by application of the BJH model in the adsorption branch of the isotherm rendered mesopores centered at 10 nm (not shown).

Similarly, Ga-AS exhibited N_2 uptake at low and high pressures. However, the total uptake was much lower that in Al-AS indicating a lower total pore volume, V_{pore} = 0.3 $cm^3\ g^{-1}$, and a BET surface area of 330 $m^2\ g^{-1}$ (Table 7.1). Application of the *t*-plot method resulted in an estimated V_{micro} = 0.15 $cm^3\ g^{-1}$, equivalent to the micropore volume in Al-AS. The much

UNIVERSITAT ROVIRA I VIRGILI
CHEMISTRY OF DAWSONITES AND APPLICATION IN CATALYSIS
Georgiana Stoica
ISBN:978-84-693-1533-0/DL:T-648-2010

lower mesopore surface area of Ga-AS indicated the presence of larger particles, in line with the TEM description.

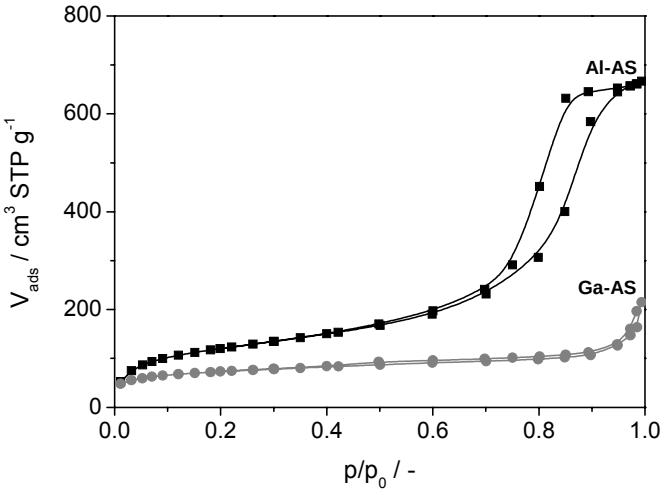

Figure 7.4. Nitrogen isotherms at 77 K of Al-AS (black) and Ga-AS (grey).

Thermal decomposition

The as-synthesized materials were subjected to thermal treatment in air at different temperatures in the range 373-873 K and the obtained materials were fully characterized with a combination of techniques. The TGA profile of Al-AS in Figure 7.5a showed the one-step weight loss at 450 K assigned to the decomposition of the ammonium aluminum carbonate hydroxide into alumina.[12] The total weight loss of Al-AS amounted to *ca.* 57%, *i.e.* less than the theoretical weight loss of pure NH_4-Al dawsonite (63%). This difference is due to the amorphous Al-containing phases present in addition to dawsonite and decomposing in the same temperature range. Assuming that these amorphous phases are aluminum (oxi)hydroxides, the dawsonite content was estimated as 74%, in agreement with the relative amount of dawsonite phase determined from chemical composition analyses, *i.e.* 70-80%. Although crystalline aluminum (oxi)hydroxides display weight loss up to higher temperatures (> 500 K),[24] this step is not expected to be discernible in the thermogravimetric profile due to the amorphous nature of the (oxi)hydroxides in Al-AS, to their small relative amount and to the low percentage of weight loss associated with their decomposition into oxides. Figure 7.5b shows the two-step thermal decomposition profile of Ga-AS, each step being assigned to one of the two phases identified by XRD. The first weight loss at 430 K amounted to 10% and was attributed to the decomposition of the gallium dawsonite phase. The transition temperatures of the two as-synthesized materials (450 K in Al-AS *vs.* 430 K in Ga-

UNIVERSITAT ROVIRA I VIRGILI
CHEMISTRY OF DAWSONITES AND APPLICATION IN CATALYSIS
Georgiana Stoica
ISBN:978-84-693-1533-0/DL:T-648-2010

AS) indicate that the thermal stability of Al-dawsonite is somewhat higher. The second weight loss of 7.5% was attributed to the dehydroxylation of GaO(OH) at higher temperatures (530-680 K). Assuming that the dawsonite phase is converted into Ga_2O_3 (*vide infra*), the theoretical weight loss for the decomposition of $NH_4GaCO_3(OH)_2$ was 48%, while the weight loss of a GaO(OH) phase can vary in the range 8.7-12.1%, depending on the synthesis method, with a transition temperature from 573 to 673 K.[24] From these data it was derived that only 20% of Ga-AS corresponded to the dawsonite phase while 80% consisted of GaO(OH). These thermogravimetric results matched the outcome from elemental analysis confirming that the as-synthesized material consists predominantly of GaO(OH) and $NH_4GaCO_3(OH)_2$.

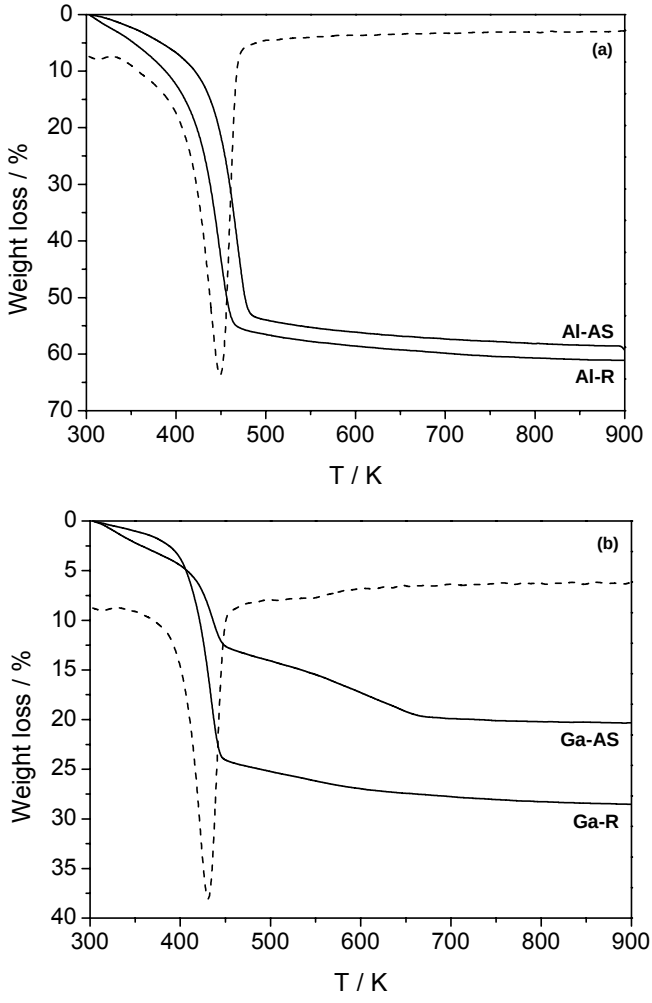

Figure 7.5. Thermogravimetric profiles (solid lines) and derivative of the weight loss (dashed lines) of selected samples upon decomposition in air at 5 K min^{-1}: (a) as-synthesized and reconstructed Al-dawsonite; (b) as-synthesized and reconstructed Ga-dawsonite.

UNIVERSITAT ROVIRA I VIRGILI
CHEMISTRY OF DAWSONITES AND APPLICATION IN CATALYSIS
Georgiana Stoica
ISBN:978-84-693-1533-0/DL:T-648-2010

Table 7.1. Characterization data of the samples.

Sample	Phases[a]	V_{pore} ($cm^3\ g^{-1}$)	V_{micro}[b] ($cm^3\ g^{-1}$)	S_{meso} ($m^2\ g^{-1}$)	S_{BET}[c] ($m^2\ g^{-1}$)
Al-AS	$NH_4AlCO_3(OH)_2$	1.27	0.14	500	839
Al-373	$NH_4AlCO_3(OH)_2$	1.28	0.12	493	832
Al-473	-	-	-	-	-
Al-573	-	1.24	0	479	479
Al-673	-	-	-	-	-
Al-873	γ-Al_2O_3	1.08	0	393	393
Al-R	$NH_4AlCO_3(OH)_2$	-	-	-	-
Al-R-373	$NH_4AlCO_3(OH)_2$	-	-	-	-
Ga-AS	$NH_4GaCO_3(OH)_2$ GaO(OH)	0.3	0.15	40	330
Ga-373	$NH_4GaCO_3(OH)_2$ GaO(OH)	0.24	0.12	143	330
Ga-473	GaO(OH)	-	-	-	-
Ga-573	GaO(OH) Ga_2O_3 (α or γ)	0.27	0	131	131
Ga-673	α-Ga_2O_3	-	-	-	-
Ga-873	α-Ga_2O_3 β-Ga_2O_3	0.2	0	85	85
Ga-R	$NH_4GaCO_3(OH)_2$ GaO(OH) α-Ga_2O_3	-	-	-	-
Ga-R-573	GaO(OH) α-Ga_2O_3	-	-	-	-

[a] Determined by powder X-ray diffraction. [b] *t*-plot method. [c] BET method.

UNIVERSITAT ROVIRA I VIRGILI
CHEMISTRY OF DAWSONITES AND APPLICATION IN CATALYSIS
Georgiana Stoica
ISBN:978-84-693-1533-0/DL:T-648-2010

The X-ray diffraction patterns of the materials obtained upon thermal treatment of Al-AS at different temperatures (Figure 7.1a) indicated that after treatment at 373 K the dawsonite phase begun to deteriorate, and after treatment at 473 K, no reflections of the dawsonite phase were present anymore. This was in agreement with the decomposition temperature of 453 K determined by thermal analysis. The diffractograms of the materials treated between 473 and 873 K showed no crystalline phase. After treatment at 873 K, broad reflections characteristic of γ-Al_2O_3 (JCPDS 29-63) became slightly discernable.

The XRD pattern of Ga-373 was analogous to that of Ga-AS, consisting of both Ga-dawsonite and GaO(OH). After treatment at 473 K, the sample showed only the reflections of GaO(OH) (Figure 7.1b), in excellent agreement with the decomposition of the dawsonite phase into an amorphous phase monitored by TGA. Thermal treatment at 573 K led to the formation of a phase with low crystallinity that can be assigned to γ-Ga_2O_3 and/or to α-Ga_2O_3. γ-Ga_2O_3 is a metastable polymorph of gallia with a cubic structure (JCPDS 6-527), often characterized by relatively low crystallinity,[25] while α-Ga_2O_3 is a polymorph of gallia with hexagonal structure (JCPDS 6-503). We propose that the dawsonite phase is the precursor of this poorly crystalline Ga_2O_3 polymorph. The exact nature of this phase could not be unequivocally determined because the α and γ polymorphs display overlapping XRD reflections,[23] they coexist in the same temperature range and both tend to convert into β-Ga_2O_3 (JCPDS 6-523) when treated at high temperatures.[25,26] After treatment at 573 K, traces of GaO(OH) were also observed. It has been reported that GaO(OH) is a precursor of α-Ga_2O_3.[27] Indeed, the reflections due to the GaO(OH) present in Ga-AS gradually decreased in intensity as a consequence of the thermal treatment between 473 and 573 K, in agreement with TGA results, and in Ga-673 the crystalline GaO(OH) phase was not detected anymore. At the same time, the reflections due to α-Ga_2O_3 became increasingly intense in Ga-673 and in Ga-873, where this polymorph coexisted with β-Ga_2O_3, *i.e.* the thermodynamically most stable polymorph of gallium oxide.[28] Summarizing, Ga-AS consisted of a dawsonite phase that, upon treatment at intermediate temperatures, transformed into a low-crystallinity Ga_2O_3 polymorph that finally converted into β-Ga_2O_3 at high temperatures; a GaO(OH) phase that upon thermal treatment was converted into α-Ga_2O_3; and possibly one or more amorphous gallium (oxy)hydroxides that converted into α- or β-Ga_2O_3 at high temperatures (> 673 K).

The remarkable resistance of Al-AS derived aluminas to sinter into γ-Al_2O_3 upon thermal treatment in the range 473-873 K was additionally demonstrated by TEM and N_2 adsorption. The particle size and morphology, and the uniform mesoporosity in the as-synthesized

UNIVERSITAT ROVIRA I VIRGILI
CHEMISTRY OF DAWSONITES AND APPLICATION IN CATALYSIS
Georgiana Stoica
ISBN:978-84-693-1533-0/DL:T-648-2010

material were kept in the calcined products (Figure 7.3). Similar to Al-AS, the morphology of the gallium oxides was preserved upon calcination and very long needles can be observed (Ga-873 in Figure 7.3).

The N_2 isotherms of the calcined samples (Figure 7.6a) were similar to those of the as-synthesized material; however, the total pore volume was slightly lower (Table 7.1). The microporosity and, consequently, the total surface area and pore volume of Al-AS might have been altered because the samples were degassed at 373 K before the measurement, causing a modification of the structure (*vide supra*). Once the dawsonite phase was decomposed, the microporosity disappeared inducing a significant decrease of the surface area. The sample calcined at 873 K experienced a marked degree of sintering with a substantial decrease of both S_{BET} and V_{pore} (Table 7.1) and thus the formation of larger γ-Al_2O_3 crystallites. Nevertheless, the surface area (S_{BET} = 393 m^2 g^{-1}) was substantially larger than that of conventional γ-aluminas (typically 150-200 m^2 g^{-1}),[29] and than that of mesostructured γ-alumina prepared using surfactants as templating agents (300-350 m^2 g^{-1}).[30]

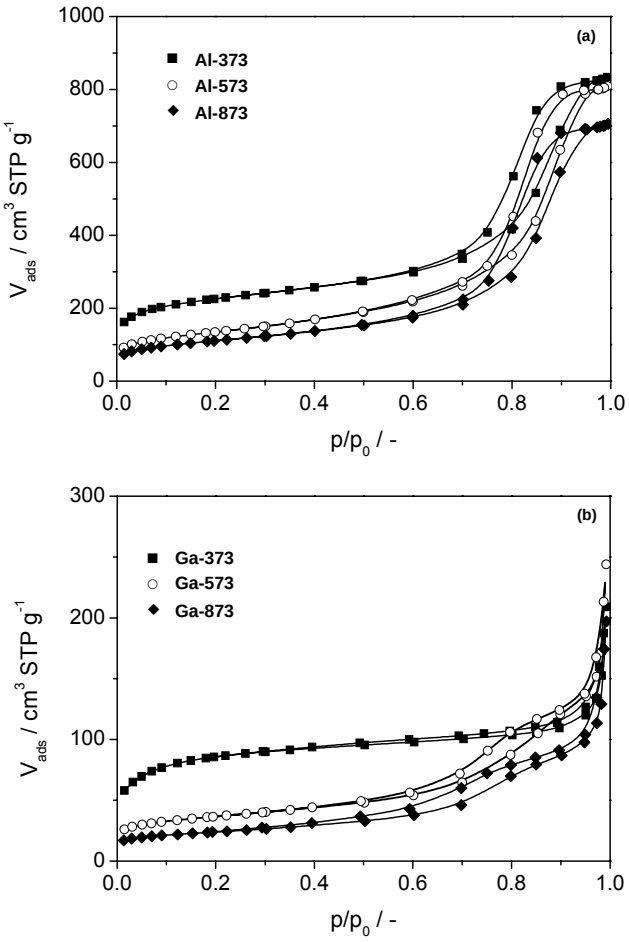

Figure 7.6. Nitrogen isotherms of the thermally treated (a) Al-AS and (b) Ga-AS at selected temperatures.

UNIVERSITAT ROVIRA I VIRGILI
CHEMISTRY OF DAWSONITES AND APPLICATION IN CATALYSIS
Georgiana Stoica
ISBN:978-84-693-1533-0/DL:T-648-2010

N_2 adsorption of Ga-373 was similar to Ga-AS due to the presence of Ga-dawsonite at this temperature (Figure 7.6b). The treatment of Ga-AS at 373 K might led to certain change in microporosity. Decomposition of the Ga-dawsonite phase resulted in a decrease of the BET surface area by 50% in Ga-573 with respect to Ga-AS, in agreement with the disappearance of the micropores in the original material (Table 7.1) and the formation of mesopores of more uniform size as indicated by the shape of the isotherms. The sintering was more pronounced at 873 K, leading to a significant decrease of the total surface area (S_{BET} = 132 m^2 g^{-1}) and pore volume (V_{pore} = 0.13 cm^3 g^{-1}) due to the formation of larger oxide particles. However, the specific surface area of Ga-873 was relatively large considering that the material consisted of more phases and that the formula weight of gallia is higher than that of alumina.

Reconstructed materials

It was proven that the oxides obtained by decomposition of ammonium aluminum dawsonite exhibit memory effect, *i.e.* they tend to undergo a reconstruction process if brought in contact with a 1 M aqueous solution of $(NH_4)_2CO_3$ at 323 K.[15,31] The reconstructed samples generally present a higher percentage of dawsonite phase compared to the parent as-synthesized material, where a fraction of amorphous species could be present. Reconstructed ammonium dawsonite (Al-R) was prepared by treatment in an aqueous ammonium carbonate solution of Al-AS thermally decomposed at 723 K. Al-R exhibited more intense and sharper dawsonite reflections compared to the parent material (Figure 7.1a). The chemical formula of Al-R, $C_{0.88}H_{7.20}N_{0.90}O_{5.80}Al$, indicated a high-purity material consisting of 90% of dawsonite, very similar to the ammonium-form of the mineral. As expected, the thermogravimetric profile of Al-R (Figure 7.5a) exhibited the one-step decomposition pattern at *ca.* 450 K described for as-synthesized dawsonites, with an increased weight loss, *i.e.* 62%.

In analogy with the experimental approach followed for the aluminum sample, a reconstructed gallium dawsonite (Ga-R) was also prepared. The reconstructed material exhibited reflections of Ga-dawsonite and, in lesser extent, reflections specific to GaO(OH) and to α-Ga_2O_3 (the latter generated by calcination of Ga-AS at 723 K) (Figure 7.1b). The ratio between the intensity of the reflections due to the dawsonite phase and those due to GaO(OH) was higher in Ga-R than in Ga-AS, in agreement with the expected higher percentage of the dawsonite phase in the reconstructed material. Chemical composition and thermal analyses of the reconstructed sample confirmed the XRD result. The chemical formula of Ga-R, $C_{0.44}H_{2.95}N_{0.38}O_{3.47}Ga$, indicated that the amount of Ga-dawsonite phase (38-44%) doubled compared to that in Ga-AS. Similar conclusions were derived from thermal

analysis. The thermogravimetric profile of Ga-R (Figure 7.5b) exhibited the one-step decomposition pattern described for as-synthesized dawsonites and the transition temperature matched well the data reported in the literature for other dawsonite-type materials (*ca.* 430 K).[31] Although the reconstruction of a Ga-dawsonite phase was not complete, the total weight loss of Ga-R was significantly higher than that of Ga-AS, due to the higher relative content of $NH_4GaCO_3(OH)_2$ in Ga-R. Similarly to previous results reported for dawsonite-derived oxides,[15] the reconstruction of Ga_2O_3 is specific to ammonium carbonate aqueous solutions and follows a dissolution-precipitation mechanism leading to a reformed material. This result indicates that reconstruction takes place independently of the presence of Al species in the starting material. Previously, reconstruction had been demonstrated for metal-substituted aluminas.[31]

3.2. Catalytic performance

The as-synthesized materials (Al-AS and Ga-AS) and those obtained by their thermal treatment in the range 373-873 K were tested in the epoxidation of cyclooctene with aqueous hydrogen peroxide. As shown in Figure 7.7 and 7.8, the Al-dawsonite derived materials displayed very different trends in catalytic performance compared with those observed with the Ga-dawsonite derived materials.

Al-dawsonite derived catalysts

The epoxide yields of the Al-dawsonite derived catalysts as a function of the temperature of the thermal treatment are reported in Figure 7.7a, while a more detailed overview of the catalytic results can be found in Table 7.2 (1^{st} catalytic run). A peculiar behavior was observed: the yield of epoxycyclooctane first decreased upon increasing the temperature of the thermal treatment, reaching a minimum at 573 K; then it gradually increased up to the thermal treatment at 873 K. This profile was markedly different from that observed for the catalytic activity of sol-gel aluminas as a function of the calcination temperature.[9] The most active catalysts were also the most selective, reaching a cyclooctene conversion of 21% with an epoxide selectivity of 97% over Al-373. The same high selectivity (97%) and a slightly lower epoxide yield (16%) were found with the as-synthesized material, Al-AS. Al-873, containing a poorly crystalline γ-Al_2O_3 phase, displayed the second highest alkene conversion (17%) among the tested catalysts, with 94% selectivity towards the epoxide. Selectivity below 90%, mainly due to the formation of 2-cycloocten-1-one as by-product, was only found with Al-573 and Al-673.

UNIVERSITAT ROVIRA I VIRGILI
CHEMISTRY OF DAWSONITES AND APPLICATION IN CATALYSIS
Georgiana Stoica
ISBN:978-84-693-1533-0/DL:T-648-2010

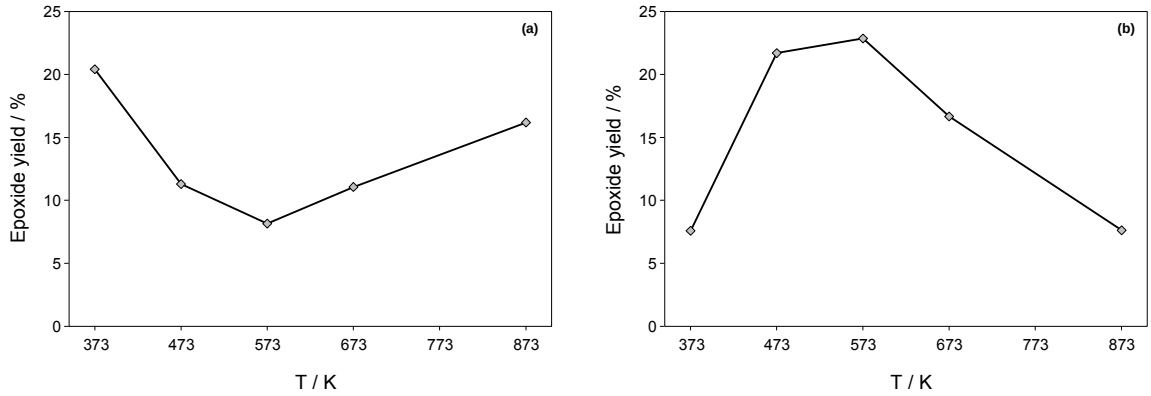

Figure 7.7. Epoxidation of cyclooctene with H_2O_2 on the catalysts obtained by thermal treatment of (a) Al-AS and (b) Ga-AS: epoxide yield as a function of the temperature of the thermal treatment.

The catalytic activity of Al-AS and Al-373 was not ascribed to the dawsonite phase but rather to amorphous aluminum (oxi)hydroxides and/or partially hydroxylated oxides formed by hydrolysis of the dawsonite during the catalytic reaction (the water is originating from the aqueous solution of hydrogen peroxide). This hypothesis was supported by the gradual disappearance of the reflections of the dawsonite phase in the XRD patterns of the used Al-AS and Al-373 catalysts (Figure 7.9a) and by the results of the recycling of these catalysts (*vide infra*). It has been proposed that the catalytically active sites are surface Al-OH groups of moderate Brønsted acidity.[5] However, a too high concentration of these sites is detrimental because it would make the catalyst surface very hydrophilic, thus preventing the approach of the apolar alkene to the active site.[32] Finding the best aluminum catalyst requires a fine balance between the population of Al-OH groups and the hydrophilicity of the surface. Accordingly, the very low catalytic activity of Al-473 and Al-573 can be correlated to a too high hydrophilicity due to the highly hydroxylated surfaces expected for the amorphous species formed upon decomposition of the dawsonite phase at these relatively low temperatures.[32] By increasing the thermal treatment temperature, the surfaces of the catalysts became more dehydroxylated and, therefore, less hydrophilic, causing an increase in catalytic activity. Treatment at 873 K led to a γ-Al_2O_3 phase, which has been reported to be the most active phase for epoxidation reactions.[5,32]

The reconstructed dawsonite was treated at 373 K, *i.e.* the thermal treatment that led to the most active catalyst derived from Al-AS, and tested in the epoxidation reaction. The obtained Al-R-373 displayed much lower catalytic activity compared to Al-373 (Table 7.2) as the amount of crystalline dawsonite in Al-R is higher than in the as-synthesized material and, therefore, its hydrolysis during the catalytic reaction to form an active phase is slower.

UNIVERSITAT ROVIRA I VIRGILI
CHEMISTRY OF DAWSONITES AND APPLICATION IN CATALYSIS
Georgiana Stoica
ISBN:978-84-693-1533-0/DL:T-648-2010

Aluminum oxide epoxidation catalysts have been reported to gradually deactivate upon recycling. This has been correlated with structural and textural changes, and poisoning of the active sites by carboxylates and diols formed during the catalytic reaction.[10] Therefore, it is important to evaluate the stability of the dawsonite-based Al-catalysts in successive runs. The catalysts were recovered from the reaction mixture after the first test, thoroughly washed with ethanol, and reused in a new epoxidation test. The recycling was repeated for a total of four cycles for each catalyst. The results are reported in Figure 7.8a and Table 7.2.

Table 7.2. Performance of the catalysts in the epoxidation of cyclooctene with H_2O_2.

Catalyst	1st run		2nd run		3rd run		4th run	
	X[a] (%)	S[b] (%)	X (%)	S (%)	X (%)	S (%)	X (%)	S (%)
Al-AS	16	97	24	97	28	98	25	97
Al-373	21	97	18	97	19	95	18	96
Al-473	12	92	31	98	26	97	23	98
Al-573	10	84	23	95	22	95	20	96
Al-673	14	80	16	93	18	94	16	95
Al-873	17	94	11	93	7	78	3	83
Al-R-373	10	97	13	97	9	96	10	95
Ga-AS	12	98	21	94	16	86	-	-
Ga-373	8	100	12	95	12	93	-	-
Ga-473	22	98	13	94	10	92	-	-
Ga-573	23	97	10	94	3	89	-	-
Ga-673	17	97	17	97	7	86	-	-
Ga-873	8	92	4	84	5	80	-	-
Ga-R-573	52	99	46	99	20	98	16	80
GaO(OH)-AS	1	88	-	-	-	-	-	-
GaO(OH)-573	6	100	-	-	-	-	-	-

[a] Conversion of cyclooctene. [b] Selectivity towards epoxycyclooctene.

UNIVERSITAT ROVIRA I VIRGILI
CHEMISTRY OF DAWSONITES AND APPLICATION IN CATALYSIS
Georgiana Stoica
ISBN:978-84-693-1533-0/DL:T-648-2010

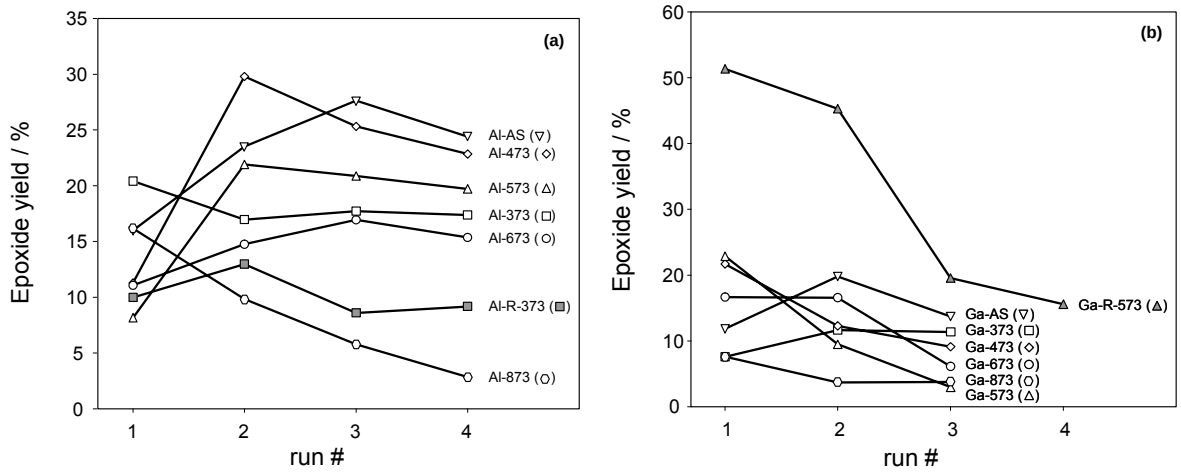

Figure 7.8. Epoxidation of cyclooctene with H_2O_2 on (a) Al-AS and (b) Ga-AS and derived products: epoxide yield upon recycling of the catalysts.

The two catalysts with the highest epoxidation activity in the first run, Al-373 and Al-873, deactivated upon recycling. The deactivation of Al-873 was relatively rapid, in line with what was reported for γ-Al_2O_3 catalysts.[9] On the other hand, Al-373 deactivated slowly and experienced only a slight decrease in activity after 4 cycles (from 20 to 17%). This result underlines the different nature of the catalytically active phases in the two samples, in agreement with what we proposed above. Strikingly, all the other catalysts, *i.e.* Al-AS, Al-473, Al-573 and Al-673, displayed an enhanced epoxidation activity in the second catalytic run. The improvement is particularly noteworthy for Al-473, for which the epoxide yield increased from 11% in the first catalytic run to 30% in the second run. After 4 h of reaction at 353 K, Al-473-rec1 displayed a similar productivity (2.04 grams of epoxide per gram of catalyst) and a 1.5 higher turnover number compared with the most active aluminum oxide catalysts previously reported, obtained by a sol-gel method from an $Al(Bu^sO)_3$ precursor.[3,5] It should be kept in mind that the TON values reported in this chapter are calculated on the basis of the total Al or Ga content, while only a small fraction of these atoms is expected to act as catalytic sites for the epoxidation (in the order of magnitude of 0.1%).[8] Therefore, conversion, selectivity, and productivity are more meaningful parameters when comparing the results of this type of Al- and Ga-catalysts with those of other catalytic systems. The epoxidation activity of Al-473 and Al-573 declined again upon further recycling, while the activity of Al-AS and Al-673 increased until the third catalytic cycle and then started to decrease. Similarly to what has been observed for Al-373, the deactivation occurred slowly and all the Al-catalysts with the exception of Al-873 still displayed a significant epoxidation activity after 4 catalytic cycles. The remarkable behavior of these Al-catalysts upon recycling was never

reported before in other aluminum oxides. In conclusion, the initial increase in the activity upon recycling, followed by a deactivation upon further reuse can be explained assuming that during the epoxidation reaction the surface of certain catalysts undergo reconstruction promoted by water and leading to the formation of highly active surface hydroxyls. The formed active species and those already existing may gradually get poisoned or themselves be subjected to structural changes leading to their disappearance during the successive catalytic runs.

XRD analysis of selected catalysts (Figure 7.9a) showed that the crystalline dawsonite phase in Al-AS and Al-373 tends to disappear during the catalytic reaction. The dawsonite phase had a higher crystallinity in Al-AS compared to Al-373. The lower degree of crystallinity in Al-373 enables a more rapid conversion of the dawsonite phase to active amorphous aluminum oxide/(oxi)hydroxides and consequently led to a higher activity in the first run but a more rapid deactivation in the following runs (Figure 7.8a). The higher degree of crystallinity of dawsonite in Al-AS implies that the conversion of the dawsonite phase to the active amorphous aluminum phases occurs more gradually and is not complete after the first catalytic run; as a consequence, the activity in the first run was lower than with Al-373 but gradually increased in the following runs (until the third). The XRD pattern of the catalyst displaying the highest activity in the second run, Al-473-rec1, showed the presence of a γ-Al_2O_3 phase with low crystallinity (Figure 7.9a), generated during the catalytic reaction from the amorphous phase formed upon treatment of Al-AS at 473 K. The incipient formation of a γ-Al_2O_3 phase can account for the fact that Al-473-rec1 displayed the highest activity among the recycled Al-catalysts, since γ-Al_2O_3 is considered to be the most active aluminum-containing phase.[5] The improved TON observed with Al-473-rec1 compared to previously reported aluminum oxides can be ascribed to the large specific surface area of the dawsonite-derived aluminum oxides/(oxi)hydroxides (Table 7.1), implying that a higher fraction of the aluminum atoms of the material are exposed on the surface and, therefore, available for the catalytic reaction. The large increase in activity upon recycling observed with Al-473 and Al-573 is in agreement with the high level of reconstruction previously found with ammonium dawsonite treated in this temperature range, while samples obtained by thermal treatment at high temperatures display higher stability and, therefore, are less prone to reconstruction.[15]

UNIVERSITAT ROVIRA I VIRGILI
CHEMISTRY OF DAWSONITES AND APPLICATION IN CATALYSIS
Georgiana Stoica
ISBN:978-84-693-1533-0/DL:T-648-2010

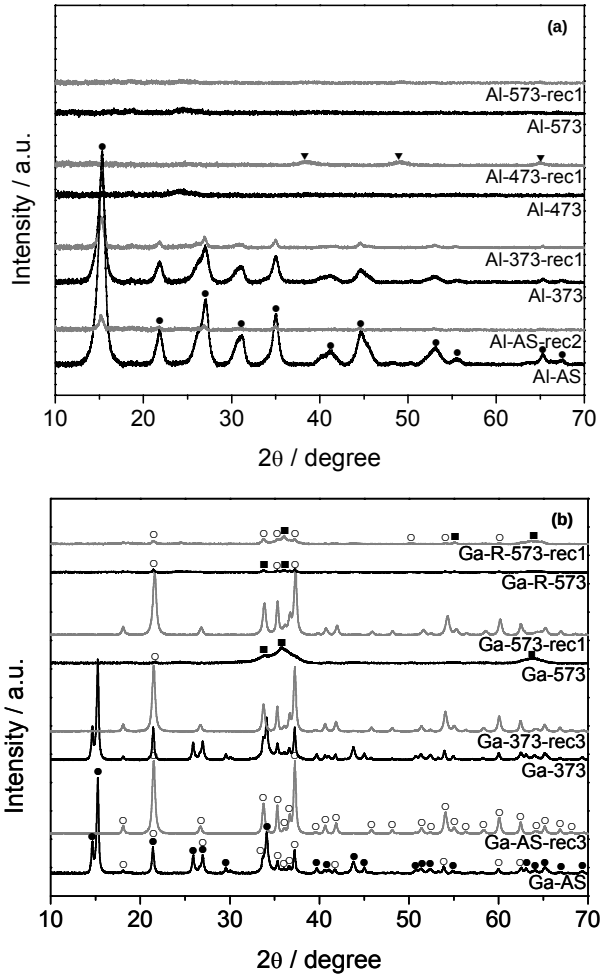

Figure 7.9. X-ray diffraction patterns of fresh (black) and reused (grey) (a) Al-AS and (b) Ga-AS and derived materials. Crystalline phases: (●) dawsonite, (▼) γ-Al_2O_3, (○) GaO(OH), and (■) α-Ga_2O_3.

In summary, the different stage at which each of the Al-catalysts reached its maximum activity can be correlated to the rate at which they undergo reconstruction. Materials that are subject to rapid structural changes will reach their maximum activity at an earlier stage compared to materials that reconstruct more gradually due to a higher degree of structural stability. Materials whose structures are sufficiently stable not to undergo reconstruction during the catalytic reaction (Al-873) displayed the highest activity in the first catalytic run. These results also point to the fact that different amorphous or low-crystallinity phases can provide a suitable equilibrium between the hydrophilicity of the surface and the number and type of Al-OH species to achieve the desired catalytic activity.

UNIVERSITAT ROVIRA I VIRGILI
CHEMISTRY OF DAWSONITES AND APPLICATION IN CATALYSIS
Georgiana Stoica
ISBN:978-84-693-1533-0/DL:T-648-2010

Ga-dawsonite derived catalysts

The approach followed for studying the gallium catalysts derived from Ga-AS was analogous to that described above for the aluminum catalysts: the as-synthesized material, Ga-AS, was subjected to thermal treatment at different temperatures in the range 373-873 K and the obtained materials were tested as catalysts in the epoxidation of cyclooctene with aqueous hydrogen peroxide. Figure 7.7b reports the epoxide yields as a function of the temperature of the thermal treatment, while Table 7.2 provides a more complete overview of the catalytic results. With all the gallium catalysts, epoxycyclooctane was formed with very high selectivity and only a low amount of by-products was observed. The approximately constant by-products yield with all Ga-catalysts, including the recycled samples, implies that lower epoxide selectivity is observed only with catalysts having low epoxidation activity. Therefore, in the following discussion the attention is focused on the differences in activity among the various gallium catalysts.

Ga-AS and the catalyst obtained after treatment at 373 K (Ga-373) displayed relatively low epoxidation activity. Upon treatment at 473 K or 573 K, Ga-catalysts with higher activity were formed, reaching a maximum epoxide yield of 23% after 4 h with Ga-573. Thermal treatment at higher temperatures caused a decrease in the activity of the catalysts (Ga-673 and Ga-873) proportional to the calcination temperature. The activities observed with the gallium catalysts derived from Ga-AS are directly connected with the type of gallium phases present in the thermally treated materials. The most active phases in the epoxidation of cyclooctene with H_2O_2 were assigned to gallium oxides with an amorphous structure or with a low level of crystallinity, in agreement with the XRD analysis of the most active catalysts, Ga-473 and Ga-573. Due to their amorphous or poor crystalline nature, these phases are expected to be rich in Ga-OH surface groups, which have been proposed to be the catalytic active centers for the epoxidation. These considerations were in agreement with what we observed for the Al-catalysts and with the results reported for aluminum and gallium oxides as epoxidation catalysts.[3,32] The catalytically active phases present in Ga-473 and Ga-573 are expected to be formed by the decomposition of the dawsonite phase of Ga-AS into partially hydroxylated gallium oxides. On the other hand, the dawsonite phase itself, present in Ga-AS and Ga-373, was not expected to be contributing to the catalytic reaction: the low epoxidation activity observed with these two materials was mainly attributed to amorphous hydroxylated gallium phases formed by hydrolysis of the dawsonite during the catalytic reaction, in agreement with the results of the recycling of these catalysts (*vide infra*), and in analogy to the results of the Al-catalysts. GaO(OH) was present as the main crystalline species in Ga-AS and Ga-373.

Similarly to what was reported for AlO(OH),[32] the GaO(OH) phase was expected to have much lower epoxidation activity compared to partially hydroxylated gallium oxides due to its high surface hydrophilicity, preventing the approach of the alkene substrate to the catalytic active sites. Indeed, a reference GaO(OH) sample gave very low cyclooctene conversion (Table 7.2), indicating that the contribution of GaO(OH) to the epoxidation activity of Ga-AS, Ga-373 and Ga-473 was minor. The low activity of Ga-AS and Ga-373 can be further motivated by the presence of micropores (Table 7.1), which have been proposed to be detrimental to the catalytic activity of this type of materials.[10] The steadily decreasing activity found passing from Ga-573 to Ga-673 and to Ga-873 indicated that the α-Ga_2O_3 and β-Ga_2O_3 crystalline phases are less suitable for catalyzing the epoxidation reaction. This can be explained by the decrease in the amount of surface Ga-OH groups and in the total surface area induced by increasing calcination temperature (Table 7.1).

Catalysts active in the epoxidation of alkenes with H_2O_2 may also catalyze the unwanted disproportionation of H_2O_2 into O_2 and H_2O. The fraction of H_2O_2 decomposed during the catalytic test with Ga-573 was determined by means of titration with Ce^{4+} as 45% of the H_2O_2 employed, corresponding to a 24% selectivity of H_2O_2 towards the epoxide. Taking into account the differences in the epoxidation conditions, these values were consistent with those found for other gallium oxide catalysts.[3]

The reconstructed Ga-R was treated at 573 K, *i.e.* the temperature that led to the most active catalyst among those derived from Ga-AS, and tested as epoxidation catalyst. The XRD pattern of Ga-R-573 (Figure 7.1b) displayed low-intensity reflections specific to GaO(OH) and to α-Ga_2O_3, indicating the largely amorphous character of the material, similarly to Ga-473 and Ga-573. Ga-R-573 displayed a much higher activity than any other catalyst presented in this study, reaching an epoxide yield of 51% with an epoxide selectivity of 99% after 4 h of reaction at 353 K (corresponding to a productivity of 2.61 grams of epoxide per gram of catalyst and a TON of 1.96 mol of epoxide per mol of Ga[33]). These catalytic results are comparable with those of the most active gallium oxide catalysts synthesized from a $GaCl_3$ precursor.[3,7] A relevant advantage of the gallium oxide catalyst derived from Ga-R compared to that prepared from $GaCl_3$ is that Ga-R-573 can be directly used for the epoxidation reaction displaying high activity and selectivity, while the gallium oxide obtained from the hydrolysis of gallium chloride still contains Cl species after thermal treatment and, therefore, showed a reduced epoxidation selectivity in the first catalytic run due to the formation of chlorinated products.[3] The higher catalytic activity observed with Ga-R-573 compared with Ga-573 confirms that the dawsonite phase, present in larger amount in the reconstructed material, is

the precursor for the catalytically active phases for the epoxidation reaction. This conclusion was supported by the low epoxidation activity found for the catalyst obtained from GaO(OH) calcined at 573 K (Table 7.2), proving that GaO(OH) was not the precursor of the most active species in Ga-573 and Ga-R-573. The catalytic properties of Ga-R-573 are the best reported so far for transition-metal-free epoxidation catalysts.[3] As mentioned above for the Al-catalysts, the TON value of this catalyst was calculated on the basis of the total Ga content and not on the fraction of these atoms that display catalytic activity. This implies that TON should be used only for comparison with other aluminum and gallium oxides. The epoxide productivity achieved with Ga-R-573 is in the same range of that of the most active heterogeneous epoxidation catalysts,[34] with the advantage that this catalyst is active with aqueous hydrogen peroxide and is devoid of transition metals.

Similarly to the aluminum oxide, gallium oxide epoxidation catalysts have been reported to gradually deactivate upon recycling.[3] Therefore, the stability of the dawsonite-based Ga-catalysts was evaluated by recycling the catalysts in successive epoxidation runs. The recycling procedure was analogous to that used for the Al-catalysts. The most active catalyst, Ga-R-573, was recycled for a total of 4 epoxidation tests, while the parent material Ga-AS and the catalysts derived from it by thermal treatment were employed for a total of 3 tests. The results of these tests are reported in Figure 7.8b and Table 7.2. Ga-AS and Ga-373 displayed an increased activity in the second catalytic run, followed in the third run by a decrease in activity leading to an epoxide yield slightly higher than in the first run. This behavior was similar to that observed with Al-AS and the derived materials, and suggested a reconstruction of the dawsonite phase into an active phase due to reaction with H_2O during the epoxidation for 4 h at 353 K. This hypothesis was supported by the absence of the reflections due the dawsonite phase in the XRD pattern of Ga-AS and Ga-373 after three catalytic runs, while high intensity reflections due to GaO(OH) were observed (Figure 7.9b).

In agreement, TGA of the reused catalysts (Annex 3) showed only the one-step weight loss profiles corresponding to GaO(OH), and the infrared results exhibited only the vibration bands specific to GaO(OH). The activity of the recycled Ga-AS and Ga-373 was ascribed to amorphous gallium oxides/oxihydroxides formed upon hydrolysis of the dawsonite, rather than to the crystalline GaO(OH). All the remaining Ga-catalysts gradually deactivated upon recycling, in line with the trends observed for gallium oxides prepared by hydrolysis of $GaCl_3$.[3] The best catalyst identified in this work, Ga-R-573, deactivated slightly in the second catalytic test and more drastically in the successive runs. However, in the forth run the catalyst still displayed a significant epoxide yield (16%). Comparing the XRD pattern of the

reused catalyst Ga-R-573-rec4 with that of Ga-R-573 (Figure 7.9b), the decrease of the catalytic performance can be connected to structural changes occurring during the catalytic reactions leading to more crystalline phases (GaO(OH) and α-Ga_2O_3), which are less catalytically active than amorphous gallium oxides (*vide supra*). Similarly, the deactivation of Ga-573 was accompanied by the formation of a crystalline GaO(OH) phase (Figure 7.9b).

4. Conclusions

A series of NH_4-Al-dawsonite and NH_4-Ga-dawsonite as-synthesized materials as well as the products obtained by their thermal decomposition or reconstruction treatment were tested in the epoxidation reaction of cyclooctene with aqueous hydrogen peroxide. The temperature at which the dawsonite precursors were treated proved to be crucial in determining the activity of the catalysts. The nature of the phases present in the Al- and Ga-catalysts was unraveled and correlated to the catalytic behavior of the materials. The difference in the trend of the catalytic activity as a function of the thermal treatment observed between the Al- and the Ga-catalysts is ascribed to the different relative content of dawsonite and of other phases in the as-synthesized materials and to the different temperatures at which the various aluminum and gallium oxihydroxides or oxides form and remain stable. The most active catalysts were also the most selective. Among the Al-catalysts, the highest activity was achieved with one of the recycled materials, Al-473-rec1, reaching a cyclooctene conversion of 31% with an epoxide selectivity of 98%. In the Ga-catalysts series, the most active material was Ga-R-573 with a cyclooctene conversion of 52% and an epoxide selectivity of 99%. These catalytic results are unsurpassed among transition-metal-free epoxidation catalysts. Similarly to what was observed previously,[3] the best gallium-catalysts proved to be more active compared to the best aluminum-catalysts. With these results, we reported for the first time the successful synthesis and characterization of gallium dawsonite and of the calcination products. Preparing a pure gallium dawsonite would enable generating, upon thermal treatment, a catalyst with high specific surface area that would be expected to display improved epoxidation activity.

Acknowledgments

Marta Santiago is acknowledged for the contribution to the characterization of the materials. Paolo Pescarmona is thanked for the extensive catalytic tests. They are gratefully thanked for the related discussions and valuable contribution to this chapter.

References

[1] G. Sienel, R. Rieth, K. T. Rowbottom; In Ullmann's Enciclopedia of Industrial Chemistry, Wiley-VCH, Weinheim, 6th Ed., 2000.

[2] B. S. Lane, K. Burgess, *Chem. Rev.* **2003**, 103, 2457.

[3] P. P. Pescarmona, K. P. F. Janssen, P. A. Jacobs, *Chem. Eur. J.* **2007**, 13, 6562.

[4] D. Mandelli, M. C. A. van Vliet, R. A. Sheldon, U. Schuchardt, *Appl. Catal. A* **2001**, 219, 209.

[5] R. Rinaldi, U. Schuchardt, *J. Catal.* **2004**, 227, 109.

[6] V. R. Choudhary, N. S. Patil, N. K. Chaudhari, S. K. Bhargava, *J. Mol. Catal. A* **2005**, 227, 217.

[7] P. P. Pescarmona, P. A. Jacobs, *Catal. Today* **2008**, 137, 52.

[8] R. Rinaldi, F. Y. Fujiwara, W. Hölderich, U. Schuchardt, *J. Catal.* **2006**, 244, 92.

[9] R. Rinaldi, J. Sepúlveda, U. Schuchardt, *Adv. Synth.* **2004**, 346, 281.

[10] R. Rinaldi, F. J. Fujiwara, U. Schuchardt, *J. Catal.* **2007**, 245, 456.

[11] A. J. Frueh, J. P. Golightly, *Can. Mineral.* **1967**, 9, 51.

[12] M. Giannos, M. Hoang, T. W. Turney, *Chem. Lett.* **1998**, 793.

[13] I. Pitsch, W. Gebner, A. Brückner, H. Mehner, S. Mohmel, D.-C. Uecker, M.-M. Pohl, *J. Mater. Chem.* **2001**, 11, 2498.

[14] M. Santiago, M. S. Yalfani, J. Pérez-Ramírez, *J. Mater. Chem.* **2006**, 16, 2886.

[15] G. Stoica, J. Pérez-Ramírez, *Chem. Mater.* **2007**, 19, 4783.

[16] A. A. Ali, M. A. Hasan, M. I. Zaki, *Chem. Mater.* **2005**, 17, 6797.

[17] S. Abelló, J. Pérez-Ramírez, *Adv. Mater.* **2006**, 18, 2436.

[18] S. Brunauer, P. H. Emmett, E. Teller, *J. Am. Chem. Soc.* **1938**, 60, 309.

[19] B. C. Lippens, J. H. de Boer, *J. Catal.* **1965**, 4, 319.

[20] P. P. Pescarmona, J. van Noyen, P. A. Jacobs, *J. Catal.* **2007**, 251, 307.

[21] C. J. Serna, J. V. Garcia-Ramos, M. J. Peña, *Spectrochim. Acta* **1985**, 41A, 697.

[22] J. W. Anthony, R. A. Bideaux, K. W. Bladh, M. C. Nichols; In Handbook of Mineralogy; Vol. V, Mineral Data Publishing: Tucson, AZ, **2007**, p. 176.

[23] Y. Zhao, R. L. Frost, J. Yang, W. N. Martens, *J. Phys. Chem. C* **2008**, 112, 3568.

[24] J. T. Kloprogge, H. D. Ruan, R. L. Frost, *J. Mater. Sci.* **2002**, 37, 1121.

[25] M. Rodríguez Delgado, C. Otero Areán, *Z. Anorg. Allg. Chem.* **2005**, 631, 2115.

[26] D. Kisailus, J. H. Choi, J. C. Weaver, W. Yang, D. E. Morse, *Adv. Mater.* **2005**, 17, 314.

[27] R. Roy, V. G. Hill, E. F. Osborn, *J. Am. Chem. Soc.* **1952**, 74, 719.

UNIVERSITAT ROVIRA I VIRGILI
CHEMISTRY OF DAWSONITES AND APPLICATION IN CATALYSIS
Georgiana Stoica
ISBN:978-84-693-1533-0/DL:T-648-2010

[28] A. Vimont, J. C. Lavalley, A. Sahibed-Dine, C. Otero Areán, M. Rodríguez Delgado, M. Daturi, *J. Phys. Chem. B* **2005**, 109, 9656.

[29] F. Schüth, K. Unger; In Handbook of Heterogeneous Catalysis, H. Knözinger, G. Ertl, J. Weitkamp, Eds.; Vol 2, Wiley-VCH, Weinheim, **1997**, pp. 72-86.

[30] Z. Zhang, T. J. Pinnavia, *J. Am. Chem. Soc.* **2002**, 124, 12294.

[31] G. Stoica, J. C. Groen, S. Abelló, R. Manchanda, J. Pérez-Ramírez, *Chem. Mater.* **2008**, 20, 3973.

[32] R. Rinaldi, U. Schuchardt, *J. Catal.* **2005**, 236, 335.

[33] When comparing the TON values, it should be taken into account that the amount of catalyst used in this set of experiments is half of what generally employed for aluminum oxides [3].

[34] D. E. De Vos, B. F. Sels, P. A. Jacobs, *Adv. Synth. Catal.* **2003**, 345, 457.

UNIVERSITAT ROVIRA I VIRGILI
CHEMISTRY OF DAWSONITES AND APPLICATION IN CATALYSIS
Georgiana Stoica
ISBN:978-84-693-1533-0/DL:T-648-2010

Annex 3

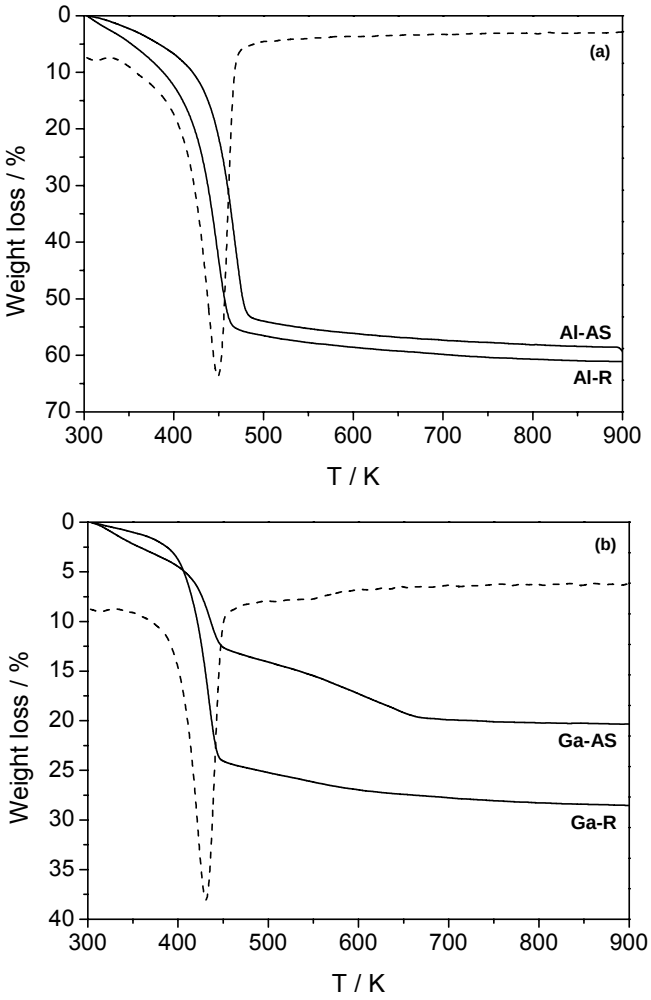

Thermogravimetry (a) of selected reused catalysts, *i.e.* Ga-AS-rec3 and Ga-373-rec3, showed the one-step weight loss profiles corresponding to GaO(OH), with a weight loss of 13-14%. The weight loss corresponding to the dawsonite phase in Ga-AS (centered at *ca.* 430 K) was not displayed anymore, and confirmed the XRD results exhibiting only reflections specific to GaO(OH) after three runs. Infrared of Ga-373-rec3 (b) underlined the presence of GaO(OH) as the only phase since the vibration bands specific to dawsonite vanished after recycling.

UNIVERSITAT ROVIRA I VIRGILI
CHEMISTRY OF DAWSONITES AND APPLICATION IN CATALYSIS
Georgiana Stoica
ISBN:978-84-693-1533-0/DL:T-648-2010

Chapter 7

UNIVERSITAT ROVIRA I VIRGILI
CHEMISTRY OF DAWSONITES AND APPLICATION IN CATALYSIS
Georgiana Stoica
ISBN:978-84-693-1533-0/DL:T-648-2010

Chapter 8

Summary and Outlook

In this thesis, the chemistry of dawsonite-type materials was extended by understanding their stability in different aqueous media, the achievement of dawsonite-hydrotalcite composites starting only from hydrotalcite, and the memory effect displayed by the dawsonite-derived aluminas in aqueous ammonium carbonate solutions. The as-such or activated dawsonites were evaluated in selected catalytic reactions: the synthesis of dimethyl carbonate by transesterification of ethylene carbonate with methanol and the epoxidation of alkenes with hydrogen peroxide.

UNIVERSITAT ROVIRA I VIRGILI
CHEMISTRY OF DAWSONITES AND APPLICATION IN CATALYSIS
Georgiana Stoica
ISBN:978-84-693-1533-0/DL:T-648-2010

Dawsonite-type compounds are crystalline double hydroxyl carboaluminates, analogues of the mineral dawsonite, $NaAlCO_3(OH)_2$. The ability to change the nature of sodium and aluminum in the structure, by other alkaline or transition metals, makes them versatile compounds. Dawsonites synthesized by the in-line dispersion-precipitation (ILDP) method are excellent precursors for aluminas with enhanced dispersion, textural properties, thermal stability, and catalytic performance.

Post-synthesis treatments of dawsonite-type materials deserve further attention and should lead to a more efficient use of these samples in catalytic applications. Thermal activation is a well-established approach, and accordingly, dawsonites are frequently used as ceramics, adsorbent, desiccant, catalyst, and catalyst support.

In this thesis, the opportunity of thermal decomposition, coupled with reconstruction in ammonium carbonate aqueous solution of the dawsonite-derived aluminas has been investigated. Additionally, the reactivity of as-synthesized dawsonites in different carbonate solutions was studied. The chemical transformations were accompanied by remarkable changes which finally led to reformed materials with improved structural, morphological, and textural properties. In situ thermal activation studies coupled with kinetic and mechanistic investigations provided valuable information for the use of dawsonites as efficient catalysts in selected basic and redox reactions.

Stability and interconversion of dawsonites

The reactivity of as-synthesized NH_4, Na, and K-dawsonites in different aqueous media in the pH range 2-14 was investigated in ***Chapter 2***. Strong acids or bases induced dissolution of these materials. The most interesting solid transformations occurred in the presence of ammonium, potassium, and sodium carbonates. NH_4-dawsonite was highly reactive and converted into Na-dawsonite and K-dawsonite in Na_2CO_3 and K_2CO_3, respectively. Additionally, the NH_4 and Na-dawsonite can be successively interconverted in the appropriate carbonate solution. K-dawsonite displayed the highest stability in these media. However, treatment of Na-dawsonite in K_2CO_3 or K-dawsonite in Na_2CO_3 solutions led to bayerite, due to high pH used. To the best of our knowledge the interconversion between different forms of dawsonites has not been reported to date.

Although the Na and NH_4-dawsonites were highly reactive, their formation kinetics is different, *i.e.* the Na to NH_4-dawsonite transformation is faster than the reverse process (1-5 h *vs.* 15-24 h). The phase transitions induced significant morphological changes; that is,

UNIVERSITAT ROVIRA I VIRGILI
CHEMISTRY OF DAWSONITES AND APPLICATION IN CATALYSIS
Georgiana Stoica
ISBN:978-84-693-1533-0/DL:T-648-2010

particles of quasi-spherical shape in the as-prepared dawsonites were transformed into acicular crystals, the thermodynamic favored geometry of the mineral dawsonite. Additional, when the NH_4-dawsonite phase was formed, the textural properties were considerably improved, displaying higher surface areas with newly developed microporosity, respectively. The overall processes followed a dissolution-precipitation mechanism, and the final compounds are the results of aluminate precipitation induced by the pH of the aqueous solution.

Dawsonite-containing composite materials

Similarly to the dawsonite-type materials, the stability of hydrotalcite-like compounds was investigated in ***Chapter 3***. We demonstrated the high reactivity of these materials in ammonium carbonate at ambient conditions, and its evolution towards composites consisting of mixtures of dawsonite, hydrotalcite and magnesium ammonium carbonate. Interestingly, we were able to achieve multicomponent composite materials starting from a single component, *i.e.* hydrotalcite, in contrast to the studies reported so far in the literature, which require starting from all the components. Two synthetic ways were followed: (i) immersion of the solid hydrotalcites in $(NH_4)_2CO_3$ solution, and (ii) exfoliation of the layered hydrotalcites in formamide, and reactive stacking of the resulting colloid in aqueous $(NH_4)_2CO_3$.It has to be highlighted that prior delamination of hydrotalcites in formamide significantly increases the reactivity of the colloidal phase in ammonium carbonate aqueous solution with respect to the parent hydrotalcite.

The composition of the structured materials can be tuned by the treatment time and Mg content. In other words, at early stages of the treatment hydrotalcites with Mg/Al ratios of 2 and 3) recovered the original layered structure, which further transformed into dawsonite-hydrotalcite composite materials. Longer treatment times and high Mg content (Mg/Al = 4) in the starting material were unfavorable for the stability of the composite due to fast hydrotalcite dissolution. The progressive transformation of hydrotalcite towards crystalline dawsonite and magnesium ammonium carbonate phases occurs *via* a dissolution-precipitation mechanism based on the ability of dissolved aluminum to crystallize as dawsonite.

UNIVERSITAT ROVIRA I VIRGILI
CHEMISTRY OF DAWSONITES AND APPLICATION IN CATALYSIS
Georgiana Stoica
ISBN:978-84-693-1533-0/DL:T-648-2010

Dawsonite reconstruction

In ***Chapters 4*** and ***5***, the reactivity of aluminas derived from thermal decomposition of dawsonite-type compounds in different aqueous solution was investigated. We demonstrated that these aluminas exhibit structural memory, *i.e.* the original mineral structure in ammonium form ($NH_4AlCO_3(OH)_2$) was reformed by treatment in aqueous solutions of ammonium carbonate under mild conditions at pH ~ 10. Alumina carbonation to dawsonite was specific to $(NH_4)_2CO_3$, and the memory property applies to dawsonite compounds with different compensating cations (NH_4^+, K^+, Na^+). Besides, the memory effect holds in aluminas doped with transition metals such as iron and chromium. These results extend the unique memory property reported so far only for the layered-double hydroxides with hydrotalcite structure to other families of mineral-like compounds.

In great contrast, treatment of calcined dawsonites in other carbonate salts such as K_2CO_3 and Na_2CO_3, and NH_4OH, NH_4Cl solutions, and water led to aluminum (oxi)hydroxides, such as bayerite, gibbsite, diaspore, and boehmite, respectively. Similarly to hydrotalcites, the term memory is used since we start from the dawsonite structure, decompose it by thermal treatment, and recover it upon specific treatment and conditions. The reconstruction was complete for the NH_4-dawsonite calcined at 523 and 723 K. The latter materials are characterized by a highly amorphous and low-density alumina phase, with a well-developed and uniform mesoporosity. Formation of larger γ-Al_2O_3 crystals by calcination at 1073 K and ultimately α-Al_2O_3 by calcination at 1473 K led to partial or no recovery, respectively.

The above chemical transformations can be explained on the basis of a dissolution-precipitation mechanism by which the aluminum dissolves to form hydroxyaluminum complexes. Depending on the pH induced by the chemical species in the aqueous solution, these complexes precipitate as dawsonite isomorphs or Al-(oxi)hydroxides. The alumina-to-dawsonite transformation is relatively fast (10-30 min depending on the temperature).

The reactivity of dawsonite-derived aluminas in carbonate solutions is higher when compared to the corresponding as-synthesized dawsonites in ***Chapter 2***, due to the higher stability of the latter materials induced by the presence of crystalline structures.

Besides the structural reorganization, the original and reconstructed dawsonites present striking differences. A significant morphological refinement and hierarchical porosity were induced by the dissolution-precipitation process with formation of the characteristic acicular particles of the mineral dawsonite with increased purity. Nanoparticles in the as-made and calcined materials transformed through complex intermediate morphologies into well-

UNIVERSITAT ROVIRA I VIRGILI
CHEMISTRY OF DAWSONITES AND APPLICATION IN CATALYSIS
Georgiana Stoica
ISBN:978-84-693-1533-0/DL:T-648-2010

crystallized acicular nanoneedles with newly developed microporosity in the reconstructed material. Our results can be of significance to improve current applications of dawsonites associated to the modified properties induced by the memory effect.

Dawsonite formation through carbonation of Al-containing compounds was reported by several authors as a final product of CO_2 mineralization, and consequently a way of reducing the carbon dioxide concentration. In this sense, a future challenge will be to investigate the potential of dawsonite-derived aluminas in carbon dioxide sequestration.

Dawsonite-derived catalysts for DMC production

Basic alumina derived by thermal activation of Na-dawsonite is efficient, selective and stable basic catalyst for the green synthesis of dimethyl carbonate by transesterification of ethylene carbonate with methanol investigated in ***Chapter 6***. The aluminate was more active than calcined hydrotalcite and magnesium oxide, and, more importantly, it can be successfully recycled. The reaction proceeds very fast (in 5 min the yield of DMC reaches 50%) and the process is material-dependent as long as the active phase is the aluminate / basic alumina, finally leading to a maximum DMC yield of *ca*. 65%. The reaction was successfully scaled up, and the agreement of the catalytic performance on the lab and bench scales was remarkable. Additionally, the mechanism of the process was assigned based on the real-time infrared spectra provided by *in situ* spectroscopic techniques.

The basic strength of Na-dawsonite derived sodium aluminate was determined using the Hammett indicators in the range 10 (medium) < H_- < 18 (strong), and it was determined that $NaAlO_2$ induced a change in the color of the indicator only between 10 < H_- < 15. This observation made us conclude that dawsonite-derived Na-aluminate is a moderate base.

The inherent characteristics of this catalyst were attractive for its use in different base-catalyzed reactions. In this purpose, we selected to test sodium aluminate in the biodiesel synthesis by transesterification of sunflower oil with methanol, and the aldol condensation reaction of citral and acetone, respectively. Fresh $NaAlO_2$ derived from Na-dawsonite activation was found to be highly active and selective in both reactions. Unfortunately, in contrast to the transesterification of ethylene carbonate with methanol, the reactions can not be efficiently recycled due to deactivation of the catalyst under the experimental conditions used. Following this investigation line, the next step will be to study on one side the deactivation of the catalyst, and secondly to make it functional for the reactions stated above.

UNIVERSITAT ROVIRA I VIRGILI
CHEMISTRY OF DAWSONITES AND APPLICATION IN CATALYSIS
Georgiana Stoica
ISBN:978-84-693-1533-0/DL:T-648-2010

Dawsonite-derived catalysts for cyclooctene epoxidation with H_2O_2

Synthesis and characterization of NH_4-Ga-dawsonite and the products of its calcination was reported for the first time herein (***Chapter 7***). NH_4-Ga-dawsonite derived materials (by calcination or reconstruction) are better catalysts than NH_4-Al-dawsonite derived samples in the epoxidation reaction of cyclooctene with aqueous hydrogen peroxide.

The thermal activation temperature is essential for the activity of the catalysts, as there is a correlation between the phases present and the catalytic behavior of the materials. The most active catalyst among all the materials tested was a reconstructed Ga-dawsonite calcined at 573 K. Both Al and Ga-catalysts displayed high epoxide selectivity, *i.e.* > 98%. It has to be mentioned that Ga-dawsonite calcined at 573 K is the best catalyst so far among all the catalysts reported in the literature for the epoxidation of cyclooctene.

However, Ga-dawsonite was poorly represented in the as-synthesized material (only 20%). Thermal decomposition and reconstruction doubled the amount of the dawsonite phase. Yet, this is far from a desired high purity compound. In this way, preparing a pure gallium dawsonite would enable generating, upon thermal treatment, a catalyst with high specific surface area, and is expected to display improved epoxidation activity.

UNIVERSITAT ROVIRA I VIRGILI
CHEMISTRY OF DAWSONITES AND APPLICATION IN CATALYSIS
Georgiana Stoica
ISBN:978-84-693-1533-0/DL:T-648-2010

Summary and Outlook

UNIVERSITAT ROVIRA I VIRGILI
CHEMISTRY OF DAWSONITES AND APPLICATION IN CATALYSIS
Georgiana Stoica
ISBN:978-84-693-1533-0/DL:T-648-2010

UNIVERSITAT ROVIRA I VIRGILI
CHEMISTRY OF DAWSONITES AND APPLICATION IN CATALYSIS
Georgiana Stoica
ISBN:978-84-693-1533-0/DL:T-648-2010

List of publications

Journals

G. Stoica, J. Pérez-Ramírez

Reforming of dawsonite by memory effect of AACH-derived aluminas, *Chem. Mater.* 19 (2007) 4783-4790.

G. Stoica, J. C. Groen, S. Abelló, R. Manchanda, J. Pérez-Ramírez

Reconstruction of dawsonite by alumina carbonation in $(NH_4)_2CO_3$, *Chem. Mater.* 20 (2008) 3973-3982.

G. Stoica, S. Abelló, J. Pérez-Ramírez

Synthesis of dimethyl carbonate by transesterification of ethylene carbonate over activated dawsonites, *ChemSusChem* 2 (4) (**2009**) 301-304.

G. Stoica, S. Abelló, J. Pérez-Ramírez

Na-dawsonite derived aluminates for DMC production by transesterification of ethylene carbonate, *Appl. Catal. A* 365 (**2009**) 252-260.

G. Stoica, M. Santiago, P. A. Jacobs, J. Pérez-Ramírez, P. P. Pescarmona

Epoxidation catalysts derived from aluminum and gallium dawsonites, *Appl. Catal. A* 371 (**2009**) 43-53.

G. Stoica, M. Santiago, S. Abelló, J. Pérez-Ramírez

Reactivity of Mg-Al hydrotalcites in solid and delaminated forms in ammonium carbonate solutions, *submitted*.

G. Stoica, J. Pérez-Ramírez

Stability and interconversion of synthetic dawsonites in aqueous media, *in preparation.*

UNIVERSITAT ROVIRA I VIRGILI
CHEMISTRY OF DAWSONITES AND APPLICATION IN CATALYSIS
Georgiana Stoica
ISBN:978-84-693-1533-0/DL:T-648-2010

S. Abelló, S. Mitchell, M. Santiago, **G. Stoica**, J. Pérez-Ramírez

Perturbing the properties layered double hydroxides by continuous coprecipitation with short residence time, *submitted*.

Conference Proceedings

G. Stoica, J. Pérez-Ramírez

Dawsonite formation by alumina treatment in $(NH_4)_2CO_3$; In *Proceedings of the 2nd International Conference on Accelerated Carbonation for Environmental and Materials Engineering*, Eds. R. Baciocchi, G. Costa, A. Polettini, R. Pomi ; Rome, Italy, **2008**, pp.63-72.

Conferences

S. Abelló, **G. Stoica**, E.V. Kondratenko, J. Pérez-Ramírez

Mixed oxides from hydrotalcite-like precursors as versatile supports for efficient nanosized gold catalysts

Poster presentation

GOLD 2006 - New Industrial Applications for Gold, Limerick, Ireland, **2006**

G. Stoica, S. Abelló, J. Pérez-Ramírez

Desarrollo de catalizadores hererogéneos para la síntesis ecoeficiente de dimetilcarbonato

Poster presentation

SECAT'07 - Congreso de la Sociedad Española de Catálisis, Bilbao, Spain, **2007**

G. Stoica, S. Abelló, J. Pérez-Ramírez

DMC synthesis by transesterification of ethylene carbonate over solid bases – Potential of activated dawsonites

Oral presentation

5 ICEC - 5th International Conference on Environmental Catalysis, Belfast, Ireland, **2008**

G. Stoica, J. Pérez-Ramírez

Carbonation of dawsonite-derived aluminas – Requirements and mechanism

Oral presentation

UNIVERSITAT ROVIRA I VIRGILI
CHEMISTRY OF DAWSONITES AND APPLICATION IN CATALYSIS
Georgiana Stoica
ISBN:978-84-693-1533-0/DL:T-648-2010

ACEME08 - Accelerated Carbonation for Environmental and Materials Engineering, Rome, Italy, **2008**

G. Stoica, M. Santiago, P. A. Jacobs, J. Pérez-Ramírez, P. P. Pescarmona

Epoxidation catalysts derived from aluminum and gallium dawsonites

Poster presentation

EuropaCatIX - Catalysis for a Sustainable World, Salamanca, Spain, **2009**

UNIVERSITAT ROVIRA I VIRGILI
CHEMISTRY OF DAWSONITES AND APPLICATION IN CATALYSIS
Georgiana Stoica
ISBN:978-84-693-1533-0/DL:T-648-2010

UNIVERSITAT ROVIRA I VIRGILI
CHEMISTRY OF DAWSONITES AND APPLICATION IN CATALYSIS
Georgiana Stoica
ISBN:978-84-693-1533-0/DL:T-648-2010

About the author

Georgiana Stoica was born on 10 July, 1980 in Bucharest, Romania. After finalizing the high-school in 1999 at Vlaicu Voda National College in Curtea de Arges, she studied Biochemistry from 1999-2003 at the University of Bucharest. After her graduation in 2003, she followed the Master in Biochemistry and Molecular Biology at the University of Bucharest from 2003-2005. In the same time, she joined the Research Centre in Molecular Biology of the University of Bucharest, investigating molecular markers by immunohystochemistry.

In 2005 she started her PhD project at the Institute of Chemical Research of Catalonia (ICIQ) in Tarragona, Spain under the supervision of Prof. Dr. Javier Pérez-Ramírez. The main focus was the activation of dawsonite-type materials for a more efficient utilization and application in catalysis. The most important results acquired during this research are enclosed in the present thesis. The author is thankful for financial support of this project offered by the FPU program (AP2005-5147) in the frame of the Spanish MICINN.

This PhD period will be followed by a post doctoral research at the Swiss Federal Institute of Technology (ETH) in Zurich focused on the catalyst design and mechanistic studies for the synthesis of methanol.